

Titre: Stress Relaxation of Growth Plate Tissue under Uniform
Compressive Load : Relationship Between Mechanical Response and
Extracellular Matrix Bio-Composition and Structure

Auteur: Samira Amini
Author:

Date: 2011

Type: Mémoire ou thèse / Dissertation or Thesis

Référence: Amini, S. (2011). Stress Relaxation of Growth Plate Tissue under Uniform
Compressive Load : Relationship Between Mechanical Response and Extracellular
Matrix Bio-Composition and Structure [Thèse de doctorat, École Polytechnique de
Montréal]. PolyPublie. <https://publications.polymtl.ca/726/>

 **Document en libre accès dans PolyPublie**
Open Access document in PolyPublie

URL de PolyPublie: <https://publications.polymtl.ca/726/>
PolyPublie URL:

**Directeurs de
recherche:** Isabelle Villemure, & Caroline D. Hoemann
Advisors:

Programme: Génie biomédical
Program:

UNIVERSITÉ DE MONTRÉAL

STRESS RELAXATION OF GROWTH PLATE TISSUE UNDER UNIFORM
COMPRESSIVE LOAD: RELATIONSHIP BETWEEN MECHANICAL
RESPONSE AND EXTRACELLULAR MATRIX BIO-COMPOSITION AND
STRUCTURE

SAMIRA AMINI

INSTITUT DE GÉNIE BIOMÉDICAL
ÉCOLE POLYTECHNIQUE DE MONTRÉAL

THÈSE PRÉSENTÉE EN VUE DE L'OBTENTION
DU DIPLÔME DE PHILOSOPHIAE DOCTOR
(GÉNIE BIOMÉDICAL)

DÉCEMBRE 2011

UNIVERSITÉ DE MONTRÉAL

ÉCOLE POLYTECHNIQUE DE MONTRÉAL

Cette thèse intitulée:

STRESS RELAXATION OF GROWTH PLATE TISSUE UNDER UNIFORM
COMPRESSIVE LOAD: RELATIONSHIP BETWEEN MECHANICAL
RESPONSE AND EXTRACELLULAR MATRIX BIO-COMPOSITION AND
STRUCTURE

présentée par : AMINI Samira

en vue de l'obtention du diplôme de : Philosophiae Doctor

a été dûment acceptée par le jury d'examen constitué de :

M. AUBIN Carl-Éric, Ph.D., président

Mme VILLEMURE Isabelle, Ph.D, membre et directrice de recherche

Mme HOEMANN Caroline, Ph.D., membre et codirectrice de recherche

M. BUSCHMANN Michael, Ph.D, membre

Mme LANGELIER Ève, Ph.D., membre

DEDICATION

*To Parham, for his unconditional love,
that more than once encouraged me to overcome difficult times*

ACKNOWLEDGEMENTS

I would like to convey my sincere gratitude to those who helped me to complete this study. First and foremost, I am genuinely grateful to my supervisor, Professor Isabelle Villemure, for her friendly guidance, continuous and substantial support, precious advice, scientific rigor and in particular her total involvement in the monitoring of this project. It was a great pleasure for me to work under her supervision. She was an endless source of encouragement to me throughout this period. Her exceptional high standards inspired me to improve my skills throughout my research at École Polytechnique de Montréal. I am deeply indebted to her for her availability at any time for consultations and discussions on my research.

I would like to thank my co-supervisor, Professor Caroline D Hoemann, for her friendly guidance, continuous support, wealth of advice, and insightful guidance on the biochemical aspect of my project. Her passion for science inspired me throughout my doctoral studies and it was an honor to work with her.

I also wish to thank Dr. Martin Lévesque, collaborator and associate professor of mechanical engineering at the Ecole Polytechnique de Montreal, for his involvement in providing advice on my third publication.

I take great pleasure in acknowledging all present and former members of the Laboratory of Pediatric Mechanobiology (LMP) of Professor Isabelle Villemure and of course my good friends. Thank you to Annie Bélisle-L'Anglais, Daniel Veilleux, Maria Laitenberger, Irene Londono, Anne-Laure Ménard, Farhad Mortazavi, Kim Sergerie, Barthélémy Valteau, Yaroslav Wakula, and Roxanne Wosu, who created lots of memorable moments for me during these years and helped me to integrate into the group. I would also like to extend my thanks to Irene Londono for being a great help during hard times and Anne-Laure Ménard for the editorial revision of the French Résumé.

I like to extend my thanks to the technical and administrative staff of the Applied mechanics section of Mechanical Engineering Department. Special thanks to Mr. Thierry Lafrance and Mr. Benedict Besner for their marvellous work on my experimental set-up.

I would like to thank present and former members of Biomaterials and Cartilage Laboratory of Professor Caroline Hoemann. I take great pleasure to specifically thank Adele Changoor,

Gaoping Chen, Anik Chevrier, Viorica Lascau-Coman, and Jun Sun for their help in the biochemical aspect of my project.

I made many friends in Montreal, and it gives me great pleasure to acknowledge the support and love I received from them. They were with me in sad and happy moments and made all these years memorable for me. I refrain from acknowledging them individually because that would take many pages, and for fear that I may inadvertently miss some of them. However, I can not help mentioning the name of my best friends, *Mahnaz, Ravid, Azin, Naser, Arezou, Alireza, Maryam, Farhad, Sara, and Ali*, who were with me during the most tragic moments of my life when I lost my grand father and my father-in-law.

I owe special gratitude to my mother, *Maman Parvin*, and my father, *Baba Hossein*, for their prayers, unconditional love, support, and encouragement throughout my entire life. I am deeply indebted to them for every success I have ever achieved. I would also thank my brother, *Ali*, for his support, love, and cheerfulness. He provided a great deal of encouragement to me during my studies and I am grateful to him.

I would like to send a heartfelt acknowledgement to my Family-in-law for the support and love I received from them. I can't help mentioning my Father-in-law who left us too early to join the invisible. He was an endless source of encouragement and love during my studies. May his soul rest in peace.

I would also like to acknowledge Canada, the province of Québec, and École Polytechnique de Montréal for giving me the opportunity to continue my studies. It is with great pleasure that I express my thanks to *Montrealers* for their kindness.

I would like to convey my gratitude to Professor Carl-Eric Aubin, Professor Michael Buschmann, and Professor Eve Langelier for accepting to participate to my Ph.D. Jury.

This project was funded by the Canada Research Chair in Mechanobiology of the Pediatric Musculoskeletal System (I.V.), the Board of Natural Sciences and Engineering Research Council of Canada (NSERC), and the MENTOR program of the Canadian Institute of Health Research (CIHR, S.A.).

Last, but most important, I would like to express my special gratitude to my lovely husband, *Parham Eslami Nejad*, for his patience, love, encouragement and support. He was an endless

source of inspiration to me for achieving my goals. He was genuinely caring during these years and I am deeply indebted to him for every single second of our life.

RÉSUMÉ

La modulation mécanique de la croissance osseuse a des implications dans la progression des déformations musculo-squelettiques telles que la scoliose idiopathique adolescente. Ce processus présente aussi un intérêt croissant pour le développement et l'amélioration des approches minimalement invasives de correction de ces déformations musculo-squelettiques en modulant localement la croissance osseuse, tout en préservant la croissance normale ainsi que les fonctions et mobilités segmentaires. La croissance longitudinale des os longs et des vertèbres s'effectue au droit des plaques de croissance, qui sont divisées en trois zones histologiques distinctes (réserve, proliférative et hypertrophique). La matrice extracellulaire de la plaque de croissance est principalement composée d'eau et de protéoglycanes imbriquées dans des fibrilles de collagène de type II, qui sont considérées comme des composants déterminants des propriétés biomécaniques des tissus cartilagineux. Des études antérieures ont étudié le comportement biomécanique des plaques de croissance, mais aucune étude n'a à ce jour analysé le comportement mécanique en compression de la plaque de croissance et de ses zones *in situ* à l'égard de sa composition biochimique et de l'organisation de ses fibres de collagène. L'objectif principal de cette étude était de déterminer les caractéristiques histomorphologiques et le comportement mécanique des plaques de croissance aux niveaux cellulaire et tissulaire, d'évaluer la composition biochimique et l'orientation des fibres de collagène de la plaque de croissance dans ses trois zones distinctes, puis d'établir des associations entre le comportement mécanique et la composition biochimique de la plaque de croissance.

Cinq groupes d'explants de plaques de croissance provenant de porcs âgés de quatre semaines ont été utilisés dans ce projet. Le premier groupe d'explants (N=12) a été utilisé pour caractériser l'histomorphologie 3D de la plaque de croissance *in situ* aux niveaux cellulaire (volume, aire surfacique, sphéricité, et rayons mineur/majeur) et tissulaire (ratio cellule/matrice extracellulaire), en utilisant un marquage fluorescent du cytoplasme cellulaire (Calcéine AM) couplé à la reconstruction 3D des coupes sériées d'images numériques confocales (logiciel IMARIS). Afin de caractériser le comportement mécanique sous compression de la plaque de croissance et de ses cellules constitutives en 3D, un second groupe d'explants de cartilage de croissance (N=6), dont les cytoplasmes cellulaires ont été marqués à la Calcéine AM, a été testé sous compression semi-confinée en relaxation de contraintes à l'aide d'un montage combinant un appareil de micro-

chargement fixé sur un microscope confocal inversé. Ces explants ont été soumis à une déformation totale de 15% (5% pré-charge et 10% de déformation) à un taux de $1.7 \times 10^{-3} \text{ s}^{-1}$ jusqu'à l'obtention de l'équilibre, suivant un critère de relaxation de $8 \times 10^{-6} \text{ N/sec}$. Des coupes sériées d'images numériques des cytoplasmes cellulaires marqués ont été acquises par microscopie confocale avant chargement et après relaxation du tissu. Des reconstructions 3D des chondrocytes dans les conditions pré- et post-charge ont été complétées à partir d'images prises séparément dans les trois zones des plaques de croissance. Différents paramètres morphométriques au niveau cellulaire (volume, aire surfacique, sphéricité et rayons mineur/majeur) et au niveau tissulaire (ratio cellule/matrice extracellulaire) ont été évalués (logiciel IMARIS) puis comparés à l'aide de tests statistiques pour les trois zones de la plaque de croissance. Afin de caractériser le comportement mécanique sous compression de la plaque de croissance au niveau tissulaire, un troisième groupe d'explants de cartilage de croissance (N=7), dont les noyaux cellulaires ont été marqués au Syto-17, a été testé sous compression semi-confinée en relaxation de contraintes à l'aide du même montage et des mêmes paramètres de chargement. Des images numériques des noyaux des chondrocytes marqués ont été acquises par microscopie confocale avant chargement et après relaxation du tissu, puis les champs de déformation 2D ont été déterminés à l'aide d'un algorithme de corrélation d'images appliqué à des paires d'images d'un même explant. Au niveau biochimique, un quatrième groupe d'explants (N=7) du même modèle animal a été analysé pour obtenir leurs contenus en eau, en glycosaminoglycanes sulfatés (S-GAG) et en hydroxyproline (OH-Pro), comme une mesure de leurs contenus en collagène, dans les trois zones histologiques de la plaque de croissance. La teneur en eau a été déterminée par pesée des tissus avant et après lyophilisation. Les contenus en collagène et en GAG ont été quantifiés à l'aide des essais d'hydroxyproline et de bleu de diméthylméthylène (DMMB), respectivement. Finalement, dans un cinquième groupe d'explants (N=7) du même modèle animal, l'organisation des fibres de collagène a été évaluée dans les trois zones histologiques de la plaque de croissance en utilisant la microscopie en lumière polarisée (PLM).

Les **caractéristiques histomorphologiques** de la plaque de croissance aux niveaux tissulaire et cellulaire sont hétérogènes et dépendent de la zone de la plaque de croissance. Des variations significatives de la morphologie des chondrocytes ont été observées entre les différentes zones histologiques. Les volumes et les aires surfaciques maximaux des chondrocytes ont été trouvés

dans la zone hypertrophique par rapport à ceux des zones de réserve et proliférative. Le volume et l'aire surfacique des chondrocytes ont augmenté d'environ cinq et trois fois respectivement en se rapprochant de la jonction chondro-osseuse à partir de la zone de réserve. Les chondrocytes de la zone proliférative ont été les cellules de formes les plus discoïdes entre les trois différentes zones histologiques. Des différences significatives ont aussi été observées concernant le ratio cellule/matrice extracellulaire entre les trois zones. Le minimum et le maximum des ratios cellule/matrice extracellulaire ont été identifiés dans les zones de réserve et proliférative, respectivement.

Les **analyses morphologiques tridimensionnelles aux niveaux tissulaire et cellulaire sous compression**, basées sur des explants marqués à la Calcéine AM, des coupes sériées d'images numériques des cytoplasmes cellulaires et des reconstructions 3D des chondrocytes dans les conditions pré- et post-chargement, démontrent que la plaque de croissance subit des déformations non uniformes sous chargement tant au niveau tissulaire qu'au niveau cellulaire, et également au niveau du ratio cellule/matrice extracellulaire. De plus grandes déformations cellulaires (changement de volume cellulaire normalisé au volume initial) ont été trouvées dans les zones proliférative et hypertrophique. Inversement, les plus faibles déformations se sont développées dans la zone de réserve. Suite à la compression, le ratio cellule/matrice extracellulaire a diminué dans les zones de réserve et hypertrophique alors qu'il a augmenté dans la zone proliférative.

L'analyse biomécanique au niveau tissulaire, basée sur des explants marqués au Syto-17, l'imagerie 2D et la corrélation numériques d'images (DIC), a démontré un comportement mécanique hétérogène dépendamment de la zone de la plaque de croissance considérée. Des déformations tissulaires axiales supérieures se sont développées dans la zone proliférative par rapport aux deux autres zones histologiques. Par ailleurs, des déformations transverses plus élevées ont été principalement trouvées dans les zones proliférative et hypertrophique par rapport à la zone de réserve. Enfin, les déformations transverses et axiales les plus faibles et les plus homogènes se sont principalement développées dans la zone de réserve.

Les **analyses biochimiques** ont indiqué que la zone de réserve a un contenu en collagène plus élevé par rapport aux zones proliférative et hypertrophique. Cependant, les contenus en eau et en GAG ont été évalués identiques dans les trois zones histologiques.

Les **caractérisations en microscopie polarisée** ont montré que les fibres de collagène de la zone de réserve sont principalement orientées parallèlement à l'interface entre la plaque de croissance et l'os, soit perpendiculairement à l'axe longitudinal des os. Toutefois, certaines fibres orientées longitudinalement ont également été observées dans cette zone. A l'inverse, les fibres de collagène ont été trouvées alignées presque exclusivement selon l'axe longitudinal de l'os, soit dans la direction de croissance, pour les zones proliférative et hypertrophique.

Au niveau histomorphologique, les hétérogénéités marquées de la taille des cellules à travers les différentes zones histologiques de la plaque de croissance sont cohérentes avec celles des études antérieures sur la morphologie des chondrocytes à l'aide de l'histologie conventionnelle et des méthodes stéréologiques. Les chondrocytes subissent les changements de forme tout en progressant de la zone de réserve à la jonction chondro-osseuse. Les chondrocytes hypertrophiques et réserves sont ronds par rapport aux chondrocytes aplatis de la zone proliférative, tel que confirmé par les valeurs significativement plus faibles de sphéricité des chondrocytes prolifératifs par rapport aux zones de réserve et hypertrophique. La morphologie tissulaire et cellulaire peut avoir des contributions notables sur le comportement de la plaque de croissance durant le processus de croissance. La capacité d'obtenir la morphométrie cellulaire *in situ* et de surveiller les changements dans la direction de la croissance pourrait améliorer notre compréhension des mécanismes par lesquels la croissance anormale est déclenchée.

Deuxièmement, les chondrocytes et leur matrice extracellulaire environnante subissent des changements morphologiques significatifs avec la compression, mais le niveau de déformation dépend de la zone histologique. Ces déformations variables sont probablement liées aux propriétés mécaniques hétérogènes des trois zones, où la zone de réserve a été trouvée plus rigide que les zones proliférative et hypertrophique dans les directions parallèle et perpendiculaire à l'axe de compression. Dans notre étude, les chondrocytes hypertrophiques ont montré les plus grandes déformations parmi les trois zones histologiques; ils pourraient ainsi être davantage susceptibles de déclencher des messages biologiques altérés, via un étirement plus important de leur membrane cellulaire, ce qui modulerait l'activité des ARN-messagers et pourrait éventuellement provoquer une décélération de croissance sous compression mécanique.

Le contenu en collagène de la plaque de croissance et l'orientation de ses fibres de collagène sont également non uniformes à travers l'épaisseur de la plaque de croissance. La dispersion aléatoire

des chondrocytes dans la zone de réserve et la disposition en colonnes des chondrocytes dans les zones proliférative et hypertrophique sont en corrélation avec l'orientation des fibres de collagène observées dans ces zones. En outre, nos données corroborent les données existantes sur le contenu biochimique de la plaque de croissance.

Enfin, le comportement biomécanique de la plaque de croissance sous compression est lié à son contenu en collagène et à l'organisation des fibres de collagène. La zone de réserve, moins sensible aux déformations comparé aux zones proliférative et hypertrophique, contient le contenu maximum en collagène avec des fibres alignées perpendiculairement à la direction de croissance. A l'inverse, les zones proliférative et hypertrophique, où un contenu en collagène inférieur et des fibres de collagène organisées longitudinalement ont été trouvés, s'avèrent plus sensibles aux déformations, tant aux niveaux cellulaire que tissulaire. La zone de réserve, plus rigide, pourrait jouer un rôle plus significatif de support mécanique comparativement aux zones proliférative et hypertrophique, qui seraient plus susceptibles d'être impliquées dans le processus de modulation de la croissance. Ces données s'ajoutent à notre compréhension de la relation entre les forces de compression subies par les chondrocytes de la plaque de croissance et de leur environnement extracellulaire.

Les principales limites de ce projet de recherche comprennent l'utilisation d'un modèle animal unique sans tenir compte des variations pouvant exister entre sites osseux et avec les stades de développement. La petite taille de l'échantillonnage ainsi que des analyses statistiques limitées pour établir des relations entre le comportement mécanique et les caractéristiques structurelles constituent aussi des limites de la présente étude. En contrepartie, cette étude est la première à offrir des informations importantes et complémentaires sur le comportement mécanique et les caractéristiques morphologiques et structurelles de la plaque de croissance ainsi que sur leurs relations pour un modèle animal avec un taux de croissance plus faible qui s'apparente davantage à celui des humains.

Les trois hypothèses de cette étude stipulaient que: 1) les trois zones de la plaque de croissance présentent différentes caractéristiques histomorphologiques, 2) les déformations cellulaires et les champs de déformation au niveau tissulaire sous compression sont non uniformes dans les trois zones de la plaque de croissance, et 3) le comportement biomécanique de la plaque de croissance en compression est relié à la composition biochimique de sa matrice extracellulaire (le contenu en

GAG et en collagène), sa teneur en eau ainsi que l'organisation de ses fibres de collagène type II dans les trois zones de la plaque de croissance. Basé sur les résultats obtenus, ces hypothèses sont vérifiées pour 1) et 2) et en partie confirmées pour 3).

En conclusion, les zones histologiques les plus activement impliquées dans la croissance longitudinale osseuse (proliférative et hypertrophique) seraient plus sensibles aux contraintes de compression aux niveaux cellulaire et tissulaire dû à leurs caractéristiques histomorphologiques et structurelles, et donc davantage susceptibles d'être impliquées dans la progression des déformations musculo-squelettiques infantile et juvénile. Une connaissance combinée de la mécanique et mécanobiologie de la plaque de croissance est essentielle afin de mieux comprendre les mécanismes par lesquels la croissance anormale est déclenchée et, à plus long terme, afin d'améliorer les approches de traitement minimalement invasive des malformations squelettiques progressives, qui exploitent directement le processus de modulation de croissance pour corriger ces déformations.

ABSTRACT

Mechanical loading has key implications in the progression of infantile and juvenile musculoskeletal deformities. Furthermore, the mechanical modulation of growth is of growing interest in the development and improvement of minimally invasive approaches that aim at modulating local bone growth while preserving the natural growth and functions of bone and bone segments. Longitudinal growth of long bones and vertebrae occurs in growth plates, which are divided into three distinct histological zones (reserve, proliferative and hypertrophic). Growth plate extracellular matrix is composed of water, large aggregating proteoglycans embedded within type II collagen fibrils, which are believed to be a critical determinant of tissue biomechanical competence. Previous studies have investigated the biomechanical behaviour of growth plates but no study up to date has comprehensively analyzed the zonal growth plate compressive mechanical behaviour *in situ* with respect to its biochemical composition and collagen fiber organization. The main objective of this study was to characterize the histomorphological characteristics and mechanical behaviour of growth plates at both cellular and tissue levels and to evaluate the biochemical composition and collagen fiber orientation of growth plate tissue in the three functionally distinct zones and to further establish associations between zonal mechanical behavior and biochemical composition of the growth plate.

Five groups of growth plate explants from 4-week old swine were used in this project. The first group of explants (N=12) was used to characterize the 3D zonal histomorphology of *in situ* growth plate at the cellular (volume, surface area, sphericity, minor/major radii) and tissue (cell/matrix volume ratio) levels using fluorescent labeling of cell cytoplasm (Calcein AM) coupled with 3D reconstruction of serial confocal sections (IMARIS software). In order to characterize the three-dimensional compressive mechanical behaviour of the growth plate tissue and its constitutive cells, a second group of growth plate explants (N = 6), labeled with Calcein AM for cell cytoplasm, were tested in semi-confined compression under stress relaxation using a loading apparatus mounted on the stage of an inverted confocal microscope. These explants were subjected to 15% compressive strain (5% pre-strain and 10% strain) at a rate of $1.7 \times 10^{-3} \text{ s}^{-1}$ until equilibrium. Serial sections of Calcein AM loaded explants were taken at two time points: prior to compression loading and after tissue relaxation. Three dimensional reconstruction of the serial sections taken pre-and post loading were completed from images taken separately in three zones

of growth plates. Morphometric parameters at cellular level (volume, surface area, sphericity, and the minor/major radii) and at tissue level (cell/extracellular matrix ratio) were evaluated (IMARIS software) and compared for the three zones of the growth plate using statistical tests. In order to characterize the compressive mechanical behaviour of the growth plate at tissue level, a third group of growth plate explants (N=7), labeled with Syto-17 for cell nuclei, were tested in semi-confined compression under stress relaxation using the same loading apparatus mounted on the stage of an inverted confocal microscope and the same loading parameters. Single images of Syto-17 loaded explants were taken at two time points: prior to compression loading and after tissue relaxation. Digital image correlation (DIC) was performed on 2D image pairs to obtain strain distribution through the growth plate thickness using a custom-designed image correlation algorithm. At the biochemical level, a fourth group of explants (N=7) from the same animal model were assayed for water content, total sulfated glycosaminoglycan (S-GAG) content and hydroxyproline (OH-Pro), as a measure of collagen content, in the three distinct histological zones. Water content was determined by weighing the tissue before and after lyophilisation. Collagen and GAG content was quantified using hydroxyproline assay and dimethylmethylene blue (DMMB) assay, respectively. Finally, in a fifth group of explants (N=7), collagen fiber organization was evaluated in the three histological zones of growth plate using polarized light microscopy.

Histomorphological analyses of growth plate at tissue and cellular levels revealed the heterogeneous and zone-dependent morphological state of the growth plate. Significant variation in the chondrocytes morphology was observed within different histological zones. Maximum chondrocytes volume and surface area were found in the hypertrophic zone compared to the reserve and proliferative zones. Chondrocyte volume and surface area increased about five- and three-fold respectively as approaching the chondro-osseous junction from the pool of reserve cells. Chondrocytes from the proliferative zone were the most discoidal cells among three different histological zones. Significant differences were also observed in cell/matrix volume ratio between the three zones. Minimum and maximum cell/matrix volume ratios were identified in the reserve and proliferative zone, respectively.

Three-dimensional morphological tissue and cellular analyses under compression, based on Calcein AM loaded explants, serial sections and quantitative morphological evaluations, prior to loading and after relaxation indicated zone-dependent biomechanical behaviour. Greater

chondrocyte bulk strains (volume decrease normalized to the initial cell volume) were found in the proliferative and hypertrophic zones, with lower chondrocyte bulk strains in the reserve zone. Following compression, the cell/matrix volume ratio decreased in the reserve and hypertrophic zones whereas it increased in the proliferative zone.

Tissue level biomechanical analyses, based on Syto-17 loaded explants, 2D imaging and digital image correlation (DIC), resulted in heterogeneous and zone-dependent mechanical behaviour of growth plate. Higher axial strains arose in the proliferative zone compared to the two other histological zones. Moreover, higher transverse strains were mainly found in the proliferative and hypertrophic zones compared to the reserve zone. On the contrary, lower and more homogeneous axial as well as transverse strains developed primarily within the reserve zone.

Biochemical analyses indicated that the reserve zone contains higher collagen content compared to the proliferative and hypertrophic zones. However, similar contents in water and GAG were obtained for all three histological zones.

Polarized microscopy investigation showed that fibers in the reserve zone were organized mainly horizontally (parallel to the growth plate/bone interface) in a radial fashion. However, some fibers were also observed as aligned in other directions in this zone. Collagen fibers were aligned almost exclusively vertically (parallel to the growth direction) in the proliferative and hypertrophic zones.

First of all, at the histomorphological level, the marked heterogeneity in cell size through the different histological zones of the growth plate observed in this study are consistent with previous studies on chondrocyte morphology using conventional histology and stereological methods. Chondrocytes undergo spatial shape changes while progressing from the reserve zone to the chondro-osseous junction. Reserve and hypertrophic chondrocytes were round relative to the flattened proliferative chondrocytes. This was confirmed by the significantly lower sphericity values of proliferative chondrocytes, as compared to reserve and hypertrophic zones. Tissue and cellular morphology may have noteworthy contribution to the growth plate behavior during growth process. Thus, the ability to obtain *in situ* cell morphometry and monitor the changes in the growth direction could improve our understanding of the mechanisms through which abnormal growth is triggered.

Secondly, chondrocytes and their surrounding extracellular matrix undergo significant zone-dependent morphological changes with compression, most probably due to heterogeneous mechanical properties characterizing the three zones, where the reserve zone was found stiffer along and perpendicular to the compression axis. In our study, hypertrophic chondrocytes showed the greatest deformations among chondrocytes of the three histological zones. Hence, hypertrophic chondrocytes could be more prone to trigger altered biological messages, potentially through cell membrane stretch, which is believed to modulate second messenger activity, and eventually cause growth deceleration under mechanical compression.

The growth plate collagen content and collagen fiber orientation were also non uniform through the growth plate thickness. Random dispersion of chondrocytes in the reserve zone and the columnar arrangement of chondrocytes in proliferative and hypertrophic zones correlate with the observed orientation of collagen fibers in these zones. Moreover, our data corroborates existing data on growth plate bio-composition.

Finally, the zone-dependent biomechanical behavior of the growth plate under compression is related to its collagen content and collagen fiber organization. Reserve zone, which was less susceptible to strains compared to proliferative and hypertrophic zones, contained the maximum collagen content with fibers aligned perpendicular to growth direction. Conversely, lower collagen content and longitudinally oriented collagen fibers were detected in the proliferative and hypertrophic zones with high proneness to strains. Overall, the proliferative and hypertrophic zones, where lower collagen levels and longitudinally organized collagen fibers were found, could be more susceptible to compressive strains at both cellular and tissue levels. The more rigid reserve zone could play a more significant role of mechanical support compared to the proliferative and hypertrophic zones, which would be more likely to be involved in the process of growth modulation. These data add to our understanding of the relationship between compressive forces experienced by growth plate chondrocytes and their extracellular environment.

The main limits of this research project include the use of a single animal model without considering the variations with site and developmental stage, the limited sample size as well as limited statistical analyses for establishing relationships between mechanical behaviour and structural characteristics. In return, this study was the first to offer significant information on the

growth plate mechanical behavior and morphological and structural characteristics as well as their relationships in an animal model with a lower growth rate that most resembles human.

The three hypotheses of this study, stating that: 1) different histomorphometrical characteristics are found within the three zones of growth plate, 2) cell deformation and strain distribution at tissue and cellular levels are non uniform within the three zones of the growth plate under uniform compressive stress, and 3) strain distribution is related to the biochemical composition of the extracellular matrix (GAG and collagen contents), the water content as well as type II collagen organization within the three zones of the growth plate, are therefore confirmed for 1) and 2) and partly confirmed for 3).

Overall, histological zones most actively involved in longitudinal bone growth (proliferative and hypertrophic) would be more susceptible to compressive strains both at cellular and tissue levels due to their histomorphological and structural characteristics, and hence more prone to be involved in the progression of infantile and juvenile musculoskeletal deformities. A combined improved knowledge of growth plate mechanics and mechanobiology is essential to better understand the possible mechanisms through which abnormal growth is triggered and to eventually improve the minimally invasive treatment approaches of progressive skeletal deformities, which directly exploit the process of growth modulation to correct these deformities.

TABLE OF CONTENTS

DEDICATION	III
ACKNOWLEDGEMENTS	IV
RÉSUMÉ.....	VII
ABSTRACT	XIII
TABLE OF CONTENTS	XVIII
LIST OF TABLES	XXIII
LIST OF FIGURES.....	XXIV
LIST OF ABBREVIATIONS	XXIX
INTRODUCTION.....	1
General organization of the thesis	3
CHAPTER 1 BACKGROUND AND REVIEW OF THE LITTERATURE	5
1.1 Longitudinal bone growth and growth plate	5
1.1.1 Longitudinal bone growth	5
1.1.2 Endochondral bone growth	5
1.1.3 Growth plate form and site.....	10
1.1.4 Growth plate composition	10
1.1.5 Growth plate ultrastructure and function	14
1.2 Growth plate mechanobiology	17
1.2.1 Mechanical modulation of bone growth.....	18
1.2.2 Musculoskeletal pathologies and treatments involving longitudinal bone growth	18
1.2.3 Effect of compression on bone growth rate	24
1.2.4 Effect of compression on growth plate histomorphometry	26
1.2.5 Effect of compression on growth plate biology	27

1.3	Growth plate mechanical behavior.....	29
1.3.1	Mechanical characteristics of cartilaginous tissue	29
1.3.2	Biphasic stress-relaxation response of growth plate in compression.....	31
1.3.3	Experimental compression tests	32
1.3.4	Quantitative tissue and cell compressive biomechanics of growth plate	35
1.4	Molecular and biochemical assays of cartilaginous tissue constituents.....	39
1.4.1	Commonly used biochemical assays for cartilaginous tissue components	39
1.4.2	Evaluation methods of growth plate bio-composition used in this thesis	40
1.4.3	Growth plate biochemical content evaluation up to date	43
1.5	Quantitative laser scanning confocal microscopy	44
1.5.1	Basic principles of the laser scanning confocal microscopy	44
1.5.2	Implications for cell and tissue biomechanics of cartilaginous tissue	48
1.6	Polarized light microscopy.....	49
1.6.1	Basic principles of polarized light microscopy	49
1.6.2	Applications in evaluation of extracellular matrix organization of hyaline cartilage	50
CHAPTER 2 PROJECT RATIONALE, HYPOTHESES AND SPECIFIC OBJECTIVES ..		52
2.1	Rationale.....	52
2.2	Thesis hypotheses and objectives.....	54
CHAPTER 3 SCIENTIFIC ARTICLE #1: THREE-DIMENSIONAL <i>IN SITU</i> ZONAL MORPHOLOGY OF VIABLE GROWTH PLATE CHONDROCYTES: A CONFOCAL MICROSCOPY STUDY.....		57
3.1	Abstract	58
3.2	Keywords	58
3.3	Introduction	58

3.4	Methods.....	62
3.4.1	Specimen preparation.....	62
3.4.2	Fluorescent labeling	63
3.4.3	Imaging protocol	64
3.4.4	Three-dimensional visualization and quantitative analysis.....	65
3.4.5	Statistical analysis	65
3.5	Results	66
3.6	Discussion	70
3.7	Acknowledgements	73
3.8	References	73
CHAPTER 4 SCIENTIFIC ARTICLE #2: TISSUE AND CELLULAR MORPHOLOGICAL CHANGES IN GROWTH PLATE EXPLANTS UNDER COMPRESSION.....		78
4.1	Abstract	79
4.2	Keywords	79
4.3	Introduction	79
4.4	Methods.....	81
4.4.1	Animal Model and Specimen Preparation	81
4.4.2	Imaging and Loading Protocol.....	83
4.4.3	Three-dimensional Reconstruction and Quantitative Analysis.....	84
4.4.4	Statistical Analysis	84
4.5	Results	85
4.6	Discussion	90
4.7	Conflict of interest statement	93
4.8	Acknowledgements	93
4.9	References	94

CHAPTER 5	SCIENTIFIC ARTICLE #3: STRESS RELAXATION OF SWINE GROWTH PLATE IN SEMI-CONFINED COMPRESSION: DEPTH DEPENDANT TISSUE DEFORMATIONAL BEHAVIOR VERSUS EXTRACELLULAR MATRIX COMPOSITION AND COLLAGEN FIBER ORGANIZATION	97
5.1	Abstract	98
5.2	Keywords	99
5.3	Abbreviations	99
5.4	Introduction	99
5.5	Methods	101
5.5.1	Animal model and tissue processing	101
5.5.2	Histological study	103
5.5.3	Imaging and mechanical loading protocols	103
5.5.4	Quantification of strain patterns using Digital image correlation	104
5.5.5	Biochemical analyses of water, collagen and GAG content	105
5.5.6	Collagen fiber organization using polarized light microscopy	106
5.5.7	Statistical analysis	107
5.6	Results	107
5.6.1	Swine growth plate zonal proportion	107
5.6.2	Strain distributions throughout growth plate thickness	108
5.6.3	Biochemical contents of 4-week old swine growth plate	112
5.6.4	Collagen fiber organization through the thickness of 4-week old swine growth plate	113
5.7	Discussion	114
5.8	Acknowledgements	119
5.9	References	119

CHAPTER 6	GENERAL DISCUSSION.....	124
6.1	Growth plate histomorphology.....	124
6.2	Growth plate mechanical behavior under compression	128
6.2.1	Three-dimensional <i>in situ</i> deformation under compressive loading	128
6.2.2	Two-dimensional <i>in situ</i> strain distribution through growth plate under compression..	129
6.3	Growth plate structural characteristics.....	131
6.4	Global discussion and overall limits of the research project.....	133
CONCLUSIONS AND RECOMMENDATIONS.....		135
BIBLIOGRAPHY		139

LIST OF TABLES

Table 1-1 : Studies on mechanical properties of growth plate tissue using stress relaxation tests.	37
Table 3-1 : Cell and tissue level morphometric analyses for the three histological zones of the growth plate (means \pm standard deviations).....	68
Table 4-1 : Cell and tissue level morphological parameters in three histological zones of growth plate at platen-to-platen compression of 0% and 15%. (mean values \pm standard deviations)	88
Table 5-1 : Mean zonal thickness proportions of the reserve, proliferative and hypertrophic zones of 4-week old ulnar growth plates.	108
Table 5-2 : (a) Average developed strains along the bone axis (\square_{yy}) and (b) average developed strains perpendicular to the bone axis (\square_{xx}) within the reserve, proliferative and hypertrophic zones of 4-week old ulnar swine growth plates under 10% uniform compressive strain.	111
Table 5-3 : Water, GAG and collagen contents in three histological zones of 4-week old swine distal ulna growth plates (mean \pm standard deviation). Both GAG and collagen contents are normalized to wet weight of the tissue.	112

LIST OF FIGURES

Figure 1-1 : Endochondral ossification process in long bones, adapted from Marieb et al. (2006) ..	5
Figure 1-2 : A typical confocal section of porcine growth plate (chondrocytes cytoplasm labeled using Calcein-AM) showing its ultrastructure and three histological zones.....	6
Figure 1-3 : Relative contribution of proliferative and hypertrophic zones in daily longitudinal growth of four different bone types from 28-day old rats at the chondro-osseous junction, adapted from Wilsman et al. (1996).....	7
Figure 1-4 : Schematic representation of different scoliotic patterns (obtained on 22 June 2011 from http://www.niams.nih.gov/Health_Info/Scoliosis/default.asp)	19
Figure 1-5 : Schematic representation of Spondylolisthesis and Spondylolysis (obtained on 22 June 2011 from http://orthoinfo.aaos.org/topic.cfm?topic=a00053)	20
Figure 1-6 : Representation of tibia vara (obtained on 3 November 2010 from http://knee-replacement-india.blogspot.com/2010/06/tibia-vara-causing-oa-knee.html)	21
Figure 1-7 : Representation of genu varum and valgum (obtained on 8 September 2010 from http://sports.jrank.org/pages/8251/genu-valgum.html)	21
Figure 1-8 : Screws and ligaments inserted at different levels between vertebral bodies (Newton et al., 2005).....	22
Figure 1-9 : Staples implanted at different levels between vertebral bodies: left panel (Wall et al., 2005) and right panel (Guille et al., 2007).	23
Figure 1-10 : (left) Staple inserted in on proximal tibial growth plate to correct idiopathic genu valgum (Courvoisier et al., 2009), (right) screw and plate (eight-plate) inserted on the distal femoral and proximal tibial growth plates (obtained on 22 June 2011 from http://www.eight-plate.com/glossary.php).	24
Figure 1-11 : Creep schematic.	30
Figure 1-12 : Stress relaxation schematic.	31

Figure 1-13 : Controlled ramp displacement applied on a cartilaginous tissue and the stress- relation response in the uniaxial compression experiment, adapted from (Mow et al., 2005).	32
Figure 1-14 : Schematic representation of confined uniaxial compression of cartilaginous tissue.	33
Figure 1-15 : Schematic representation of unconfined uniaxial compression of cartilaginous tissue.	34
Figure 1-16 : Schematic representation of indentation of cartilaginous tissue.	35
Figure 1-17 : Schematic representation of confocal microscope light path (dash lines show the out-of-focus light and simple lines represent the in-focus light).	45
Figure 1-18 : Simplified light path of confocal microscope.	46
Figure 3-1 : (Right) Porcine ulnar growth plate shown as a light purple line at the physis/bone junction (inside the rectangular box). (Left) Histological section of the growth plate showing its three zones: reserve (R), proliferative (P), and hypertrophic (H).	59
Figure 3-2 : (A) Growth plate location on the porcine radius-ulna complex. (B) Punching of the ulna perpendicular to the growth plate/bone junction for recovery of the 4 mm diameter sample. (C) Recovered growth plate sample. (D) Growth plate semicylindrical samples cut parallel to the sample longitudinal axis.	62
Figure 3-3 : Calcein AM concentration and cellular viability. (A) Confocal section of growth plate chondrocytes loaded with 0.5 mM Calcein AM and 1 mM EthD-1 and showing very good cell viability (B) Confocal section of growth plate chondrocytes loaded with 5 mM Calcein AM and 1 mM EthD-1 and showing decreased cellular viability, as confirmed with EthD-1 taken up by the chondrocytes.	64
Figure 3-4 : Projected three-dimensional image of Calcein AM loaded <i>in situ</i> growth plate chondrocytes obtained from a four-week old porcine distal ulna (10×).	66
Figure 3-5 : Chondrocyte shape and size showed zonal heterogeneity in growth plate. The morphology of the chondrocyte was determined from the surface of the cell cytoplasm.	

- Chondrocytes are aligned along the growth direction except the cell marked by *, which is perpendicular to growth direction.67
- Figure 3-6 : Cell level morphometrical parameters: (A) chondrocytes volume, (B) chondrocytes surface volume, (C) chondrocytes minor radius, (D) chondrocytes major radius, (E) chondrocytes sphericity and tissue level morphometrical parameter (F) cell/matrix volume ratio evaluated in 4-week old swine growth plates (mean values \pm standard deviations). Significant differences among the three histological zones are shown with thick connecting lines (—) and significant differences between two histological zones are shown with thin connecting lines (—). (cell level morphological parameters: *p-value \leq 0.05, tissue level parameter: **p-value \leq 0.001).69
- Figure 4-1 : (Right) Typical confocal section of a fluorescently labelled porcine growth plate showing its three histological zones: reserve (R), proliferative (P) and hypertrophic (H). (Left) Growth plate cylindrical plug extracted using a 6 mm biopsy punch. (Center) The growth plate site is located between the metaphysis and secondary ossification center of the epiphysis.....82
- Figure 4-2 : Experimental set up: (A) custom-made loading apparatus mounted on the stage of an inverted laser scanning confocal microscope (B) Schematic of the loading apparatus.83
- Figure 4-3 : Typical experimental stress relaxation curves of growth plate samples undergoing semi-confined compression at 5% pre-strain (A) followed by 10% strain (B) at a strain rate of $1.7\text{E-}3\text{ s}^{-1}$85
- Figure 4-4 : Typical three-dimensional reconstructed chondrocytes in each histological zone before compression (intact) and after compression and relaxation.....86
- Figure 4-5 : Morphometrical changes at cellular level ((a) volume, (b) surface area, (c) minor radius, (d) major radius and (e) sphericity) and tissue level ((f) cell/matrix volume ratio) in response to 15% uniform tissue compression. Significant differences between pre-compression and post-relaxation parameters are shown with asterisks (p-value \leq 0.05).89
- Figure 5-1 : (A) Growth plate site located between the metaphysis and secondary ossification center of the epiphysis, where the longitudinal growth occurs. (B) Typical confocal section of a swine growth plate fluorescently labeled using Syto-17 showing the three histological

zones: reserve zone (RZ), proliferative zone (PZ) and hypertrophic zone (HZ). (C) Growth plate cylindrical sample extracted using a 6 mm biopsy punch perpendicular to the growth plate/bone junction.102

Figure 5-2 : (A) Experimental set-up consisting of a custom-made loading apparatus mounted on the stage of an inverted laser scanning confocal microscope. (B) Growth plate semi-cylindrical sample being sandwiched between the two platens of the loading apparatus in a bath of HBSS. (C) Schematic of the experimental set-up.103

Figure 5-3 : Image correlation results for a swine ulnar growth plate sample (GP#4) undergoing 10% uniaxial compressive strain between initial and final images: (A) initial 512×512 confocal image (before loading); (B) final 512×512 confocal image (after loading and relaxation); (C) region of interest (ROI) covering three histological zones of growth plate, which was cropped out from the final image and used in DIC algorithm; (D) calculated strain map along loading direction (ϵ_{yy}); (E) calculated strain map perpendicularly to the loading direction (ϵ_{xx}).109

Figure 5-4 : Variations in strain developed across swine growth plates under 10% uniform compressive strain, normalized to growth plate zone thicknesses. The strains were averaged on a pixel by pixel basis to compute the “average” strains in each histological zone. Each point on each curve represents an average of ϵ_{yy} distributions as observed along the x axis (perpendicular to loading direction) of the imaged growth plates. Each curve stands for the average of strain distribution along the y axis (in loading direction). 0-1, 1-2, and 2-3 on the abscissa represent the reserve zone, the proliferative zone, and the hypertrophic zone, respectively.110

Figure 5-5 : Biochemical composition of the three histological zones of 4-week old swine growth plates. Significant differences between the histological zones are shown with connecting lines (*p-value \leq 0.05 and **p-value \leq 0.005).113

Figure 5-6 : A typical presentation of collagen orientation in birefringent swine growth plate at (a) 45°, (b) 90° and (c) 135° relative to the analyzer. At 45° vertically oriented collagen network is present in the proliferative and hypertrophic zones. At 135°, a mainly horizontally oriented collagen network is present in RZ. Panel (d) shows an adjacent section stained with Safranin-O/Fast-Green, with the histological zones as indicated (RZ: reserve

zone, PZ: proliferative zone, HZ: hypertrophic zone, and MB: metaphyseal bone. The analyzer direction (A) is marked on the panel (a). All angles are relative to the analyzer filter. The scale bar is 250 μ m.....	114
Figure 6-1 : Frequency distribution of chondrocytes volume within the three different zones of porcine growth plate. Polynomial curves were fitted to the data.	126
Figure 6-2 : Superposition of 2D confocal images of chondrocytes labeled with Calcein AM and Ethidium homodimer-1 through the growth plate thickness.	127
Figure 6-3 : Changes in chondrocytes volume within three histological zones of growth plate with two repeated confocal scans.	129
Figure 6-4 : Typical experimental stress relaxation curve of growth plate samples undergoing a two-step semi-confined compression	131

LIST OF ABBREVIATIONS

ADAMTS	Aggrecanases, adamalysin-thrombospondins
ANOVA	analysis of variance
CO ₂	Carbone dioxyde
DIC	Digital image correlation
DMMB	1,9-dimethylmethylene blue
ECM	Extracellular matrix
FGFs	Fibroblast growth factors
GAG	Glycosaminoglycan
GH	Growth hormone
HBSS	Hank's balanced salt solution
HZ	Hypertrophic zone
IGF-I, II	Insulin-like growth factor –I and –II
IGFs	Insulin-like growth factor
IHC	Immunohistochemistry
MMP	Metalloproteinases
O ₂	Oxygene
OH-Pro	Hydroxyproline
PLM	Polarized light microscopy
PG	Proteoglycan
PZ	Proliferative zone
RA	Retinoic acid
ROI	Region of interest
RZ	Rezerve zone

S-GAG	Sulfated glycosaminoglycan
TGFβs	Transforming growth factor
VEGF	Vascular endothelial growth factor

INTRODUCTION

The longitudinal growth of bones is synchronized by hormones, genetics, nutrition, and mechanical factors, which regulate the normal development of bones (Ballock & O'Keefe, 2003b; Bonnel, Dimeglio, Baldet, & Rabischong, 1984; LeVeau & Bernhardt, 1984; I. A. Stokes, Mente, Iatridis, Farnum, & Aronsson, 2002). It has been clinically shown that mechanical loads are essential for normal growth. However, when excessive, these loads are involved in the progression of musculoskeletal deformities such as adolescent idiopathic scoliosis, neuromuscular disease, spondylolisthesis, the genu varum/valgum, tibia vara and other deformities (Bonnel et al., 1984; Frost, 1990; LeVeau & Bernhardt, 1984), through a phenomenon called the mechanical modulation of bone growth. The mechanical modulation of bone growth is also of growing interest in the development and improvement of minimally invasive approaches aiming to exploit local modulation of growth to correct the deformities while preserving the natural growth of bone as well as the functions and mobility of the bone segments.

Growth plates are the site of the longitudinal bone growth, which occurs through a process of interstitial expansion and endochondral ossification of growth plate cartilage. These cartilaginous disks at the ends of long bones and vertebrae are responsible for bone growth until complete ossification of the growth plate at maturity (C. E. Farnum & N. J. Wilsman, 1998; Fujii et al., 2000; LeVeau & Bernhardt, 1984). The shape, size and arrangement of the constitutive cells of the growth plate, the chondrocytes, as well as biochemical composition of the extracellular matrix define three distinct morphological zones: the reserve zone, the proliferative zone and the hypertrophic zone (Breur, VanEnkevort, Farnum, & Wilsman, 1991; Buckwalter et al., 1985). Differentiation and hypertrophy of chondrocytes are the result of a complex spatio-temporal process that occurs through these three histological zones, where the columns of chondrocytes are bone growth functional units (Alvarez et al., 2000; Hunziker & Schenk, 1989).

Growth plate extracellular matrix is composed of water, large aggregating proteoglycans embedded within type II collagen fibrils as well as short chain type X collagen, exclusively in the hypertrophic zone, which all provide the growth plate with its mechanical stiffness (Mwale, Tchetina, Wu, & Poole, 2002) and functions such as promoting/synchronizing the cell differentiation. Type II collagen, one of the major extracellular components of growth plate, forms a highly organized fibrillar network, which is believed to be a critical determinant of tissue

biomechanical competence (Speer, 1982). This collagen network has the ability to entrap large, hydrophilic proteoglycan molecules.

The mechanisms by which growth plate chondrocytes modulate longitudinal bone growth are still not well understood. Hypertrophy (changes in cell volume and height), proliferation of chondrocytes as well as matrix synthesis have been identified as the most important factors in both normal and mechanically modulated growth of long bones (Ballock & O'Keefe, 2003a; I. A. Stokes, Clark, Farnum, & Aronsson, 2007; I. A. Stokes et al., 2002; Villemure & Stokes, 2009; Wilsman, Farnum, Green, Lieferman, & Clayton, 1996; Wilsman, Farnum, Lieferman, Fry, & Barreto, 1996). Furthermore, one of the important mechanisms through which chondrocytes may respond to changes in their environment in both normal and mechanically modulated growth is directly through deformation of the cellular membrane. However, *in situ* three-dimensional visualization and zonal characterization of growth plate morphometry at both cellular and tissue levels have not been documented yet.

The growth plate mechanobiology, i.e. the effect of mechanical stimuli on the tissue biological responses, was studied *in vivo* in different animal models (Alberty, Peltonen, & Ritsila, 1993; Apte & Kenwright, 1994; Farnum et al., 2000; I. A. Stokes, Aronsson, Dimock, Cortright, & Beck, 2006; I. A. Stokes et al., 2002). There is convincing evidence that static forces alter the longitudinal bone growth, increased pressure on the growth plates retards growth and a reduced pressure accelerates it (Bonnell et al., 1984; I. A. Stokes et al., 2006). Many authors refer to this phenomenon by designating the Hueter-Volkmann law. Different approaches have been used to interpret the role of compressive loading in regulating growth plate and chondrocytes activity ranging from studies at the tissue and extracellular level to experiments at the cell level (Bachrach, 1995; Cohen, Chorney, Phillips, Dick, & Mow, 1994; Cohen, Lai, & Mow, 1998; Radhakrishnan, Lewis, & Mao, 2004; Sergerie, Lacoursiere, Levesque, & Villemure, 2009; Villemure, Cloutier, Matyas, & Duncan, 2007; Wosu, Sergerie, Levesque, & Villemure, 2011). However, up to date, no study has comprehensively analyzed the zonal growth plate compressive mechanical behavior at cellular and tissue levels with respect to the biochemical composition and type II fibrillar collagen organization of growth plates.

The main objective of the present research project was to characterize histomorphological (cell and tissue morphology) and structural (biochemical composition, fibrillar collagen organization)

characteristics as well as mechanical behaviour (in terms of developed strains) of growth plate at cellular and tissue levels in its three distinct histological zones. To do this, different techniques such as confocal microscopy combined with fluorescent labelling, polarized microscopy, digital image correlation, and biochemical assays have been used.

General organization of the thesis

This dissertation includes six chapters and is submitted as a "thesis by articles". The first chapter includes a literature review required to achieve a sufficient understanding of the issues and methods used in this research project. The topics covered are the anatomy and basic physiology of growth plates, the mechanical modulation of growth and associated pathologies, the state of knowledge on mechanobiology of the growth plate and the state of knowledge on the mechanical behaviour of growth plate tissue. Finally, confocal microscopy and polarized light microscopy concepts were described as the techniques which were used in the present project.

The second chapter describes the hypotheses and clarifies the objectives of the research project including the methodological framework. The body of this doctoral thesis is composed of three principal articles presented in Chapters 3 to 5. Chapter 3 presents the first article entitled: “*Three-dimensional in situ zonal morphology of viable growth plate chondrocytes: a confocal microscopy study*” which was published in Journal of Orthopaedic Research. This scientific article addresses the three-dimensional zonal morphology of viable growth plate at cellular and tissue levels and presents a confocal microscopy approach combined with fluorescent labeling of the tissue. This chapter answers the first objective of this research project. The fourth chapter includes the second scientific article entitled: “*Tissue and Cellular Morphological Changes in Growth Plate Explants under Compression*” which was published in Journal of Biomechanics. This study addresses three-dimensional deformations of chondrocytes and growth plate tissue in all histological zones of growth plates under compression using stress relaxation tests. This chapter answers the first step of the second objective of the research project. The fifth chapter presents the last article entitled “*Stress relaxation of swine growth plate in semi-confined compression: depth dependant tissue deformational behavior versus extracellular matrix composition and collagen fiber organization*” which revision was recently submitted to Biomechanics and Modeling in Mechanobiology. The growth plate mechanical behaviour evaluated using the digital image correlation (DIC) technique as well as corresponding biochemical

composition and collagen fiber orientation in its three functionally distinct zones are presented in this chapter. This chapter deals with the second step of the second objective as well as the third, fourth and fifth objectives of this thesis. The final chapter (Chapter 6) contains a general discussion on the research project followed by a conclusion and recommendations for future related projects.

CHAPTER 1 BACKGROUND AND REVIEW OF THE LITTERATURE

1.1 Longitudinal bone growth and growth plate

1.1.1 Longitudinal bone growth

The longitudinal growth of long bones and vertebrae occurs through the process of endochondral ossification, i.e. through the synthesis of a cartilaginous growth plate, which then transforms into bone. Although in humans the growth rate decreases until skeletal maturity at around 18-20 years, periods of accelerated growth are observed in childhood and adolescence. The closure of the growth plate marks the completion of longitudinal growth, usually in late adolescence (Villemure & Stokes, 2009).

1.1.2 Endochondral bone growth

Ossification is always done through another tissue whether fibrous connective tissue or cartilaginous tissue. The ossification taking place primarily through a fibrous connective tissue is called intramembranous ossification, whereas the ossification through a hyaline cartilage is called endochondral ossification. Figure 1-1 illustrates the process of endochondral ossification of long bones, also referred to as longitudinal bone growth.

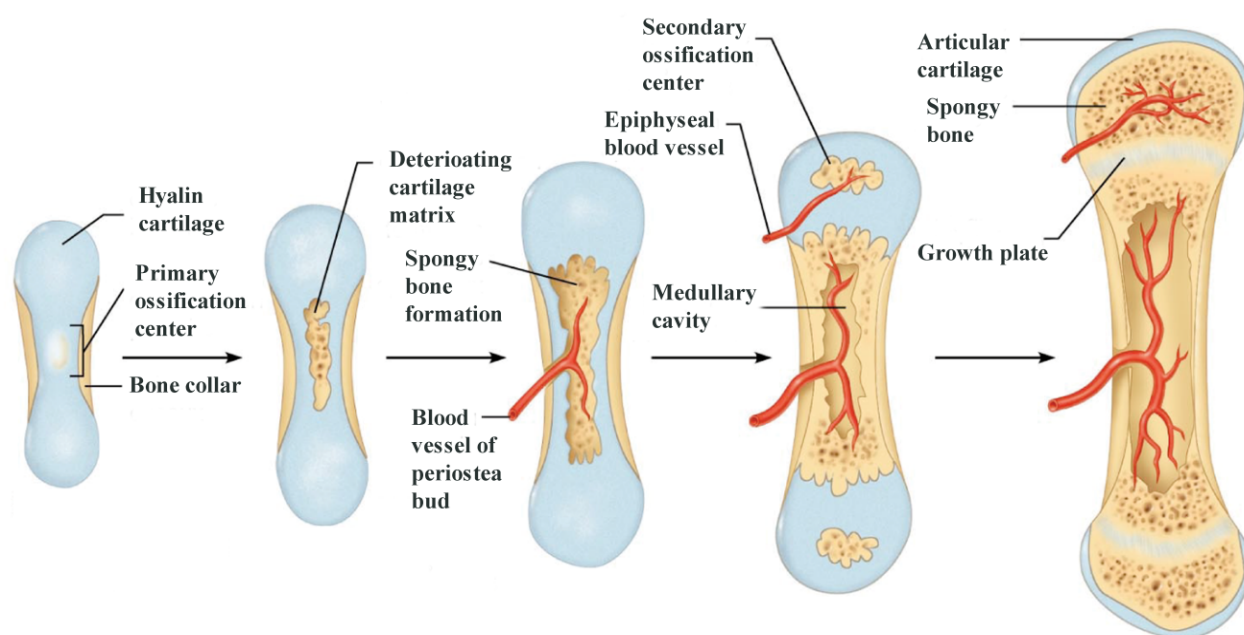


Figure 1-1 : Endochondral ossification process in long bones, adapted from Marieb et al. (2006).

Longitudinal bone growth is the result of a complex spatio-temporal process, which operates through three zones of the cartilaginous growth plate (the reserve, the proliferative, and the hypertrophic (Figure1-2)), where the columns of chondrocytes are the functional units of longitudinal growth of long bones (Alvarez et al., 2000; Hunziker & Schenk, 1989).

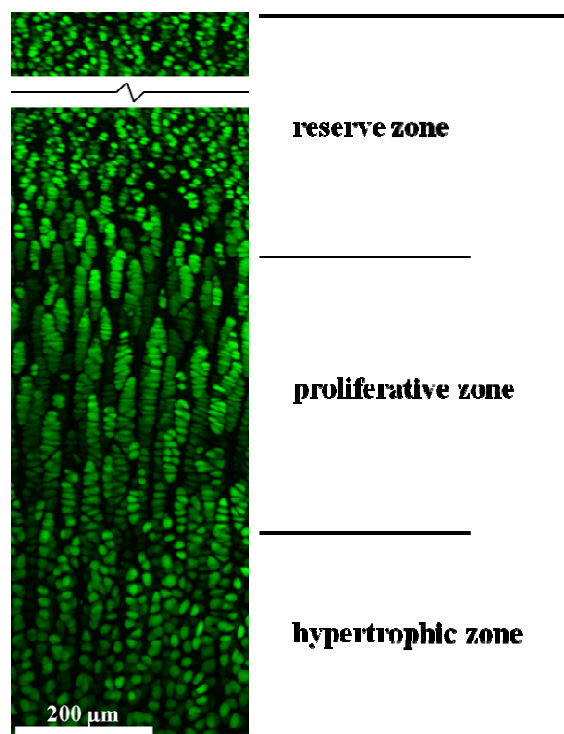


Figure 1-2 : A typical confocal section of porcine growth plate (chondrocytes cytoplasm labeled using Calcein-AM) showing its ultrastructure and three histological zones.

In the growth plate, chondrocytes proliferate, hypertrophy, synthesize extracellular matrix and die. This process of interstitial growth takes place in conjunction with chondrocytes of the same column and in a particular, synchronized and predefined order (Farnum & Wilsman, 1993; Hunziker & Schenk, 1989). Chondrocytes are constantly dividing and piled in front of the epiphysis pushing older cells toward the diaphysis. While chondrocytes degenerate at the chondro-osseous junction, osteoblasts ossify them to form new bone tissue. This phenomenon is called endochondral ossification.

Proliferation and hypertrophy of chondrocytes (Breur et al., 1991; Buckwalter et al., 1985; Buckwalter, Mower, Ungar, Schaeffer, & Ginsberg, 1986; Hunziker & Schenk, 1989; Wilsman, Farnum, Green, et al., 1996; Wilsman, Farnum, Leiferman, et al., 1996) play a major role in the process of longitudinal growth. Synthesis and degradation of the extracellular matrix are also key

elements in longitudinal growth of long bones (Alvarez et al., 2000; Breur et al., 1991; Buckwalter et al., 1986; Cowell, Hunziker, & Rosenberg, 1987; Hunziker, 1994; Hunziker & Schenk, 1989; Wilsman, Farnum, Leiferman, et al., 1996). Indeed, the matrix remodeling can regulate cell shape and volume, and is hence involved in the spatio-temporal sequence of proliferation, hypertrophy and chondrocytes migration (Alvarez et al., 2000). The relative contribution of proliferative and hypertrophic zones in the daily elongation of bones is shown in Figure 1-3 for four different bones from rats (Wilsman, Farnum, Leiferman, et al., 1996).

Overall, Wilsman et al. (Wilsman, Farnum, Leiferman, et al., 1996) showed that the largest contribution to the daily growth in all bones came from cellular hypertrophy (40-60%) and extracellular matrix synthesis in the hypertrophic zone (15-30%), which together represents almost 75% of the total contribution. Matrix synthesis in the proliferative zone (15-20%) and especially chondrocyte proliferation (10%) had a minimal, although significant influence on longitudinal growth, concluding that hypertrophy remains the most important factor for longitudinal growth.

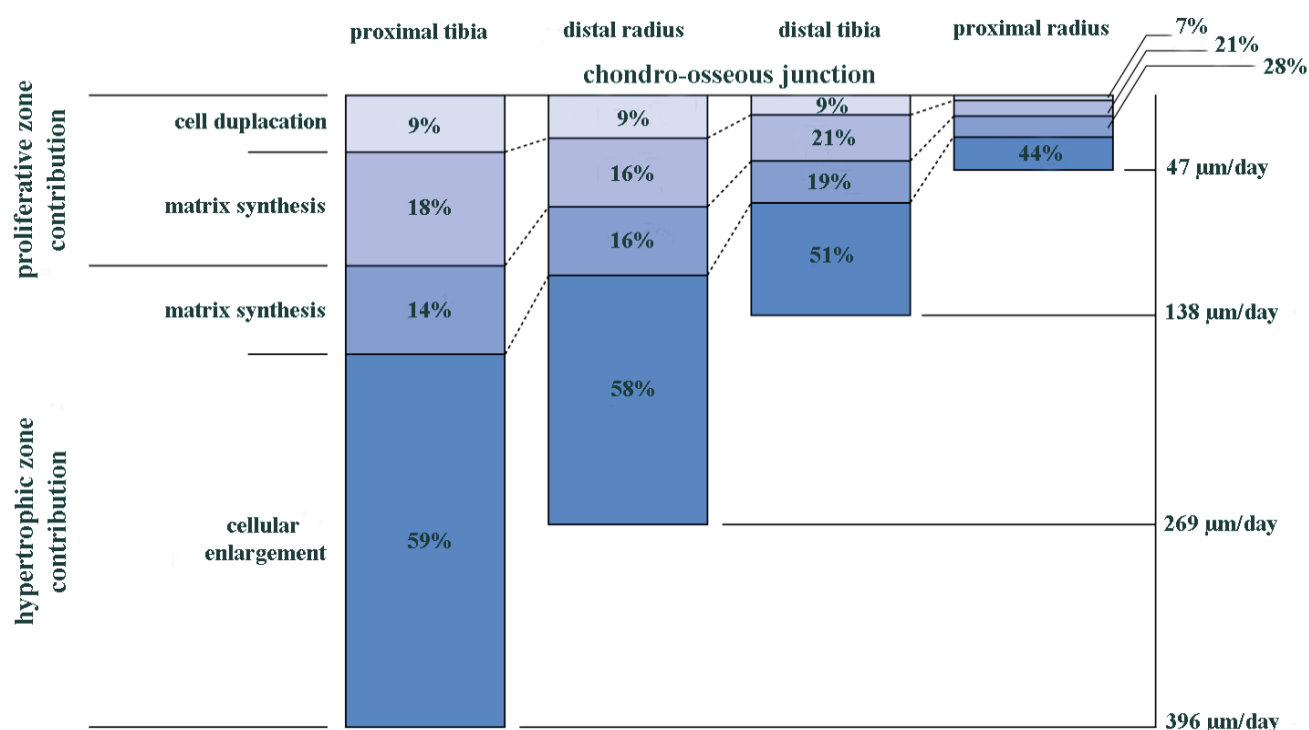


Figure 1-3 : Relative contribution of proliferative and hypertrophic zones in daily longitudinal growth of four different bone types from 28-day old rats at the chondro-osseous junction, adapted from Wilsman et al. (1996).

1.1.2.1 Biological regulation of bone growth

Biological mechanisms involved in the growth process are regulated by various factors including:

- ☑ Systemic hormones including growth hormone GH (Isaksson, Jansson, & Gause, 1982; Russell & Spencer, 1985; Thorngren & Hansson, 1974; Wit, Kamp, & Rikken, 1996), , IGF-I (insulin-like growth factor I) (Baker, Liu, Robertson, & Efstratiadis, 1993; Schoenle, Zapf, Humbel, & Froesch, 1982), thyroid hormones T3 and T4 (Bassett, Swinhoe, Chassande, Samarut, & Williams, 2006; Leger & Czernichow, 1989) and androgenic steroids during puberty and estrogens (Cassorla et al., 1984; Coxam et al., 1996; Cutler, 1997; Takano, Aizawa, Irie, Kokubun, & Itoi, 2007; Zung et al., 1999). They are necessary to allow bone to grow at the same pace on the left and right sides of the body (Rauch, 2005);
- ☑ PTHrP protein (parathyroidhormone-related protein), which plays an important role in endochondral ossification by increasing the synthesis of extracellular matrix in the growth plates. The expression of PTHrP protein is also influenced by mechanical loads (Tanaka et al., 2005).
- ☑ Growth factors are polypeptides known to affect growth and cell differentiation in bone and cartilage. There are several main types of growth factors: IGFs (insulin-like growth factors) and TGFβs (transforming growth factors) (Zerath et al., 1997) The FGFs (fibroblast growth factors) (Hutchison, Bassett, & White, 2007) and VEGF (vascular endothelial growth factor) (van der Eerden, Karperien, & Wit, 2003) are also involved in the regulation of longitudinal bone growth. Finally, it has also been shown that RA (retinoic acid) is associated with chondrocyte maturation during endochondral ossification (Iwamoto et al., 1993; W. Wang & Kirsch, 2002).
- ☑ Transmembrane proteins, such as the integrins, which allow communication between cells and matrix (Egerbacher & Haeusler, 2003; Hausler, Helmreich, Marlovits, & Egerbacher, 2002);
- ☑ The nutrients (Hunziker, 1994).
- ☑ Genetic factors (Hunziker, 1994; Hunziker & Schenk, 1989)

Certain biological factors influence the production of various matrix components which are important for growth and remodeling. Indeed, it has been shown that IGF-I (Demarquay et al., 1990; Wroblewski & Edwall-Arvidsson, 1995), TGF- β 1 (Ballock et al., 1993; Thorp, Anderson, & Jakowlew, 1992) and GH (Monson, Halevy, Gertler, Hurwitz, & Pines, 1995) stimulate the expression of type II collagen. The expression of this same component is however inhibited by bFGF (Wroblewski & Edwall-Arvidsson, 1995) and by retinoic acid (Yoshida et al., 2001). IGF-I and IGF-II as well as retinoic acid stimulate the expression of collagen type X (Yoshida et al., 2001). The expression of collagen type X is inhibited by TGF- β 1 (Ballock et al., 1993) and PTHrP (O'Keefe et al., 1997). The expression of proteoglycans is also stimulated by IGF-I and IGF-II (Leach, Richards, Praul, Ford, & McMurtry, 2007), however, it is inhibited by retinoic acid (Yoshida et al., 2001) and bFGF (Makower, Wroblewski, & Pawlowski, 1988). It should be noted that extracellular matrix components are also influenced by the enzymes, particularly metalloproteinases (or MMPs) and aggrecanases (Abbaszade et al., 1999; Keeling & Herrera, 2008; M. D. Tortorella et al., 1999).

1.1.2.2 Environmental regulation of bone growth

In addition to biological factors already mentioned such as hormones, growth factors, nutrients and genetic factors, the mechanical environment also affects the behavior of the growth plate. The mechanical environment is a very important factor of influence on the functioning of the growth plate; however, its role in growth is not yet clearly defined (Arriola, Forriol, & Canadell, 2001; Farnum et al., 2000; Niehoff, Kersting, Zaucke, Morlock, & Bruggemann, 2004; Ohashi, Robling, Burr, & Turner, 2002; I. A. Stokes, 2002; I. A. Stokes et al., 2006; I. A. Stokes et al., 2007; I. A. Stokes, Gwadera, Dimock, Farnum, & Aronsson, 2005). The known effects of mechanical loading on the growth process is presented in section 1.2. Vascularization of the growth plate is also a significant factor in the growth regulation (Trueta & Trias, 1961). It is generally accepted that growth plate is vascularized during early childhood, even if this theory does not reach consensus (Jaramillo et al., 2004; Wirth et al., 2002). In the subsequent growth, growth plate regulatory elements like growth factors and systemic hormones come from three vascularization systems: that of the metaphyseal junction, of the epiphyseal junction, and of the perichondrium (Trueta & Trias, 1961; Williams, Zipfel, Tinsley, & Farnum, 2007; Wirth et al., 2002). The transport of molecules from the epiphyseal and metaphyseal junctions is done partly

by diffusion and partly by convection (Williams et al., 2007). To allow convection, a pressure gradient is therefore required between the bone and growth plate cartilage. That is the reason why the mechanical loading of the growth plate could interfere with this transport. A suppression of the first vascularization system (metaphyseal junction) seems to induce a thickening of proliferative and hypertrophic zones of growth plate and an abnormal endochondral ossification (Trueta & Little, 1960). The chondrocytes terminal differentiation was disrupted and led to accumulation of chondrocytes instead of disappearing (Trueta & Trias, 1961). Suppression in the second vascularization system (epiphyseal junction) seems to induce a large cellular disorganization and disruption in chondrocytes proliferation (Brashear, 1963; Trueta & Little, 1960; Trueta & Trias, 1961).

1.1.3 Growth plate form and site

Growth plates are cartilaginous discs at the ends of long bones and vertebrae. In the long bones, they are located between the epiphysis and the metaphysis, whereas in human vertebrae, where there is no epiphysis, they are located between the intervertebral disc and the vertebral body. There are also growth plates in the posterior parts of the vertebrae, called the neurocentral junctions. The following sections describe the structure and function of the growth plate and its respective zones, as well as their composition.

1.1.4 Growth plate composition

1.1.4.1 Chondrocytes

Chondrocytes are the constitutive cells that are found specifically in cartilage. Their main function is the synthesis and degradation of the extracellular matrix components, i.e. collagens and proteoglycans, as well as the secretion of enzymes that degrade these components (Mow, Gu, & Chen, 2005; Mow & Hung, 2001). The shape and arrangement of chondrocytes in the growth plate differ from one zone to another (Ballock & O'Keefe, 2003b; Bonnel et al., 1984; Buckwalter et al., 1985; C. E. Farnum & N. J. Wilsman, 1998).

1.1.4.2 Extracellular matrix

The extracellular matrix consists of a network of collagen fibrils embedded in a complex, highly hydrated proteoglycans and hyaluronic acid aggregate whose concentrations vary from one

histological zone to another (Alvarez et al., 2000; Poole, Matsui, Hinek, & Lee, 1989; Sandell, Sugai, & Trippel, 1994).

Collagen

Collagen, the most common protein in the human body, is the main structural component of the growth plate extracellular matrix. Collagen is formed by the polymerization of five tropocollagen into fibrils, a molecule composed of three alpha chains arranged in a helix (Mow & Hung, 2001; Ratcliffe & Mow, 1996). Collagen forms small fibrils with an architectural arrangement that varies through the hyaline cartilage depth. For example, in articular cartilage, collagen fibrils are organized in parallel to the articular surface in the superficial zone while they are randomly oriented in the middle zone and are perpendicular to the articular surface in the deep zone. Such a structure gives the cartilage the ability to withstand loads in tension, and retain glucosaminoglycans (GAG) into a coherent wholesome. This structure also provides a permeability effect producing a frictional drag of the fluid, which provides the extracellular matrix the ability to withstand compression. Although several types of collagen exist, hyaline cartilage contains types II, IX, X and XI, and of these, the concentration of type II collagen is the highest, except in the hypertrophic zone. This high concentration in the reserve and proliferative zones helps the prevention of premature calcification and efficient distribution of loads (Mow & Hung, 2001; Niehoff et al., 2004; Radhakrishnan et al., 2004; Ratcliffe & Mow, 1996). Type IX collagen is also a fibrillar collagen. It is still composed of three α chains, but also a proteoglycan glycosaminoglycan chain which is covalently bound to its α chains (Bruckner, Vaughan, & Winterhalter, 1985; van der Rest & Mayne, 1988). It is covalently bound to the fiber surface of type II collagen (Diab, Wu, & Eyre, 1996; Eyre, Apon, Wu, Ericsson, & Walsh, 1987; Ruggiero et al., 1993; van der Rest & Mayne, 1988). It is highly expressed in the growth plate (Ballock & O'Keefe, 2003a), although in much smaller amounts than type II collagen (Balmain et al., 1995). Ballock et al. (Ballock & O'Keefe, 2003a) postulated that collagen type IX allows type II collagen to interact with other components of the extracellular matrix and is also likely to participate in growth control and thickness of type II collagen fibers (Balmain et al., 1995). Type XI collagen is another fibrillar collagen of the extracellular matrix and is composed of three α chains (Francomano, 1995; Suttmoller, Bruijn, & de Heer, 1997). It is linked to type II collagen by structural links (Pihlajamäki et al., 1999; Ruggiero et al., 1993; Sandell et al., 1994). Although it is less important than type II collagen (Balmain et al., 1995; Sandell et al., 1994), it is also

highly expressed in the growth plate (Ballock & O'Keefe, 2003a). Similar to type IX collagen, it plays a role in controlling growth and fiber thickness of type II collagen (Balmain et al., 1995). Type X collagen, a nonfibrillar collagen which consists of three identical $\alpha 1$ chains but shorter than those of other types of collagen (Sutmuller et al., 1997), is found only in the hypertrophic zone of growth plates and serves to facilitate the calcification of the extracellular matrix (Poole et al., 1989; Sutmuller et al., 1997) and to maintain its structure to compensate for other collagen types (Burdan et al., 2009; Mwale et al., 2002). Furthermore, Anderson (1995) reported rather a structural role and support for type X collagen in the extracellular matrix of growth plate.

Proteoglycan

Proteoglycans are polysaccharides composed of a long core protein linked to chains of glycosaminoglycans. The aggrecan, a gigantic assembly of proteoglycans, which is formed of at least 100 molecules of chondroitin sulfate and keratan sulfate (Sandell et al., 1994), is one of the most abundant proteins in hyaline cartilage. In combination with collagen, it serves to retain the interstitial fluid in cartilage, and thus to provide the osmotic pressure necessary for the compressive strength of cartilage tissue (Ballock & O'Keefe, 2003b; Mow & Hung, 2001; Radhakrishnan et al., 2004; Ratcliffe & Mow, 1996). It is now well accepted that proteoglycan aggregation promotes immobility of the proteoglycans within the collagen network, adding stability and rigidity to the extracellular matrix of cartilaginous tissue (Mow et al., 1989). Proteoglycans (aggrecan, but also versicane, decorin, biglycan, fibromodulin, lumican of the glypican, chondroitin and agrin (Ballock & O'Keefe, 2003a; Hausser, Ruegg, Brenner, & Ksiazek, 2007; Radhakrishnan et al., 2004; van der Eerden et al., 2003)) are found in different proportions depending on the histological zone (Radhakrishnan et al., 2004). In particular, decorin covers the collagen fibers (Ballock & O'Keefe, 2003a). Agrin appears to play an important role in bone growth; mice lacking the producing gene presented decreased growth and less type II collagen and aggrecan in the extracellular matrix of their growth plates (Hausser et al., 2007).

Water

Water is the most abundant component of the hyaline cartilage. It is responsible for the transport of gases, nutrients and waste product between chondrocytes and the surrounding matrix through

fluid exchanges. It is also responsible for controlling the mechanical behavior under load due to its movement within the tissue (Mow & Hung, 2001; Ratcliffe & Mow, 1996).

Matrix Metalloproteinase

Matrix Metalloproteinases (MMPs) are proteolytic enzymes that contribute to matrix remodeling. There are four subgroups of metalloproteinases: collagenases, gelatinases, stromelysins and membrane type metalloproteinases (Takahashi, Onodera, Bae, Mitani, & Sasano, 2005). The collagenases are capable of breaking the peptide bonds of collagen. There are three types of MMPs in human growth plate: MMP1 or collagenase 1, MMP8 or collagenase 2 and MMP13 or collagenase 3. The MMP13 (or collagenase 3) is a protease involved in the degradation of type II and type X collagen as well as the degradation of aggrecan and other proteoglycans (Knauper et al., 1996; Mitchell et al., 1996). MMP13 also contributes to extracellular matrix remodeling during endochondral ossification (Stickens et al., 2004). Of the stromelysins, MMP3 is also a degrader of type II and type X collagen, which also degrades collagen type IX and XI (Keeling & Herrera, 2008). Other MMPs have been investigated, such as MMP-2, MMP-9, MMP-10, MMP-11 and MMP-14. MMP-2 and MMP-9 are gelatinases (Takahashi et al., 2005), MMP-2 degrades denatured type II collagen (Patterson, Atkinson, Knauper, & Murphy, 2001), and both have a role in activation of other MMPs at least *in vitro* (Haeusler, Walter, Helmreich, & Egerbacher, 2005). MMP-14 is a membrane-type metalloproteinase capable of degrading type II collagen and aggrecan and has been detected in humans in all areas of the growth plate (Haeusler et al., 2005).

Aggrecanase

The aggrecanase proteolytic enzymes are members of the ADAMTS family of proteins (a disintegrin and metalloproteinase with thrombospondin motifs). The aggrecanase degrades proteoglycans, and more specifically aggrecan. ADAMTS-4 (or aggrecanase I) degrades aggrecan and versicane while ADAMTS-5 (or aggrecanase II) degrades aggrecan (Abbaszade et al., 1999; M. Tortorella et al., 2000).

1.1.4.3 Structural and physical interaction among growth plate components

The interaction between collagen, proteoglycan and water is believed to have an important role in regulating the structural organization of hyaline cartilage (Mow & Hung, 2001). The structure and physical interactions of proteoglycans aggregates is believed to influence the properties of the extracellular matrix of hyaline cartilage (Ratcliffe & Mow, 1996). The closely spaced sulfate

and carboxyl groups fixed along the proteoglycan chains leave a high concentration of fixed negative charges in solution at physiological pH (Donnan osmotic pressure) (Mow & Hung, 2001). This charge-charge repulsive force is likely to extend the proteoglycans into the fibrillar collagen network, structurally. To maintain electroneutrality, the fixed negative charges attract counter- and co-ions into the tissue, giving rise to a swelling pressure given by Donnan osmotic pressure. This swelling pressure would be balanced by subjecting the collagen network to a pre-stress of a significant magnitude, confining the proteoglycans to 20% of their free solution volume (Mow & Hung, 2001; Mow & Ratcliffe, 1997; Setton, Gu, Lai, & Mow, 1995).

As stated by Mow et al. (2005), when an external compressive force is applied to the cartilaginous tissue, an instantaneous deformation is caused which is primarily controlled by the change in the proteoglycans molecular volume. This external force causes internal pressure in the extracellular matrix to exceed the swelling pressure which leads to flowing of the interstitial water out of the tissue. This will increase the proteoglycans concentration within the tissue which will in turn increase the Donnan osmotic pressure (charge-charge repulsive force) and bulk compressive stress until they come to equilibrium with the external force. In this manner, Mow et al. concluded that the ability of proteoglycans to resist compression arises from two mechanisms: (a) the Donnan osmotic swelling pressure associated with fixed anionic groups on the glycosaminoglycans and (b) the bulk compressive stiffness of the collagen-proteoglycan matrix.

1.1.5 Growth plate ultrastructure and function

Growth plates are responsible for the longitudinal growth of bones, a process that continues until the closure of the growth plate at skeletal maturity (Ballock & O'Keefe, 2003b; Bonnel, et al., 1984; Rauch, 2005; van der Eerden, et al., 2003). As already stated, it is histologically composed of three structurally distinct zones the reserve zone, the proliferative zone and the hypertrophic zone (Figure 1-2) (Breur et al., 1991; Buckwalter et al., 1985; Buckwalter et al., 1986; C. E. Farnum & N. J. Wilsman, 1998; Hunziker & Schenk, 1989; Hunziker, Schenk, & Cruz-Orive, 1987), although some authors divide the growth plate otherwise (Buckwalter et al., 1986; Farnum et al., 2000; Leger & Czernichow, 1989; Murphy, Nagase, & Brinckerhoff, 1988; Roach & Clarke, 2000). Each zone presents variations in the chondrocytes size, shape, orientation and function. The proportion of each zone can vary with anatomical location, the animal model and

the developmental stage (Buckwalter et al., 1985; C. E. Farnum & N. J. Wilsman, 1998; Hunziker & Schenk, 1989; Rauch, 2005).

Reserve zone

The reserve zone is adjacent to the chondro-osseous junction of the epiphysis of the bone. It consists of a sparse and non-homogeneous distribution of nearly spherical chondrocytes (Buckwalter et al., 1985), also known as stem cells in a dense extracellular matrix consisting of a high concentration of fibrils of type II collagen positioned randomly in proteoglycans and water (Abad et al., 2002; Buckwalter et al., 1985). In animal models of larger size, the reserve zone occupies the largest proportion of the growth plate. The thickness of this zone decreases with developmental stage, in parallel with that of the complete growth plate (C. E. Farnum & N. J. Wilsman, 1998; Hunziker & Schenk, 1989; Sergerie et al., 2009). The matrix/cell volume ratio is much higher in the reserve zone compared to the other zones (Ballock & O'Keefe, 2003a; Farnum, Lee, O'Hara, & Urban, 2002). Indeed, the matrix/cell volume ratio decreases dramatically, approaching the chondro-osseous junction. It was shown that the ratio reached values above 9 in the reserve zone, was between 4 and 8 in the proliferative zone and decreased significantly to values below 1 in the hypertrophic zone (Farnum et al., 2002).

The major functions of the reserve zone can be categorized based on the major structural components. Production and maintenance of a dense extracellular matrix by chondrocytes provide storage of all the nutrients and components required in the growth process (Ballock & O'Keefe, 2003b). The chondrocytes in this area serve as a reservoir of stem cells to the growth plate and then go through a proliferative stage (Buckwalter et al., 1985; Rauch, 2005). Finally, the chondrocytes in this zone secrete two factors: the first factor, growth plate-orienting morphogen, serves to organize the cells into columns in the proliferative zone and the second, hypertrophy-inhibiting morphogen, to prevent premature cell expansion (i.e. hypertrophy) during the growth process (Abad et al., 2002). This latter aspect explains the presence of two distinct zones on one hand and hypertrophy on the other hand in the growth plate. The amount of chondrocytes and their differentiation capabilities, which are directly related to growth rate, decrease with age (Schrier et al., 2006). In large animals, the extracellular matrix of the reserve area is the thickest and the stiffest part of the growth plate.(C. E. Farnum & N. J. Wilsman, 1998; Sergerie et al., 2009) (Schrier et al., 2006). It would serve as an important structural support for

the longitudinal growth, especially in larger species where this process occurs over a longer period (C. E. Farnum & N. J. Wilsman, 1998). Abad et al. (Abad et al., 2002) have shown that, following the separation of the reserve zone from the other two zones, the area isolated can regenerate both underlying zones, i.e. the proliferative and the hypertrophic zones. Therefore, the reserve zone is central to the growth plate and contributes to its overall structural organization and function.

Proliferative zone

The proliferative zone consists of flattened chondrocytes, which are organized in columns parallel to the direction of longitudinal growth (Buckwalter et al., 1985; C. E. Farnum & N. J. Wilsman, 1998). Their cell cycle is fast, which causes a high concentration of chondrocytes compared to other areas (Buckwalter et al., 1985; Buckwalter et al., 1986; Hunziker & Schenk, 1989). Meanwhile, the proliferation rate changes with the developmental stage and, in general, there is an increase in cell number in these columns during periods of rapid growth (Farnum & Wilsman, 1993; C. E. Farnum & N. J. Wilsman, 1998). With age, the amount of chondrocytes and the thickness of this zone decreases due to the reduction of stem cells from the reserve zone and proliferation capacity (Schrier et al., 2006). This decrease also coincides with the shape change of these cells, as they approach the hypertrophic zone (Buckwalter et al., 1985). The extracellular matrix of this zone is composed of a high concentration of collagen, especially type II, which is oriented along the longitudinal axis of the growth plate (Fujii et al., 2000; Hunziker & Schenk, 1989).

The main role of this zone is the proliferation of chondrocytes, which is one of the main factors affecting the rate of longitudinal growth (Wilsman, Farnum, Green, et al., 1996). Cell proliferation is necessary to maintain a balance between the production of cartilage on one hand and chondrocytes apoptosis and calcification of the matrix at the metaphyseal chondro-osseous junction on the other hand (C. E. Farnum & N. J. Wilsman, 1998; Nilsson & Baron, 2004). The chondrocytes in this zone also contribute to the synthesis and degradation of the extracellular matrix. Proliferative metalloproteinases (MMPs) MMP2 and MMP9 (Takahashi et al., 2005) and MMP13 (Alvarez et al., 2000) are also synthesized in this zone.

Hypertrophic zone

The hypertrophic zone, located between the metaphysis and the proliferative zone is often divided into two sub-zones: the pre-hypertrophic zone or transition zone, and hypertrophic zone. The transition zone consists of chondrocytes arranged in columns that began to increase in volume (Ballock & O'Keefe, 2003a; Rauch, 2005). This increase in volume continues in the hypertrophic zone until they reach five to ten times the original size of chondrocytes in conjunction with differentiation cessation, the synthesis of type X collagen and decrease in type II collagen (Mwale et al., 2002). Because of cell hypertrophy, this zone is the most deficient in extracellular matrix, which is less stiff compared to other zones of the growth plate (Sergeie et al., 2009) and therefore more susceptible to fractures. There is a significant synthesis of extracellular matrix in the hypertrophic zone (Buckwalter et al., 1986; van der Eerden et al., 2003), which is much higher than the synthesis in the proliferative zone (Buckwalter et al., 1986; Hunziker & Schenk, 1989). More specifically, the chondrocytes synthesize type II and type X collagens (Alvarez et al., 2000; Poole et al., 1989; Sandell et al., 1994), MMP13 (Alvarez et al., 2000; Ballock & O'Keefe, 2003a) and aggrecanases (Mitani et al., 2006). Both ADAMTS-4 and ADAMTS-5 are mainly expressed in mature and hypertrophic chondrocytes (Mitani et al., 2006). The fibers of type II and type X collagens remain oriented along the longitudinal axis (Fujii et al., 2000). Finally, at the end of hypertrophic zone, i.e. the junction with the bone metaphysis, is the site of cell death or apoptosis, where matrix calcification occurs followed by the vascular invasion and production of new bone (Buckwalter et al., 1985; C. E. Farnum & N. J. Wilsman, 1998; Rauch, 2005).

The cellular hypertrophy, together with proliferation, is largely responsible for longitudinal growth observed following expansion in the volume of chondrocytes (Ballock & O'Keefe, 2003a; C. E. Farnum & N. J. Wilsman, 1998; Wilsman, Farnum, Leiferman, et al., 1996). The rate of chondrocytic expansion, and thus the growth rate vary depending on the site of growth, i.e. in small or large bone, age and animal species (Ballock & O'Keefe, 2003a; Buckwalter et al., 1985; Kuhn, Hornovich, & Lee, 1993).

1.2 Growth plate mechanobiology

An interdisciplinary branch of biomechanics, which studies the effect of mechanical loads on the biological responses of organs and tissues, is called mechanobiology (Stoltz & Wang, 2002; van der Meulen & Huiskes, 2002). In the case of growth plates, it is the study of the association

between different types of mechanical loading and the resulting effects on the biological components of the growth plate and, consequently, their effect on the resulting bone growth process. This process is called the mechanical modulation of bone growth. Understanding the relationship between these two aspects (mechanical and biological components) allows better understanding the development and progression of musculoskeletal diseases and intervening in the design and improvement of their treatment approaches. Furthermore, the development of tissue-engineered organs and tissues, where quantitative data is required both at the structural and compositional levels, depends on the progress in mechanobiology (van der Meulen & Huiskes, 2002). Controlling and modulating mechanical stimuli is an essential step to develop appropriately engineered organs that integrate and function properly with the host. The next section covers various aspects of the mechanical modulation of bone growth and certain diseases associated with non-physiological loading of immature bones, i.e. on the growth plates.

1.2.1 Mechanical modulation of bone growth

Mechanical forces are essential to the growth process (Lerner, Kuhn, & Hollister, 1998; LeVeau & Bernhardt, 1984; Niehoff et al., 2004) and they usually have a modulatory effect on this process (R. L. Duncan & Turner, 1995). Several studies define the modulation of bone growth by the Hueter-Volkman law, which states that increased sustained pressure on the growth plates decreased bone growth and, conversely, a decrease in pressure accelerates bone growth (Bonnell et al., 1984; Lerner et al., 1998; Niehoff et al., 2004; Rauch, 2005; I. A. Stokes et al., 2006; I. A. Stokes et al., 2007).

1.2.2 Musculoskeletal pathologies and treatments involving longitudinal bone growth

It is clear that bone growth modulation mechanism is a key element in the progression of infantile and juvenile musculoskeletal deformities such as adolescent idiopathic scoliosis and neuromuscular diseases (Bonnell et al., 1984; Frost, 1990; LeVeau & Bernhardt, 1984). It turns out that this process is also of utmost importance and of a growing interest in the development and improvement of minimally invasive approaches modulating local bone growth while preserving the natural growth of bone, the bone segment function and mobility.

1.2.2.1 Mechanical modulation of bone growth and progression of musculoskeletal pathologies

Longitudinal growth is particularly sensitive to its mechanical environment during developmental stages of rapid growth (R. L. Duncan & Turner, 1995; Niehoff et al., 2004). The following section describes some examples of musculoskeletal deformities resulting from non-physiological mechanical loads applied to the immature skeleton during growth.

Musculoskeletal disorders affecting the spine:

Adolescent idiopathic scoliosis

Scoliosis (Figure 1-4) is an asymmetric, three-dimensional and very widespread spinal deformity that can be congenital, related to neuromuscular conditions, or idiopathic in nature. In the case of adolescent idiopathic scoliosis, the deformity develops and progresses during puberty, particularly among girls. Due to the curved shape of the spine, growth is hampered on the growth plates of vertebrae located on the concave side of the scoliotic curvature, while it continues on the convex side, which further accentuates the deformation, which progresses in a self-sustaining manner (LeVeau & Bernhardt, 1984; I. A. Stokes, 2002).

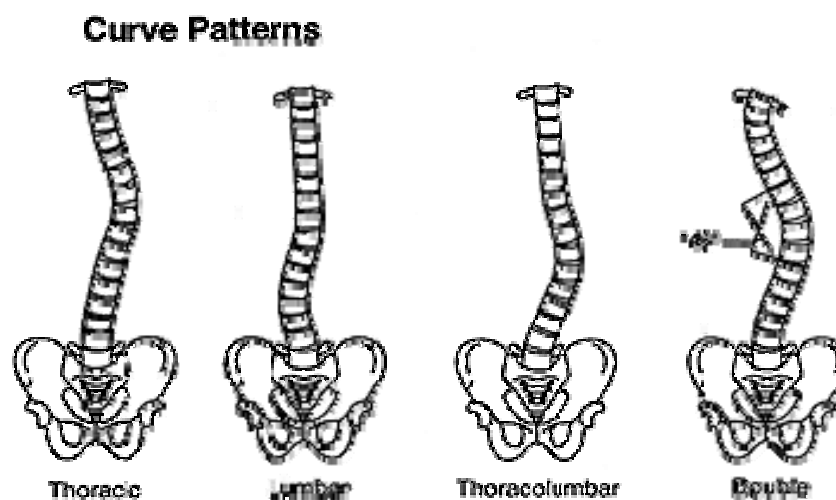


Figure 1-4 : Schematic representation of different scoliotic patterns (obtained on 22 June 2011 from http://www.niams.nih.gov/Health_Info/Scoliosis/default.asp)

Spondylolisthesis / Spondylolysis

Spondylolisthesis and spondylolysis (Figure 1-5) are spinal deformities caused by a non-congenital defect in the pars (located between the upper and lower articular processes of the vertebrae) (Beutler et al., 2003; Fredrickson, Baker, McHolick, Yuan, & Lubicky, 1984; LeVeau & Bernhardt, 1984; Newman, 1955; Sakai, Sairyo, Suzue, Kosaka, & Yasui). Spondylolysis is essentially a fracture of the pars, while spondylolisthesis includes the fracture aforementioned and slipping past the affected vertebra located underneath. Spondylolysis is often a precursor of spondylolisthesis (Beutler et al., 2003; Fredrickson et al., 1984; LeVeau & Bernhardt, 1984; Newman, 1955). The cause of spondylolysis is often due to cyclic external loading. Progression of spondylolisthesis may be related to the fact that the vertebral growth plate is the weakest part of the spine and is sensitive to stress, particularly anterior shear, causing a shift at this level (Hu, Tribus, Diab, & Ghanayem, 2008; Sairyo et al., 2001). These conditions are frequently found in children, particularly males, who practice a lot of physical activity such as gymnastics and swimming, where the cause of the fracture is probably related to cyclic loading in hyperextension. The lumbar spine is the most affected because it supports more weight (LeVeau & Bernhardt, 1984).

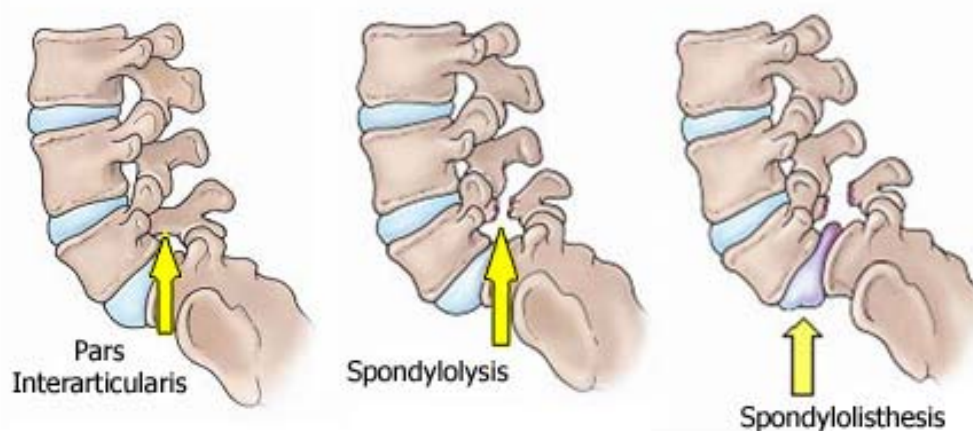


Figure 1-5 : Schematic representation of Spondylolisthesis and Spondylolysis (obtained on 22 June 2011 from <http://orthoinfo.aaos.org/topic.cfm?topic=a00053>)

Musculoskeletal disorders affecting the joints:

Tibia vara

Tibia vara (Figure 1-6), also known as Blount disease, is a condition characterized by disturbance of normal growth in the inner part of the upper tibia. Tibia vara causes a bowlegged gait, and can

impair the knees significantly. Although the cause is unknown, it is believed to be largely due to non-physiological loading on one side of the growth plate.



Figure 1-6 : Representation of tibia vara (obtained on 3 November 2010 from <http://knee-replacement-india.blogspot.com/2010/06/tibia-vara-causing-oa-knee.html>)

Genu varum / valgum / recurvatum

The presence of abnormal forces during development can create many defects in the knee. The genu recurvatum is due to a malposition in utero, which forces the knees to grow in extension rather than flexion. The genu varum deformity is marked by medial angulation of the leg from the thigh, giving the appearance of an arc (Figure 1-7). There is usually curved towards the outside of the femur and tibia. The genu valgum is a deviation to the outside of the axis of the lower limb, which forces the knees to touch while the ankles are separated (Figure 1-7). It is believed that genu varum and genu valgum occur because of unequal loads across the growth plate.

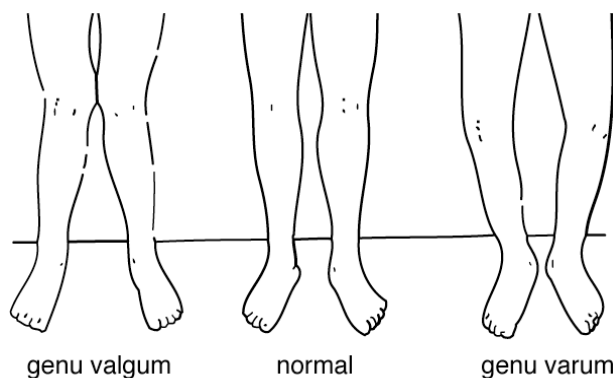


Figure 1-7 : Representation of genu varum and valgum (obtained on 8 September 2010 from <http://sports.jrank.org/pages/8251/genu-valgum.html>)

1.2.2.2 Mechanical modulation of bone growth and treatment of musculoskeletal pathologies

Modulation of local growth is exploited in the development of minimally invasive approaches for the treatment of musculoskeletal pathologies. Orthopedic treatments currently used are based, rather loosely, on simple observations and the exact physiological response to external stimuli remains unknown.

Adolescent idiopathic scoliosis

Screws and ligaments (Braun, Akyuz, Ogilvie, & Bachus, 2005; Newton et al., 2005) (Figure 1-8) and staples (Betz, D'Andrea, Mulcahey, & Chafetz, 2005; Guille, D'Andrea, & Betz, 2007; Wall, Bylski-Austrow, Kolata, & Crawford, 2005) (Figure 1-9) are two examples of minimally invasive approaches, i.e. approaches that involve less surgical risks and complications and preserve growth and segment function, for the treatment of idiopathic scoliosis. In both cases, the implants are inserted in two adjacent vertebrae in order to modulate the local growth and restore the symmetry of the vertebral bodies. The principle of these two types of implants is therefore based on the mechanobiological response of the immature vertebral bodies (Hueter-Volkman law) subjected to static mechanical loading. Each technique has proven effective; it appears that the screws and ligaments would be preferable to staples since they allow a better correction of scoliosis and a higher osseointegration. However, the surgical procedure is more invasive in case of screws and ligaments compared to the staples.

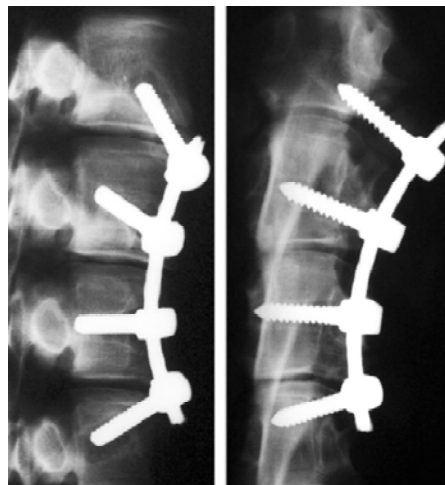


Figure 1-8 : Screws and ligaments inserted at different levels between vertebral bodies (Newton et al., 2005)



Figure 1-9 : Staples implanted at different levels between vertebral bodies: left panel (Wall et al., 2005) and right panel (Guille et al., 2007).

Tibia vara

The treatment of Blount's disease ranges from simple observation to the wearing of orthotic braces to surgery. Decisions about the appropriate treatment for each child depend mostly upon the age of the child at the time of diagnosis and the severity of bowing of the legs. If the bowing worsens, or is detected in a 2-4 years old child, Blount's disease is usually best treated with the use of orthotic braces that are fitted by an orthopaedic surgeon and worn on the child's legs. These braces, referred to as KAFP braces, which stands for Knee-Ankle-Foot Prosthetic, extend from top of the thigh to the tips of the toes, following underneath the feet. The goal is to gradually guide the growth of the legs towards a straighter position of the legs, so that the knees and feet are aligned properly, without bowing. Based on the severity of the deformity, conventional osteotomy or asymmetrical physal compression using an external apparatus will be used to correct the deformity.

Genu varum / valgum / recurvatum

Hemiepiphysiodesis is an attractive method in growing children to allow “guided growth” to correct the angular deformity. Stapling and eight-plate are two examples of hemiepiphysiodesis, a minimally invasive treatment of deformities at knee level (Courvoisier, Eid, & Merloz, 2009; Wiemann, Tryon, & Szalay, 2009) (Figure 1-10). In both cases, the implants are inserted on the proximal tibial and/or distal femoral growth plates depending on the type of deformity in order to modulate the local bone growth and restore the symmetry of legs.

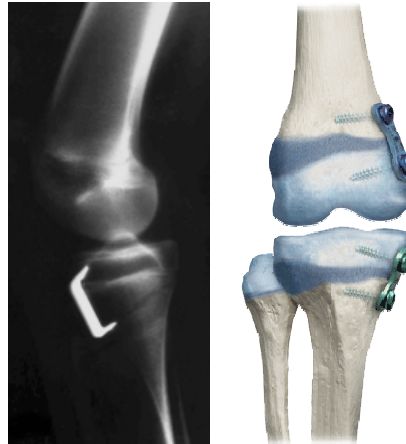


Figure 1-10 : (left) Staple inserted in on proximal tibial growth plate to correct idiopathic genu valgum (Courvoisier et al., 2009), (right) screw and plate (eight-plate) inserted on the distal femoral and proximal tibial growth plates (obtained on 22 June 2011 from <http://www.eight-plate.com/glossary.php>).

1.2.3 Effect of compression on bone growth rate

Mechanical loads are characterized by three main parameters: the type of loading, the amplitude of loading and the loading time. The load may be static or dynamic compression, tension, torsion or shear. Its magnitude can vary from very small amplitudes to amplitudes completely non-physiological. Finally, the load can be applied for a short period of time or for an extended period. In this section, we are interested in the effects of static and dynamic compressive loading on the growth rate.

Mechanical loading may slow or accelerate bone growth rate (Cohen et al., 1998; Frost, 1990; Mankin & Zaleske, 1998; I. A. Stokes, 2002), although the time required between the stimulus and the change of growth as such is not yet precisely characterized (I. A. Stokes, 2002). Since the discovery of the Hueter-Volkmann law, many studies have been conducted *in vivo* on different animal models to characterize and quantify this relationship. Early studies suggest that even a small increase in physiological compression retards growth. This would suggest that there is no real threshold that triggers the phenomenon (Alberty et al., 1993; Arkin & Katz, 1956; Aronsson, Stokes, Rosovsky, & Spence, 1999; Farnum et al., 2000; I. A. F. Stokes, Spence, Aronsson, & Kilmer, 1996). Recently, it was concluded that the relationship between load and mechanical

modulation of growth is linear; this concept is supported by a study conducted on two different bones (vertebra, tibia) of three animal models (rat, rabbit, calf) (I. A. Stokes et al., 2006).

In the case of longitudinal growth, the growth rate can be expressed as a change in length divided by a time interval. The growth rate is often measured using fluorochromes, such as calcein, which binds specifically to the extracellular matrix during mineralization (Alvarez et al., 2000; Breur, Lapierre, Kazmierczak, Stechuchak, & McCabe, 1997; Breur et al., 1991; Farnum et al., 2000; Hunziker & Schenk, 1989; I. A. Stokes et al., 2006; I. A. Stokes et al., 2007; I. A. Stokes et al., 2005; Valteau, Grimard, Londono, Moldovan, & Villemure, 2011; Wilsman, Farnum, Green, et al., 1996; Wilsman, Farnum, Leiferman, et al., 1996). Using multiple injections and histology techniques, it is possible to determine the growth rate by measuring the distance between markers or between a simple marker and the bone forehead. It is also possible to measure the bone length on radiographs or directly on the subject post-mortem.

The **type of loading** (static or dynamic, compression or tension) is an important factor which affects growth rate (Simon, 1978). An earlier study has shown that static loading has more effects on growth mechanisms while dynamic loading influences more the remodeling mechanisms (Mankin & Zaleske, 1998). More recently, in a study by Valteau et al. (2011), the effect of finely controlled equivalent static versus dynamic compression on the growth rate was investigated. It has been shown that growth rate was reduced in both static and dynamic loading conditions in a similar manner showing that dynamic loading is as effective as static loading in modulating bone growth with less detrimental effects on the growth plate. It is also noteworthy to mention that it is also believed that the gravitational force is sufficient to affect the epiphyseal growth (Arkin & Katz, 1956). The type of loading in terms of compression or tension has also been shown to be a contributing factor affecting growth rate. Stokes et al. (2002) has shown that there is a significant reduction in the growth rate of compressed vertebrae of rats. However, the difference was not significant for the vertebrae loaded in tension. On the other hand, the hypertrophic zone thickness, the hypertrophic chondrocytic height and number of proliferative chondrocytes correlated with the growth rate in both tension and compression loading (I. A. Stokes et al., 2007; I. A. Stokes et al., 2002). It was shown that growth rate positively correlates with all aforementioned histological parameters (hypertrophic zone thickness, hypertrophic chondrocytic height and number of proliferative chondrocytes).

The **loading magnitude** is also an important parameter (LeVeau & Bernhardt, 1984; Niehoff et al., 2004; Ohashi et al., 2002; Scott, 1957; Simon, 1978; I. A. Stokes, 2002; I. A. Stokes et al., 2006; I. A. Stokes et al., 2007). While a minimum required compression seems to allow normal growth and ossification (C. E. Farnum & N. J. Wilsman, 1998), a load too high (0.6 MPa (Villemure & Stokes, 2009)) may result in cessation of longitudinal bone growth. It has been shown that longitudinal growth rate is inversely proportional to the magnitude of the static compression (Bonnell, Peruchon, Baldet, Dimeglio, & Rabischong, 1983) and is linked to the magnitude of dynamic compression (Ohashi et al., 2002). More recently, it was shown by Stokes et al. (2007) that the growth rate was significantly altered in response to different magnitudes of loading in vertebral and tibial growth plates of rats, calves and rabbits.

The **loading time** is another significant factor that has been shown to affect bone growth rate (Alberty et al., 1993; Frost, 1990; Ohashi et al., 2002; Scott, 1957; I. A. Stokes et al., 2005). The longer the load is maintained, the higher the growth reduction would be.

1.2.4 Effect of compression on growth plate histomorphometry

The growth plate histomorphometry is the histological analysis of its morphological characteristics and includes measurements defining the arrangement and general organization of chondrocytes, the total growth plate thickness, its histological zones thicknesses, etc. The histomorphometry of mechanically loaded growth plates was studied both *in vitro* and *in vivo* in various animal models (Alberty et al., 1993; Apte & Kenwright, 1994; Farnum et al., 2000; Sergerie et al., 2011; I. A. Stokes et al., 2006; I. A. Stokes et al., 2007; I. A. Stokes et al., 2002; Valteau et al., 2011).

Morphology of the growth plate

To date, it has been shown that, with compression, chondrocytes lose their columnar alignment (Alberty et al., 1993; Farnum et al., 2000; Sergerie et al., 2011). Chondrocytes in the proliferative zone are shown to be less numerous in response to compression (Farnum et al., 2000; I. A. Stokes et al., 2007; Valteau et al., 2011). However, the columnar density of proliferative chondrocytes was shown to remain unchanged (Valteau et al., 2011). The hypertrophic chondrocytes were shown to be less numerous, smaller in height and in volume in response to compressive loading (Alberty et al., 1993; Farnum et al., 2000; C. E. Farnum & N. J. Wilsman, 1998; I. A. Stokes et

al., 2007). Moreover, the reduction in hypertrophic chondrocytes height following static compressive loading was reported more significant than dynamic compressive loading (Valteau et al., 2011).

Growth plate and its histological zones thicknesses

Although a study by Trueta and Trias (1961) has shown that growth plate thickness increased under static compression, the microscopic measurements showed that total growth plate thickness was reduced following static compression (Alberty et al., 1993; I. A. Stokes et al., 2007; Villemure et al., 2005), reducing not only the proliferative zone thickness (Alberty et al., 1993; I. A. Stokes et al., 2007) but also the hypertrophic zone thickness (Alberty et al., 1993; Farnum et al., 2000; C. E. Farnum & N. J. Wilsman, 1998; I. A. Stokes, 2002; I. A. Stokes et al., 2007). More recently, a study by Valteau et al. (2011) reported a more significant reduction in growth plate thickness following *in vivo* static loading compared to dynamic loading on rat caudal vertebrae. Nevertheless, in an *in vitro* study by Sergerie et al. (2011), overall growth plate thickness decreased non-significantly following static and dynamic compressive loading.

1.2.5 Effect of compression on growth plate biology

1.2.5.1 Effect of compression on growth plate cellular proliferation

The effect of mechanical loading on cell proliferation has also been extensively studied (Alberty et al., 1993; Apte & Kenwright, 1994; Basso & Heersche, 2006; Ehrlich, Mankin, & Treadwell, 1972; Farnum et al., 2000; C.E. Farnum & N.J. Wilsman, 1998; Ohashi et al., 2002; Othman, Thonar, & Mao, 2007; Revel et al., 1992; X. Wang & Mao, 2002). Chondrocytes number was reduced, but their proliferation was not ceased when subjected to static forces in compression (Ehrlich et al., 1972; Farnum et al., 2000; C.E. Farnum & N.J. Wilsman, 1998). However, *in vivo* physiological dynamic loading was shown to increase the number of chondrocytes in the proliferative (Revel et al., 1992) and hypertrophic zone (Ohashi et al., 2002). In terms of cell division measured by BrdUrd, a decrease in cell division in the proliferative zone was observed following static compressive loading (Alberty et al., 1993; C.E. Farnum & N.J. Wilsman, 1998). However, the cells were shown to still actively proliferate (Farnum et al., 2000). Nevertheless, as shown in a recent study, the proliferation index was not influenced significantly by mechanical compression of vertebral and proximal tibial growth plates (I. A. Stokes et al., 2007).

1.2.5.2 Effect of compression on extracellular matrix components

The protein detection approaches characterize qualitatively the abundance of one or more specific protein in a specific tissue or a cell. Three major techniques which are extensively used in research are the *western blot*, *radioactive isotopic labeling*, and *immunohistochemistry*.

The *Western Blot* technique is an experimental technique used to detect specific proteins in a tissue. Gel electrophoresis separates proteins according to the length of polypeptides or based on the three-dimensional structure of the protein. The proteins are then transferred to a membrane where they are detected using specific antibodies. Detecting and reading the results can be achieved by autoradiography, fluorescence or radioactive detection (Kurien & Scofield, 2006).

Radioactive isotopic labeling is used to track the passage of a molecule in a system. Radioactive isotopes are included in the chemical composition of the molecule and are then detected by mass spectrometry or infrared spectroscopy (Bonnell et al., 1984; Seinsheimer & Sledge, 1981; Zioudrou, Fujii, & Fruton, 1958).

Immunohistochemistry (IHC) is used to detect qualitatively specific proteins in cells or tissues. By a chain of reactions, specific antibodies bind to proteins. Some molecular markers are specific to one phase as cell proliferation or apoptosis. Immunohistochemistry is widely used in research to understand the distribution, localization and differences in protein expression in different biological tissues, with or without a treatment. The detection and visualization can be made by counter-staining or immunofluorescence (Nerlich, 2003).

A limited number of studies have investigated the effect of static or cyclic compression on the expression of certain key proteins of the growth plate extracellular matrix using these techniques.

Type II and Type X collagen

Under static compressive loading, a decreased expression of type II and type X collagens was reported (Cancel, Grimard, Thuillard-Crisinel, Moldovan, & Villemure, 2009; Niehoff et al., 2004). *In vivo* studies on dynamically loaded rats have shown that the expression of type II collagen and type X collagen was neither modified by cyclic loading (Ohashi et al., 2002; Tang & Mao, 2006) nor by voluntary exercise in a running wheel (Niehoff, et al., 2004). Nevertheless, in an *in vitro* study on swine ulnar growth plates, an increase in type II collagen expression was observed under dynamic loading (Sergerie et al., 2011).

Aggrecan

Aggrecan expression was reported to remain unchanged under *in vivo* static (Cancel et al., 2009) and dynamic (Tang & Mao, 2006) compressive loading. However, *in vitro* results (Sergerie et al., 2011) showed that aggrecan expression decreased under static compressive loading and increased under dynamic compressive loading

1.3 Growth plate mechanical behavior

The mechanical behavior of cartilaginous tissue is used to describe the response of the material under specific loading conditions (Mow et al., 2005; Mow & Hung, 2001). To better understand the biomechanical behavior of cartilaginous tissue, it should be regarded as a multiphase material with two major phases which both are immiscible and incompressible: a fluid phase composed of water and ions and a solid phase composed of collagen, proteoglycan, other proteins and the chondrocytes.

1.3.1 Mechanical characteristics of cartilaginous tissue

With the combination of two major phases (fluid phase composed of water and ions and solid phase composed of collagen, proteoglycan, other proteins and the chondrocytes) cartilaginous tissue has specific behavioral characteristics under loading condition. The two important characteristics of cartilaginous tissue are viscoelasticity and anisotropy. This section summarizes the mechanical characteristics of cartilaginous tissue.

1.3.1.1 Viscoelasticity

Cartilaginous tissues are regarded as viscoelastic materials, meaning that if subjected to a constant load or a constant deformation, their response varies with time (Mow et al., 2005; Mow & Hung, 2001; Mow & Ratcliffe, 1997). In general, the response of such materials can be modeled as a combination of the response of an elastic solid and a viscous fluid. The two fundamental responses of viscoelastic materials are creep (Figure 1-11) and stress relaxation (Figure 1-12). When a viscoelastic material is subjected to a constant load, creep happens. In this case, the viscoelastic material responds with a rapid initial strain followed by a time-dependent and progressively increasing strain to the equilibrium point (Figure 1-11). In the case of stress relaxation, the viscoelastic material is subjected to a constant strain. Typically, the viscoelastic

material responds with a high initial stress followed by a time-dependent and progressively decreasing stress, which is required to maintain the applied deformation (Mow et al., 2005; Mow & Hung, 2001) (Figure 1-12).

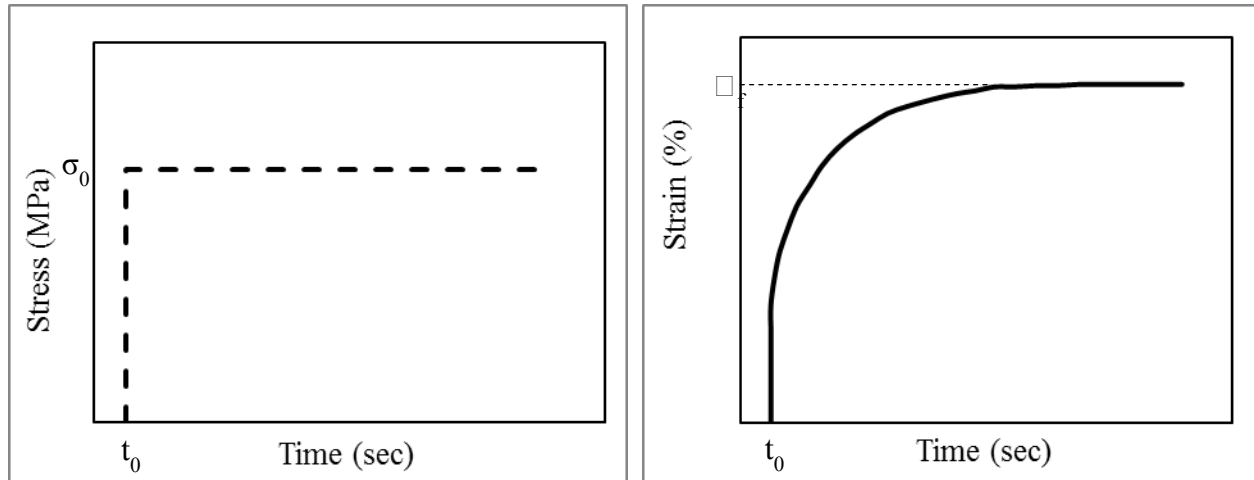


Figure 1-11 : Creep schematic.

It is noteworthy to mention that during the creep and stress relaxation responses of the cartilaginous tissue, a heterogeneous compressive strain field is developed in the extracellular matrix of the tissue. In a study by Villemure et al. (2007), in response to *in situ* stress relaxation, a non homogenous strain field was developed through the thickness of rat growth plates.

The creep and stress-relaxation phenomena can be caused by different mechanisms. They can come from either an intrinsic viscosity of the material (also known as flow independent viscosity) or the flow of interstitial fluid through the solid phase (also known as flow dependent viscosity). In the case of cartilaginous tissues, the viscoelasticity is primarily explained by the frictional drag (or flow dependent viscosity) resulting from the movement of water through porous extracellular matrix. The intrinsic viscosity of collagens and proteoglycans also play a role, however smaller (Mak, 1986; Mow et al., 2005; Mow & Hung, 2001).

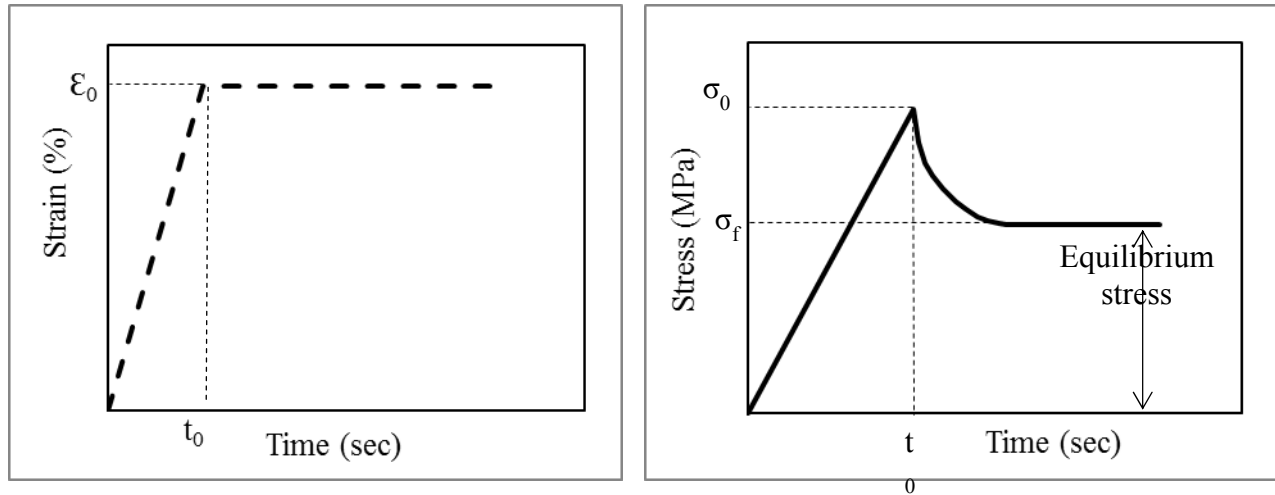


Figure 1-12 : Stress relaxation schematic.

1.3.1.2 Anisotropy

Unlike isotropic materials, which have identical properties in all directions, mechanical properties of anisotropic materials depend on the direction in which they are measured. Since the composition and structure of growth plate is heterogeneous (as mentioned in earlier sections), it is assumed as an anisotropic material (Mow et al., 2005).

1.3.2 Biphasic stress-relaxation response of growth plate in compression

The stress relaxation response of a cartilaginous tissue in a one dimensional compression test is shown in Figure 1-13. In this case, the tissue is compressed with a constant strain rate until the nominal strain (ϵ_0) is reached (curve O-A-B: Figure 1-13, left panel). Beyond that point, the nominal deformation is maintained (curve B-C-D: Figure 1-13, left panel). The stress relaxation response of the cartilaginous tissue to this type of deformation is shown in the right panel of Figure 1-13. During the constant compression phase (curve O-A-B: Figure 1-13, right panel), the stress rises continuously until the maximum stress (σ_0) is reached, corresponding to the nominal strain (ϵ_0). During the stress relaxation phase, which starts right after the maximum stress is reached, the stress continuously decreases until an equilibrium is reached (curve B-C-D: Figure 1-13, right panel). The stress increase in the compression phase is associated with the exudation of the interstitial fluid and the compaction of the solid matrix, while the stress relaxation phase is caused by relief of the high compaction region near the platens, which apply the compression

force by fluid re-flow within the porous extracellular matrix (Mow et al., 2005; Mow & Hung, 2001).

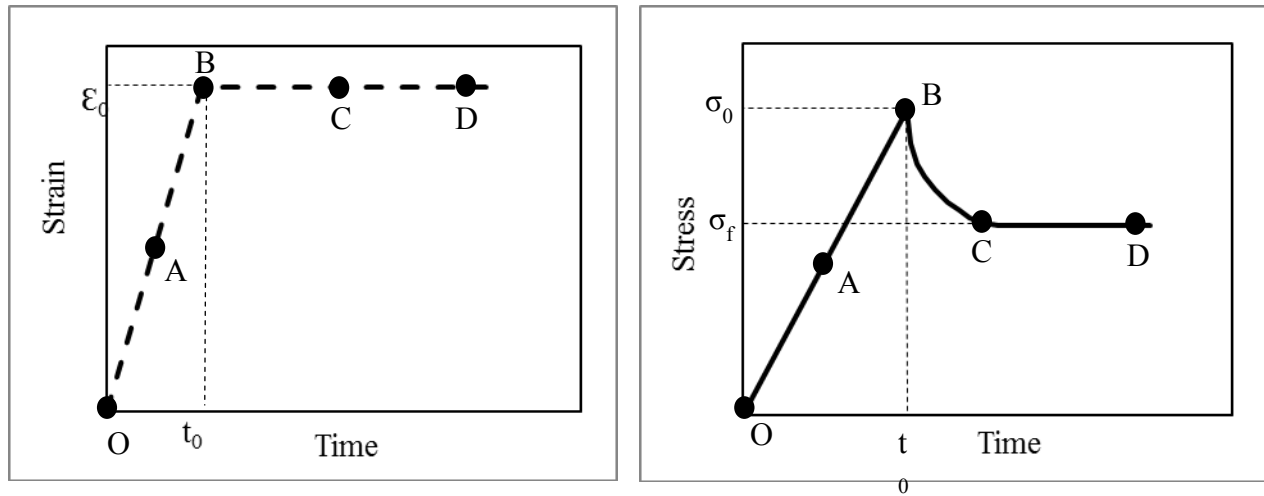


Figure 1-13 : Controlled ramp displacement applied on a cartilaginous tissue and the stress-relation response in the uniaxial compression experiment, adapted from (Mow et al., 2005).

The stress relaxation process will stop when the developed stress within the cartilaginous tissue reaches the stress generated by the intrinsic compressive modulus of the solid matrix for the applied ϵ_0 (Mow et al., 2005; Mow & Hung, 2001). It is important to emphasize that in cartilaginous tissue under physiological loading condition, high stresses are difficult to maintain due to the stress relaxation response, which rapidly attenuates the developed stress within the tissue (Mow et al., 2005; Mow & Hung, 2001).

1.3.3 Experimental compression tests

Basically, a compression test involves the application of an axial load compressing the cylindrical sample (Callister, 2002). Typical testing configurations to study the time-dependent creep or stress relaxation response of cartilaginous tissues are confined compression, unconfined compression and indentation. During these tests, samples of cartilage tissue are usually immersed in a saline solution such as Hanks' Balanced Salt Solution (HBSS). The choice of test depends on the problem studied and available technical resources.

1.3.3.1 Confined compression

In confined compression, the sample is placed in a closed, impermeable metallic chamber with fixed dimensions where it is compressed with a porous filter. The fluid is exuded axially (along the direction of compression) through the tissue surface in contact with the filter (Figure 1-14). This type of experiment is difficult to achieve due to three technical difficulties: first, it is not possible to achieve perfect confinement as most mathematical models require. Secondly, the confining chamber prevents nutrients from reaching the explants under test (Mow, Wang, & Hung, 1999). Finally, the confining chamber could also add the effects of friction during compression and interdigitation of the tissue against the filter can increase resistance (Mak, 1986; Mow et al., 2005; Schinagl, Gurskis, Chen, & Sah, 1997).

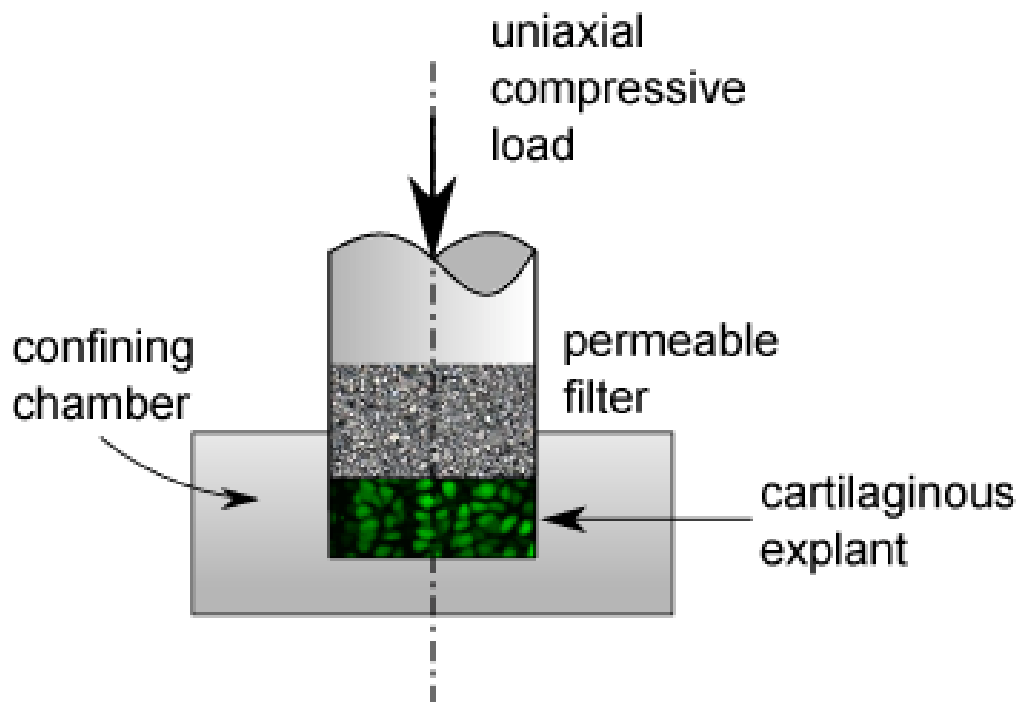


Figure 1-14 : Schematic representation of confined uniaxial compression of cartilaginous tissue.

1.3.3.2 Unconfined compression

In unconfined compression, cartilaginous tissue is compressed between two smooth, impermeable metallic platens, and the fluid exudates only in the radial direction (Figure 1-15). Samples must be cut, but the dimensions are less strict than the confined compression test. The

important point to note is that in unconfined compression test, the strain in the axial direction is always compressive while the strain in the radial direction is always tensile.

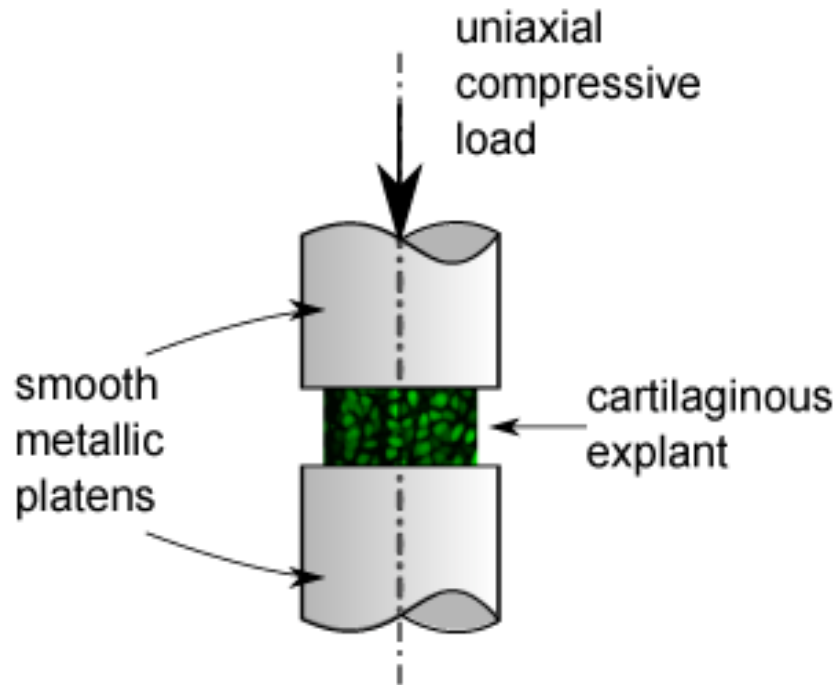


Figure 1-15 : Schematic representation of unconfined uniaxial compression of cartilaginous tissue.

1.3.3.3 Indentation

Indentation is a process where a material is compressed locally by a rigid a porous or nonporous indenter (Figure 1-16). When using biological tissues, the indenter is often porous and has a rounded end, although it can also be flat (Jin & Lewis, 2004; Lu et al., 2004; Mow et al., 2005).

Indentation is often used because of its ease of implementation that does not require prior preparation of tissues. The test can be performed with the cartilage still attached to the subchondral bone, which allows the determination of mechanical properties *in situ* (Julkunen, Korhonen, Herzog, & Jurvelin, 2008; Mow et al., 2005). However, it is difficult to standardize the mechanical properties determined from these tests because they depend on the size and shape of the indenter and the sample status. According to these pros and cons, the usefulness of *in situ* indentation testing versus *in vitro* unconfined or confined compression testing of isolated cartilaginous tissue is still a matter of debate.

Other forms of indentation include microindentation with atomic force microscopy and nanoindentation. These tests use smaller indenters and forces much smaller than the standard tests (micro- or nano-newtons), thereby simplifying the modeling of tissues due to low magnitudes used (DiSilvestro & Suh, 2001; Gupta, Lin, Ashby, & Pruitt, 2009; Radhakrishnan et al., 2004). In addition, it is possible to perform tests on smaller samples or different parts of the sample, allowing studying the variation of the mechanical behavior with depth.

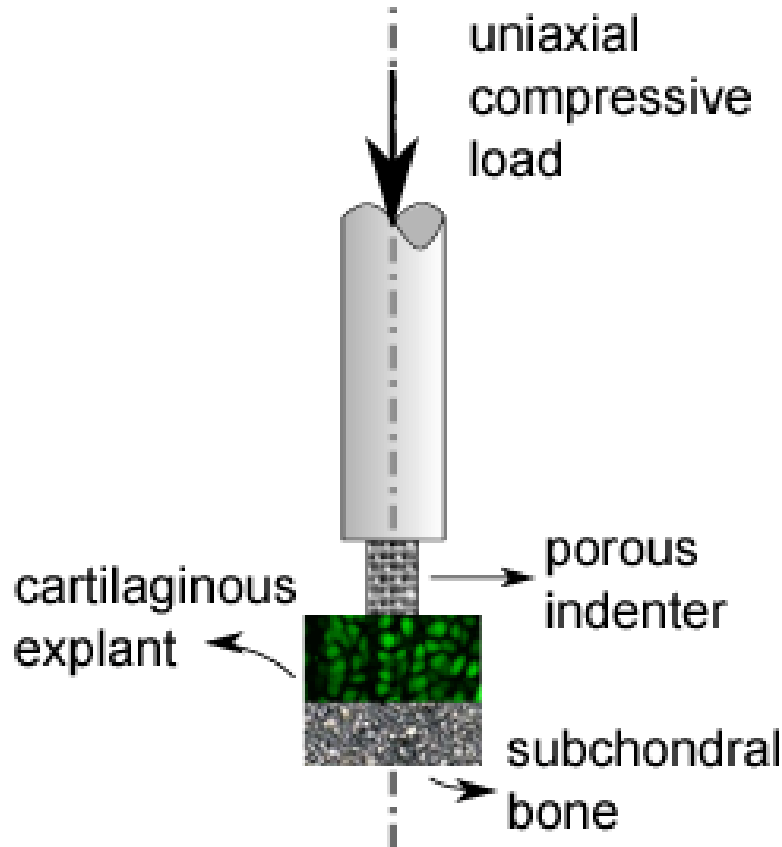


Figure 1-16 : Schematic representation of indentation of cartilaginous tissue.

1.3.4 Quantitative tissue and cell compressive biomechanics of growth plate

The two most abundant protein molecules of the extracellular matrix, collagens and proteoglycans, and their interactions as well as water, which is the most abundant component of cartilaginous tissue, contribute directly to the mechanical behavior of cartilaginous tissue (Mow & Hung, 2001). Considering that the cell-extracellular matrix composite varies greatly across the thickness of the growth plate, the mechanical properties are different depending on the

histological zone (Radhakrishnan et al., 2004; Villemure et al., 2007). Chondrocytes retain their characteristic phenotype by extracellular matrix (collagen and proteoglycan) synthesis, however, their density variation are detectable through growth plate tissue, which would also contribute to mechanical characteristics of the growth plate tissue.

A number of different approaches have been used to interpret the role of physical stimuli in regulating growth plate and chondrocytes activity ranging from studies at the tissue and extracellular level to experiments at the cell level. Each level of study provides specific information on the effect of growth plate loading in confined or unconfined compression along and the growth direction as well as indentation. The following sections will briefly summarize the current state of knowledge of cartilaginous tissues, especially growth plates, compressive biomechanics by confined or unconfined compression or indentation tests, at the tissue, cellular and extracellular levels.

1.3.4.1 Tissue

Different *in vitro* studies have previously investigated intrinsic mechanical properties of growth plates (Cohen et al., 1994), growth plate regions (chondroepiphysis/reserve zone region and the proliferative/hypertrophic zones) (Cohen et al., 1998) or growth plate histological zones (Sergerie et al., 2009) and with developmental stage (Wosu et al., 2011) under uniaxial compression using different animal models. These data were extracted either directly from experimental data or by an optimization algorithm. It should be noted that the mechanical testing protocols were not identical, which has an effect on the mechanical properties obtained respectively. Table 1-2 summarizes the studies on growth plate tissue to extract its mechanical properties and their respective experimental protocols.

The obtained mechanical properties from four month old bovine growth plates subjected to unconfined uniaxial compression showed that the reserve zone/chondroepiphysis was the least permeable and transverse and axial Young's moduli were approximately twice as large as the other regions of the growth plate (Cohen et al., 1998). Complementary results were obtained for the newborn porcine growth plates, investigating the three zones separately (Sergerie et al., 2009). More recently, a study on porcine growth plates has explicitly characterized the intrinsic mechanical properties of growth plates at different developmental stages. Swine growth plates were shown to become more flexible and permeable with age (Wosu et al., 2011).

Table 1-1 : Studies on mechanical properties of growth plate tissue using stress relaxation tests.

study	animal model	age	explants	experimental protocol
Wosu et al., 2011	Swine	0-18 weeks	4mm Ø, fresh, tested in HBSS	pre-strain: 5% strain : 15% strain rate: $1.5 \times 10^{-3} \text{s}^{-1}$ relaxation: 0.05g/min
Sergerie et al., 2009	Swine	newborn	4mm Ø, fresh, tested in HBSS	pre-strain: 5% strain : 15% strain rate: $1.5 \times 10^{-3} \text{s}^{-1}$ relaxation: 0.05g/min
Bursac et al., 1999	Bovine	3-4 weeks	7mm Ø, frozen at -20°C, tested in PBS+protease inhibitors	pre-strain: 3% strain rate : $0.115 \mu\text{m/s}$ relaxation: 3kPa/16 min
Cohen, 1998	Bovine	4 months	6.35mm Ø, fresh, tested in 0.15 M unbuffered NaCl	pre-strain: 0.03 MPa strain : 10% strain rate: $7.6 \times 10^{-4} \text{s}^{-1}$
Cohen, 1994	Bovine	12-18 months	6.35mm Ø, fresh, tested in 0.15 M unbuffered NaCl+Protease inhibitor	pre-strain: 0.03 MPa strain : 20%

Despite several studies on the mechanical properties of growth plate, the mechanical behavior of growth plate in terms of tissue deformation under compressive loading was studied to a lesser extent. Growth plate deformation, as measured by change in thickness, has been characterized under various loading conditions using chemical fixation followed by light microscopy (Sergerie et al., 2011). Local strain measurements in growth plate explants have been also reported under equilibrium static loading conditions using optical methods, by tracking distances between cells (Bachrach, 1995) or with digital image correlation (DIC)(Villemure et al., 2007). Digital image correlation is one of the latest noncontact, nondestructive, and direct approaches for quantifying

intratissue and intracellular deformations. In this method, strain maps are produced based on sequentially recorded images. Strain maps are typically made using surface markers, a pattern matching technique establishing correspondence between pairs of digital images of a tissue under load (Bay, 1995). This technique has been recruited in trabecular bone (Bay, 1995), spinal segments (Bay, Yerby, McLain, & Toh, 1999), tendons (Bey, Song, Wehrli, & Soslowky, 2002) and extensively in articular cartilage (Canal, Hung, & Ateshian, 2008; Erne et al., 2005; Guilak, Ratcliffe, & Mow, 1995; Schinagl et al., 1997; Schinagl, Ting, Price, & Sah, 1996; C. C. Wang, Chahine, Hung, & Ateshian, 2003; C. C. B. Wang, Jian-Ming, Ateshian, & Hung, 2002) in order to quantify developed strain patterns. Villemure et al. (2007) also characterized the strain distribution through cartilaginous growth plate in pubertal rats and showed that strain distribution with lower strains developed in the proliferative zone under compressive loading.

1.3.4.2 Cell

One important mechanism by which mammalian cells may perceive alterations in their physical environment is through cellular deformation (Sachs, 1991; Watson, 1991). Several studies have previously investigated the mechanical behavior of articular cartilage at cell level. Articular chondrocyte volume *in situ* has been shown to be altered by as much as ~20%, under physiological levels of matrix deformation (Freeman, Natarajan, Kimura, & Andriacchi, 1994; Guilak, 1995; Guilak & Hung, 2005; Guilak et al., 1995). Theoretical and experimental measurements of cellular deformation in response to applied loading also indicate that the magnitude and distribution of cell deformations will vary with depth in articular cartilage (Bachrach et al., 1995; Guilak & Hung, 2005; Guilak et al., 1995). Furthermore, cell morphology is implicated in the regulation of cell differentiation, phenotypic expression and proliferation (Watson, 1991). Changes in cell shape or size could initiate signals through stretch-activated ion channels on the cells plasma membrane, which may further regulate second messenger activity (Sachs, 1991; Watson, 1991). Different studies on growth plate tissue have indeed characterized a strong relationship between bone growth rate and chondrocyte hypertrophy (Breur et al., 1991; Buckwalter et al., 1985; Hunziker & Schenk, 1989; I. A. Stokes et al., 2007).

Despite several *in vivo* studies that used conventional histology methods combined to chemical fixation to characterize cell morphology in terms of chondrocytic height and volume in mechanically modulated growth plates (Sergerie et al., 2009; I. A. Stokes et al., 2007; Valteau et

al., 2011) (see section 1.2.4), no study up to date evaluated compression induced morphological characteristics of intact growth plate chondrocytes maintained within their extracellular matrix under various loading conditions. Nevertheless, several *in situ* studies have extensively addressed three-dimensional deformation of articular chondrocytes under compressive loading conditions at cellular (Guilak et al., 1995; Choi et al., 2007) and intracellular (Guilak, 1995) levels.

1.3.4.3 Extracellular matrix

Little is known about growth plate extracellular matrix deformation under compressive loading condition. Radhakrishnan et al. (Radhakrishnan et al., 2004) used microindentation to determine the variation of the Young's modulus of the extracellular matrix along the growth plate thickness in six week old rabbit growth plates. It was found that the matrix stiffness increased non-linearly from the reserve zone to the mineralization zone. Bachrach et al (1995) used a technique to evaluate tissue strain by measuring the change in the distance between the chondrocytes in bovine growth plate. However, no significant differences were found between the zones in different directions.

1.4 Molecular and biochemical assays of cartilaginous tissue constituents

Cartilaginous growth plate, as stated previously, is a unicellular tissue, with a biphasic, viscoelastic extracellular matrix primarily composed of water, collagens (mostly type II, as well as types VI, IV and X), glycosaminoglycan-bearing proteoglycans (mostly aggrecan, as well as biglycan and decorin), and hyaluronic acid. This section briefly focuses on generally accepted methods used to quantify components of cartilaginous tissue.

1.4.1 Commonly used biochemical assays for cartilaginous tissue components

According to Hoemann et al. (2004a), quantification of cartilaginous tissue components depends on their solubilization, which can be achieved by thorough proteolytic digestion. Papain digestion at high temperature (60°C) will melt the collagen helix, thereby facilitating collagen proteolysis and fully solubilize glycosaminoglycans, by cleaving the core protein. According to Hoemann et al. (C. D. Hoemann, 2004a, 2004b), parallel quantification of GAG and hydroxyproline content is feasible using the protein-solubilized cartilaginous tissue. Several studies developed direct GAG-dye binding colorimetric assays to measure collagen content by hydroxyproline assay from acid-

hydrolyzed samples (Burleigh, Barrett, & Lazarus, 1974; Stegemann & Stalder, 1967; Woessner, 1961) and GAG content by dimethyl methylene blue (DMMB) assay (Chandrasekhar, Esterman, & Hoffman, 1987; Farndale, Buttle, & Barrett, 1986; Farndale, Sayers, & Barrett, 1982). According to Stegemann et al. (Stegemann & Stalder, 1967), among all different techniques for the determination of collagen content, hydroxyproline assay is regarded as a relatively specific and sensitive assay. Assays which detect chemically modified uronic acid derived from released GAGs were also extensively used to extract total proteoglycan content of cartilaginous tissue (Mort & Roughley, 2007). According to Mort (2007), to date, the most widely used method for GAG quantification is the spectrophotometric DMMB assay. However, prior to development of the DMMB assay, the most widely accepted technique for GAG quantification used uronic acid analysis via carbazole reaction. Two important advantages of uronic acid assay over DMMB analysis are that uronic acid assay (1) is independent of GAG size and degree of sulfation, and hence can detect all uronic acid-containing products of GAG catabolism and (2) is able to detect both hyaluronic acid and sulfated GAGs (Mort & Roughley, 2007). So, even though the uronic acid assay is tedious to be carried out, there might still be occasions that unique features of uronic acid warrant its use. However, according to Mort (Mort & Roughley, 2007), the DMMB assay gained wide acceptance because it is quick, easy and cheap to perform.

Water content is also an important characteristic of cartilaginous tissue, since it is the most abundant constituent of cartilaginous tissue extracellular matrix. Among all imaging and physical methods for water content evaluation of cartilaginous tissue, the gold standard is the freeze-drying of the tissue.

The following section will focus on the biochemical methods used in the present thesis to evaluate growth plate biocomposition.

1.4.2 Evaluation methods of growth plate bio-composition used in this thesis

As previously described, GAG and collagen contents can be quantified in parallel using the papain-digested cartilaginous tissue (C. D. Hoemann, 2004a). The following sections concentrate on the principles of the biochemical assays used in this thesis to evaluate the water content, collagen content, and GAG content of cartilaginous growth plate. It is noteworthy that growth plate explants were all flash-frozen immediately in liquid nitrogen right after tissue extraction, labeled and stored at -80°C until biochemical analysis.

1.4.2.1 Water content evaluation

The water content can be determined using tissue weights prior to and following the lyophilization of tissue at -40°C for 24 hours using standard freeze dry systems. Lyophilization is a process which extracts the water from tissue using a simple principle of physics called sublimation. Sublimation is the transition of a substance from the solid state to the vapor state, without first passing through an intermediate liquid phase. To extract water from tissue, the process of lyophilization consists of:

- ☑ Freezing the tissue using the liquid nitrogen so that the water in the tissue become ice, this step is usually referred to as pre-freezing step;
- ☑ Under vacuum condition, sublimating the ice directly into water vapor;
- ☑ Drawing off the water vapor.

According to Hoemann et al. (2004a), water content determination by lyophilization will degrade cellular RNA and labile proteins. Therefore, samples designated to the biochemical analyses will be normalized to wet weight.

1.4.2.2 Protein solubilization

Papain, which is a sulfhydryl protease from papaya, can be used to degrade most proteins substrates in cartilaginous tissue for different biochemical assays including hydroxyproline assay for collagen content and DMMB assay for glycosaminoglycans.

Farndale et al. (1986) were the first to suggest the use of Papain to solubilize cartilage for analysis of GAG content by DMMB assay. According to Worthington Manual ("Papain assay: Worthington enzymes and biochemicals," 2011), the optimal temperature of hydrolysis is 25°C. However, digestion at 60°C is essential to denature insoluble collagen and to access the alpha chains (Farndale et al., 1986). Full solubilization of matrix and cellular proteins facilitates biochemical detection assays of solubilized components (Heinegard & Paulsson, 1984). Mineralized bone will not solubilize with Papain, and the presence of bone in digested samples will leave an insoluble residue that should be centrifuged out of the sample prior to biochemical assays. Papain was repeatedly reported to be active at pH 6.0 (Kim, Sah, Doong, & Grodzinsky, 1988), pH 6.5 (Buschmann, Gluzband, Grodzinsky, Kimura, & Hunziker, 1992), pH 6.8 (Farndale et al., 1986), and pH 7.5 (C. D. Hoemann, Sun, Chrzanowski, & Buschmann, 2002).

1.4.2.3 Collagen content evaluation

The original protocol of hydroxylproline assay was introduced by Woessner (1961). The hydroxyproline assay used in this thesis is based on the modified versions (Burleigh et al., 1974; Stegemann & Stalder, 1967) of the original protocol. This assay is based on the fact that hydroxyproline is a major component of protein collagen (Stegemann & Stalder, 1967). According to Hoemann et al. (2004a, 2004b), the basic idea of the hydroxyproline assay is that type II collagen has approximately 13.2% of its total mass as hydroxyproline. Once the concentration of hydroxyproline is known, the collagen content may be deducted. In hydroxyproline assay, chemical reaction is used to reveal the presence of hydroxyproline in hydrolysed tissue. The basic steps of the hydroxyproline assay are as follows:

- ☑ Hydrolysis of all amino acids with heat and acid;

This step is done using 6N HCl for 18 hours at 110°C in a Pasteur oven. The presence of GAG in the hydrolysis step results in caramelization or blacking of the samples. Thus, decolorizing is necessary before neutralizing the samples using an ion exchange resin.

- ☑ Neutralizing the samples using NaOH.
- ☑ Oxidization of hydroxyproline residues using Chloramine T solution as an oxidizing agent;
- ☑ Inactivation of oxidizing reagent;
- ☑ Colorimetric reaction of Ehrlich's reagent with oxidized hydroxyproline to form chromophore.
- ☑ Reading the color using a spectrophotometer at 560 nm.

Pure hydroxyproline is used as standard. The standard curve needs to be proceeded in parallel with the samples to extrapolate the concentrations.

1.4.2.4 Proteoglycan content evaluation

Sulfated Glycosaminoglycans (s-GAGs) are known to yield metachromatic reactions with several basic dyes. The interaction causes a shift in absorption observed from the blue end of the visible spectrum towards the red. Disadvantage in the use of most dyes is that the high concentration of the dye solution causes the precipitation of the dye-polyanion aggregate and consequently the

measurement in a spectrophotometer cannot be done. Dimethylmethylene blue (DMMB) is one of the dyes that was identified to give strong metachromatic reaction with sulfated glycosaminoglycans.

Dimethylmethylene blue (DMMB) was first introduced by Taylor et al. (1969) for histological detection of sulphated GAGs. Dimethylmethylene blue was found to give robust metachromatic reaction with s-GAGs (Humbel & Etringer, 1974) when the dye associates with repeating negative charges on the GAGs resulting in stacking of the dye molecules and a shift in the absorption maximum. Ever since, the DMMB assay is widely accepted as a quick and simple method of measuring s-GAGs. The assay has also been largely improved by Farndale et al. (1986; 1982) with more stable reagents, by eliminating the interference of other anionic macromolecules such as DNA, and by discriminating between different kinds of sulfated GAGs by prior digestion with GAG specific enzymes.

Shark Chondroitin Sulfate C sodium salt can be used as standard in this assay and the standard curve needs to be proceeded in parallel with the samples to extrapolate the concentrations. Standard curve concentration range used in this thesis is 0.125-1.25 μg . The Optical Density of the DMMB standard solutions are read along with the samples at 530 nm using a microplate reader to confirm that the standard curve is accepted and solutions been made correctly. A pilot assay needs to be done prior to the actual assay to determine sample dilution in order to fall inside the linear standard curve.

1.4.3 Growth plate biochemical content evaluation up to date

Biochemical content of growth plate including water content, collagen content, and proteoglycan content was previously reported both biochemically (Alini, Matsui, Dodge, & Poole, 1992; Cohen et al., 1992; Matsui, Alini, Webber, & Poole, 1991; Mwale et al., 2002; Wuthier, 1969) and morphologically (Buckwalter et al., 1986) in different histological zones, over consecutive strata, or anatomical regions of the growth plate.

In a study by Wuthier et al. (1969), collagen and water content of fetal calf legs were evaluated using hydroxyproline assay and lyophilization, respectively. It was shown that collagen represented about 60% of the extracellular matrix in the reserve zone and decreased progressively in proliferative and hypertrophic zone to 22%. Moreover, the water content was shown to be

indistinguishable in three histological zones representing more than 80% of the tissue weight. Cohen et al. (1992) evaluated the biochemical content of growth plate in bovine distal femur. It was demonstrated that the center of the growth plate has a significantly lower water content than other anatomical regions. Furthermore, the collagen content evaluated using hydroxyproline assay was found to be the highest in the anterior region while the proteoglycan content evaluated by DMMB assay was the lowest in this anatomical region. In a study by Alini et al. (1992) on fetal calves, analysis of hydroxyproline revealed lower overall collagen content in the hypertrophic zone, where type X collagen is being synthesized in the extracellular matrix.

In a study by Buckwalter et al. (1986) on mice, the relative volume of collagen decreased from the reserve zone to the hypertrophic zone in both territorial and interterritorial matrices. Moreover, total amount of proteoglycan evaluated by uronic acid assay per unit of extracellular matrix increased from the proliferative zone to the hypertrophic zone as reported by Matsui et al. (1991) in 16 sequential strata of fetal bovine tibial growth plates. However, the sulfated glycosaminoglycan content as measured by DMMB assay only showed a modest increase from the first stratum in the proliferative zone to the last stratum in the hypertrophic zone (Mwale et al., 2002).

To our knowledge, no study up to date evaluated growth plate biochemical content in animal models with lower growth rates, which most resemble humans.

1.5 Quantitative laser scanning confocal microscopy

Confocal microscopy is an optical imaging technique that overcomes the limit of conventional microscopes to observe specimens that are thicker than the focal plane using increased optical resolution and contrast of microscopic images by using point illumination and a spatial pinhole to eliminate out-of-focus light. Laser scanning confocal microscopy enables the reconstruction of three-dimensional structures from the obtained images. The following section briefly explains the principles of confocal microscopy and its implications in cell and tissue biomechanics.

1.5.1 Basic principles of the laser scanning confocal microscopy

In conventional microscopy techniques, the scattered light from out-of-focus planes makes the images blurry. This problem is usually addressed by mechanically cutting the biological samples into thin slices ($\sim 5\mu\text{m}$). Minsky was the first one who found a solution to this problem and

invented the stage scanning confocal microscopy (Minsky, 1961). The essential feature of the confocal technique is that the illumination and detection is confined to the same spot in the specimen keeping scattered light from contributing to detected signals.

Although confocal microscope was invented almost 50 years ago, within the past decades this technique became a powerful tool with the incorporation of laser light sources as well as advances in fluorescent microscopy, fast optical scanners, and digital image acquisition and processing techniques. Furthermore, non-invasive imaging of biological samples and improved resolution compared to conventional techniques are two well-recognized characteristics (Pawley, 1995).

A schematic illustration of the confocal microscope light path is shown in Figure 1-17. Light from a point light source is reflected from a beam splitter through the microscope objective to focus the light within the thick tissue at the desired focal depth. Placing a pinhole at the focal point of the objective lens, only the light from the illuminated spot within the tissue is allowed to be collected by the detector. As only one point in the sample is illuminated at a time, two- and three-dimensional images are built up by scanning the whole sample. In order to have three-dimensional intensity profile of the sample, a series of focal planes can be imaged within the sample. The accurate and controlled focusing can be achieved by controlled stepper motors that are attached to the fine focus knob of the microscope.

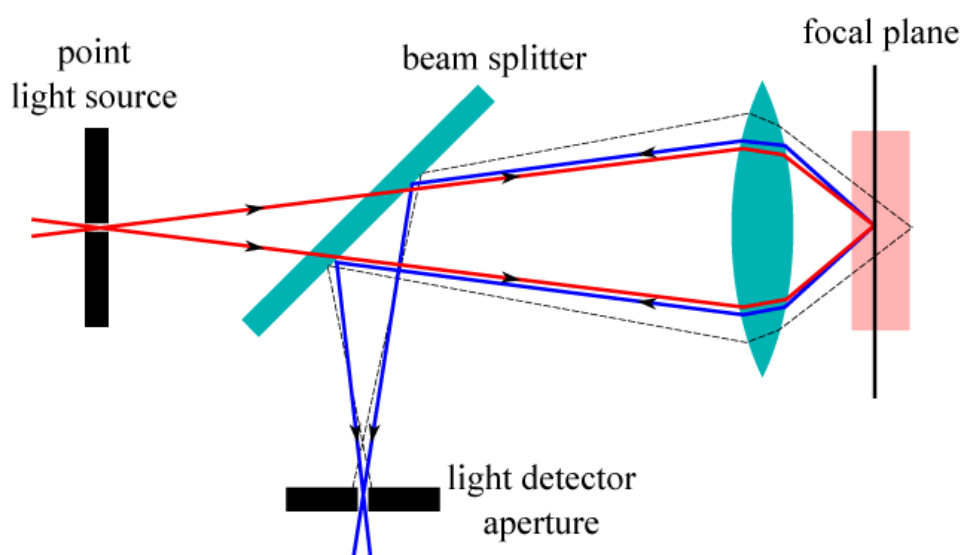


Figure 1-17 : Schematic representation of confocal microscope light path (dash lines show the out-of-focus light and simple lines represent the in-focus light).

1.5.1.1 Optical resolution

Optical resolution in microscopy is often assessed either by means of an optical unit termed the *Rayleigh* criterion or by full width at half maximum (FWHM) criterion of the point source intensity profile.

The Rayleigh criterion is defined in terms of the minimum resolvable distance between two point sources of light generated from a sample maintaining their distinct intensity profiles and is not dependent upon the magnification used to produce the image. According to the Rayleigh criterion, two closely spaced point sources are distinct if they are farther apart than the distance at which the principal maximum of first intensity profile coincides with the first minimum of the second intensity profile. Based on the Rayleigh criterion, a 26.5% dip in brightness appears between the two maxima, giving rise to the probability of peak separation (Pawley, 1995).

The FWHM criterion is a measure of the confocal spot size. The width of the confocal spot in any direction is defined as the distance between two positions along that direction on the intensity profile at half of the maximum intensity (Pawley, 1995). Using the FWHM criterion, two point sources can be considered resolved when distance between their maximum intensity is equal to or bigger than the width of the confocal spot.

Lateral resolution

In confocal case, both the illumination and light collection paths need to be considered in resolution calculations. So, the whole optical system cannot be reduced to a single lens but should rather be simplified to a two lens system, as shown in Figure 1-18.

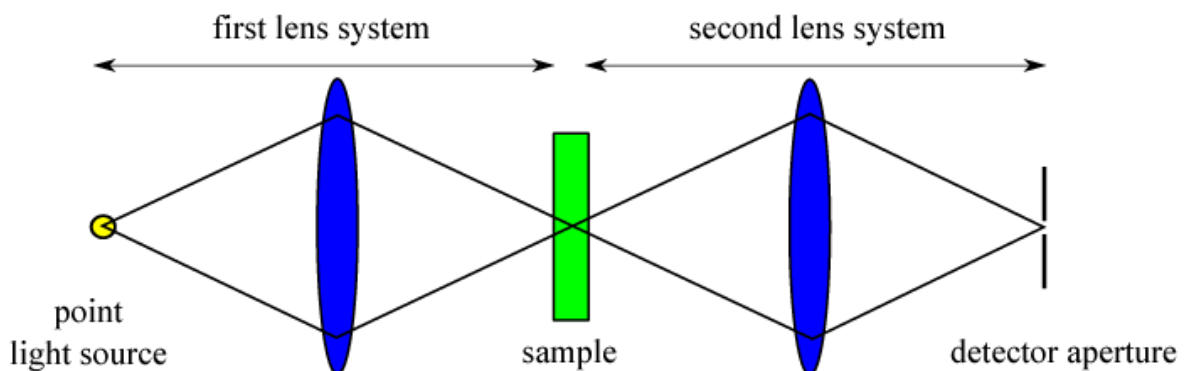


Figure 1-18 : Simplified light path of confocal microscope.

Using the Rayleigh criterion of a 26.5% 'dip', the lateral (in x-y plane) resolution is defined as (Webb, 1996):

$$\text{Lateral resolution} = 0.44 \frac{\lambda}{n \sin \alpha} \quad 1-1$$

where λ is the wave-length of the light being collected, n is the refractive index of the medium, and α is the half angle of the cone of light captured by the objective lens.

Axial resolution

Although the lateral resolution improvement compared to conventional microscopy is of utmost importance in confocal microscopy, the main reason behind the extensive use of confocal microscopes in biology is a result of its axial resolution.

One way to obtain the axial resolution of confocal microscope is to consider the variation of the total power that reaches the detector plane when a point reflector is moved through the focus. According to Webb (1996), the axial resolution is defined as:

$$\text{Axial resolution} = 1.5 \frac{\lambda}{n \sin^2 \alpha} \quad 1-2$$

where λ is the wave-length of the light being collected, n is the refractive index of the medium, and α is the half angle of the cone of light captured by the objective lens.

It is noteworthy to mention that resolution in the x-y plane varies only with the first power of numerical aperture, whereas axial resolution varies with the square of the numerical aperture. This important difference means that lateral resolution and axial resolution both improve with increasing numerical aperture, but z-axis resolution improves more dramatically.

1.5.1.2 The Nyquist Theorem

The sampling criterion most commonly relied upon is based on the well known Nyquist Theorem, which specifies the sampling interval required to reconstruct a pure sine wave as a function of its frequency. The Nyquist Theorem suggest sampling two times for each optically resolved unit (Webb & Dorey, 1995). Since in reality perfect reconstruction of the original signal from the sampled data requires an ideal low pass filter which are unavailable, a factor of 2.3 is usually considered as a minimum practical sampling frequency (Webb & Dorey, 1995). The spatial sampling criterion certainly affects the ability of the confocal microscope to provide

intensity data for accurate quantitative measurements. The optimal sampling procedure helps avoiding under- and oversampling.

1.5.1.3 Effect of photobleaching

The phenomenon of photobleaching occurs when a fluorophore permanently loses the ability to fluoresce due to photon-induced chemical damage. Photo-bleaching of the fluorescent dye while imaging using a confocal microscope is a well known phenomenon whereby the emission intensity of the dye decreases as a function of total irradiation. Thus, the speed of the scan and the excitation power determine the amount of bleaching in obtaining an image. This effect can be minimized by reducing the excitation source energy while taking images.

1.5.1.4 Precision

Besides the photobleaching effect that would introduce errors, precision of the system is also of utmost importance. The precision can be obtained using fluorescent microspheres of known diameter and volume on the same order of the magnitude of the imaged detail (cells for instance). The same protocol (image acquisition, deconvolution, reconstruction) used for the actual samples should be applied for the microspheres.

1.5.2 Implications for cell and tissue biomechanics of cartilaginous tissue

The widespread use of confocal laser scanning microscopy (CLSM) and the development of many useful fluorescent probes have made it possible to observe the cellular structure by labeling the cells and perform two-dimensional studies of tissue structure and three-dimensional studies of cell morphology. Confocal laser scanning microscopy (CLSM) has allowed the detection of fluorescence signals with high spatial and temporal resolution from uniformly thin optical sections at different depths of tissue (Blatter, 1999). Furthermore, this technique provides a non-invasive means of determination of morphometric parameters and examination of intact, viable tissues.

Optical cell sections obtained with CLSM is used for three-dimensional reconstruction of subcellular structures and for quantitative analysis of cell volume of various cell types. Three-dimensional visualization technique using confocal microscopy has been applied to sub-tissue structures in cartilaginous tissue such as cell nuclei (Guilak, 1995), cell membrane (Bush,

Parisinos, & Hall, 2008; Guilak, 1994) and pericellular matrix (Choi et al., 2007; Youn, Choi, Cao, Setton, & Guilak, 2006). This technique has also been applied to extracellular matrix (Choi et al., 2007; Youn et al., 2006). Furthermore, this technique has been widely used in cartilaginous tissue mechanics. Different studies used CLSM to record images of labeled cells prior to and after loading to evaluate the strain developed in articular cartilage (Choi et al., 2007; Guilak, 1995; Guilak et al., 1995; Knight et al., 2006; Lee et al., 2000), growth plate (Villemure et al., 2007), intervertebral disc (Desrochers & Duncan, 2010; N. A. Duncan, 2006; Michalek, Buckley, Bonassar, Cohen, & Iatridis, 2009), and tendon (Arnoczky, Lavagnino, Whallon, & Hoonjan, 2002) at cell and tissue levels.

1.6 Polarized light microscopy

The polarized light microscope is designed to observe and image specimens that are visible due to their optically anisotropic character. From qualitative and quantitative analysis of anisotropic materials using polarized light microscopy, information can be obtained about the spatial orientation of microscopic constituents of biological materials such as fibrillar collagen network. In the following paragraphs, the theoretical basis and the practical aspects of linear polarized light microscopy (PLM) in evaluation of the fibrillar collagen network in hyaline cartilage is summarized.

1.6.1 Basic principles of polarized light microscopy

Polarized light is the light with vibration that travels within a single plane while light from an ordinary light source that vibrates in random direction is called non-polarized light. Polarized light microscopy is a microscopy technique that is performed using light microscope with two filters, polarizer and analyzer, added in the light path (Modis, 1991). The first filter, the polarizer, is positioned beneath the microscope stage after the light source somewhere before the sample ensuring the transmission of linearly polarized light to the sample.

If the material, through which the light passes, is optically anisotropic, the linear polarized light is divided into two linearly polarized light rays (ordinary and extraordinary) having mutually perpendicular vibration directions, an effect called birefringence (Modis, 1991). The split happens when the incident polarized light interacts with the valence electrons of the anisotropic material. These two rays are perpendicular to each other each at 45° with respect to the vibration

plane of the incident polarized light and have the same amplitude but different velocities passing through the sample. Both rays are slowed down when passed through the birefringent sample, but with a phase difference.

The second filter, the analyzer, is normally positioned after the sample above the objectives at 90° to the polarizer. The analyzer merges the two slowed down rays by superposition to construct a resultant image observed at the eyepiece. The orientation of the analyzer is to ensure passing the light with a polarization that is altered passing through the material. The intensity of the resulting signal therefore indicates regions of the tissue that are optically anisotropic and oriented.

Birefringence is basically the numerical difference between the extraordinary and ordinary rays when they are recombined at the analyzer. Biological anisotropic samples such as fibrillar collagen due to their oriented microscopic structure are birefringent. In case of fibrillar collagen network, the ordinary beam is independent of direction while the extraordinary beam is in the same plane as the long axis of the collagen fibres.

1.6.2 Applications in evaluation of extracellular matrix organization of hyaline cartilage

Collagen network organization was extensively characterized within articular cartilage. In unstained sections of articular cartilage, the birefringence is almost exclusively due to the organization of type II collagen fibers, while proteoglycans contribute to 6% of total birefringence (Kiraly et al., 1997). In case of intact articular cartilage, collagen network is reported highly organized and birefringent in the superficial and deep zones. However, the transitional zone is non-birefringent and no significant organization is reported in this zone (Arokoski et al., 1996; Hughes, Archer, & ap Gwynn, 2005; Kaab, Gwynn, & Notzli, 1998; Kiraly et al., 1997; Korhonen et al., 2002; Rieppo et al., 2003; Speer & Dahners, 1979). Polarized light microscopy was also used to define different regions of birefringent and non-birefringent within articular cartilage repair tissues (Mainil-Varlet et al., 2003; Roberts et al., 2003) as well as quantitative measurements within repair cartilage (Langsjo et al., 2010; Vasara et al., 2006). More recently, polarized light technique was used to develop a new score for collagen organization in articular cartilage repair tissue (Changoor et al., 2011; Langsjo et al., 2010; Vasara et al., 2006). Polarized light microscopy was also used to determine collagen orientation

in intact meniscus (Aspden, Yarker, & Hukins, 1985; Skaggs, Warden, & Mow, 1994) or to examine the potential of autologous (Bruns, Kahrs, Kampen, Behrens, & Plitz, 1998; Bruns, Kampen, Kahrs, & Plitz, 2000) or allogeneic (Rodeo et al., 2000) transplantation of meniscal replacement. Unlike meniscus and articular cartilage, little is known about collagen organization of cartilaginous growth plate in its three histological zones. Polarized light microscopy was once recruited to characterize collagen architecture within rabbit metatarsal, from the secondary ossification center to the metaphyseal bone including the perichondrial ring and ossification groove (Speer, 1982). Results of this study indicated that the type II collagen fibers are oriented vertically in the proliferative and hypertrophic zones of the growth plate.

CHAPTER 2 PROJECT RATIONALE, HYPOTHESES AND SPECIFIC OBJECTIVES

2.1 Rationale

The anatomical, physiological, biochemical and biomechanical literature review led to identifying the following key aspects, which are directly related to this research project:

- ☑ The growth plate, divided in three structurally distinct zones, is responsible for endochondral bone growth;
- ☑ The growth plate is a cartilaginous tissue comprising chondrocytes embedded in a viscoelastic extracellular matrix principally composed of the following key elements: water (the most abundant component of the extracellular matrix), collagens (mainly type II as well as type X exclusively in hypertrophic zone), glycosaminoglycan GAG-bearing proteoglycans (mainly aggrecan);
- ☑ These components of the extracellular matrix are believed to contribute to mechanical properties of cartilaginous tissue.
- ☑ Different biochemical and molecular assays can be used for quantification of extracellular matrix components. Quantification of growth plate extracellular matrix components depends on their solubilization, which can be achieved by exhaustive proteolytic digestion;
- ☑ Type II collagen, one of the major extracellular components of growth plate, forms a highly organized fibrillar network which is believed to be a critical determinant of tissue biomechanical competence. The orientation of these fibers can be determined using qualitative polarized light microscopy.
- ☑ **However, quantification of growth plate extracellular matrix key elements as well as evaluation of type II collagen fibers orientation have not been done in an animal model with low growth rate and long period of growth that most resembles human.**
- ☑ Chondrocytes hypertrophy, extracellular matrix synthesis and chondrocytes proliferation are the three most important factors involved in endochondral bone growth;

- ☑ One important mechanism through which chondrocytes may respond to changes in their environment via changes in the synthesis/degradation of the extracellular matrix is directly through deformation of the cellular membrane, which regulates several features of chondrocytes differentiation such as chondrocyte morphology and volume;
- ☑ Conventional histology and stereological techniques combined with chemical fixation have been used to characterize growth plate morphometric parameters in different animal species. **However, three-dimensional *in situ* zonal characterization of growth plate morphometry at both cellular and tissue levels have not been documented yet.**
- ☑ In addition to growth factors, hormones, nutrients, and genetics, mechanical forces are known to regulate bone growth process as explained by Hueter-Volkmann law and therefore, to significantly influence pathological processes involving the growth plate. Moreover, clinical evidence indicates that physiological mechanical stimuli are critical for normal growth and development of bones;
- ☑ The inhomogeneous structure and composition of growth plate induces depth- and strain-dependent mechanical behavior within the tissue.
- ☑ **Nevertheless, based on available studies, little is known about *in situ* compression induced deformations at tissue and cellular levels in three histological zones of intact growth plates of bigger animal models that resemble humans the most.**
- ☑ **Furthermore, the zonal growth plate compressive mechanical behavior with respect to its corresponding extracellular matrix bio-composition and structure has not been fully addressed;**
- ☑ The mechano-transduction mechanisms involved in the process of bone growth modulation can only be studied with a suitable model for the mechanical perturbation of a cell within its extracellular matrix. Based on previous studies, the virtual sectioning properties of laser scanning confocal microscopy (LSCM) is ideally suited for three-dimensional quantitative morphometric model of intact chondrocyte within its extracellular matrix.

2.2 Thesis hypotheses and objectives

Analysis of these key elements has led to the principal hypotheses of this research process:

H1. Three-dimensional histomorphological characteristics of the growth plate at cellular (volume, surface area, major/minor radii and sphericity) and tissue (cell/matrix volume ratio) levels are non-uniform and change with its histological zone.

H2. In response to uniform compressive loading, non-uniform three-dimensional cellular strain as well as two-dimensional tissue strain will develop depending on the histological zone under study.

H3. Biochemical composition (collagen, GAG and water content) and type II collagen fiber orientation change with the histological zone throughout the growth plate thickness.

H4. Developed strain within the three zones of the growth plate is related to the corresponding biochemical composition (collagen, GAG and water content) as well as type II collagen fiber organization.

In order to verify the hypotheses of this thesis, immature swine growth plates were chosen as the animal model due to their lower growth rate and longer period of growth that most resemble humans compared to rodents and rabbits that was extensively used in the literature.

The following specific objectives will help to verify the research hypotheses:

Objective 1: To characterize three-dimensional tissue and cell morphometry of intact swine growth plates using laser scanning confocal microscopy.

This objective has three main components that aim to describe the three-dimensional morphometry of intact chondrocytes in their extracellular matrix.

Step 1: To identify the optimal fluorescent probe concentration and incubation time for swine ulnar growth plates.

Step 2: To verify the imaging and the reconstruction parameters using fluorescent latex beads of known dimensions.

Step 3: To visualize and quantify *in situ* three-dimensional zonal growth plate morphology at the cell and tissue levels using fluorescence labeling of cell cytoplasm coupled with three-dimensional reconstruction of serial confocal sections.

The first step consists of a preliminary study on viability testing of swine growth plate chondrocytes using dual staining of cell cytoplasm and dead cell nucleus in order to determine the optimal probe concentration and incubation time in order to avoid the cytotoxic effects of the probe or its degradation products.

The second step aims for experimental calibration of the imaging and reconstruction parameters using fluorescent Fluoresbrite (TM) latex beads of known diameters and volumes. The beads are reconstructed in the same conditions as the ones used to image growth plate chondrocytes.

The third step is to record digital images of chondrocytes labeled using optimal probe concentration obtained in the first component by laser scanning confocal microscope. The subsequent step is to deconvolve and reconstruct serial confocal sections using a commercially available software in order to characterize three-dimensional morphometry of swine growth plates.

Objective 2: To characterize *in situ* 2D and 3D deformations at the tissue and cellular levels, respectively for the three zones of porcine growth plates using laser scanning confocal microscopy combined with a loading apparatus;

This objective is comprised of two principal steps to quantify cellular and tissue deformations.

Step 1: To identify three-dimensional cell deformations for three histological zones of swine growth plate.

Step 2: To characterize two-dimensional strain distribution through swine growth plate thickness at tissue level.

The first step focuses on quantifying three-dimensional deformations of chondrocytes in all histological zones of swine growth plates under compression using stress relaxation tests. Digital images of chondrocytes labeled with optimal probe concentration obtained (step 1 of objective 1) were recorded using laser scanning confocal microscope within the three histological zones of growth plate prior to compression loading and after tissue relaxation. The serial confocal sections were deconvolved and reconstructed using a commercially available software in order to characterize three-dimensional deformation of chondrocytes under compressive loading.

The second step aims at characterizing the two dimensional tissue strain distributions through swine growth plate thickness under uniaxial loading using stress relaxation tests. Digital two-

dimensional images of labeled growth plate were recorded using laser scanning confocal microscopy in three histological zones of growth plate prior to compression loading and after tissue relaxation. Digital image correlation was used to evaluate strain distribution across the thickness of growth plate.

Objective 3: To evaluate the biochemical content (water, collagen and GAG) of the three zones of the porcine growth plates using appropriate biochemical assays;

This objective includes the evaluation of collagen content using Hydroxyproline assay, GAG content using dimethylmethylin blue assay (DMMB), and water content using lyophilization in the three histological zones of growth plates.

Objective 4: To evaluate type II fibrillar collagen organization within the three histological zones of the growth plate using polarized microscopy.

In this objective of the research project, polarized light microscopy is used to characterize the fibrillar collagen organization within the three histological zones of the growth plate.

Objective 5: To establish relationships between the mechanical behaviour and the biochemical composition and collagen organization of the three zones of the growth plate.

This objective aims at determining possible associations between mechanical behaviour of the growth plate zones and the corresponding structural characteristics (biocomposition and collagen organization).

CHAPTER 3 SCIENTIFIC ARTICLE #1: THREE-DIMENSIONAL *IN SITU* ZONAL MORPHOLOGY OF VIABLE GROWTH PLATE CHONDROCYTES: A CONFOCAL MICROSCOPY STUDY

This chapter introduces the first article written in the context of this thesis and responds to the first objective of this thesis as detailed in Chapter 2.

This article was published in *Journal of orthopaedic research* © 2010 Orthopaedic Research Society in November 2010.

The contribution of the first author in the preparation, obtaining the results, writing and literature review of this paper is estimated at 85%.

Three-Dimensional In Situ Zonal Morphology of Viable Growth Plate Chondrocytes: A Confocal Microscopy Study

Samira Amini,^{1,2} Daniel Veilleux,³ Isabelle Villemure^{1,2}

¹Department of Mechanical Engineering, École Polytechnique de Montréal, P.O. Box 6079, Station Centre-Ville, Montreal, Quebec, Canada H3C 3A7, ²Sainte-Justine University Hospital Center, 3175 Côte-Ste-Catherine Rd., Montreal, Quebec, Canada H3T 1C5, ³Department of Chemical Engineering, École Polytechnique de Montréal, P.O. Box 6079, Station Centre-Ville, Montreal, Quebec, Canada H3C 3A7

Received 30 April 2010; accepted 4 October 2010

Published online 30 November 2010 in Wiley Online Library (wileyonlinelibrary.com). DOI 10.1002/jor.21294

Detailed description of the contribution of different authors:

Samira Amini: Design, obtaining the results, analysis, interpretation of results, article writing and editing, responsible for the integrity of the work.

Daniel Veilleux: Obtaining, analysis, and interpretation of the results.

Isabelle Villemure: Design, interpretation of results, review of the article, responsible for the integrity of the work.

3.1 Abstract

Longitudinal growth, occurring in growth plates with structurally distinct zones, has clinical implications in treatment of progressive skeletal deformities. This study documents the three-dimensional morphology of chondrocytes within histological zones of growth plate using confocal microscopy combined with fluorescent labeling techniques. Three-dimensional reconstruction of Calcein AM labeled chondrocytes was made from stacks of confocal images recorded *in situ* from 4-week old swine growth plates. Three-dimensional quantitative morphological measurements were further performed and compared at both tissue and cell levels. Chondrocyte volume and surface area increased about five- and three-fold respectively approaching the chondro-osseous junction from the pool of reserve cells. Chondrocytes from the proliferative zone were the most discoidal cells (sphericity of 0.81 ± 0.06) among three histological zones. Minimum and maximum cell/matrix volume ratios were identified in the reserve (11.0 ± 2.2) and proliferative zones (16.8 ± 3.0) respectively. Evaluated parameters revealed the heterogeneous and zone-dependent morphological state of the growth plate. Tissue and cellular morphology may have noteworthy contribution to the growth plate behavior during growth process. The ability to obtain *in situ* cell morphometry and monitor the changes in the growth direction would offer better understanding of the mechanisms through which abnormal growth is triggered.

3.2 Keywords

Chondrocyte, Confocal microscopy, Fluorescent labeling, Growth plate, Three-dimensional morphology.

3.3 Introduction

Longitudinal bone growth has clinical implications in the pathogenesis and treatment of juvenile and adolescent progressive skeletal deformities. This process takes place within the growth plates, located between the metaphysis and the epiphysis of long bones, and involves a tempo-spatial progression of chondrocytes within three adjacent histological zones—the reserve (R), proliferative (P), and hypertrophic (H) zones (Ballock & O'Keefe, 2003a; C. E. Farnum & N. J. Wilsman, 1998) (Figure 3-1). Bone growth results from a complex interplay between cellular division in the proliferative zone, cellular enlargement in the hypertrophic zone and controlled

synthesis and degradation of the extracellular matrix throughout the growth plate. Histology and cell morphology (Buckwalter et al., 1985) of the growth plate are heterogeneous along the three zones. In the reserve zone, cells are randomly dispersed through the matrix alone or in couples (Ballock & O'Keefe, 2003b; C. E. Farnum & N. J. Wilsman, 1998; Johnstone, Leane, Kolesik, Byers, & Foster, 2000). In the proliferative zone, chondrocytes have a flattened appearance and are organized in columns (Ballock & O'Keefe, 2003b). Chondrocytes located at epiphyseal end of the proliferative zone divide rapidly while chondrocytes located at metaphyseal end of the proliferative columns start to increase in size towards the hypertrophic zone (Breur, Turgai, Vanenkevort, Farnum, & Wilsman, 1994; Buckwalter et al., 1986; Hunziker & Schenk, 1989; Hunziker et al., 1987; Kember, 1960, 1978). In the hypertrophic zone, cell division stops and terminal differentiation associated with a large increase in cell volume begins (Ballock & O'Keefe, 2003b).

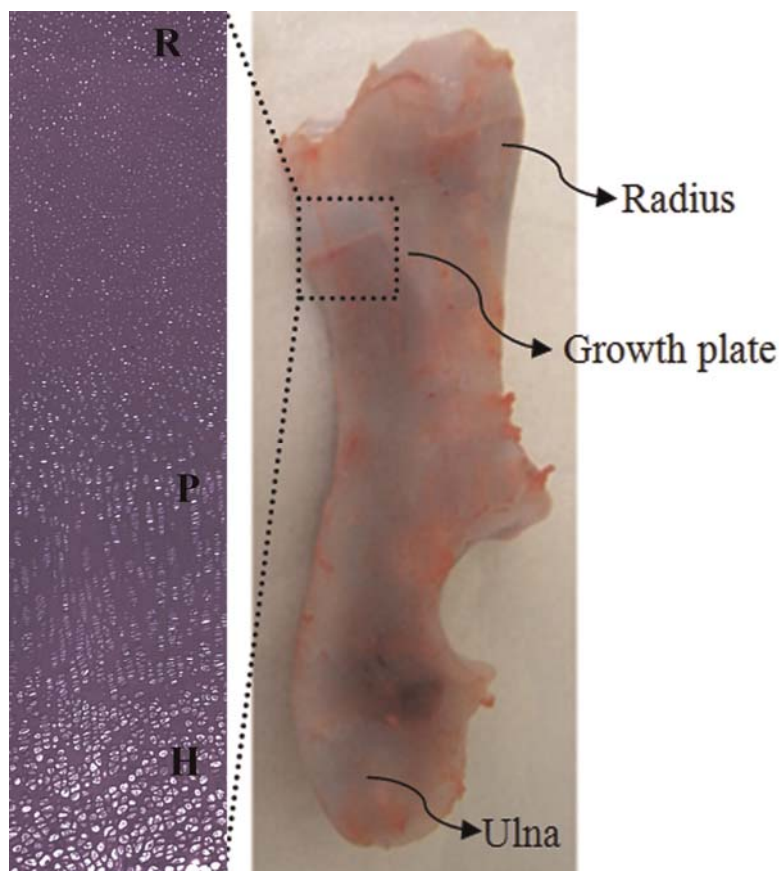


Figure 3-1 : (Right) Porcine ulnar growth plate shown as a light purple line at the physis/bone junction (inside the rectangular box). (Left) Histological section of the growth plate showing its three zones: reserve (R), proliferative (P), and hypertrophic (H).

The mechanisms by which growth plate chondrocytes modulate longitudinal bone growth are still not well understood. Hypertrophy (changes in cell volume and height), proliferation of chondrocytes as well as matrix synthesis have been implicated as the most important factors in both normal and mechanically modulated growth of long bones (Ballock & O'Keefe, 2003a; I. A. Stokes et al., 2007; I. A. Stokes et al., 2002; Wilsman, Farnum, Green, et al., 1996; Wilsman, Farnum, Leiferman, et al., 1996). It has been suggested that the final volume and shape of hypertrophic chondrocytes are important factors in determining the rate of longitudinal bone growth. The several-fold chondrocytic hypertrophy is believed to contribute to the major portion of long bone growth, with the remainder due to matrix synthesis in proliferative and hypertrophic zones as well as chondrocyte proliferation (Eerola, Elima, Markkula, Kananen, & Vuorio, 1996; Farnum & Wilsman, 2001; Hunziker & Schenk, 1989; Kember, 1960, 1978; Villemure & Stokes, 2009; Wilsman, Farnum, Green, et al., 1996). According to Hunziker and Schenk (Hunziker & Schenk, 1989) the normal growth process of long bones is mostly controlled by the morphometric modulation of chondrocyte phenotype. A strong linear relationship was indeed established between hypertrophic chondrocytes volume and longitudinal bone growth rate in both tibial and radial growth plates of three animal species (rats, mice, and pigs) (Breur et al., 1991; Buckwalter et al., 1985; Hunziker & Schenk, 1989). The differential growth of various bones also appears to be related to size differences in hypertrophic chondrocytes (Breur et al., 1994; Breur et al., 1991; Buckwalter et al., 1986; Hunziker & Schenk, 1989; Wilsman, Farnum, Leiferman, et al., 1996). In growth plates undergoing rapid growth, such as in the femur, chondrocytes hypertrophy to a greater extent than do chondrocytes in growth plates from less rapidly growing bones, such as in the radius (Eerola et al., 1996; Farnum & Wilsman, 2001). In an *in vivo* study on rat caudal growth plates, the degree of mechanically modulated growth was found to correlate with hypertrophic chondrocytes enlargement in the direction of growth (I. A. Stokes et al., 2002). One of the important mechanisms through which chondrocytes may respond to changes in their environment in both normal and mechanically modulated growth is directly through deformation of the cellular membrane. Hence, characterization of the shape and volume of growth plate chondrocytes is of utmost importance in understanding the role of the chondrocyte membrane deformation in signal transduction. Furthermore, cell volume regulation has been previously shown to influence matrix synthesis in cartilaginous tissue and would consequently have a significant impact on the integrity of the extracellular matrix (Hall, 1995; Kerrigan & Hall, 2008;

Urban, Hall, & Gehl, 1993), suggesting that chondrocytic enlargement and matrix synthesis are strongly correlated (Villemure & Stokes, 2009). Conventional histology and stereological techniques combined with chemical fixation have been used to characterize two- and three-dimensional growth plate morphometric parameters in different animal species both at tissue and cell levels (Breur et al., 1994; Breur et al., 1991; Buckwalter et al., 1985; Buckwalter et al., 1986; C. E. Farnum & N. J. Wilsman, 1998; Glade & Belling, 1984; Hunziker & Schenk, 1989).

In studies on the rat model at prepubertal, growth spurt, and mature developmental stages, it was demonstrated that, from the proliferative zone to the hypertrophic zone, chondrocyte volume enlarges up to 10-fold while chondrocyte height increases up to 5-fold (Breur et al., 1994; Hunziker & Schenk, 1989; Hunziker et al., 1987). In a study by Buckwalter et al. (1986) on 35-day-old mice model, a five time increase in chondrocyte volume was reported from the resting zone to the late hypertrophic zone. These morphological changes result in a reduced extracellular matrix volume per unit tissue volume in the direction of growth. The three-dimensional visualization and morphological evaluation of cells within their extracellular matrix has been increasingly used due to advances in confocal microscopy techniques (Bush, Hall, & Macnicol, 2008). In a study by Bachrach (1995) the volume of bovine growth plate chondrocytes was quantified *in situ* following compression for the three zones of the growth plate using confocal microscopy combined with fluorescent labeling of the chondrocyte cytoplasm. In a more recent study, the structure of ovine physis and the spatial arrangement of chondrocytes during late fetal development were investigated using confocal microscopy coupled with CMFDA labeling of cells (Johnstone et al., 2000). This method was also used to quantify human chondrocyte volume exclusively within the central region of the hypertrophic zone (Huntley, Bush, Hall, & Macnicol, 2003). Furthermore, three dimensional imaging using two photon laser scanning microscopy was recently used to investigate the mechanism of hypertrophy by quantifying the osmotic sensitivity of chondrocytes in terms of cell volume in a rat model (Bush, Parisinos, et al., 2008). However, *in situ* three-dimensional visualization and zonal characterization of growth plate morphometry at both cellular and tissue levels have not been documented yet.

The objective of this study was to characterize the three-dimensional zonal morphology of *in situ* growth plate chondrocytes both at the cell and tissue levels using fluorescence labeling of cell cytoplasm coupled with three-dimensional reconstruction of serial confocal sections. This knowledge will provide a useful scientific basis for mechanobiological and biomechanical studies

aiming at an improved understanding of the processes of bone development and of mechanically modulated bone growth.

3.4 Methods

3.4.1 Specimen preparation

Twelve forelimbs of 4-week-old pigs were obtained within 3 h of slaughter from a local abattoir. The radius-ulna complex joints were disarticulated under sterile conditions and distal ulnar growth plates were dissected (Figure 3-2). Cylindrical full depth explants of growth plate/metaphyseal bone were then harvested using 4 mm diameter biopsy punches (Figure 3-2A–C). The biopsy punch was inserted perpendicularly to the bone/growth plate junction (Figure 3-2B), which is visible (light purple line) on the ulna (Figure 3-1) in order to have growth plate samples oriented along the bone growth direction.

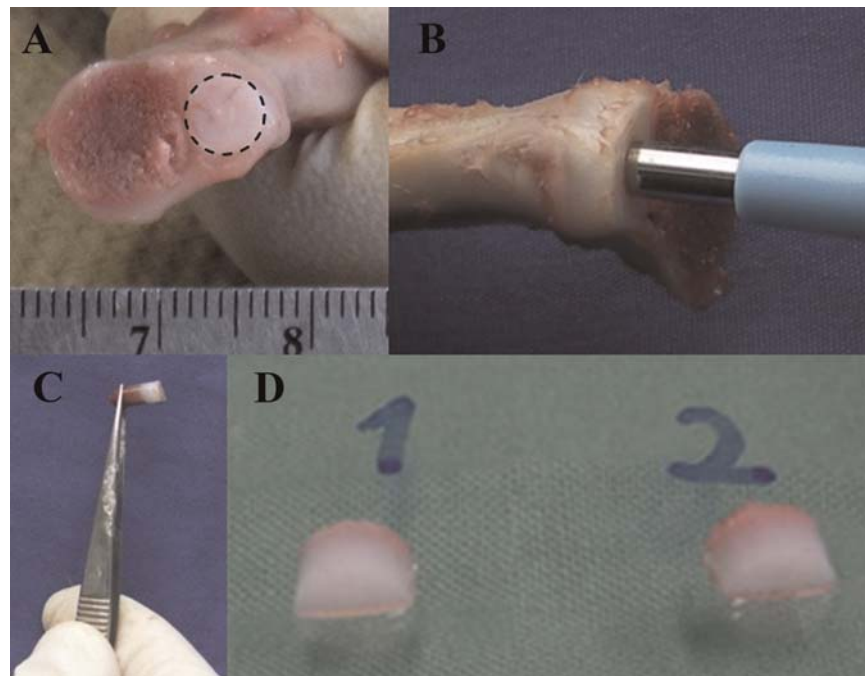


Figure 3-2 : (A) Growth plate location on the porcine radius-ulna complex. (B) Punching of the ulna perpendicular to the growth plate/bone junction for recovery of the 4 mm diameter sample. (C) Recovered growth plate sample. (D) Growth plate semicylindrical samples cut parallel to the sample longitudinal axis

Upper and lower surfaces of the resulting cylindrical samples were trimmed using a Vibratome (Vibratome 1500 Sectioning System) to obtain two parallel surfaces and to provide the thickness of each growth plate sample. Using the same system, samples were further cut into halves (N=24) parallel to the longitudinal axis of the sample to expose the growth plate on the resulting planar surface (Figure 3-2D). Growth plate explants were kept in HBSS (Hank's Balanced Salt Solution), physiological pH, and osmotic pressure (308 mOsm) at room temperature (no longer than 15 min) before staining to avoid drying. The procedures of dissection, tissue preparation, and microscopy were all carried out the same day.

3.4.2 Fluorescent labeling

Samples used for three-dimensional morphological analysis were stained with Calcein AM (Molecular Probes, Invitrogen, Montreal, Canada). The fluorescent calcein, which is retained in the cytoplasm of live cells, was shown to be a suitable measure of cell volume (Alvarez-Leefmans, Altamirano, & Crowe, 1995). However, as reported previously (Johnson, 1998) increasing the fluorescence signal levels by raising the intracellular probe concentration are often counterproductive. In order to avoid the cytotoxic effects of the probe or its degradation products, the optimal stain concentration was determined in a preliminary study using viability testing using dual staining of cell cytoplasm (Calcein AM, Molecular Probes, Invitrogen, Montreal, Canada) and dead cell nucleus (Ethidium homodimer-1 (EthD-1), Molecular Probes, Invitrogen). This study confirmed that higher concentrations of Calcein AM could cause significant staining of dead cells (nuclei labeled using EthD-1). As presented in Figure 3-3, 10-fold increase in Calcein AM concentration led to decreased viability and EthD-1 was taken by the chondrocytes. Using this technique, the minimum stain concentration that indicates maximal counts of green cells whose nuclei were not significantly labeled with EthD-1 was chosen as the optimal stain concentration. Prior to imaging, each individual specimen was immersed in a solution of 0.5 mM Calcein AM with sHBSS (sterile Hank's Balanced Salt Solution) and incubated for 30 min at 37°C in an atmosphere of 95% O₂ and 5% CO₂.

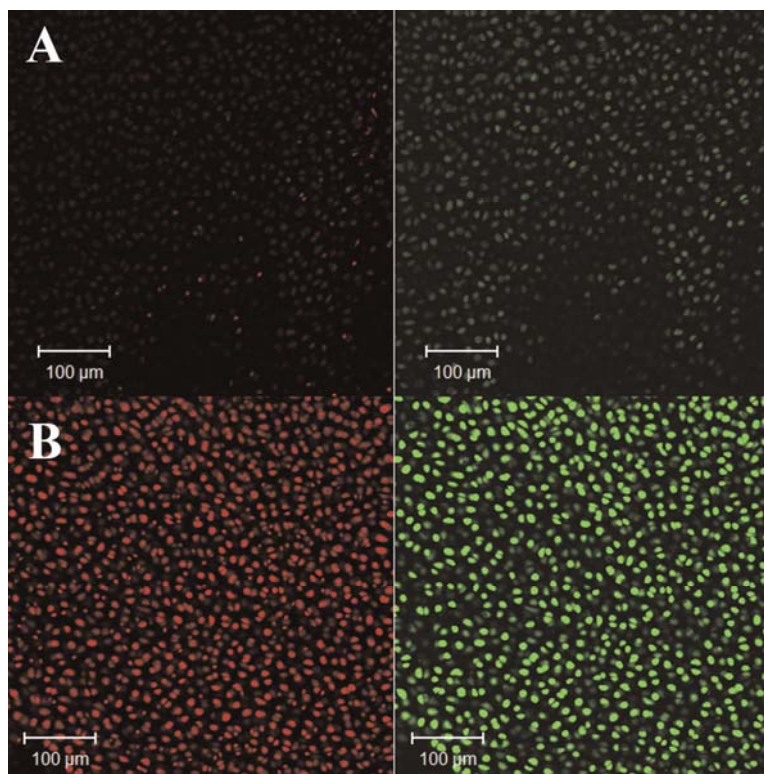


Figure 3-3 : Calcein AM concentration and cellular viability. (A) Confocal section of growth plate chondrocytes loaded with 0.5 mM Calcein AM and 1 mM EthD-1 and showing very good cell viability (B) Confocal section of growth plate chondrocytes loaded with 5 mM Calcein AM and 1 mM EthD-1 and showing decreased cellular viability, as confirmed with EthD-1 taken up by the chondrocytes.

3.4.3 Imaging protocol

For each growth plate semi-cylindrical sample (N=24), volume images (z-stack) of *in situ* Calcein AM-loaded chondrocytes were acquired in two randomly chosen fields in each histological zone using an inverted laser scanning confocal microscope (LSM 510, Carl Zeiss, Jena, Germany). In each field, a total of 1–5 chondrocytes were randomly selected for analysis, for a total of 264 analyzed chondrocytes (reserve zone: n=86; proliferative zone: n=80; hypertrophic zone: n=98). Serial sections of 512×512 pixels were taken using a LD Plan-Neofluar ×40: 0.6 NA objective (Zeiss) with 0.5 mm section intervals (Nyquist acquisition in axial direction) to a depth of ~50–150 μm (which was deep enough in tissue to avoid cutting effects). Argon laser (excitation: 488 nm) was set to permit optimal image quality with minimal dye bleaching, at 15% of full power. Complementary experiments (data not shown) showed that

photobleaching was negligible and not causing significant changes in chondrocyte volume using 15% full power of argon laser. The emission was detected using a 500–550 nm band-pass filter. Each section was averaged over two frames.

3.4.4 Three-dimensional visualization and quantitative analysis

Confocal serial images of chondrocytes loaded with Calcein AM provided a strongly homogeneous and clearly defined signal from the extracellular matrix, which showed negligible fluorescence, hence resulting in a high signal to noise ratio. Prior to three-dimensional reconstruction, optical sections were deconvolved using Huygens software (Huygens Essential, Scientific Volume Imaging BV, Hilversum, The Netherlands) in order to partially remove intrinsic distortion of microscopic images. These images were then reconstructed in 3D using Imaris software (Bitplane, Inc., Zurich, Switzerland), which was previously calibrated to determine the adequate cut-off intensity value determining the cell's boundary with the surrounding matrix. In this experimental calibration, fluorescent Fluoresbrite (TM) latex beads (Polysciences, Inc., Warrington, PA) of known diameters ($10.16 \pm 0.1 \mu\text{m}$) and volumes ($549 \mu\text{m}^3$) (similarly to the study done by Bush and Hall (Bush & Hall, 2001)) were reconstructed in the same conditions as those used to image growth plate chondrocytes. The measured beads' diameter ($10.88 \pm 1.3 \mu\text{m}$) confirmed the parameters used to record and reconstruct 3D images. Quantitative morphological analyses at both tissue and cell levels were then performed using IMARIS 6.0 software (Bitplane). For cell level visualization and analyses, individual chondrocytes were isolated as regions of interest and reconstructed to assess cell level morphological parameters such as cell volume (μm^3), cell surface area (μm^2), sphericity ($(\mu\text{m}^3)^{2/3}/\mu\text{m}^2$) as well as minor and major radii (μm). At the tissue level, cell/matrix volume ratio ($\mu\text{m}^3/\mu\text{m}^3$) was extracted from the 3D reconstructed tissue images in different histological zones of the growth plate. Cell/matrix volume ratio was defined as the ratio of green voxels (3D pixels) volume showing chondrocytes labeled with Calcein AM to the total volume of the three-dimensional image excluding chondrocyte volume.

3.4.5 Statistical analysis

Basic statistical analyses were completed (means \pm standard deviations) for individual parameters studied at cell level (cell volume, cell surface area, cell sphericity, minor radius, and major

radius) and at tissue level (cell/matrix volume ratio) on each set of data (reserve, proliferative, and hypertrophic zones) based on the number of ulnae (N) and on the number of imaged chondrocytes (n). A one-way ANOVA for repeated measurements was carried out to determine whether the difference between the mean values of each investigated parameter reached a certain level of significance (p-value ≤ 0.05 at cell level and p-value ≤ 0.001 at tissue level) for each of the three zones of the growth plate. The post hoc comparisons between data sets were performed using the Tukey's method. Data were processed using statistical analysis software (Statistica 8.0, Statsoft, Inc., Tulsa, OK)

3.5 Results

Growth plate sample thicknesses varied between 3,200 and 4,600 μm with an average of 3,980 μm . Figure 3-4 presents a 3D iso-view of a typical ulnar porcine growth plate, showing the spatial distribution of the reserve (R), proliferative (P), and hypertrophic (H) chondrocytes along the growth plate thickness. Chondrocyte morphology, defined as the surface of cell cytoplasm, varied significantly among the different histological zones of the physis, as shown by the three-dimensional reconstructed images of chondrocytes (Figure 3-5).

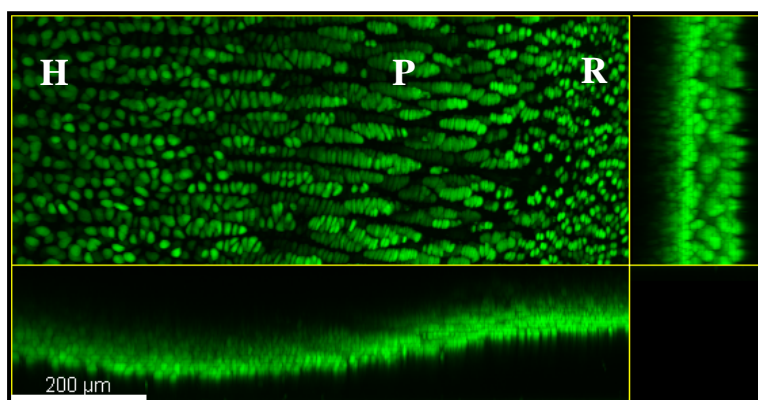


Figure 3-4 : Projected three-dimensional image of Calcein AM loaded *in situ* growth plate chondrocytes obtained from a four-week old porcine distal ulna (10 \times).

Table 3-1 summarizes cell level morphometric analyses. Data are also shown graphically in Figure 3-6, with the results of the comparative ANOVA analyses. The maximum chondrocyte volume was found in the hypertrophic zone ($5331.6 \pm 1585.8 \mu\text{m}^3$), while the minimum was found ($1242.1 \pm 289.5 \mu\text{m}^3$) in the reserve zone. Chondrocyte volume increased of about fivefold from the reserve to the hypertrophic zone along the direction of growth. Chondrocyte surface area

increased threefold from the stem cell pool in the reserve zone ($603.0 \pm 96.9 \mu\text{m}^2$) to the calcification border in the hypertrophic zone ($1613.1 \pm 341.7 \mu\text{m}^2$). Chondrocytes from the proliferative were the least spherical cells (sphericity of 0.81 ± 0.06) among three different histological zones but became more spherical towards the hypertrophic zone (sphericity = 0.91 ± 0.05).

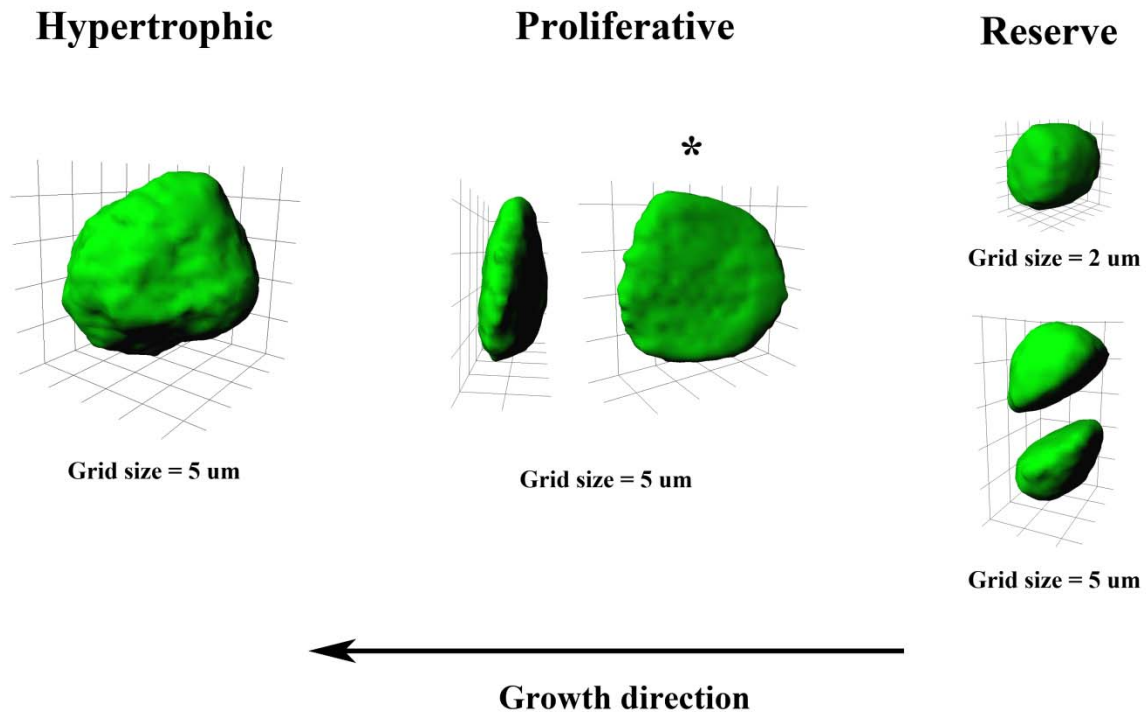


Figure 3-5 : Chondrocyte shape and size showed zonal heterogeneity in growth plate. The morphology of the chondrocyte was determined from the surface of the cell cytoplasm. Chondrocytes are aligned along the growth direction except the cell marked by *, which is perpendicular to growth direction.

In the growth direction, the minor chondrocytic radius did not change significantly from the reserve to the proliferative zone, while a 60% increase was observed from the proliferative to the hypertrophic zone. Conversely, the major chondrocytic radius showed a significant increase (70%) from the chondrocyte pool in the reserve zone to the cellular division zone. However, no measurable change was observed from proliferative to the hypertrophic zones. The increase in cell volume in the growth direction is thus accompanied by an increase in both the major (51.5%) and the minor (75%) chondrocytic radii. Statistically significant differences were found in

chondrocyte volume (Figure 3-6A) and surface area (Figure 3-6B) among the three histological zones. Chondrocyte minor radius (Figure 3-6C) showed significant differences between the hypertrophic zone and the reserve zone as well as between the hypertrophic zone and the proliferative zone whereas the chondrocyte major radius (Figure 3-6D) significantly differed between the reserve zone and the two other zones. Significant difference was also found between the proliferative zone and both reserve and hypertrophic zones for chondrocyte sphericity (Figure 3-6E).

Table 3-1 : Cell and tissue level morphometric analyses for the three histological zones of the growth plate (means \pm standard deviations)

cell level data	Histological zone		
	reserve (n=86)	proliferative (n=80)	hypertrophic (n=98)
volume (μm^3)	1242.1 \pm 289.5* (ii, iii)	2767.5 \pm 691.7*(i, iii)	5331.6 \pm 1585.8*(i, ii)
surface area (μm^2)	603.0 \pm 96.9*(ii, iii)	1194.5 \pm 217.3*(i, iii)	1613.1 \pm 341.7*(i, ii)
sphericity ($(\mu\text{m}^3)^{2/3}/\mu\text{m}^2$)	0.92 \pm 0.04	0.81 \pm 0.06*(i, iii)	0.91 \pm 0.05
major radius (μm)	8.9 \pm 1.1*(ii, iii)	13.1 \pm 1.4	13.5 \pm 1.9
minor radius (μm)	5.1 \pm 0.5	5.3 \pm 0.9	8.9 \pm 1.2*(i, ii)
tissue level data	(n=12)	(n=12)	(n=12)
cell/matrix volume ratio (%)	11.0 \pm 2.2** (ii, iii)	16.8 \pm 3.0** (i, iii)	14.8 \pm 3.0** (i, ii)
overall growth plate thickness (μm)		3980 \pm 420	
*Statistically significant (p-value \leq 0.05) compared to the reserve (i), proliferative(ii) and hypertrophic (iii) zone			
** Statistically significant (p-value \leq 0.001) compared to the reserve (i), proliferative(ii) and hypertrophic (iii) zone			

Morphometric analyses at the tissue level are also summarized in Table 3-1. Significant difference was observed in cell/matrix volume ratio (Figure 3-6F) between the three zones of the physis. Minimum cell/matrix volume ratio (11.0 \pm 2.2%) was identified in the reserve zone. It then substantially increased to 17.0 \pm 3% in the proliferative zone and decreased to 15.0 \pm 3% in the hypertrophic zone.

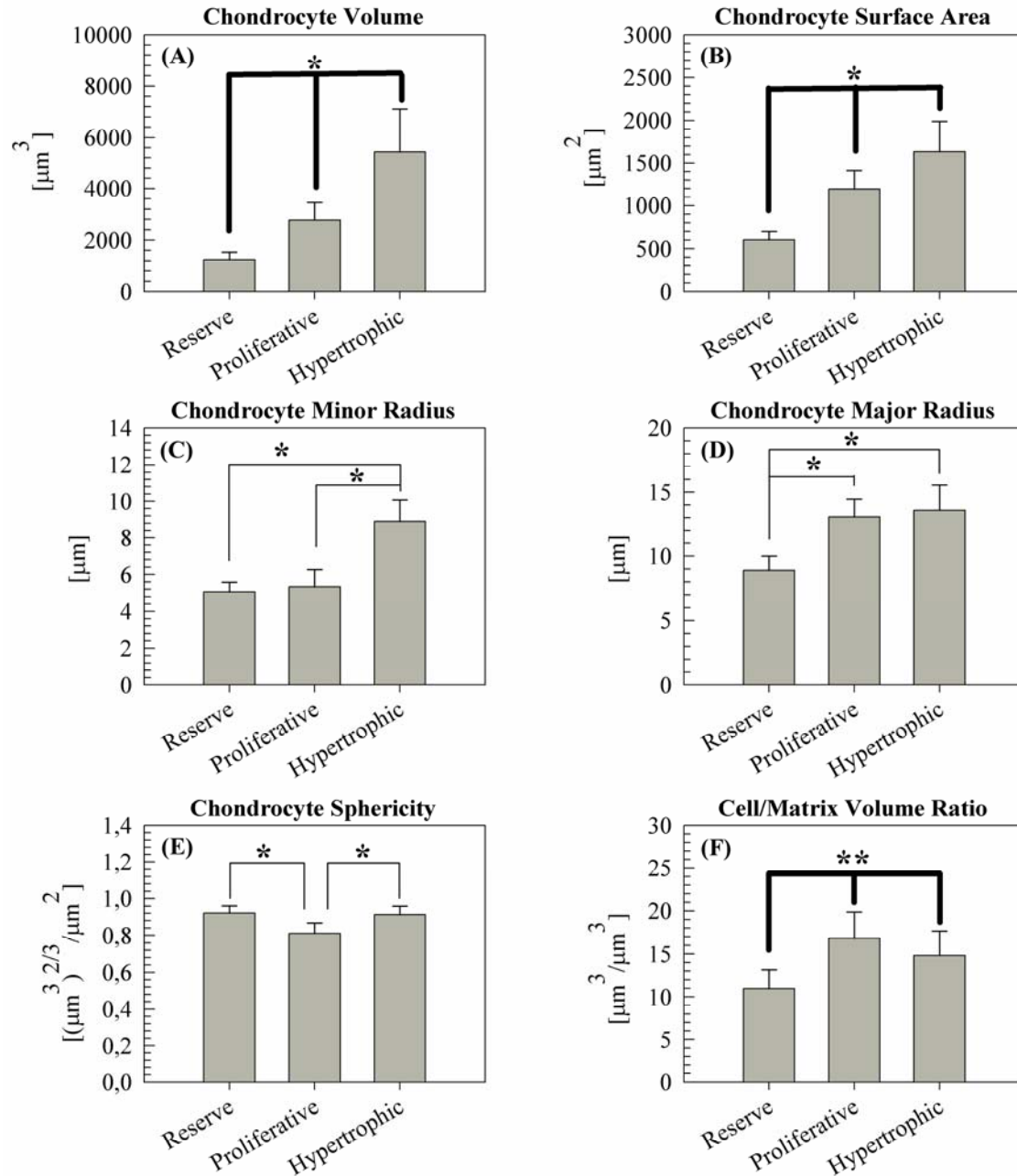


Figure 3-6 : Cell level morphometrical parameters: (A) chondrocytes volume, (B) chondrocytes surface volume, (C) chondrocytes minor radius, (D) chondrocytes major radius, (E) chondrocytes sphericity and tissue level morphometrical parameter (F) cell/matrix volume ratio evaluated in 4-week old swine growth plates (mean values \pm standard deviations). Significant differences among the three histological zones are shown with thick connecting lines (—) and significant differences between two histological zones are shown with thin connecting lines (—). (cell level morphological parameters: *p-value \leq 0.05, tissue level parameter: **p-value \leq 0.001).

3.6 Discussion

This study aimed at documenting *in situ* three-dimensional morphology of growth plates at tissue and cellular levels. Although chondrocyte volume was reported in sequential optical sections through rat growth plate thickness (Bush, Parisinos, et al., 2008) and exclusively in human hypertrophic chondrocytes (Huntley et al., 2003), this study provides for the very first time a direct and noninvasive three-dimensional characterization of the *in situ* size and shape of chondrocytes, as well as cellular versus matrix density information in the three histological zones of growth plate based on fluorescent labeling techniques of cell cytoplasm. Chondrocyte morphology was quantified without fixation or physical sectioning of the tissue, which could cause changes in the physical aspect of chondrocytes and their surrounding extracellular matrix.

There is a marked heterogeneity in cell size through the different histological zones of the growth plate. Observed differences in chondrocyte size are consistent with previous studies on chondrocyte morphology using conventional histology and stereological methods (Breur et al., 1991; Hunziker & Schenk, 1989; Hunziker et al., 1987). In a study carried out by Breur et al. (1994) the mean chondrocyte volume was characterized in rat proximal tibial growth plates divided into eight horizontal strata of equal heights. Estimated mean chondrocyte volume in the first six strata indicates similar magnitude to those measured for reserve and proliferative chondrocytes in the present study. Moreover, volume of hypertrophic chondrocytes of radial and tibial growth plates of 3- and 5-week-old pigs (Breur et al., 1991) are compatible with our results. In addition, our results are in good agreement with two recent studies reporting chondrocyte volume in rat and bovine models (Bush, Hall, et al., 2008; Bush, Parisinos, et al., 2008). Cell volume increase has been consistently reported as approaching the chondro-osseous junction in different animal species (C. E. Farnum & N. J. Wilsman, 1998; Hunziker & Schenk, 1989). In our study, chondrocyte volume and surface area increased five and three times, respectively, in the direction of growth from the reserve zone to the hypertrophic zone. In a study by Buckwalter et al. (1986), chondrocyte volume was characterized from the reserve zone to the late hypertrophic zone in the mouse tibial growth plates. This fivefold increase in cell volume through the growth plate thickness is in good agreement with the results reported in the present study. However, these changes do not corroborate with a previous study in rat tibial growth plates (Hunziker & Schenk, 1989), which showed a greater (9-fold) cell volume increase from the proliferative to the hypertrophic zone. At least two major reasons could explain this difference. First, chemical

fixation technique, which would result in proteoglycan loss in the matrix and could cause changes in the aspect of chondrocytes and their surrounding matrix (Eggli, Herrmann, Hunziker, & Schenk, 1985) was used in the earlier study while chondrocytes were maintained intact in their extracellular matrix in our study. Furthermore, the absence of intracellular signaling in fixation techniques may inhibit regulatory mechanisms such as volume change (Kerrigan & Hall, 2008) through the cytoskeleton, and could eventually affect the evaluated morphological parameters. Secondly, different animal models as well as developmental stage could contribute to these differences. Cartilaginous growth plates are heterogeneous in terms of cell and tissue morphology as previously reported in two-dimensional studies in literature (Ballock & O'Keefe, 2003a, 2003b; C. E. Farnum & N. J. Wilsman, 1998) and is confirmed by our three-dimensional study. Thus, this nonhomogeneity in terms of morphology was expected in this study. The nonhomogeneity observed in both cellular and tissue morphology of the growth plate among its three histological zones would also lead to a heterogeneous biological response of either zones or chondrocytes to physical stimuli such as mechanical loading. It is thought that these heterogeneous changes would trigger nonhomogenous altered messages through the growth plate thickness and could eventually modulate the growth process by preferentially and/or sequentially affecting chondrocytes in certain growth plate zones.

Chondrocytes undergo several spatially oriented shape changes while progressing from the resting, proliferative to maturation stages along the growth direction. Reserve and hypertrophic chondrocytes were round relative to the marked flattened proliferative chondrocytes. This was confirmed by the significantly lower sphericity values of proliferative chondrocytes, as compared to reserve and hypertrophic zones. There is a slight but not significant cell flattening in the growth direction from the reserve to the proliferative zone. However, their average dimension perpendicular to growth direction changes significantly. Proliferative chondrocytes then hypertrophied along the growth direction with no significant enlargement noticed perpendicularly to growth direction in chondrocytes from proliferative to hypertrophic zones. Several stereological studies have demonstrated that the main portion of cellular enlargement is the result of water absorption in the hypertrophic zone (Buckwalter et al., 1986; Farnum et al., 2002; Hunziker et al., 1987). Conversely, a recent *in situ* study on rat growth plate chondrocytes (Bush, Parisinos, et al., 2008) found no significant difference between chondrocyte osmotic properties in the proliferative and hypertrophic zones, which would hence confirm hypertrophy as the

mechanism in charge of bone elongation. Both swelling and an increase in organelle number or size would most probably contribute to chondrocyte hypertrophy.

Differences in chondrocyte shape and organization along growth plate thickness could be related to depth-dependent arrangement of collagen fibrils and proteoglycan distribution in growth plate extracellular matrix. Chondrocytes in the reserve zone were round and randomly scattered in the extracellular matrix of the growth plate with no special alignment, while flattened proliferative and spherical hypertrophied chondrocytes were aligned along the direction of bone growth. In a study by Eggli et al. (1985), pericellular matrix (PCM) of chondrocytes in rat tibial growth plates has been shown to consist exclusively of proteoglycans. Presence of PCM around a cell is fully dependent on the preservation of these proteoglycans *in situ* as extraction of the proteoglycans by standard chemical fixation was found to result in profound changes in chondrocytes shape and size (Eggli et al., 1985). Considering the dense proteoglycan coat in proliferative PCM as compared to the hypertrophic and reserve PCM (Eggli et al., 1985) in which proteoglycan coats are less compact, the specific proliferative chondrocyte shape could be dictated by proteoglycan distribution in their PCM. In a study by Fujii et al. (2000) collagen fibrils were shown to be randomly oriented in the reserve zone as compared to their longitudinal orientation in the two other zones. The random arrangement of chondrocytes in the reserve zone, compared to the highly organized columnar cell arrangement in the proliferative and hypertrophic zones, could be controlled by the collagen fibril network at the tissue level.

Differences in cell/matrix volume ratio may explain the mechanical property of growth plate tissue. The cell/matrix volume ratio increased from the pool of the reserve zone to the proliferative zone, but decreased in the hypertrophic zone. This decrease from the proliferative zone to the hypertrophic zone is a new observation that could be explained by the compact columnar organization in the proliferative zone compared to the hypertrophic zone which leads to higher cellularity in this zone. Overall, the average cell/matrix volume ratio significantly increased approaching the calcification zone, which is consistent with published studies reporting an increase in cell/matrix volume ratio values from the resting to the hypertrophic zones (Farnum et al., 2002). Combining these morphological results with a biomechanical study on the same growth plate model (Sergerie et al., 2009) shows that the zone with the lowest cell/matrix volume ratio, that is the reserve zone, provides the highest rigidity, suggesting that the extracellular matrix (ECM) would have a greater contribution to mechanical properties as compared to

chondrocytes. However, other factors, such as intrinsic mechanical properties of the ECM, chondrocyte alignment, collagen fiber arrangement in each histological zone, might also influence the overall mechanical properties of each growth plate zone.

In conclusion, the present study investigated the *in situ* three-dimensional morphometry of growth plate tissue through its thickness. Growth plate morphology is heterogeneous among its three zones at both cellular and tissue levels. Chondrocytes are generally believed to represent the functional units for longitudinal bone growth. However, the mechanisms by which chondrocytes modulate longitudinal bone growth are unknown. Nonetheless, changes in chondrocyte height and volume have been implicated (Hunziker & Schenk, 1989; Hunziker et al., 1987). Furthermore, changes in chondrocyte shape, size, and volume within the growth plate are believed to play a role in the process of mechanical signal transduction that could eventually alter the bone growth process. One proposed pathway through which cells may observe changes in their mechanical environment is directly through deformation of the cellular membrane (Sachs, 1991; Watson, 1991). Hence, an important step toward understanding the role of chondrocyte membrane deformation in signal transduction is to characterize the shape and volume of growth plate chondrocytes. In this light, the ability to measure *in situ* cell morphology directly and monitor the changes in the direction of growth would allow a better understanding of the possible mechanisms through which abnormal growth is triggered

3.7 Acknowledgements

This research project was funded by the Canada Research Chair in Mechanobiology of the Pediatric Musculoskeletal System (I.V.), the Natural Sciences and Engineering Research Council of Canada (NSERC) and the MENTOR training program of Canadian Institutes of Health Research (CIHR, S.A.). Authors would like to thank Roxanne Wosu for the editorial revision of the document.

3.8 References

Alvarez-Leefmans, F. J., Altamirano, J., & Crowe, W. E. (1995). Use of ion-selective microelectrodes and fluorescent probes to measure cell volume. In K. Jacob & S. J. Dixon (Eds.), *Methods in neurosciences* (Vol. 27, pp. 361-391). London: Academic Press.

- Bachrach, N. M. (1995). *Growth plate chondrocyte deformation in situ and a biphasic inclusion model for cells within hydrated soft tissues*. (Ph.D.), Columbia University, New York.
- Ballock, R. T., & O'Keefe, R. J. (2003a). The biology of the growth plate. *J Bone Joint Surg Am*, 85-A(4), 715-726.
- Ballock, R. T., & O'Keefe, R. J. (2003b). Physiology and pathophysiology of the growth plate. *Birth Defects Res C Embryo Today*, 69(2), 123-143.
- Breur, G. J., Turgai, J., Vanenkevort, B. A., Farnum, C. E., & Wilsman, N. J. (1994). Stereological and serial section analysis of chondrocytic enlargement in the proximal tibial growth plate of the rat. *Anat Rec*, 239(3), 255-268.
- Breur, G. J., VanEnkevort, B. A., Farnum, C. E., & Wilsman, N. J. (1991). Linear relationship between the volume of hypertrophic chondrocytes and the rate of longitudinal bone growth in growth plates. *J Orthop Res*, 9(3), 348-359.
- Buckwalter, J. A., Mower, D., Schafer, J., Ungar, R., Ginsberg, B., & Moore, K. (1985). Growth-plate-chondrocyte profiles and their orientation. *J Bone Joint Surg Am*, 67(6), 942-955.
- Buckwalter, J. A., Mower, D., Ungar, R., Schaeffer, J., & Ginsberg, B. (1986). Morphometric analysis of chondrocyte hypertrophy. *J Bone Joint Surg Am*, 68(2), 243-255.
- Bush, P. G., & Hall, A. C. (2001). The osmotic sensitivity of isolated and *in situ* bovine articular chondrocytes. *Journal of orthopaedic research : official publication of the Orthopaedic Research Society*, 19(5), 768-778.
- Bush, P. G., Hall, A. C., & Macnicol, M. F. (2008). New insights into function of the growth plate: clinical observations, chondrocyte enlargement and a possible role for membrane transporters. *J Bone Joint Surg Br*, 90(12), 1541-1547.
- Bush, P. G., Parisinos, C. A., & Hall, A. C. (2008). The osmotic sensitivity of rat growth plate chondrocytes *in situ*; clarifying the mechanisms of hypertrophy. *J Cell Physiol*, 214(3), 621-629.
- Eerola, I., Elima, K., Markkula, M., Kananen, K., & Vuorio, E. (1996). Tissue distribution and phenotypic consequences of different type X collagen gene constructs in transgenic mice. *Ann N Y Acad Sci*, 785, 248-250.

- Eggli, P. S., Herrmann, W., Hunziker, E. B., & Schenk, R. K. (1985). Matrix compartments in the growth plate of the proximal tibia of rats. *Anat Rec*, 211(3), 246-257.
- Farnum, C. E., Lee, R., O'Hara, K., & Urban, J. P. (2002). Volume increase in growth plate chondrocytes during hypertrophy: the contribution of organic osmolytes. *Bone*, 30(4), 574-581.
- Farnum, C. E., & Wilsman, N. J. (1998). chapter 13: Growth plate cellular function. In J. A. Buckwalter, M. G. Ehrlich, L. J. Sandell & S. B. Trippel (Eds.), *Advances in the basis and clinical understanding of the growth plate*. (pp. 203-223). Chicago, IL: American Academy of Orthopaedic Surgeons.
- Farnum, C. E., & Wilsman, N. J. (2001). Converting a differentiation cascade into longitudinal growth: stereology and analysis of transgenic animals as tools for understanding growth plate function. *Curr Opin Orthop*, 12, 428-433.
- Fujii, T., Takai, S., Arai, Y., Kim, W., Amiel, D., & Hirasawa, Y. (2000). Microstructural properties of the distal growth plate of the rabbit radius and ulna: biomechanical, biochemical, and morphological studies. *Journal of orthopaedic research : official publication of the Orthopaedic Research Society*, 18(1), 87-93.
- Glade, M. J., & Belling, T. H., Jr. (1984). Growth plate cartilage metabolism, morphology and biochemical composition in over- and underfed horses. *Growth*, 48(4), 473-482.
- Hall, A. C. (1995). Volume-sensitive taurine transport in bovine articular chondrocytes. *The Journal of physiology*, 484 (Pt 3), 755-766.
- Huntley, J. S., Bush, P. G., Hall, A. C., & Macnicol, M. F. (2003). Looking at the living human growth plate. *CMAJ*, 168(4), 459-460.
- Hunziker, E. B., & Schenk, R. K. (1989). Physiological mechanisms adopted by chondrocytes in regulating longitudinal bone growth in rats. *J physiol*, 414, 55-71.
- Hunziker, E. B., Schenk, R. K., & Cruz-Orive, L. M. (1987). Quantitation of chondrocyte performance in growth-plate cartilage during longitudinal bone growth. *J Bone Joint Surg Am*, 69(2), 162-173.
- Johnson, I. (1998). Fluorescent probes for living cells. *Histochem J*, 30(3), 123-140.

- Johnstone, E. W., Leane, P. B., Kolesik, P., Byers, S., & Foster, B. K. (2000). Spatial arrangement of physeal cartilage chondrocytes and the structure of the primary spongiosa. *J Orthop Sci*, 5(3), 294-301.
- Kember, N. F. (1960). Cell division in endochondral ossification. A study of cell proliferation in rat bones by the method of tritiated thymidine autoradiography. *J Bone Joint Surg Br*, 42B, 824-839.
- Kember, N. F. (1978). Cell kinetics and the control of growth in long bones. *Cell Tissue Kinet*, 11(5), 477-485.
- Kerrigan, M. J., & Hall, A. C. (2008). Control of chondrocyte regulatory volume decrease (RVD) by $[Ca^{2+}]_i$ and cell shape. *Osteoarthritis Cartilage*, 16(3), 312-322.
- Sachs, F. (1991). Mechanical transduction by membrane ion channels: a mini review. *Mol Cell Biochem*, 104(1-2), 57-60.
- Sergerie, K., Lacoursiere, M. O., Levesque, M., & Villemure, I. (2009). Mechanical properties of the porcine growth plate and its three zones from unconfined compression tests. *J Biomech*, 42(4), 510-516.
- Stokes, I. A., Clark, K. C., Farnum, C. E., & Aronsson, D. D. (2007). Alterations in the growth plate associated with growth modulation by sustained compression or distraction. *Bone*, 41(2), 197-205.
- Stokes, I. A., Mente, P. L., Iatridis, J. C., Farnum, C. E., & Aronsson, D. D. (2002). Enlargement of growth plate chondrocytes modulated by sustained mechanical loading. *J Bone Joint Surg Am*, 84-A(10), 1842-1848.
- Urban, J. P., Hall, A. C., & Gehl, K. A. (1993). Regulation of matrix synthesis rates by the ionic and osmotic environment of articular chondrocytes. *J Cell Physiol*, 154(2), 262-270.
- Villemure, I., & Stokes, I. A. (2009). Growth plate mechanics and mechanobiology. A survey of present understanding. *J Biomech*, 42(12), 1793-1803.
- Watson, P. A. (1991). Function follows form: generation of intracellular signals by cell deformation. *FASEB J*, 5(7), 2013-2019.

- Wilsman, N. J., Farnum, C. E., Green, E. M., Lieferman, E. M., & Clayton, M. K. (1996). Cell cycle analysis of proliferative zone chondrocytes in growth plates elongating at different rates. *J Orthop Res*, 14(4), 562-572.
- Wilsman, N. J., Farnum, C. E., Lieferman, E. M., Fry, M., & Barreto, C. (1996). Differential growth by growth plates as a function of multiple parameters of chondrocytic kinetics. *J Orthop Res*, 14(6), 927-936.

CHAPTER 4 SCIENTIFIC ARTICLE #2: TISSUE AND CELLULAR MORPHOLOGICAL CHANGES IN GROWTH PLATE EXPLANTS UNDER COMPRESSION

This chapter introduces the second article written in the context of this thesis and responds to the second step of the second objective of this thesis as detailed in Chapter 2.

This article was published in *Journal of Biomechanics*© 2010 Elsevier Ltd. in June 2010.

The contribution of the first author in the preparation, obtaining the results, writing and literature review of this paper is estimated at 85%.

Journal of Biomechanics 43 (2010) 2582–2588



Contents lists available at ScienceDirect

Journal of Biomechanics

journal homepage: www.elsevier.com/locate/jbiomech
www.JBiomech.com



Tissue and cellular morphological changes in growth plate explants under compression

Samira Amini^{a,b}, Daniel Veilleux^c, Isabelle Villemure^{a,b,*}

^a Department of Mechanical Engineering, École Polytechnique of Montreal, P.O. Box 6079, Station "Centre-Ville", Montréal, Québec, Canada H3C 3A7

^b Sainte-Justine University Hospital Center, 3175 Côte-Ste-Catherine Rd., Montréal, Québec, Canada H3T 1C5

^c Department of Chemical Engineering, École Polytechnique of Montreal, P.O. Box 6079, Station "Centre-Ville", Montréal, Québec, Canada H3C 3A7

Detailed description of the contribution of different authors:

Samira Amini: Design, obtaining the results, analysis, interpretation of results, article writing and editing, responsible for the integrity of the work.

Daniel Veilleux: Obtaining and analysis of the results.

Isabelle Villemure: Design, interpretation of results, review of the article, responsible for the integrity of the work.

4.1 Abstract

The mechanisms by which mechanical loading may alter bone development within growth plates are still poorly understood. However, several growth plate cell or tissue morphological parameters are associated with both normal and mechanically modulated bone growth rates. The aim of this study was to quantify *in situ* the three-dimensional morphology of growth plate explants under compression at both at cell and tissue levels. Growth plates were dissected from ulnae of immature swine and tested under 15% compressive strain. Confocal microscopy was used to image fluorescently labeled chondrocytes in the three growth plate zones before and after compression. Quantitative morphological analyses at both cell (volume, surface area, sphericity, minor/major radii) and tissue (cell/matrix volume ratio) levels were performed. Greater chondrocyte bulk strains (volume decrease normalized to the initial cell volume) were found in the proliferative (35.4%) and hypertrophic (41.7%) zones, with lower chondrocyte bulk strains (24.7%) in the reserve zone. Following compression, the cell/matrix volume ratio decreased in the reserve and hypertrophic zones by 24.3% and 22.6% respectively, whereas it increased by 35.9% in the proliferative zone. The 15% strain applied on growth plate explants revealed zone-dependent deformational states at both tissue and cell levels. Variations in the mechanical response of the chondrocytes from different zones could be related to significant inhomogeneities in growth plate zonal mechanical properties. The ability to obtain *in situ* cell morphometry and monitor the changes under compression will contribute to a better understanding of mechanisms through which abnormal growth can be triggered.

4.2 Keywords

Growth plate, Chondrocytes, Compression, Bulk strain, Three-dimensional morphology, Confocal microscopy, Fluorescent labeling.

4.3 Introduction

Longitudinal bone growth has clinical implications in pediatric orthopaedics. This process takes place within the cartilaginous growth plate located at both ends of long bones. Cell shape, size and arrangement as well as tissue composition define three histologically distinct zones within the growth plate: the reserve (R), proliferative (P) and hypertrophic (H) zones (Figure 4-1), where

each zone plays a specific role in the growth process (C.E. Farnum & N.J. Wilsman, 1998; Hunziker & Schenk, 1989). Starting from the pool of chondrocytes in the reserve zone, chondrocytes divide in the proliferative zone, followed by a volumetric enlargement of chondrocytes in the hypertrophic zone (Hunziker & Schenk, 1989; Wilsman, Farnum, Leiferman, et al., 1996).

Growth plates are sensitive to their surrounding mechanical environment (Farnum et al., 2000; I. A. Stokes, 2002; I. A. Stokes et al., 2006; X. Wang & Mao, 2002). Early clinical observations have established that mechanical loading can modulate bone growth. Mechanical modulation of growth was first elucidated by the Hueter Volkmann law, where increased pressure on the growth plate retards growth and reduced pressure accelerates it (I. A. Stokes et al., 2006; I. A. Stokes et al., 2007; Villemure & Stokes, 2009). The phenomenon of mechanical growth modulation is implicated in the pathogenesis and treatment of infantile progressive skeletal deformities, such as adolescent idiopathic scoliosis, hyperkyphosis, genu varus/valgus and others (Frost, 1990; Mao & Nah, 2004). Several *in vivo* and *in vitro* studies provide evidence that growth plate chondrocytes sense their mechano-environment and respond to signals generated by mechanical loading of the tissue (Cancel et al., 2009; Gray, Pizzanelli, Grodzinsky, & Lee, 1988; Gray, Pizzanelli, Lee, Grodzinsky, & Swann, 1989; I. A. Stokes et al., 2007; I. A. Stokes et al., 2002; Villemure et al., 2005). Recently, an *in vivo* study on growth plates of three different animal species revealed that growth retardation under compression is associated with a reduced number of proliferative chondrocytes and a decreased chondrocytic enlargement occurring in the hypertrophic zone, with the latter having the greatest effects on bone growth changes (I. A. Stokes et al., 2007). It was also shown that chondrocytes proliferative activity reduces following increased compressive loading (Farnum et al., 2000; C.E. Farnum & N.J. Wilsman, 1998). However, the underlying mechanisms through which chondrocytes sense mechanical loading and eventually alter bone longitudinal growth process remain poorly understood.

Cell morphology is implicated in the regulation of cell differentiation, phenotypic expression and proliferation (Watson, 1991). Changes in cell shape or size could initiate signals through stretch-activated ion channels on the cells plasma membrane, which may further regulate second messenger activity (Sachs, 1991; Watson, 1991). Different studies on growth plate tissue have indeed characterized a strong relationship between bone growth rate and chondrocyte

hypertrophy (Breur et al., 1991; Buckwalter et al., 1985; Hunziker & Schenk, 1989; I. A. Stokes et al., 2007; I. A. Stokes et al., 2002). Conventional histology combined to chemical fixation has been used to characterize cell morphology in terms of chondrocytic height and volume in both normal and mechanically modulated growth plates (Breur et al., 1991; Buckwalter et al., 1985; Buckwalter et al., 1986; Hunziker & Schenk, 1989; I. A. Stokes et al., 2006; I. A. Stokes et al., 2007). An alternative approach to characterize cartilaginous tissue morphology is three-dimensional reconstruction of tissue using digital microscopic images (Bush, Parisinos, et al., 2008; Bush, Wokosin, & Hall, 2007; Guilak, 1994; Youn et al., 2006). In two recent *in situ* studies, compressive local strains both at tissue and cell levels (Bachrach, 1995) and continuous strain patterns along the growth plate thickness under compression (Villemure et al., 2007) have been determined using an experimental assembly combining a loading apparatus with a confocal microscope. These studies confirmed the non-homogeneous mechanical response of growth plate to loading through its three histological zones. Similar configurations have been extensively used to address articular cartilage 3D deformation under compression loading at both tissue (C. C. B. Wang et al., 2002), cellular (Guilak et al., 1995) and intracellular (Guilak, 1995) levels. However, little is known about compression induced 3D morphological characteristics of intact growth plate chondrocytes maintained within their extracellular matrix. This information would further help us to understand the *in situ* effect of the mechanical environment on the biological response of growth plate chondrocytes. The aim of this study was to quantify *in situ* the three-dimensional growth plate morphology under compression at both cell and tissue levels using fluorescence labeling techniques combined with three-dimensional reconstruction of serial confocal sections.

4.4 Methods

4.4.1 Animal Model and Specimen Preparation

Distal ulnae from four-week old swine were obtained within 3 h of slaughter from a local abattoir. Full depth explants of epiphyseal bone/growth plate/metaphyseal bone (N=6) were harvested along the bone longitudinal axis using 6 mm diameter biopsy punches (Figure 4-1). For each sample, upper and lower surfaces of the disks were trimmed using a Vibratome (Vibratome 1500 Sectioning System) to obtain two parallel surfaces and to provide the thickness of each

growth plate sample. Using a custom made tissue slicer (Zivic Instruments, USA), each cylindrical specimen was further cut into semi-cylindrical halves parallel to the longitudinal axis of the sample to expose the growth plate along the resulting planar surface. Growth plate explants were kept in HBSS at room temperature before staining to avoid drying. Each semi-cylindrical specimen was then incubated in a solution of 0.5 mM Calcein AM (membrane-permeant dye, Molecular Probes) for 30 min at 37 °C in an atmosphere of 95% O₂ and 5% CO₂ to fluorescently label live chondrocytes cytoplasm. The optimal stain concentration was previously determined using viability testing with dual staining of cell cytoplasm (Calcein AM, Molecular Probes) and dead cell nucleus (Ethidium homodimer-1, Molecular Probes).

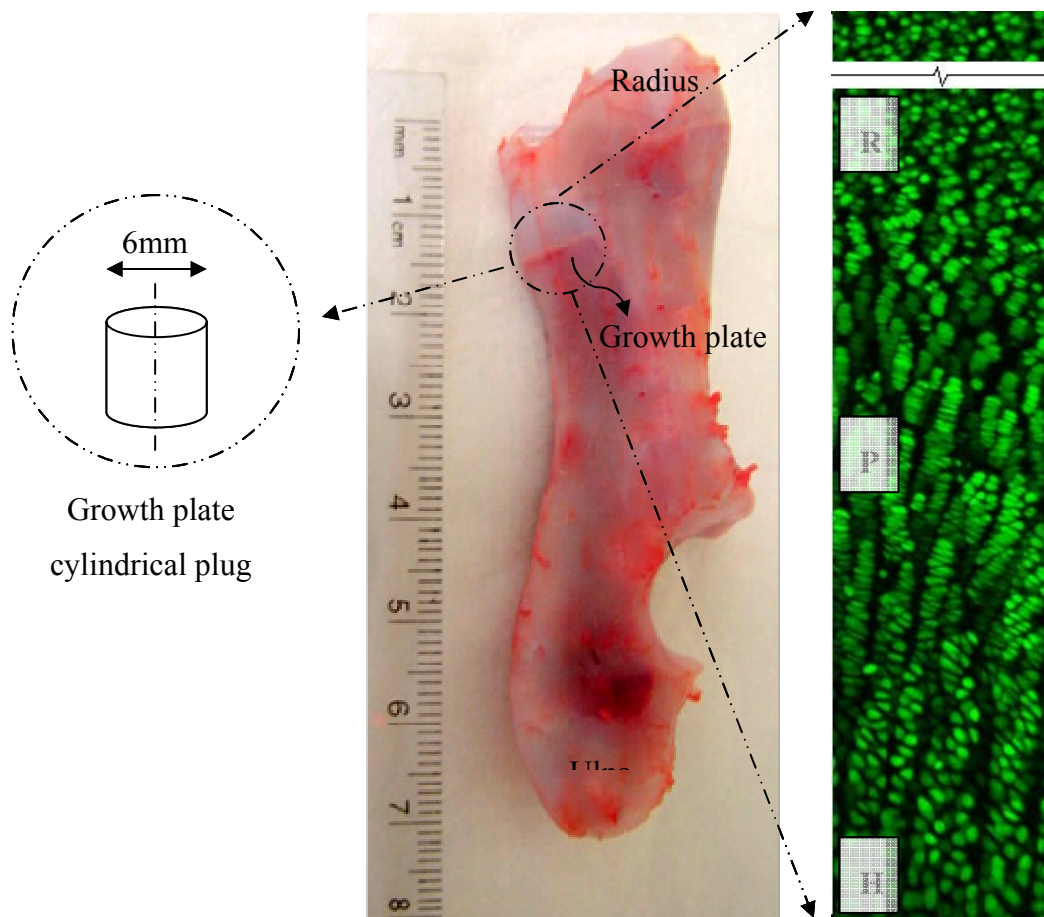


Figure 4-1 : (Right) Typical confocal section of a fluorescently labelled porcine growth plate showing its three histological zones: reserve (R), proliferative (P) and hypertrophic (H). (Left) Growth plate cylindrical plug extracted using a 6 mm biopsy punch. (Center) The growth plate site is located between the metaphysis and secondary ossification center of the epiphysis.

4.4.2 Imaging and Loading Protocol

Following staining, each semi-cylindrical explant was placed in a custom-made loading apparatus (Figure 4-2), mounted on the stage of an inverted laser scanning confocal microscope (LSM 510 Carl Zeiss Inc., Germany), similar to other studies on articular cartilage (Guilak, 1995; Guilak et al., 1995) and growth plate (Villemure et al., 2007).

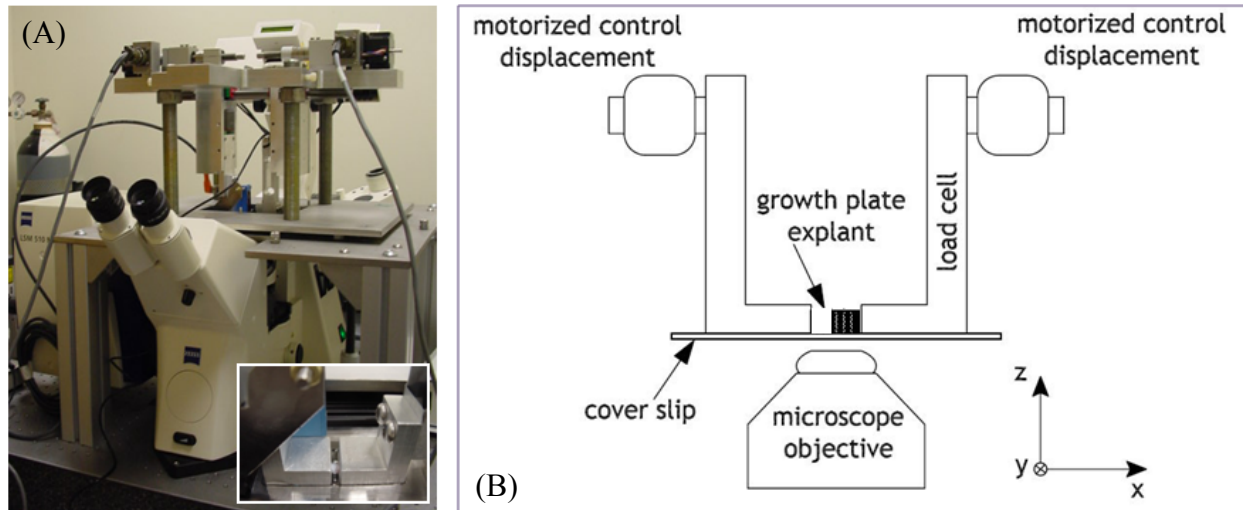


Figure 4-2 : Experimental set up: (A) custom-made loading apparatus mounted on the stage of an inverted laser scanning confocal microscope (B) Schematic of the loading apparatus.

The exposed flat edge of the explant was put against a clean cover slip placed over the microscope objective and sandwiched between the two platens to apply semi-confined compression. Uniaxial compressive load was then applied at the metaphyseal (fixed) and epiphyseal (mobile) edges of the explants. The platens displacement along the longitudinal axis of the explants was controlled by a custom designed software (Lab View, National Instruments, Inc., USA) and the resulting applied forces were recorded by a single point load cell (Tede-Huntleigh, Intertechonology Inc.). For each sample, a pre-strain (5%) was first applied to establish uniform contact between the explant and two platens, followed by a stress relaxation test (10% strain), both at a strain rate of $1.7 \times 10^{-3} \text{ s}^{-1}$. The relaxation period was fixed at 20 min based on a relaxation criterion of $8 \times 10^{-6} \text{ N/s}$ allowing samples to reach a relaxed state. The explant was kept moist during the whole test with sHBSS. For each of the 12 semi-cylindrical samples, a random field of view was chosen in one of the three histological zones. For each selected field, serial

sections of 512×512 pixels were recorded using a 40×: 0.6 NA objective with a 1.27 µm section intervals at a depth of ~50–150 µm at two time points: prior to compression loading and after tissue relaxation. In each field, a total of 1–6 chondrocytes and 1–4 regions were randomly selected for cell and tissue level analysis, respectively. A 488 line of an argon laser was set to permit optimal image quality with minimal dye bleaching, at 15% of full power (Guilak, 1994, 1995). Complementary experiments (data not shown) showed that photobleaching was negligible following two volume images and not causing significant changes in chondrocytes volume. The images were collected using a 500–550 nm band-pass filter. The procedures of dissection, tissue preparation and microscopy were all carried out on the same day.

4.4.3 Three-dimensional Reconstruction and Quantitative Analysis

In order to determine chondrocyte boundary, a cut-off intensity value between cells and matrix was chosen according to an experimental calibration of IMARIS software performed prior to the experiments using fluorescent Fluoresbrite (TM) latex beads (Polyscience Inc., Warrington) (Bush & Hall, 2003; Bush et al., 2007) of known diameter (10.16 ± 0.1 µm) and volume (549 µm³) in the same conditions as the ones used to image growth plate chondrocytes. Prior to three-dimensional reconstruction, optical sections were deconvolved using Huygens software (Huygens Essential, Scientific Volume Imaging BV) in order to partially remove intrinsic distortion of 3D microscopic images. Three-dimensional reconstruction and quantitative morphological analyses at both tissue and cell levels were performed using IMARIS 6.0 software (Bitplane). For cell level analysis, individual chondrocytes were isolated at regions of interest and reconstructed to assess morphological parameters including cell volume, cell surface area and sphericity ($\pi^{1/3}(6V)^{2/3}/A$, V: cell volume, A: cell surface area). At tissue level, cell/matrix volume ratio was extracted from the 3D reconstructed tissue in different histological zones of the growth plate.

4.4.4 Statistical Analysis

Data were expressed as means ± standard deviations for each morphological parameter studied either at cell level (cell volume, cell surface area, cell sphericity, minor and major radii) or at tissue level (cell/matrix volume ratio) on each set of data (pre-compression and post-relaxation) in the three histological zones based on the number of semi-cylindrical samples (12) and number

of chondrocytes chosen (n). A one-way ANOVA for repeated measurements was carried out to determine whether the difference between the mean values of each investigated parameter reached a certain level of significance ($p\text{-value} \leq 0.05$) depending upon the level of compression (prior to compression: 0% and following compression: 15%). The post-hoc comparisons between data sets were performed using the Tukey's method. Data were processed using a statistical analysis software (Statistica 7.0, Statsoft Inc.)

4.5 Results

Ulnar growth plate samples were obtained from pigs of average weight 3.35 ± 2.13 kg and their thicknesses varied between 2300 and 3800 μm with a mean value of 3170 ± 520 μm . Typical experimental stress relaxation curves obtained for growth plate semi-cylinder samples in response to 15% platen-to-platen strain are shown in Figure 4-3.

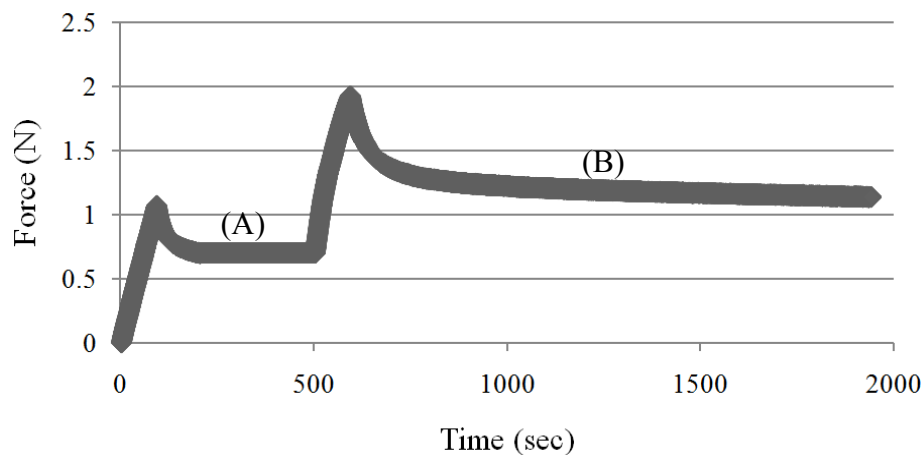


Figure 4-3 : Typical experimental stress relaxation curves of growth plate samples undergoing semi-confined compression at 5% pre-strain (A) followed by 10% strain (B) at a strain rate of $1.7\text{E-}3 \text{ s}^{-1}$.

Typical 3D reconstructed morphology of growth plate chondrocytes in each histological zone before compression (top) and after compression and relaxation (bottom) is presented in Figure 4-4. Chondrocytes exhibited three-dimensional shape changes among the three histological zones of the growth plate. Pre-compression and post-relaxation morphometric data are summarized in Table 4-1 and graphically presented in Figure 4-5 for both cell and tissue levels. A total of 48 and

68 chondrocytes were analyzed in order to assess intact and loaded cell level morphology respectively.

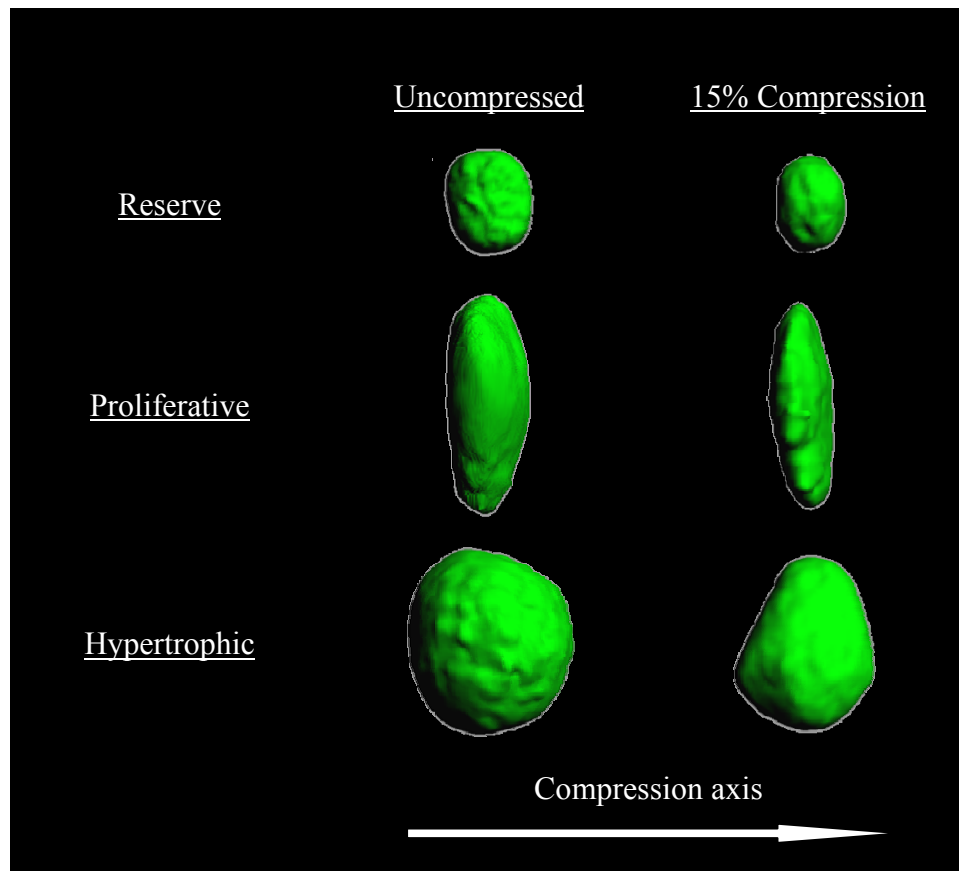


Figure 4-4 : Typical three-dimensional reconstructed chondrocytes in each histological zone before compression (intact) and after compression and relaxation

At 15% compression, chondrocytes volume decreased in the three histological zones. Corresponding chondrocytes bulk strain (volume decrease normalized to the initial cell volume) reached 24.7%, 35.4%, and 41.7% in the reserve, proliferative and hypertrophic zones respectively (Figure 4-5a). Chondrocytes surface area also decreased in all histological zones following uniaxial compression. Corresponding chondrocyte surface area changes reached 6.9% in the reserve zone, 30.7% in the proliferative zone and 22.9% in the hypertrophic zone (Figure 4-5b). Chondrocytes also underwent a decrease in the major and minor radii as well as sphericity following compression in all histological zones. The greatest decrease in minor chondrocytic radius occurred in the proliferative zone (19.6%), while the lowest was in the reserve zone (8.5%) (Figure 4-5c). Following compression, the highest decrease for major radius (18.3%) was

detected in hypertrophic chondrocytes as compared to proliferative (14.1%) and reserve zone (11.2%) (Figure 4-5d). The highest sphericity change happened in the hypertrophic zone (14.6%), compared to the two other zones (Figure 4-5e). Following compression, the cell/matrix volume ratio decreased by 24% and 23% in the reserve and hypertrophic zones respectively, whereas it increased by 36% in the proliferative zone (Figure 4-5f).

In response to the 15% platen-to-platen strain, chondrocytes volume (Figure 4-5a) and major radius (Figure 4-5d) significantly decreased for chondrocytes from the three zones.

No significant change was detected in reserve chondrocytes surface area (Figure 4-5b) and minor radius (Figure 4-5c) following compression as compared to proliferative and hypertrophic chondrocytes, where corresponding changes reached significance. Chondrocytes also underwent a significant decrease in sphericity, except in the proliferative zone (Figure 4-5e). Cell/matrix volume ratios showed significant decreases (Figure 4-5f) in the reserve and hypertrophic zones and a significant increase in the proliferative zone.

Table 4-1 : Cell and tissue level morphological parameters in three histological zones of growth plate at platen-to-platen compression of 0% and 15%. (mean values \pm standard deviations)

		Reserve zone		Proliferative zone		Hypertrophic zone	
		0%	15%	0%	15%	0%	15%
		(n=21)	(n=25)	(n=17)	(n=22)	(n=10)	(n=21)
Cell level data	Volume (μm^3)	1250.6 \pm 233.3	940.7 \pm 229.3	2103.6 \pm 544.7	1359.1 \pm 276.3	5190.55 \pm 757.6	3023.9 \pm 996.5
	Surface area (μm^2)	667.7 \pm 85.9	621.6 \pm 142.4	1299.1 \pm 300.0	900.7 \pm 115.1	1780 \pm 335.8	1372.1 \pm 447.5
	Minor radius (μm)	4.7 \pm 0.5	4.3 \pm 0.7	4.6 \pm 0.9	3.7 \pm 0.6	8.7 \pm 0.7	7.1 \pm 1.0
	Major radius (μm)	10.7 \pm 1.1	9.5 \pm 1.6	12.8 \pm 1.5	11.0 \pm 1.3	14.2 \pm 1.4	11.6 \pm 2.0
	Sphericity ($(\mu\text{m}^3)^{2/3}/\mu\text{m}^2$)	0.84 \pm 0.05	0.76 \pm 0.10	0.66 \pm 0.12	0.59 \pm 0.11	0.89 \pm 0.04	0.76 \pm 0.09
		(n=11)	(n=14)	(n=14)	(n=10)	(n=6)	(n=6)
Tissue level data	Cell/matrix volume ratio ($\mu\text{m}^3/\mu\text{m}^3$)	0.13 \pm 0.02	0.10 \pm 0.03	0.18 \pm 0.03	0.24 \pm 0.05	0.17 \pm 0.02	0.13 \pm 0.02

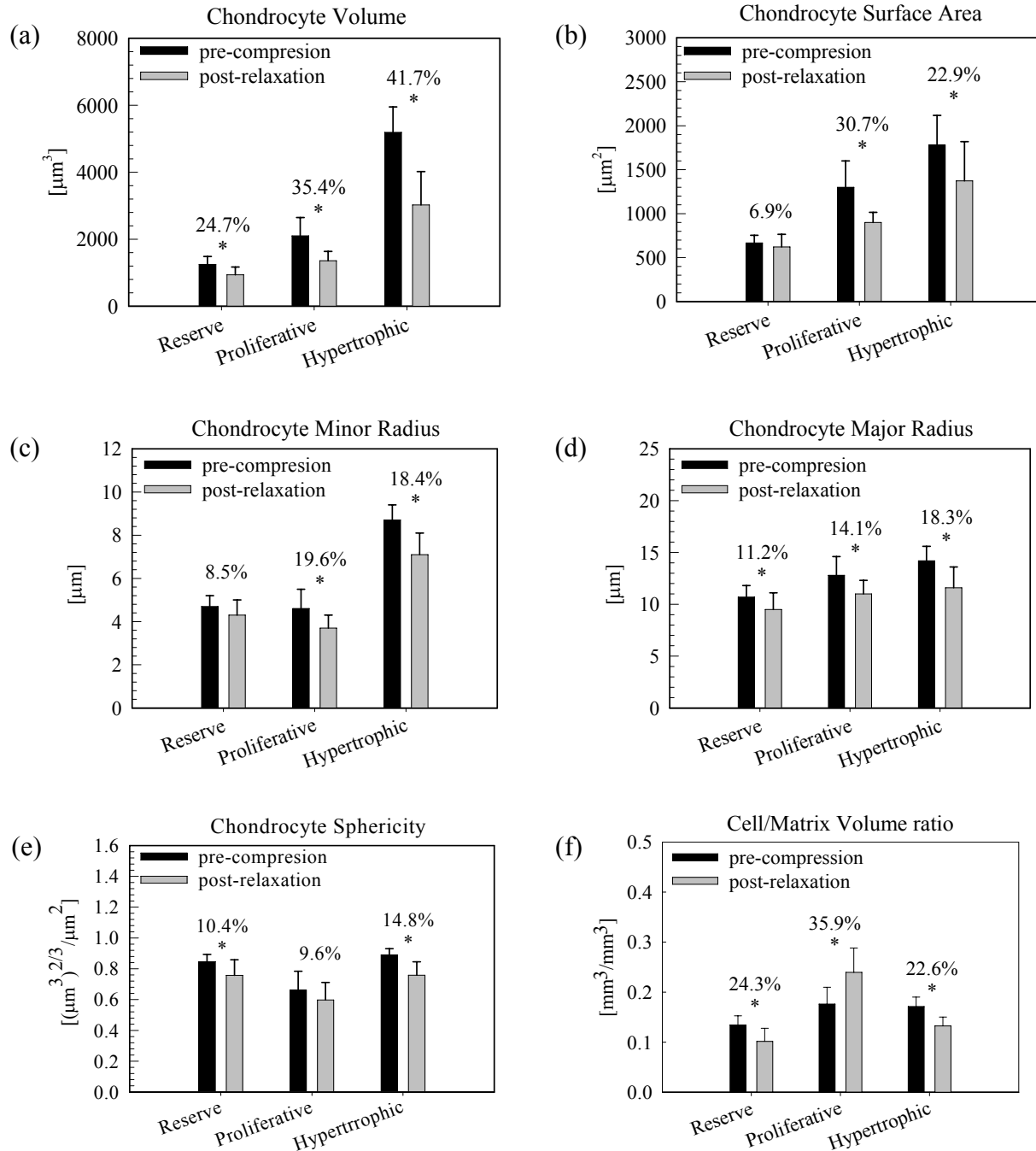


Figure 4-5 : Morphometrical changes at cellular level ((a) volume, (b) surface area, (c) minor radius, (d) major radius and (e) sphericity) and tissue level ((f) cell/matrix volume ratio) in response to 15% uniform tissue compression. Significant differences between pre-compression and post-relaxation parameters are shown with asterisks (p-value ≤ 0.05).

4.6 Discussion

The aim of this study was to characterize compression induced morphological changes in growth plate tissue at both cellular and tissue levels using stress relaxation tests under semi-confined compression combined with confocal microscopy and fluorescent labeling techniques. Morphometric results are in agreement with published studies on growth plate chondrocyte morphology based on conventional histology and stereological techniques (Farnum et al., 2002; Hunziker & Schenk, 1989).

Chondrocytes undergo significant zone-dependent shape and size changes with compression, most probably related to heterogeneous mechanical properties characterizing the three growth plate zones. In response to compression, larger changes in volume and surface area were found in the hypertrophic and proliferative zones. Significant differences have been reported in Young's modulus among the three growth plate zones, where the reserve zone was found twice as stiff as the proliferative and hypertrophic zones along the compression axis and about three times stiffer in the transverse plane (Sergerie et al., 2009). Although no study up to date addressed the mechanical properties of the chondrocytes in the different growth plate zones, some recent studies evaluated the Young's modulus of chondrocytes in the different layers of

articular cartilage using indentation combined with atomic force microscopy (Darling, Zauscher, & Guilak, 2006), micropipette aspiration (Trickey, Lee, & Guilak, 2000) and unconfined compression (Leipzig & Athanasiou, 2005; Shieh & Athanasiou, 2006). All these studies suggested that chondrocytes from the superficial zone, which resemble the most the chondrocytes from the reserve zone of the growth plate, are significantly stiffer than chondrocytes found in the middle/deep layers. Considering the greater reserve zone mechanical rigidity at tissue and cell levels, reserve chondrocytes would undergo lower mechanical deformation compared to proliferative and hypertrophic chondrocytes. Proliferative and hypertrophic zones were also reported three times as permeable as the reserve zone in the radial direction (Sergerie et al., 2009) and that could further contribute to higher chondrocyte deformations in these two more flexible zones. Fluid flow through a more permeable matrix would cause little frictional strain and hence zones with higher permeability would be more prone to undergo higher tissue and cellular deformations. It should be noted that observed chondrocyte bulk strains were much greater than

the applied platen-to-platen strain; they reached 1.7, 2.3 and 2.8 times 15% strain, respectively, for the reserve, proliferative and hypertrophic zones. This emphasizes that the structural role of the extracellular matrix is of utmost importance in the mechanical behaviour of soft tissues.

The reverse trends observed for changes in cell/matrix volume ratio could be related to zonal chondrocytes arrangement and to relative cellular/intercellular strains developing within the three zones. Decreases in cell/matrix volume ratio for the reserve and hypertrophic zones are reverse in the proliferative zone, where an increase in the cell/matrix volume ratio was observed. This implies that proliferative chondrocytes undergo less deformation compared to their extracellular matrix, whereas higher deformations develop in chondrocytes of the reserve and hypertrophic zones compared to their surrounding extracellular matrix. In a 2D study carried out by Bachrach (Bachrach, 1995), higher compressive strains were reported in the extracellular matrix compared to the chondrocytes in the proliferative zone and this trend was reported as reverse in the reserve zone, similar to our results. The highly compact columnar organization of chondrocytes in the proliferative zone of the growth plate, compared to their less columnar arrangement in the hypertrophic zone and their random distribution in an abundant extracellular matrix in the reserve zone, as well as the non-homogenous cell density in different histological zones of the growth plate and mechanical properties at cellular and matrix level could also contribute to these observed differences in deformation sharing between chondrocytes and their surrounding extracellular matrix.

The depth dependent bio-composition of growth plate extracellular matrix could partly address the deformational state of growth plate chondrocytes. Type II collagen and aggrecan are the two main structural components of the growth plate extracellular matrix that are believed to provide tissue with its mechanical rigidity. Alini et al. (1992) characterized type II collagen and proteoglycan distributions within bovine fetal tibial growth plates in 16 horizontal strata of equal heights. Type II collagen content exhibited a gradual decrease from the proliferative to the hypertrophic zones, whereas proteoglycan content increased as chondrocytes hypertrophy in the growth direction. More recently, a qualitative evaluation by Mwale et al. (2002) on the same animal model confirmed that type II collagen reaches its lowest content in the hypertrophic zone and that proteoglycans are maximized in regions where mineral deposition is initiated in the proliferative zone through regions of the hypertrophic zone neighboring the chondro-osseous

junction, where mineral deposition reaches its maximum (Mwale et al., 2002). Considering the important structural role of both type II collagen and proteoglycan in the mechanical behaviour of cartilaginous tissue, chondrocytes surrounded by extracellular matrix of low collagen/proteoglycan contents would be expected to undergo higher deformations upon compression. In our study, the gradual increase observed in chondrocyte bulk strains from the reserve to hypertrophic zones could be explained by the corresponding decrease in collagen content along growth plate thickness, but not by the concurrent increase in proteoglycan content. Therefore, the heterogeneous depth-dependent growth plate matrix composition cannot fully address the chondrocytes deformational state observed along the growth plate thickness, suggesting that the three-dimensional interaction of growth plate structural elements (proteoglycans, collagen fibrils and the interstitial fluid) overall determines chondrocytes deformation under tissue compression. However, the lowest cell density in the reserve zone, as quantified by cell/matrix volume ratio at 0% compression, should not be overlooked. The abundant extracellular matrix in the reserve zone could also protect the chondrocytes from high degree of deformation under compression loading.

Hypertrophic chondrocyte strains could contribute to reported decreasing growth rate in response to growth plate compression as stated by Hueter-Volkmann law. There is experimental evidence that chondrocytic hypertrophy is of utmost importance in both normal and mechanically modulated bone growth. Normal bone growth rates are highly related to chondrocyte shape remodeling (Hunziker & Schenk, 1989). A high degree of correlation has been established between hypertrophic chondrocytes volume and longitudinal bone growth rate (Breur et al., 1991; Buckwalter et al., 1985; Hunziker & Schenk, 1989). Wilsman et al. (1996), revealed that 50% of the difference between the growth rates of different growth plates would be explained by differing chondrocytes height in the hypertrophic zone. In addition, experimental studies have shown that proportional changes in bone growth rate following loading was mostly explained by changes in the number of proliferating chondrocytes and in the amount of chondrocyte hypertrophy (I. A. Stokes et al., 2006; I. A. Stokes et al., 2007; I. A. Stokes et al., 2005). In our study, hypertrophic chondrocytes showed the greatest deformations among chondrocytes from the three histological zones. Hence, hypertrophic chondrocytes could then be more inclined to trigger altered biological messages, potentially thorough cell membrane stretch, which is believed

to modulate second messenger activity (Sachs, 1991; Watson, 1991), and eventually cause growth deceleration under mechanical compression.

Although the 3D deformation of articular cartilage under compression loading has been extensively studied at both tissue and cellular levels, this study provides, for the very first time, an *in situ* three-dimensional morphological analysis of growth plate cell and tissue under compression. Our findings suggest that the growth plate and its constitutive chondrocytes undergo significant heterogeneous and zone-dependent deformation, where the proliferative and hypertrophic chondrocytes experience greater bulk strains as compared to the reserve zone. Variations in the mechanical response of chondrocytes from different zones could be related to significant inhomogeneities in growth plate zonal mechanical properties and histomorphology. This knowledge on chondrocytes mechanical response is very important for growth plate mechanobiology, where the effects of mechanical loading on the physis biological response and the resulting endochondral growth rate are investigated. Based on obtained results, the less rigid hypertrophic and proliferative chondrocytes would be more likely to trigger abnormal endochondral growth under compressive loading. Future studies of the deformational behaviour of growth plate at tissue and cellular levels with aging or disease would also offer a better understanding of physis physiology and pathology

4.7 Conflict of interest statement

There are no conflicts of interest related to this manuscript.

4.8 Acknowledgements

The authors acknowledge the participation of Catherine Boyer and Thierry Lafrance in the experimental set-up design. This research project was funded by the Canada Research Chair in Mechanobiology of the Pediatric Musculoskeletal System (I.V.), the Natural Sciences and Engineering Research Council of Canada (NSERC) and the MENTOR training program of Canadian Institutes of Health Research (CIHR, S.A.).

4.9 References

- Alini, M., Y. Matsui, et al., 1992. The extracellular matrix of cartilage in the growth plate before and during calcification: changes in composition and degradation of type II collagen. *Calcif Tissue Int* 50(4): 327-35.
- Bachrach, N. M. (1995). *Growth plate chondrocyte deformation in situ and a biphasic inclusion model for cells within hydrated soft tissues*. (Ph.D.), Columbia University, New York.
- Breur, G. J., B. A. VanEnkevort, et al., 1991. Linear relationship between the volume of hypertrophic chondrocytes and the rate of longitudinal bone growth in growth plates. *Journal of orthopaedic research* 9(3): 348-59.
- Buckwalter, J. A., D. Mower, et al., 1985. Growth-plate-chondrocyte profiles and their orientation. *The Journal of bone and joint surgery. American volume* 67(6): 942-55.
- Buckwalter, J. A., D. Mower, et al., 1986. Morphometric analysis of chondrocyte hypertrophy. *The Journal of bone and joint surgery. American volume* 68(2): 243-55.
- Bush, P. G. and A. C. Hall, 2003. The volume and morphology of chondrocytes within non-degenerate and degenerate human articular cartilage. *Osteoarthritis Cartilage* 11(4): 242-51.
- Bush, P. G., C. A. Parisinos, et al., 2008. The osmotic sensitivity of rat growth plate chondrocytes *in situ*; clarifying the mechanisms of hypertrophy. *J Cell Physiol* 214(3): 621-9.
- Bush, P. G., D. L. Wokosin, et al., 2007. Two-versus one photon excitation laser scanning microscopy: critical importance of excitation wavelength. *Front Biosci* 12: 2646-57.
- Cancel, M., G. Grimard, et al., 2009. Effects of *in vivo* static compressive loading on aggrecan and type II and X collagens in the rat growth plate extracellular matrix. *Bone* 44(2): 306-15.
- Choi, J. B., I. Youn, et al., 2007. Zonal changes in the three-dimensional morphology of the chondron under compression: the relationship among cellular, pericellular, and extracellular deformation in articular cartilage. *J biomech* 40(12): 2596-603.
- Darling, E. M., S. Zauscher, et al., 2006. Viscoelastic properties of zonal articular chondrocytes measured by atomic force microscopy. *Osteoarthritis Cartilage* 14(6): 571-9.

- Farnum, C. E., R. Lee, et al., 2002. Volume increase in growth plate chondrocytes during hypertrophy: the contribution of organic osmolytes. *Bone* 30(4): 574-81.
- Farnum, C. E., A. Nixon, et al., 2000. Quantitative three-dimensional analysis of chondrocytic kinetic responses to short-term stapling of the rat proximal tibial growth plate. *Cells, tissues, organs* 167(4): 247-58.
- Farnum, C. E. and N. J. Wilsman, 1998. Effects of distraction and compression on growth plate function. In: J. A. Buckwalter, M. G. Ehrlich, L. J. Sandell and S. B. Trippel, (Eds.), *Skeletal Growth and Development*. AAOS, Rosemont, pp. 517-530.
- Frost, H. M., 1990. Skeletal structural adaptations to mechanical usage (SATMU): 3. The hyaline cartilage modeling problem. *The Anatomical record* 226(4): 423-32.
- Gray, M. L., A. M. Pizzanelli, et al., 1988. Mechanical and physiochemical determinants of the chondrocyte biosynthetic response. *Journal of orthopaedic research* 6(6): 777-92.
- Gray, M. L., A. M. Pizzanelli, et al., 1989. Kinetics of the chondrocyte biosynthetic response to compressive load and release. *Biochimica et biophysica acta* 991(3): 415-25.
- Guilak, F., 1994. Volume and surface area measurement of viable chondrocytes *in situ* using geometric modelling of serial confocal sections. *J Microsc* 173(Pt 3): 245-56.
- Guilak, F., 1995. Compression-induced changes in the shape and volume of the chondrocyte nucleus. *J Biomech* 28(12): 1529-41.
- Guilak, F., A. Ratcliffe, et al., 1995. Chondrocyte deformation and local tissue strain in articular cartilage: a confocal microscopy study. *J Orthop Res* 13(3): 410-21.
- Hunziker, E. B. and R. K. Schenk, 1989. Physiological mechanisms adopted by chondrocytes in regulating longitudinal bone growth in rats. *The Journal of physiology* 414: 55-71.
- Leipzig, N. D. and K. A. Athanasiou, 2005. Unconfined creep compression of chondrocytes. *J Biomech* 38(1): 77-85.
- Mao, J. J. and H. D. Nah, 2004. Growth and development: hereditary and mechanical modulations. *American journal of orthodontics and dentofacial orthopedics* 125(6): 676-89.

- Mwale, F., E. Tcheta, et al., 2002. The assembly and remodeling of the extracellular matrix in the growth plate in relationship to mineral deposition and cellular hypertrophy: an *in situ* study of collagens II and IX and proteoglycan. *J Bone Miner Res* 17(2): 275-83.
- Sachs, F., 1991. Mechanical transduction by membrane ion channels: a mini review. *Molecular and cellular biochemistry* 104(1-2): 57-60.
- Sergerie, K., M. O. Lacoursiere, et al., 2009. Mechanical properties of the porcine growth plate and its three zones from unconfined compression tests. *Journal of biomechanics* 42(4): 510-6.
- Shieh, A. C. and K. A. Athanasiou, 2006. Biomechanics of single zonal chondrocytes. *J Biomech* 39(9): 1595-602.
- Stokes, I. A., 2002. Mechanical effects on skeletal growth. *Journal of musculoskeletal & neuronal interactions* 2(3): 277-80.
- Stokes, I. A., D. D. Aronsson, et al., 2006. Endochondral growth in growth plates of three species at two anatomical locations modulated by mechanical compression and tension. *Journal of orthopaedic research* 24(6): 1327-34.
- Stokes, I. A., K. C. Clark, et al., 2007. Alterations in the growth plate associated with growth modulation by sustained compression or distraction. *Bone* 41(2): 197-205.
- Stokes, I. A., J. Gwadera, et al., 2005. Modulation of vertebral and tibial growth by compression loading: diurnal versus full-time loading. *Journal of orthopaedic research* 23(1): 188-95.
- Stokes, I. A., P. L. Mente, et al., 2002. Enlargement of growth plate chondrocytes modulated by sustained mechanical loading. *J Bone Joint Surg Am* 84-A(10): 1842-8.
- Trickey, W. R., G. M. Lee, et al., 2000. Viscoelastic properties of chondrocytes from normal and osteoarthritic human cartilage. *J Orthop Res* 18(6): 891-8.
- Villemure, I., M. A. Chung, et al., 2005. Static compressive loading reduces the mRNA expression of type II and X collagen in rat growth-plate chondrocytes during postnatal growth. *Connective tissue research* 46(4-5): 211-9.

CHAPTER 5 SCIENTIFIC ARTICLE #3: STRESS RELAXATION OF SWINE GROWTH PLATE IN SEMI-CONFINED COMPRESSION: DEPTH DEPENDANT TISSUE DEFORMATIONAL BEHAVIOR VERSUS EXTRACELLULAR MATRIX COMPOSITION AND COLLAGEN FIBER ORGANIZATION

This chapter introduces the third article written in the context of this thesis and responds to the second (step two), third, fourth and fifth objectives of this thesis as detailed in Chapter 2.

This article was accepted for publication in *Biomechanics and Modeling in Mechanobiology* © Springer in December 2011.

The contribution of the first author in the preparation, obtaining the results, writing and literature review of this paper is estimated at 85%.

Detailed description of the contribution of different authors:

Samira Amini: Design, obtaining the results, analysis, interpretation of results, article writing and editing, responsible for the integrity of the work.

Farhad Mortazavi: Analysis of the DIC results.

Jun Sun: Technical help (biochemical content evaluation).

Martin Levesque: Review of the article.

Caroline Hoemann: Design, interpretation of results, review of the article, responsible for the integrity of the work.

Isabelle Villemure: Design, interpretation of results, review of the article, responsible for the integrity of the work.

5.1 Abstract

Introduction: Mechanical environment is one of the regulating factors involved in the process of longitudinal bone growth of the cartilaginous growth plate. Non-physiological compressive loading can lead to infantile and juvenile musculoskeletal deformities particularly during growth spurt. We hypothesized that tissue mechanical behavior in sub-regions (reserve, proliferative and hypertrophic zones) of the growth plate is related to its collagen and proteoglycan content as well as its collagen fiber orientation.

Objectives: To characterize the strain distribution through growth plate thickness and to evaluate biochemical content and collagen fiber organization of the three histological zones of growth plate tissue.

Methods: Distal ulnar growth plate samples (N=29) from 4-week old pigs were analyzed histologically for collagen fiber organization (N=7) or average zonal thickness (N=8), or trimmed into the three average zones, based on the estimated thickness of each histological zone, for biochemical analysis of water, collagen and glycosaminoglycan content (N=7). Other samples (N=7) were tested in semi-confined compression under 10% compressive strain. Digital images of the fluorescently labeled nuclei were concomitantly acquired by confocal microscopy before loading and after tissue relaxation. Strain fields were subsequently calculated using a custom-designed 2D digital image correlation algorithm.

Results: Depth-dependent compressive strain patterns and collagen content were observed. The proliferative and hypertrophic zone developed the highest axial and transverse strains, respectively, under compression compared to the reserve zone, in which the lowest axial and transverse strains arose. The collagen content per wet mass was significantly lower in the proliferative and hypertrophic zones compared to the reserve zone, and all three zones had similar glycosaminoglycan and water content. Polarized light microscopy showed that collagen fibers were mainly organized horizontally in the reserve zone and vertically aligned with the growth direction in the proliferative and hypertrophic zones.

Discussion: Higher strains were developed in growth plate areas (proliferative and hypertrophic) composed of lower collagen content and of vertical collagen fiber organization. The stiffer

reserve zone, with its higher collagen content and collagen fibers oriented to restrain lateral expansion under compression, could play a greater role of mechanical support compared to the proliferative and hypertrophic zones, which could be more susceptible to be involved in an abnormal growth process.

5.2 Keywords

growth plate, mechanical behavior, biochemical content, collagen fiber orientation, polarized light microscopy, mechanobiology, confocal microscopy, compressive strain, digital image correlation (DIC).

5.3 Abbreviations

DIC: digital image correlation, ROI: region of interest, DMMB: 1,9-dimethylmethylene blue, OH-Pro: hydroxyproline, GAG: glycosaminoglycan, S-GAG: sulfated glycosaminoglycan, PG: proteoglycan.

5.4 Introduction

In addition to growth factors, hormones, nutrients and genetics, mechanical forces can modulate the rate of bone growth (Cancel et al., 2009; Farnum et al., 2000; C. E. Farnum & N. J. Wilsman, 1998; I. A. Stokes et al., 2006; I. A. Stokes et al., 2002). This phenomenon is a key factor in the progression of infantile and juvenile musculoskeletal deformities such as adolescent idiopathic scoliosis, neuromuscular disease, spondylolisthesis, and varus and valgus deformities (Bonnell et al., 1984; Frost, 1990; LeVeau & Bernhardt, 1984). The mechanical modulation of growth is also a concept of growing interest in the development and improvement of minimally invasive approaches that locally target bone growth modulation to correct these segmental deformities while preserving the growth plate and segment mobility.

Longitudinal growth of vertebrae and long bones occurs through an interstitial expansion process and endochondral ossification of cartilaginous growth plates. The shape, size and arrangement of growth plate chondrocytes dictate three structurally distinct morphological zones: the reserve zone, proliferative and hypertrophic zones (Ballock & O'Keefe, 2003b; C. E. Farnum & N. J. Wilsman, 1998; Hunziker & Schenk, 1989). Growth plate extracellular matrix (ECM) is

comprised of water, large aggregating proteoglycans (PG) embedded within type II collagen fibrils as well as short chain type X collagen exclusively in the hypertrophic zone, which all provide the growth plate with its mechanical stiffness (Mwale et al., 2002).

Type II collagen, one of the major extracellular components of growth plate, forms a highly organized fibrillar network which is believed to be a critical determinant of tissue biomechanical competence (Speer, 1982). This collagen network has the ability to entrap large, hydrophilic proteoglycan molecules. During compressive loading, the collagen network resists lateral expansion and interstitial fluid is forced out through the dense proteoglycan matrix, pressurizing the fluid and allowing for resistance to loading. Polarized light microscopy (PLM) is suitable for evaluating the collagen architecture, since it is sensitive to collagen fiber organization (Speer, 1982).

At the biomechanical level, different *in vitro* studies have investigated intrinsic mechanical properties of growth plates (Cohen et al., 1994), growth plate regions (chondroepiphysis/reserve zone region and the proliferative/hypertrophic zones) (Cohen et al., 1998) or growth plate histological zones (Sergerie et al., 2009) and with developmental stage (Wosu et al., 2011) under uniaxial compression using different animal models. Regional variations in rat tibial growth plate mechanical behavior have also been determined under uniaxial compression in terms of continuous strain patterns (Villemure et al., 2007). Moreover, in a study by Radhakrihan et al. (2004), growth plate extracellular matrix elastic moduli were evaluated through growth plate thickness using combined micro-indentation and atomic force microscopy. More recently, chondrocyte mechanical behavior under uniaxial compression in three histological zones of swine growth plate was determined (Amini, Veilleux, & Villemure, 2010).

Up to date, no study has comprehensively analyzed the zonal growth plate compressive mechanical behavior with respect to its biochemical composition and collagen fiber organization. A few experimental studies have aimed to correlate the mechanical properties of the growth plate in tension with its biochemical composition. In a study by Cohen et al. (1992) on bovine growth plates under tension, the tangent modulus and ultimate stress correlated well by anatomical site with the collagen concentration as measured by hydroxyproline content. Conversely, in a study on rabbit growth plates (Fujii et al., 2000), no correlation was found between the tensile

mechanical properties of each histological zone and its corresponding collagen content. However, the inconclusive results of this last study maybe due to the evaluation of collagen content in five consecutive equal sections, which overlapped the growth plate histological zones.

In this study, it is hypothesized that the deformational behavior of large animal growth plates under compression is zone-dependent and related to its zonal biochemical composition and collagen fiber organization. The objective is to determine the strain distribution within swine growth plates, using the digital image correlation (DIC) technique, as well as their corresponding biochemical composition and collagen fiber orientation in the three functionally distinct zones: reserve, proliferative, and hypertrophic. This would further our understanding of the effect of tissue structural characteristics on the biological functioning of growth plate under the daily effect of the mechanical environment, which is continuously experienced by growth plates. At the mechanobiological level, this knowledge could help establishing which growth plate zone would be more inclined to trigger abnormal endochondral growth upon compressive loading.

5.5 Methods

5.5.1 Animal model and tissue processing

Distal ulnae (N=29) of 4-week old swine (body mass= 3.73 ± 0.30 kg; N=14) were obtained from the same local abattoir within 3 hours of slaughter and after removing the epiphysis with a scalpel blade, growth plate cylindrical samples (N=1 per ulna) were extracted using 6 mm diameter biopsy punches (Figure 5-1) perpendicular to the growth plate/bone junction. Following sample extraction, four separate groups were implemented: (a) histological group (N=8) to quantify the zonal average thickness of each zone (b) mechanical group (N=7), in which a compression protocol was implemented, (c) biochemical group (N=7) for biochemical content evaluation and (d) another histological group (N=7) for characterization of collagen organization. Following dissection, samples in group (a) and (d) were fixed in 4% paraformaldehyde at 4°C. Decalcification was achieved by rocking samples placed in 10% EDTA (pH 7.0) at 4°C for 3-5 days prior to paraffin embedding. Samples designated for the mechanical group were kept moist using HBSS (Hank's Balanced Salt Solution, physiological pH and osmotic pressure (308 mOsm)) and held on ice. They were trimmed on their upper and lower surfaces using a

Vibratome (Vibratome 1500 Sectioning System) to obtain two parallel surfaces and to provide the thickness of each growth plate sample (resolution of height adjustment of 5 μm). The samples were further bisected along the longitudinal growth axis using a custom-made tissue slicer (Zivic Instruments, Pittsburgh, USA) to obtain a flat surface in the longitudinal plane. Semi-cylindrical samples were then immersed in a solution of 5 μM Syto-17 (Molecular probes, Invitrogen, Montreal, Canada) for 30 min at room temperature to fluorescently label chondrocytes nuclei. For the biochemical samples, the three zones were sequentially trimmed from the complete growth plate as reported previously by Sergerie et al. (2009) using the Vibratome based on the zone proportions evaluated from the histological study. The samples were immediately flash-frozen using liquid nitrogen and stored at -80°C until biochemical analysis.

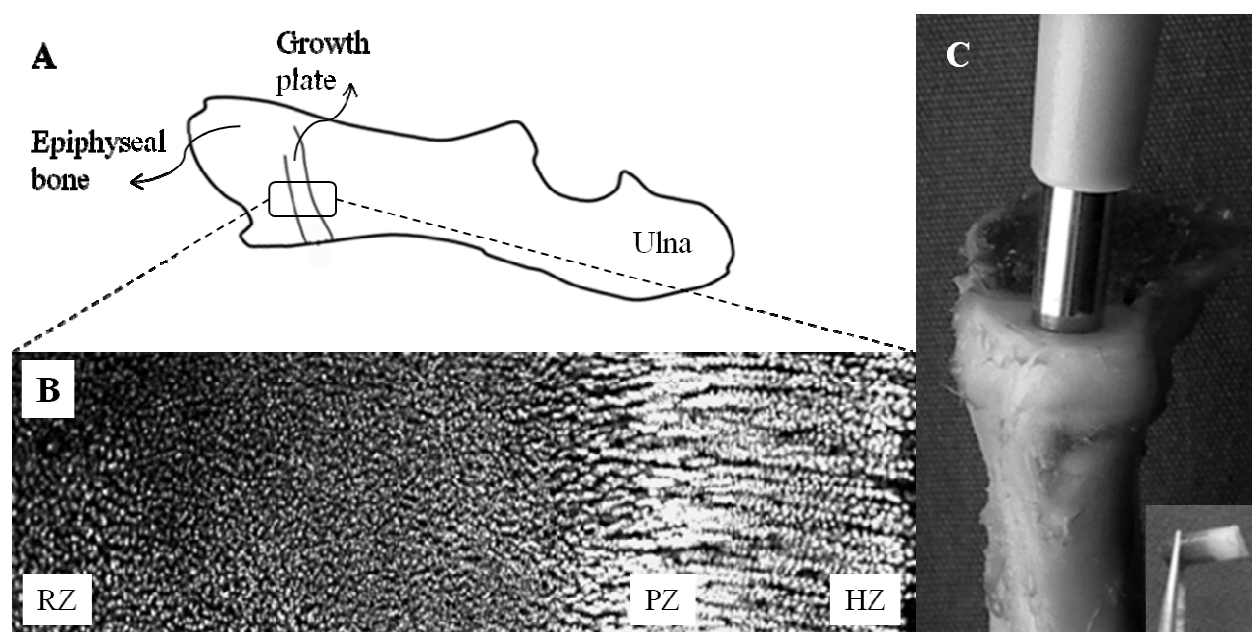


Figure 5-1 : (A) Growth plate site located between the metaphysis and secondary ossification center of the epiphysis, where the longitudinal growth occurs. (B) Typical confocal section of a swine growth plate fluorescently labeled using Syto-17 showing the three histological zones: reserve zone (RZ), proliferative zone (PZ) and hypertrophic zone (HZ). (C) Growth plate cylindrical sample extracted using a 6 mm biopsy punch perpendicular to the growth plate/bone junction.

5.5.2 Histological study

In order to quantify the average thickness of the three zones of 4-week old swine growth plate prior to the biochemical study, a histological study (N=8) was first performed. Four histological sections (5 μ m) along the bone growth axis, taken from different levels within the sample using a rotary microtome (Leica RM 2145), were stained with toluidine blue and digital images were taken (2.5 \times magnification) using a microscope (Leica DMR with a Retiga Qimaging Camera). Based on the presence of mineralized bone, and distinctive chondrocyte cell morphology in each zone (Ballock & O'Keefe, 2003a; C. E. Farnum & N. J. Wilsman, 1998), growth plate and individual zone thicknesses were measured with Digimizer (v3.0) image analysis software at ten different locations per histological section, for a total of 40 measurements per sample.

5.5.3 Imaging and mechanical loading protocols

Each Syto-17-stained semi-cylindrical sample of the mechanical group was placed in a custom-made loading apparatus (Amini et al. 2010) mounted on the stage of an inverted confocal microscope (LSM 510 Carl Zeiss Inc., Germany) (Figure 5-2). The flat edge of the sample was positioned on a clean cover slip placed over the microscope objective and sandwiched between two platens to apply semi-confined compression (Figure 5-2C).

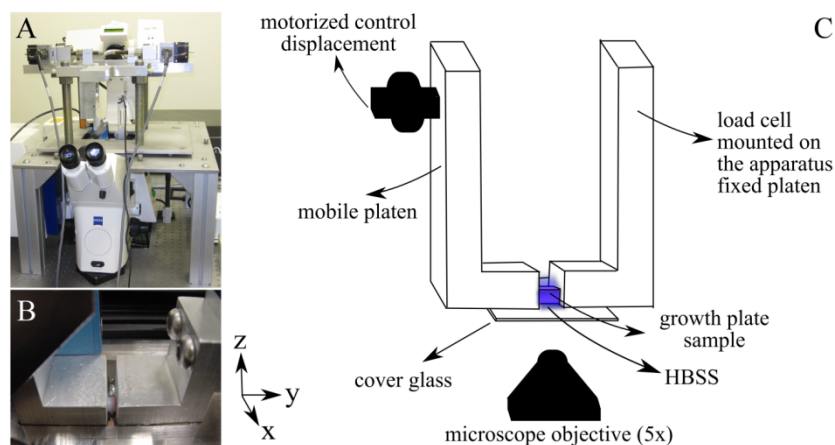


Figure 5-2 : (A) Experimental set-up consisting of a custom-made loading apparatus mounted on the stage of an inverted laser scanning confocal microscope. (B) Growth plate semi-cylindrical sample being sandwiched between the two platens of the loading apparatus in a bath of HBSS. (C) Schematic of the experimental set-up.

The sample was kept moist throughout the test with HBSS. Uniaxial compressive load was applied at the epiphyseal edge of the sample. The platens displacement along the longitudinal axis of the sample was controlled by a custom designed software (Lab View, National Instruments, Inc., USA) and the resulting applied forces were recorded by a single point load cell (Tedea-Huntleigh, Intertechnology Inc.).

Following first contact between platens and sample (0.1-0.2 N compression), a two-step stress relaxation test was performed sequentially for platen-to-platen strain values of 5% and 10%, at a strain rate of $1.7 \times 10^{-3} \text{ s}^{-1}$. A relaxation criterion of $8 \times 10^{-6} \text{ N/s}$ was used to allow the sample reaching a relaxed state, which was determined in a preliminary study. Digital images (512×512 pixels: $5.09 \times 5.09 \text{ } \mu\text{m/pixel}$) of fluorescently labeled chondrocyte nuclei were recorded before applying the two-step stress relaxation test and after final relaxation of the tissue using an EC Plan-Neofluar $5 \times / 0.16$ NA lens (Carl Zeiss Inc., Jena, Germany) from the central region of each sample. The 633 nm line of a He-Ne laser was used for excitation and images were collected using a BP 650-710 filter.

5.5.4 Quantification of strain patterns using Digital image correlation

Digital Image Correlation (DIC) is one of the optical measurement techniques enabling full-field strain measurements in samples under loading. DIC is based on establishing spatial correspondences between two images acquired from the same test specimen; one image in the unloaded state and one image at the same location in the loaded state.

In the present study, displacements and strains were calculated based on the movement and distortion of the growth plate samples (labeled GP1-GP7), which were analyzed using a DIC technique similar to the studies by Cheng et al. (2002) and Tong (2005). Confocal images were saved in TIF format and imported into a custom programmed MATLAB R2010a DIC software. For each image, a region of interest (ROI) with an approximate size of 120×300 pixels covering the three histological zones of the growth plate was further extracted. The objective of the DIC technique was to find continuous displacement fields using nonlinear minimization of the similarity criterion (C) defined in Equations (5-1) to (5-3):

$$C = \sum_i \sum_j \left[\frac{I_{ref}(x_i, y_j) - I_0^{ref}}{\Delta I_{ref}} - \frac{I_{def}(\tilde{x}_i, \tilde{y}_j) - I_0^{def}}{\Delta I_{def}} \right]^2 \quad (5-1)$$

$$I_0 = \frac{1}{N \times M} \sum_{i,j} I(x_i, y_j) \quad (5-2)$$

$$\Delta I = \sqrt{\sum_{i,j} (I(x_i, y_j) - I_0)^2} \quad (5-3)$$

Where N and M are the ROI dimensions. I_{ref} and I_{def} are the reference and deformed image grey levels distributions, respectively. The summation is performed over all pixels in the ROI. (x, y) and (\tilde{x}, \tilde{y}) denote coordinates in the reference and deformed configurations, which are related by displacement components u and v as defined in Equation (5-4):

$$u = \tilde{x} - x, \quad v = \tilde{y} - y \quad (5-4)$$

In order to estimate continuous displacements, B-Splines were used to express displacement components (Cheng et al., 2002; Tong, 2005). Thus, the minimization scheme seeks out for the best B-Splines parameters producing the minimum dissimilarity between images, i.e. Equation (5-1). A four-point bicubic interpolation scheme (Lehmann, Gonner, & Spitzer, 1999) was then used in the algorithm to evaluate the objective function presented in Eq. (1a) at sub-pixel positions. The presented approach was implemented using MATLAB software routines. The algorithm performance was evaluated a priori with the aid of artificial displacements imposed on a sample image according to previously reported procedures (Cheng et al., 2002). Resulting uncertainty measurements were found similar to the evaluations by Cheng et al. (2002).

DIC was performed on confocal images recorded before applying the two-step stress relaxation test and after final relaxation period at either 0% (reference) or 10% (deformed) compressive loading to obtain displacement components. The Lagrangian strain tensors were then directly determined using partial derivatives of displacement components.

5.5.5 Biochemical analyses of water, collagen and GAG content

Samples of the biochemical group were assayed for water content, total sulfated glycosaminoglycan (S-GAG) content and hydroxyproline (OH-Pro) as a measure of collagen content. Water content was determined by weighing the tissue before and after lyophilization at

40°C for 24 hours using Labcono freeze dry system (Labcono Corp., Kansas City, USA). Collagen and GAG content was quantified according to previously described methods (C. D. Hoemann et al., 2002). Samples were papain-digested in 125 µg/mL papain solution for 16 h at 60°C. A portion of the solubilized sample was used to evaluate GAG content by the spectrophotometric 1,9-dimethylmethylene blue (DMMB) assay (C. D. Hoemann, 2004a). The difference in absorbance at 530 and at 590 nm read, done using a Tecan plate reader (Tecan Group Ltd., Männedorf, Switzerland) for each sample, was compared to a standard curve (12.5-125 µg/mL) derived from shark chondroitin sulfate (C4384, Sigma, Montreal, Canada) made in the PBE (phosphate EDTA buffer) solution. Another portion of the papain-digested sample was further hydrolyzed in 6 N HCl for 18 h at 110°C according to Hoemann et al. (2004a; 2002). Aliquots of the hydrolyzed sample were oxidized with chloramine-T hydrate and quantified following the colorimetric reaction with Ehrlich's reagent. The absorbance was read at 560 nm for samples and standards (hydroxyproline, 0.5–5 µg/mL) using Beckman spectrophotometer (Beckman Coulter, Inc., Brea, USA). Collagen content was evaluated assuming that 13.2% of the collagen mass originated from hydroxyproline residues (C. D. Hoemann, 2004a). Both GAG and collagen contents were normalized to tissue wet weight.

5.5.6 Collagen fiber organization using polarized light microscopy

Using a rotary microtome (Leica RM 2145), 5 µm thick sections were prepared at a representative level within all the 7 samples from group (d) (see Methods section 2.1). All sections analyzed by PLM were deparaffinized and rehydrated for mounting unstained (Changoor et al., 2011; C. Hoemann et al., 2011) using a sequence of baths including toluene (Fisher Scientific Canada, Ottawa ON, Canada), a graded ethanol series (Commercial Alcohols, QC, Canada), and distilled water. They were then dehydrated in a second series of ethanol baths, toluene, and mounted unstained in Permount (Fisher Scientific, Hampton, New Hampshire, USA). To positively identify the three histological zones in unstained sections, an adjacent section was stained with Safranin O for bright field microscopy. Grey-scale PLM images at 5x magnification were generated in all three growth plate zones with a microscope (Zeiss Axiolab) using a CCD Camera (Hitachi HV-F22 Progressive Scan Colour 3-CCD). According to Changoor et al (2010), for optimal image contrast, each grey-scale PLM image was used to

extract the green plane followed by 2 “sharp” deconvolution steps (Northern Eclipse v7.0, Empix Imaging Inc., Mississauga, ON, Canada). Separate images were merged (MosaicJ plugin, ImageJ v.1.42q, National Institutes of Health, USA) to generate a single image that comprised the entire growth plate thickness.

5.5.7 Statistical analysis

Basic statistical analysis (mean, standard deviation) was performed for parameters of the histological group (thicknesses), mechanical group (compressive strains) and biochemistry group (water, collagen and GAG contents) for each set of data (reserve, proliferative and hypertrophic zones). A one-way ANOVA for repeated measurements was carried out to determine whether the effect of zone on each biochemical parameter and the amount of developed strain was significant. The post-hoc comparisons between data sets were performed using the Tukey’s method to examine if the difference between the mean values of investigated parameters for each of the three zones reached a certain level of significance ($p\text{-value} < 0.05$). Data were processed using Statistica 10.0 (Statsoft Inc., Tulsa, OK, USA) software.

5.6 Results

5.6.1 Swine growth plate zonal proportion

Results of histological analyses are summarized in Table 5-1. The average thickness of the 4-week old ulna growth plate was $3370\text{ }\mu\text{m}$ ($N=8$ histological samples). Proportions of the reserve, proliferative and hypertrophic zones of 4-week old ulnar growth plates were evaluated at $70.6\pm 7.7\%$, $16.3\pm 4.7\%$ and $13.1\pm 4.1\%$, respectively. These proportions were further used to sequentially trim the three zones from the complete growth plate for the biochemical assays.

Table 5-1 : Mean zonal thickness proportions of the reserve, proliferative and hypertrophic zones of 4-week old ulnar growth plates.

Zonal thickness normalized to complete growth plate thickness (%)	
Reserve zone (N=8)	70.6 ± 7.7
Proliferative zone (N=8)	16.3 ± 4.7
Hypertrophic zone (N=8)	13.1 ± 4.1

5.6.2 Strain distributions throughout growth plate thickness

In the mechanical group, complete growth plate sample thicknesses varied between 3400 and 4100 μm with an average of 3670 ± 260 μm . Confocal images showed a random dispersion of chondrocytes within the reserve zone and a typical columnar arrangement of chondrocytes within the proliferative and hypertrophic zones prior to loading (Figure 5-3A) and after relaxation of the tissue (Figure 5-3B).

A typical region of interest (ROI) chosen for strain pattern generation is shown in Figure 5-3C. Strain distributions were non uniform across the growth plate thickness in all seven samples (Figure 5-3D). Growth plates were predominantly under compression, with peak compressive strains ranging between 10% to 30%, which is 1 to 3 times higher than the overall applied strain of 10%. Strain patterns also showed limited regions of weak tension with the maximum tensile strain ranging from 2% to ~8%. When comparing growth plate images and corresponding strain maps, strain distributions matched up with the growth plate histological zones in all samples (Figure 5-3C, D). Table 2a presents the resulting average developed axial strains (ϵ_{yy}) within the reserve, proliferative and hypertrophic zones. Developed average axial compressive strains ranged between 1.3-2.9%, 4.3-11.3%, and 0.3-8.6% within reserve, proliferative, and hypertrophic zones, respectively. Higher axial compressive strains were principally located in the proliferative zone, while low axial compressive strains were mainly found in the reserve zone and partly in the hypertrophic zone (Figure 5-3D). Modest strains were found in transverse direction (ϵ_{xx}) through growth plate thickness (Table 5-2b), as graphically shown in Figure 5-3E for GP4.

Higher transverse strains were developed in the proliferative and hypertrophic zones compared to the reserve zone.

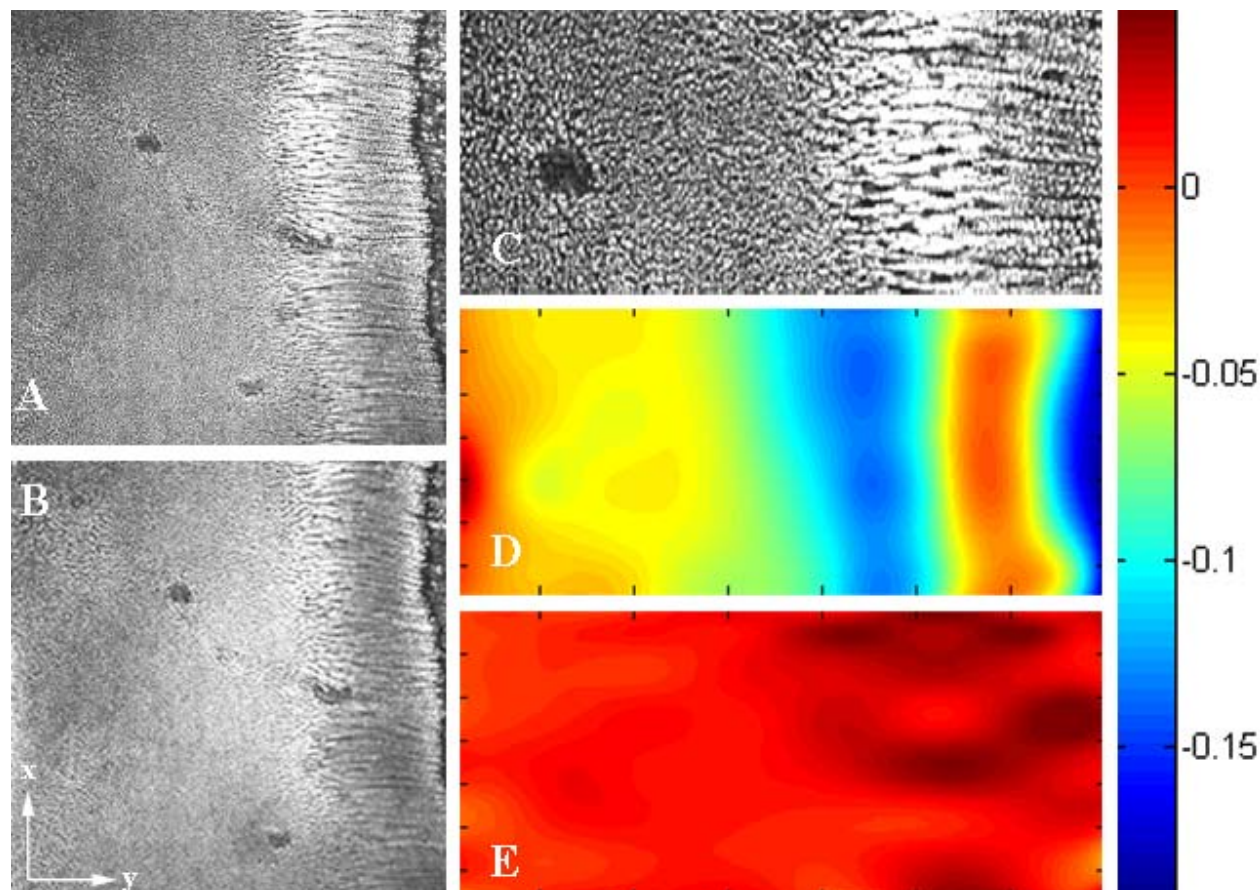


Figure 5-3 : Image correlation results for a swine ulnar growth plate sample (GP#4) undergoing 10% uniaxial compressive strain between initial and final images: (A) initial 512×512 confocal image (before loading); (B) final 512×512 confocal image (after loading and relaxation); (C) region of interest (ROI) covering three histological zones of growth plate, which was cropped out from the final image and used in DIC algorithm; (D) calculated strain map along loading direction (ϵ_{yy}); (E) calculated strain map perpendicularly to the loading direction (ϵ_{xx}).

Figure 5-4 presents quantitative strain variations developed across growth plates, which depths were normalized to corresponding growth plate zone thicknesses. Average strain curves obtained in all samples followed a similar pattern, with peak compressive strains in the proliferative zone compared to the two other zones. These data show the heterogeneous mechanical behavior

through growth plate thickness under compressive loading, which represents each histological zone as different functional units of the growth plate under loading.

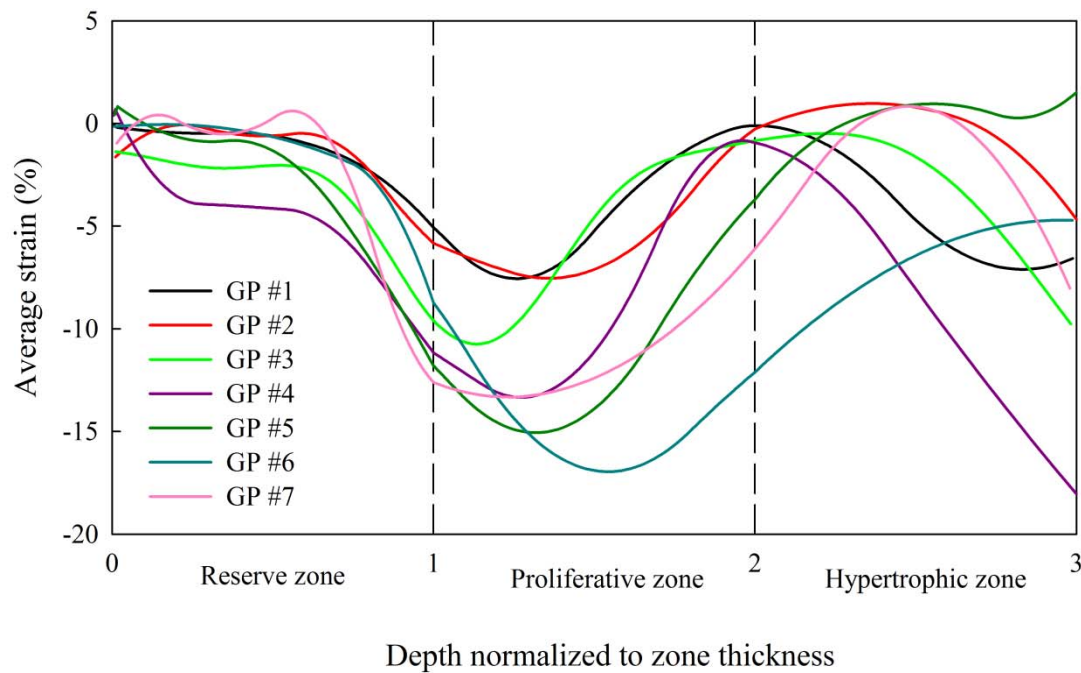


Figure 5-4: Variations in strain developed across swine growth plates under 10% uniform compressive strain, normalized to growth plate zone thicknesses. The strains were averaged on a pixel by pixel basis to compute the “average” strains in each histological zone. Each point on each curve represents an average of ϵ_{yy} distributions as observed along the x axis (perpendicular to loading direction) of the imaged growth plates. Each curve stands for the average of strain distribution along the y axis (in loading direction). 0-1, 1-2, and 2-3 on the abscissa represent the reserve zone, the proliferative zone, and the hypertrophic zone, respectively.

ANOVA analyses showed that the effect of zone on developed strain among the three histological zones was significant ($p < 0.005$). Univariate results on developed compressive strains along the bone axis (ϵ_{yy}) with Tukey post-hoc tests showed statistically significant differences between the proliferative zone and the two other histological zones (Table 5-2a: reserve zone ($p < 0.005$) and hypertrophic zone ($p < 0.05$)). Moreover, univariate results on developed transverse strains (ϵ_{xx}) with Tukey post-hoc tests presented statistically significant differences among the three histological zones (Table 5-2b).

Table 5-2 : (a) Average developed strains along the bone axis (\square_{yy}) and (b) average developed strains perpendicular to the bone axis (\square_{xx}) within the reserve, proliferative and hypertrophic zones of 4-week old ulnar swine growth plates under 10% uniform compressive strain.

(a) \square_{yy} strain (%)			
(Mean \pm Standard deviation)			
GP #	Reserve zone	Proliferative zone	Hypertrophic zone
1	-1.3 \pm 1.3	-4.3 \pm 3.1	-4.1 \pm 3.0
2	-1.4 \pm 1.8	-5.5 \pm 2.5	-0.3 \pm 1.8
3	-1.8 \pm 1.7	-5.4 \pm 4.1	-2.5 \pm 2.4
4	-4.9 \pm 2.7	-8.6 \pm 4.7	-8.6 \pm 5.7
5	-2.9 \pm 3.5	-10.5 \pm 3.3	-1.0 \pm 1.5
6	-1.6 \pm 2.6	-14.5 \pm 6.0	-7.0 \pm 5.0
7	-2.4 \pm 4.1	-11.3 \pm 3.0	-2.0 \pm 2.8
Average	-2.3 \pm 1.3^{**ii}	-8.6 \pm 3.7^{**i, *iii}	-3.6 \pm 3.1^{*ii}

(b) \square_{xx} strain (%)			
(Mean \pm Standard deviation)			
GP #	Reserve zone	Proliferative zone	Hypertrophic zone
1	0.31 \pm 0.50	0.04 \pm 1.0	0.61 \pm 1.8
2	0.60 \pm 0.74	0.71 \pm 0.62	0.65 \pm 0.78
3	0.69 \pm 0.66	0.93 \pm 0.71	1.4 \pm 0.97
4	1.2 \pm 0.60	2.7 \pm 1.1	2.6 \pm 1.3
5	0.56 \pm 0.26	1.3 \pm 1.0	2.5 \pm 3.4
6	0.34 \pm 0.69	1.3 \pm 1.1	2.5 \pm 2.7
7	0.16 \pm 0.38	1.2 \pm 0.73	1.5 \pm 1.4
Average	0.55 \pm 0.34^{*ii, *iii}	1.2 \pm 0.80^{*i, *iii}	1.7 \pm 0.87^{*i, *ii}

* Statistically significant (p -value ≤ 0.05) compared to the reserve (i), proliferative(ii) or hypertrophic (iii) zone

** Statistically significant (p -value ≤ 0.005) compared to the reserve (i), proliferative(ii) or hypertrophic (iii) zone

5.6.3 Biochemical contents of 4-week old swine growth plate

Table 5-3 summarizes biochemical content analyses. Data are also shown graphically in Figure 5-5, with the results of post-hoc comparisons between data sets. Highest water and GAG content (normalized to wet weight) were found in the proliferative zone ($83.6 \pm 5.1\%$ and $54.9 \pm 8.0 \mu\text{g}/\text{mg}$, respectively) while lower water and GAG content was detected in the reserve zone ($79.7 \pm 1.9\%$ and $51.5 \pm 4.5 \mu\text{g}/\text{mg}$, respectively). The maximum collagen content was found in the reserve zone ($79.0 \pm 5.0 \mu\text{g}/\text{mg}$ wet weight), while the minimum was found in the hypertrophic zone ($46.3 \pm 18.4 \mu\text{g}/\text{mg}$ wet weight). Collagen content showed a 41% decrease from the reserve zone to the hypertrophic zone along the growth direction.

Table 5-3 : Water, GAG and collagen contents in three histological zones of 4-week old swine distal ulna growth plates (mean \pm standard deviation). Both GAG and collagen contents are normalized to wet weight of the tissue.

Histological zone	Collagen content	Water content	PG content
	OH-Pro ($\mu\text{g}/\text{mg}$ wet wt)	(% of mg wet wt)	s-GAG ($\mu\text{g}/\text{mg}$ wet wt)
Reserve (n=7)	$79.0 \pm 5.0^{*ii, **iii}$	79.7 ± 1.9	51.5 ± 4.5
Proliferative (n=7)	$53.3 \pm 13.6^{*i}$	83.6 ± 5.1	54.9 ± 8.0
Hypertrophic (n=7)	$46.3 \pm 18.4^{**i}$	81.3 ± 5.9	53.0 ± 14.1

* Statistically significant ($p\text{-value} \leq 0.05$) compared to the reserve (i), proliferative(ii) or hypertrophic (iii) zone

** Statistically significant ($p\text{-value} \leq 0.005$) compared to the reserve (i), proliferative(ii) or hypertrophic (iii) zone

ANOVA tests showed significant differences in collagen content among the three histological zones ($p < 0.005$). No significant effect was detected on the water content and GAG content (normalized to wet weight) among the three growth plate zones. Univariate results on collagen content with Tukey post-hoc tests showed statistically significant differences between the reserve zone and the two other histological zones (Table 5-3: proliferative zone ($p < 0.05$) and hypertrophic zone ($p < 0.005$)).

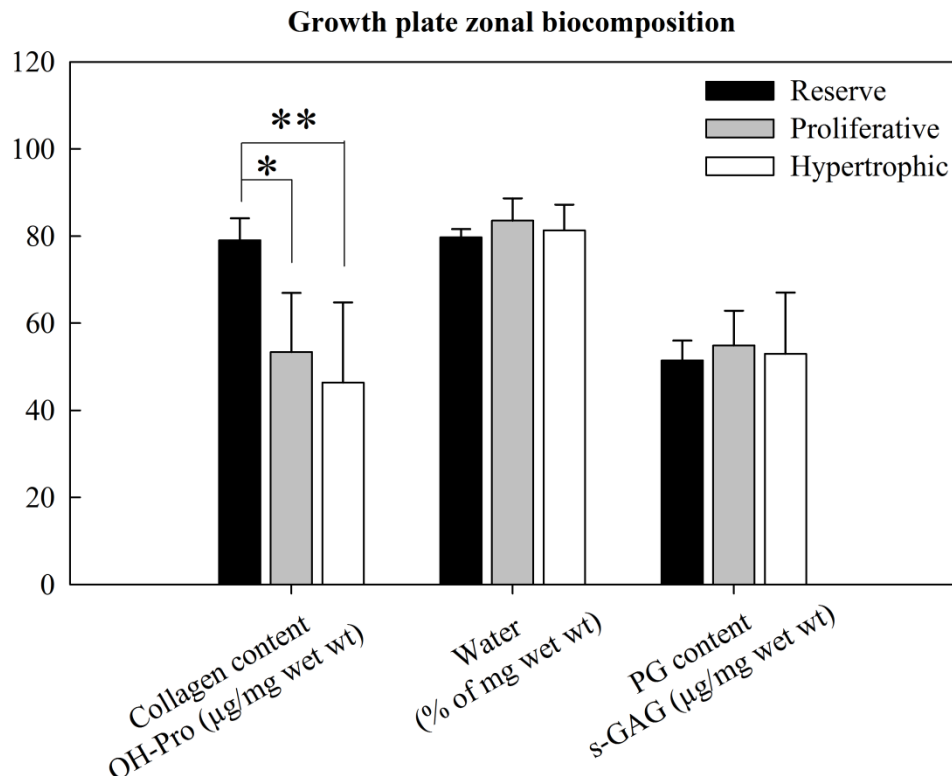


Figure 5-5 : Biochemical composition of the three histological zones of 4-week old swine growth plates. Significant differences between the histological zones are shown with connecting lines (*p-value \leq 0.05 and **p-value \leq 0.005).

5.6.4 Collagen fiber organization through the thickness of 4-week old swine growth plate

Differences in birefringence were observed through the growth plate zones (Figure 5-6). Fibers in the reserve zone were organized mainly horizontally in a radial fashion (parallel to the growth plate/bone interface). However, some fibers were also observed as aligned in other directions in this zone. Collagen fibers were aligned almost exclusively vertically (parallel to the growth direction) in the proliferative and hypertrophic zones. A decrease in the transverse width of the longitudinal septa between chondrocytes columns combined with an increase in the intensity of birefringence was observed as chondrocytes undergo proliferation, hypertrophy, and increased cell diameter.

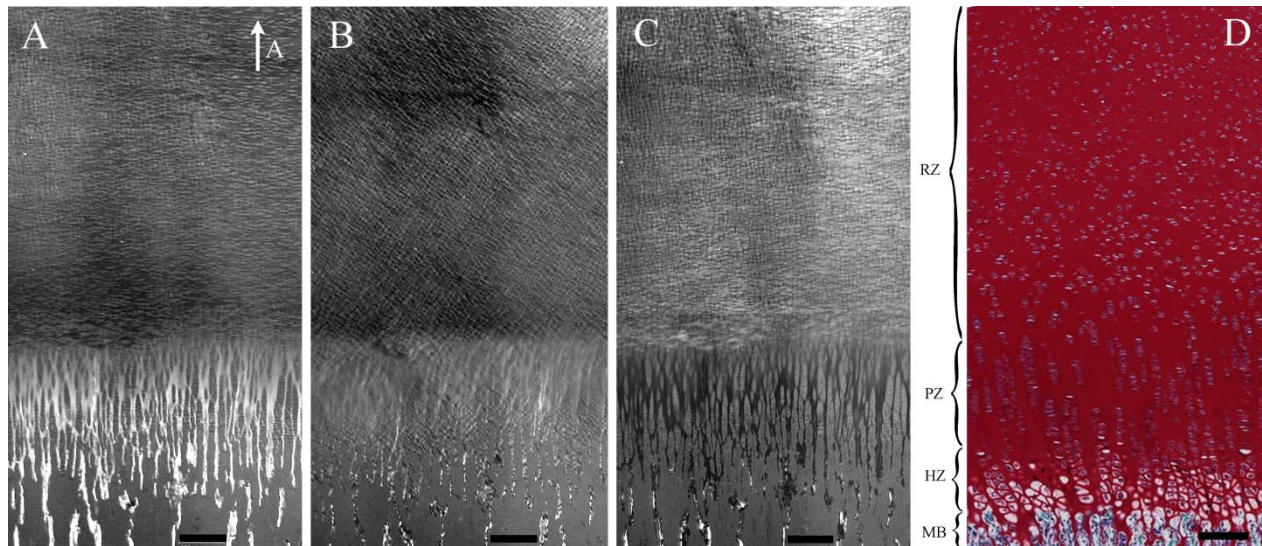


Figure 5-6 : A typical presentation of collagen orientation in birefringent swine growth plate at (a) 45°, (b) 90° and (c) 135° relative to the analyzer. At 45° vertically oriented collagen network is present in the proliferative and hypertrophic zones. At 135°, a mainly horizontally oriented collagen network is present in RZ. Panel (d) shows an adjacent section stained with Safranin-O/Fast-Green, with the histological zones as indicated (RZ: reserve zone, PZ: proliferative zone, HZ: hypertrophic zone, and MB: metaphyseal bone). The analyzer direction (A) is marked on the panel (a). All angles are relative to the analyzer filter. The scale bar is 250 μ m.

5.7 Discussion

The compressive deformational behavior of the growth plate was non uniform and zone dependent. In response to uniaxial compression, higher axial strains were developed within the proliferative zone compared to two other histological zones. Higher transverse strains mainly arose in the proliferative and hypertrophic zones compared to reserve zone. Conversely, lower, more homogenous axial strains as well as transverse strains were developed primarily within the reserve zone of 4-week old swine growth plates. These results corroborate moderately with existing knowledge of growth plate tissue mechanics. A biomechanical study on newborn (day 0) swine ulnar growth plates reported significant differences among Young's moduli of the three growth plate histological zones, along with a slightly larger ($\sim 200\ \mu$ m) growth plate thickness (Sergerie et al., 2009). The reserve zone was found two times stiffer than the proliferative and hypertrophic zones along the compression axis and about twice as stiff in the transverse plane. A

more recent study on the morphology of 4-week old swine growth plate chondrocytes under compression revealed non uniform and zone dependent mechanical behavior of the compressed chondrocytes (Amini et al., 2010). In this latter study, cellular strains in terms of cell volume change under compression were evaluated in the three histological zones. Reserve chondrocytes were shown to experience lower bulk compressive strains while chondrocytes from the proliferative and hypertrophic zones underwent high compressive bulk strains. Nevertheless, results obtained in these porcine models do not corroborate with the reported strain patterns in rat tibial growth plates under compression (Villemure et al., 2007), where lower strains were mainly located in the proliferative zone and higher compressive strains were found in the reserve and hypertrophic zones. Three major reasons could address these differences. Firstly, rat growth plates used in that study originated from a small animal model, which has been reported to have a very narrow reserve zone compared to larger animal models, such as the swine (C. E. Farnum & N. J. Wilsman, 1998). Given that the sizable reserve zone in large species is believed to serve as a mechanical support to the actively growing chondrocytes of the growth plate (C. E. Farnum & N. J. Wilsman, 1998; Sergerie et al., 2009), substantial thicker reserve zone could certainly contribute to the shift in minimum developed strain from the proliferative zone in small animal models to the reserve zone in large animal models. Secondly, different developmental stages (infantile in the present study and adolescent in the previous rodent study) could contribute to the observed difference between mechanical behavior of rat tibial and swine ulnar growth plates under uniaxial compression. Indeed, growth plate mechanical properties were shown to vary nonlinearly with developmental stage (Wosu et al., 2011). Finally, the influential effect of bio-compositional differences in growth plate extracellular matrix between species and developmental stages should not be neglected.

Intra-sample behavioral heterogeneity in terms of average strain in the hypertrophic zone when compared to the other two histological zones could be explained by type X collagen which is exclusively found in this histological zone. The reserve and proliferative zones look relatively homogenous between the samples compared to the hypertrophic zone where both average strain magnitude and shape shows great variation among samples. The intra animal difference in type X collagen which is believed to be involved in cartilage mineralization in the hypertrophic zone (Gannon et al., 1991) could contribute to the intra-sample behavioral heterogeneity in the

hypertrophic zone when compared to the other two histological zones. Differential rates of cell apoptosis or collagen remodeling could also contribute to variable weakening of the hypertrophic zone compressive properties (Vu et al., 1998).

The growth plate has a non uniform collagen content but similar GAG and water content through its thickness. Results indeed showed a significant decrease in collagen content from the reserve zone to the chondro-osseus junction. A similar gradient of collagen content was previously reported both biochemically (Alini et al., 1992; Wuthier, 1969) and morphologically (Buckwalter et al., 1986). A study by Wuthier et al. (1969) on fetal calves showed that collagen represented about 60% of the extracellular matrix in the reserve zone and decreased progressively in proliferative and hypertrophic zone to 22%. In a study by Alini et al. (1992) on fetal calves, analysis of hydroxyproline revealed lower overall collagen content where type X collagen is being synthesized in the extracellular matrix in the hypertrophic zone. In a study by Buckwalter et al. (1986) on mice, the relative volume of collagen decreased from the reserve zone to the hypertrophic zone in both territorial and interterritorial matrices. Furthermore, the average water content in the present study was similar to the formerly reported values in bovine distal femur (Cohen et al., 1992) and fetal calf legs (Wuthier, 1969). Moreover, total amount of proteoglycan evaluated by uronic acid assay per unit of extracellular matrix increased from the proliferative zone to the hypertrophic zone as reported by Matsui et al. (1991) in 16 sequential strata of fetal bovine tibial growth plates. However, the sulfated glycosaminoglycan content as measured by DMMB assay only showed a modest increase from the first stratum in the proliferative zone to the last stratum in the hypertrophic zone (Mwale et al., 2002). The amount of sulfated glycosaminoglycan measured in the present study is in agreement with the results presented in the latter study when averaging the s-GAG content over strata of the same histological zones. Moreover, in a study by Byers et al. (1997), structural changes in large proteoglycans were characterized in different histological zones of ovine growth plate. An increasing portion of unsulfated residues was reported in this study while approaching the chondro-osseus junction. To summarize, our data corroborates existing data on growth plate bio-composition and extends them in the same animal model with lower growth rates, which most resemble humans, to show that collagen has a dominant influence on compressive behavior.

The growth plate collagen fiber orientation was non uniform through its thickness. Random dispersion of chondrocytes in the reserve zone and the columnar arrangement of chondrocytes in proliferative and hypertrophic zones correlate with orientation of collagen fibers in these zones. The increase in the intensity of birefringence with decreasing the width of the longitudinal septa from the proliferative zone to the hypertrophic zone could be due to an increased collagen concentration in the septa as a result of cellular hypertrophy, where the expanding cells compress the matrix, as suggested by Speer (1982).

The non uniform and zone-dependent compressive deformational behavior of the ulnar growth plate could be partly explained by collagen content and collagen fiber organization across growth plate zones. In response to uniaxial semi-confined compression, the reserve zone, where the highest collagen content was detected, demonstrated higher stiffness as measured by the smaller developed strain compared to the proliferative zone. Conversely, the proliferative zone, with lower detected collagen content, developed higher compressive strains compared to two other zones. It should be noted that no association was found between axial strains and collagen content in the hypertrophic zone. In contrast to the possible association between compressive behavior and collagen content, no direct association can be established between either total proteoglycan content or water content and growth plate compressive behavior. The collagen organization was also found to play an important role in the developed zonal strain patterns. The reserve zone with mostly horizontal collagen fibers offers higher resistance to lateral expansion when compressed. This forces the interstitial fluid out through the dense proteoglycan matrix and highly pressurizes the fluid and would offer resistance to developing axial strains, whereas in the proliferative zone the vertically oriented collagen network would not offer enough resistance to lateral expansion as measured by higher transverse strains and consequently the fluid would be poorly pressurized which would lead to development of higher axial strains in this zone. On the other hand, although hypertrophic zone with vertically oriented collagen network offers lower resistance to lateral expansion, higher axial strains were not developed in this zone. It is noteworthy to mention that the incorporation of collagen type X, which is exclusively found in the hypertrophic zone, in the collagen type II positive matrix should not be neglected. Further studies are indeed required to confirm if type II collagen fibers and type X collagen are the major players in growth plate mechanobiology in this early developmental stage.

Major compressive strain developing within the proliferative zone could contribute to decreasing growth rate in response to increasing compression on the growth plate. Mechanical loading is one of the key factors which are believed to modulate bone development (Cancel et al., 2009; Farnum et al., 2000; C. E. Farnum & N. J. Wilsman, 1998; I. A. Stokes et al., 2006; I. A. Stokes et al., 2002). The transduction of mechanical signals to growth plate chondrocytes most likely rises from local tissue strains (Villemure & Stokes, 2009), which eventually lead to modulating second messenger activity through chondrocytes membrane stretch (Sachs, 1991; Watson, 1991). In parallel, experimental evidence indicates that biological events occurring within the proliferative and hypertrophic zones are critical in growth plate mechanobiology (I. A. Stokes et al., 2007; Villemure & Stokes, 2009). In the present study, the maximum average strains were located in regions overlapping the proliferative and hypertrophic zones. These two compliant zones, the proliferative and hypertrophic, could then be critical mechanotransductive zones and more likely to trigger abnormal endochondral growth upon compressive mechanical loading. To our knowledge, this is the first in situ study relating mechanical, biochemical, and histological architecture of the growth plate.

In conclusion, 4-week old porcine ulnar growth plates showed lower axial and transverse strain, higher collagen levels, and horizontally organized collagen fibers in the reserve zone, whereas higher axial and transverse strain, lower collagen levels, and vertically organized collagen fibers were found in the proliferative and hypertrophic zones. These data add to our understanding of the fundamental relationship between compressive forces experienced by growth plate chondrocytes and their extracellular environment structural characteristics. This information would further help us to better understand the effect of the mechanical environment on the biological response of growth plate. Therapies aiming to direct or influence pathologic growth plate maturation should take into consideration that the histological zones involved in longitudinal growth (proliferative and hypertrophic) are more susceptible to compressive strain. A combined improved knowledge of growth plate mechanics and mechanobiology is essential to better understand the possible mechanisms through which abnormal growth is triggered and to eventually improve the minimally invasive treatment approaches of progressive skeletal deformities, which directly exploit the process of growth modulation to correct these deformities.

5.8 Acknowledgements

The authors acknowledge the participation of Catherine Boyer, Thierry Lafrance and Bénédict Besner in the experimental set-up design. Thank you to Parham Eslami Nejad, Irene Londono and Adele Changoor for their technical assistance. This research project was funded by the Canada Research Chair in Mechanobiology of the Pediatric Musculoskeletal System (I.V.) and the MENTOR training program of Canadian Institutes of Health Research (S.A.). Salary support is acknowledged from the Fonds de la Recherche sur la Santé du Québec (C.D.H.) and Piramal Healthcare (J.S.).

5.9 References

- Alini, M., Matsui, Y., Dodge, G. R., & Poole, A. R. (1992). The extracellular matrix of cartilage in the growth plate before and during calcification: changes in composition and degradation of type II collagen. *Calcif Tissue Int*, 50(4), 327-335.
- Amini, S., Veilleux, D., & Villemure, I. (2010). Tissue and cellular morphological changes in growth plate explants under compression. *J Biomech*, 43(13), 2582-2588. doi:S0021-9290(10)00280-0 [pii]10.1016/j.jbiomech.2010.05.010 [doi]
- Ballock, R. T., & O'Keefe, R. J. (2003a). The biology of the growth plate. *J Bone Joint Surg Am*, 85-A(4), 715-726.
- Ballock, R. T., & O'Keefe, R. J. (2003b). Physiology and pathophysiology of the growth plate. *Birth Defects Res C Embryo Today*, 69(2), 123-143. doi:http://dx.doi.org10.1002/bdrc.10014
- Bonnel, F., Dimeglio, A., Baldet, P., & Rabischong, P. (1984). Biomechanical activity of the growth plate. Clinical incidences. *Anat Clin*, 6(1), 53-61.
- Buckwalter, J. A., Mower, D., Ungar, R., Schaeffer, J., & Ginsberg, B. (1986). Morphometric analysis of chondrocyte hypertrophy. *J Bone Joint Surg Am*, 68(2), 243-255.
- Byers, S., van Rooden, J. C., & Foster, B. K. (1997). Structural changes in the large proteoglycan, aggrecan, in different zones of the ovine growth plate. *Calcif Tissue Int*, 60(1), 71-78.

- Cancel, M., Grimard, G., Thuillard-Crisinel, D., Moldovan, F., & Villemure, I. (2009). Effects of in vivo static compressive loading on aggrecan and type II and X collagens in the rat growth plate extracellular matrix. *Bone*, 44(2), 306-315. doi:S8756-3282(08)00778-3 [pii] 10.1016/j.bone.2008.09.005 [doi]
- Changoor, A., Tran-Khanh, N., Methot, S., Garon, M., Hurtig, M. B., Shive, M. S., & Buschmann, M. D. (2011). A polarized light microscopy method for accurate and reliable grading of collagen organization in cartilage repair. *Osteoarthritis Cartilage*, 19(1), 126-135. doi:S1063-4584(10)00351-1 [pii]10.1016/j.joca.2010.10.010 [doi]
- Cheng, P., Sutton, M., Schreier, H., & McNeill, S. (2002). Full-field speckle pattern image correlation with B-Spline deformation function. *Experimental Mechanics*, 42(3), 344-352. doi:10.1177/001448502321548445
- Cohen, B., Chorney, G. S., Phillips, D. P., Dick, H. M., Buckwalter, J. A., Ratcliffe, A., & Mow, V. C. (1992). The microstructural tensile properties and biochemical composition of the bovine distal femoral growth plate. *Journal of orthopaedic research : official publication of the Orthopaedic Research Society*, 10(2), 263-275. doi:10.1002/jor.1100100214 [doi]
- Cohen, B., Chorney, G. S., Phillips, D. P., Dick, H. M., & Mow, V. C. (1994). Compressive stress-relaxation behavior of bovine growth plate may be described by the nonlinear biphasic theory. *Journal of orthopaedic research : official publication of the Orthopaedic Research Society*, 12(6), 804-813. doi:10.1002/jor.1100120608 [doi]
- Cohen, B., Lai, W. M., & Mow, V. C. (1998). Transversely isotropic biphasic model for unconfined compression of growth plate and chondroepiphysis. *Journal of Biomechanical Engineering, Transactions of the ASME*, 120(4), 491-496.
- Farnum, C. E., Nixon, A., Lee, A. O., Kwan, D. T., Belanger, L., & Wilsman, N. J. (2000). Quantitative three-dimensional analysis of chondrocytic kinetic responses to short-term stapling of the rat proximal tibial growth plate. *Cells, tissues, organs*, 167(4), 247-258.
- Farnum, C. E., & Wilsman, N. J. (1998). chapter 13: Growth plate cellular function. In J. A. Buckwalter, M. G. Ehrlich, L. J. Sandell & S. B. Trippel (dir.), *Advances in the basis and*

clinical understanding of the growth plate. (pp. 203-223). Chicago, IL: American Academy of Orthopaedic Surgeons.

- Frost, H. M. (1990). Skeletal structural adaptations to mechanical usage (SATMU): 3. The hyaline cartilage modeling problem. *Anat Rec*, 226(4), 423-432. doi:10.1002/ar.1092260404 [doi]
- Fujii, T., Takai, S., Arai, Y., Kim, W., Amiel, D., & Hirasawa, Y. (2000). Microstructural properties of the distal growth plate of the rabbit radius and ulna: biomechanical, biochemical, and morphological studies. *J Orthop Res*, 18(1), 87-93.
- Gannon, J. M., Walker, G., Fischer, M., Carpenter, R., Thompson, R. C., Jr., & Oegema, T. R., Jr. (1991). Localization of type X collagen in canine growth plate and adult canine articular cartilage. *Journal of orthopaedic research : official publication of the Orthopaedic Research Society*, 9(4), 485-494. doi:10.1002/jor.1100090404
- Hoemann, C., Kandel, R., Roberts, S., Saris, D. B. F., Creemers, L., Mainil-Varlet, P., . . . Buschmann, M. D. (2011). International Cartilage Repair Society (ICRS) Recommended Guidelines for Histological Endpoints for Cartilage Repair Studies in Animal Models and Clinical Trials. *Cartilage*, 2(2), 153-172. doi:10.1177/1947603510397535
- Hoemann, C. D. (2004). Cartilage and Osteoarthritis. In F. De Ceuninck, M. Sabatini & P. Pastoreau (dir.), *Methods in Molecular Medicine*. (2004/08/10e éd., Vol. 101, pp. 127-156). doi:1-59259-821-8:127 [pii]10.1385/1-59259-821-8:127 [doi]
- Hoemann, C. D., Sun, J., Chrzanowski, V., & Buschmann, M. D. (2002). A multivalent assay to detect glycosaminoglycan, protein, collagen, RNA, and DNA content in milligram samples of cartilage or hydrogel-based repair cartilage. *Anal Biochem*, 300(1), 1-10. doi:10.1006/abio.2001.5436 [doi] S0003269701954363 [pii]
- Hunziker, E. B., & Schenk, R. K. (1989). Physiological mechanisms adopted by chondrocytes in regulating longitudinal bone growth in rats. *J physiol*, 414, 55-71.
- Lehmann, T. M., Gonner, C., & Spitzer, K. (1999). Survey: interpolation methods in medical image processing. *IEEE Trans Med Imaging*, 18(11), 1049-1075. doi:10.1109/42.816070 [doi]

- LeVeau, B. F., & Bernhardt, D. B. (1984). Developmental biomechanics. Effect of forces on the growth, development, and maintenance of the human body. *Phys Ther*, 64(12), 1874-1882.
- Matsui, Y., Alini, M., Webber, C., & Poole, A. R. (1991). Characterization of aggregating proteoglycans from the proliferative, maturing, hypertrophic, and calcifying zones of the cartilaginous physis. *J Bone Joint Surg Am*, 73(7), 1064-1074.
- Mwale, F., Tchetina, E., Wu, C. W., & Poole, A. R. (2002). The assembly and remodeling of the extracellular matrix in the growth plate in relationship to mineral deposition and cellular hypertrophy: an in situ study of collagens II and IX and proteoglycan. *J Bone Miner Res*, 17(2), 275-283.
- Radhakrishnan, P., Lewis, N. T., & Mao, J. J. (2004). Zone-specific micromechanical properties of the extracellular matrices of growth plate cartilage. *Annals of Biomedical Engineering*, 32(2), 284-291. doi:<http://dx.doi.org10.1023/B:ABME.0000012748.41851.b4>
- Sachs, F. (1991). Mechanical transduction by membrane ion channels: a mini review. *Molecular and cellular biochemistry* 104(1-2), 57-60.
- Sergerie, K., Lacoursiere, M. O., Levesque, M., & Villemure, I. (2009). Mechanical properties of the porcine growth plate and its three zones from unconfined compression tests. *J Biomech*, 42(4), 510-516. doi:S0021-9290(08)00587-3 [pii]10.1016/j.jbiomech.2008.11.026 [doi]
- Speer, D. P. (1982). Collagenous architecture of the growth plate and perichondrial ossification groove. *J Bone Joint Surg Am*, 64(3), 399-407.
- Stokes, I. A., Aronsson, D. D., Dimock, A. N., Cortright, V., & Beck, S. (2006). Endochondral growth in growth plates of three species at two anatomical locations modulated by mechanical compression and tension. *J Orthop Res*, 24(6), 1327-1334. doi:10.1002/jor.20189 [doi]
- Stokes, I. A., Clark, K. C., Farnum, C. E., & Aronsson, D. D. (2007). Alterations in the growth plate associated with growth modulation by sustained compression or distraction. *Bone*, 41(2), 197-205. doi:S8756-3282(07)00372-9 [pii] 10.1016/j.bone.2007.04.180 [doi]

- Stokes, I. A., Mente, P. L., Iatridis, J. C., Farnum, C. E., & Aronsson, D. D. (2002). Enlargement of growth plate chondrocytes modulated by sustained mechanical loading. *J Bone Joint Surg Am*, 84-A(10), 1842-1848.
- Tong, W. (2005). An evaluation of digital image correlation criteria for strain mapping applications. *Strain*, 41(4), 167-175. doi:10.1111/j.1475-1305.2005.00227.x
- Villemure, I., Cloutier, L., Matyas, J. R., & Duncan, N. A. (2007). Non-uniform strain distribution within rat cartilaginous growth plate under uniaxial compression. *Journal of Biomechanics*, 40(1), 149-156. doi:http://dx.doi.org10.1016/j.jbiomech.2005.11.008
- Villemure, I., & Stokes, I. A. (2009). Growth plate mechanics and mechanobiology. A survey of present understanding. *Journal of Biomechanics*, 42(12), 1793-1803. doi:S0021-9290(09)00270-X [pii]
10.1016/j.jbiomech.2009.05.021 [doi]
- Vu, T. H., Shipley, J. M., Bergers, G., Berger, J. E., Helms, J. A., Hanahan, D., . . . Werb, Z. (1998). MMP-9/gelatinase B is a key regulator of growth plate angiogenesis and apoptosis of hypertrophic chondrocytes. *Cell*, 93(3), 411-422.
- Watson, P. A. (1991). Function follows form: generation of intracellular signals by cell deformation. *The FASEB journal* 5(7), 2013-2019.
- Wosu, R., Sergerie, K., Levesque, M., & Villemure, I. (2011). Mechanical properties of the porcine growth plate vary with developmental stage. *Biomech Model Mechanobiol*. doi:10.1007/s10237-011-0310-6 [doi]
- Wuthier, R. E. (1969). A zonal analysis of inorganic and organic constituents of the epiphysis during endochondral calcification. *Calcif Tissue Res*, 4(1), 20-38.

CHAPTER 6 GENERAL DISCUSSION

The present thesis aimed at characterizing the histomorphological characteristics and mechanical behaviour of growth plates at the cellular and tissue levels and at evaluating their biochemical composition and collagen fiber orientation in the three functionally distinct zones. The characterization of histomorphological characteristics, mechanical behaviour and structural characteristics of growth plate tissue allowed finding an association between these key elements, which raise certain hypotheses about the effect of loading on the growth process. This discussion is a summary and a complement to the discussions presented in each scientific article in sections 3.6, 4.6 and 5.7.

6.1 Growth plate histomorphology

One of the important mechanisms through which cells may respond to changes in their environment in both normal and mechanically modulated growth is directly through deformation of cellular membrane (Sachs, 1991; Watson, 1991). In this light, one of the important steps toward understanding the role of chondrocyte membrane deformation in signal transduction is to characterize the shape and volume of growth plate chondrocytes. Moreover, it has been suggested that the final volume and shape of hypertrophic chondrocytes are important factors in determining the rate of longitudinal bone growth, both in normal bone development (Buckwalter & Mower, 1987; Buckwalter et al., 1986; Hunziker & Schenk, 1989) and in mechanically modulated bone growth (I. A. Stokes et al., 2007; Villemure & Stokes, 2009). Finally, changes in cell volume have been previously shown to influence the matrix synthesis in cartilaginous tissue and will consequently have a significant impact on the integrity of the extracellular matrix (Hall, 1995; Kerrigan & Hall, 2008; Urban et al., 1993; Villemure & Stokes, 2009). That is why we decided to address growth plate morphology in the first place (Article No.1).

The first objective of this thesis was to characterize the three-dimensional histomorphology of growth plate within its three distinct histological zones (reserve, proliferative, hypertrophic) at cellular and tissue levels. In this thesis, characterization of growth plate histomorphology was done using a combination of experimental (tissue dissection, fluorescent labeling of cell cytoplasm and confocal microscopy) and analytical (deconvolution and three-dimensional

reconstruction) techniques. Procedures, experimental tests and analyses conducted as part of this objective of the research project helped to highlight the following conclusions:

- ☑ Growth plate morphology is heterogeneous among its three zones at both cellular and tissue levels.
- ☑ There is marked heterogeneity in cell sizes through the different histological zones of the growth plate. Chondrocyte volume increased about five-fold from the reserve to the hypertrophic zones along the direction of growth. Chondrocytes surface area increased three-fold from the stem cell pool in the reserve zone to the calcification border in the hypertrophic zone.
- ☑ Chondrocytes undergo several spatially-oriented shape changes while progressing from the resting to the proliferative to maturation stages along the growth direction. Chondrocytes in the reserve zone were round and randomly scattered in the extracellular matrix of growth plate with no special alignment, while flattened proliferative and spherical hypertrophied chondrocytes were aligned along the direction of bone growth.
- ☑ The average cell/matrix volume ratio significantly increased approaching the calcification zone, which is consistent with published studies reporting a 9-time increase in cell/matrix volume ratio values from the resting to the hypertrophic zones.

Additional items of discussion are discussed below.

Up to date, conventional histology and stereological techniques combined to chemical fixation have been widely used to characterize two- and three-dimensional growth plate morphometric parameters (Bachrach, 1995; Breur et al., 1994; Breur et al., 1991; Buckwalter et al., 1985; Buckwalter et al., 1986; C. E. Farnum & N. J. Wilsman, 1998; Glade & Belling, 1984; Hunziker & Schenk, 1989). However, *in situ* three-dimensional visualization and zonal characterization of growth plate morphometry at both cellular and tissue levels have not been documented yet. This objective provides for the very first time a direct and non-invasive three-dimensional measurement of the *in situ* size and shape of growth plate chondrocytes without fixation or physical sectioning of the tissue. Chemical fixation technique is believed to result in proteoglycan loss in the matrix and to cause changes in the aspect of chondrocytes and their surrounding

matrix (Egglı et al., 1985). Furthermore, the absence of intracellular signaling in fixation techniques may inhibit the regulatory mechanisms such as regulatory volume change mechanism (through the cytoskeleton for example) and eventually would affect the evaluated morphological parameters (Kerrigan & Hall, 2008).

Chondrocyte volume is not sufficient by itself to assign a growth plate chondrocyte to a specific zone, especially at the reserve/proliferative and proliferative/hypertrophic transitions (C. E. Farnum & N. J. Wilsman, 1998). As shown in Figure 6-1, there is a clear overlap in frequency distribution of chondrocytes volume within histological zones of growth plate.

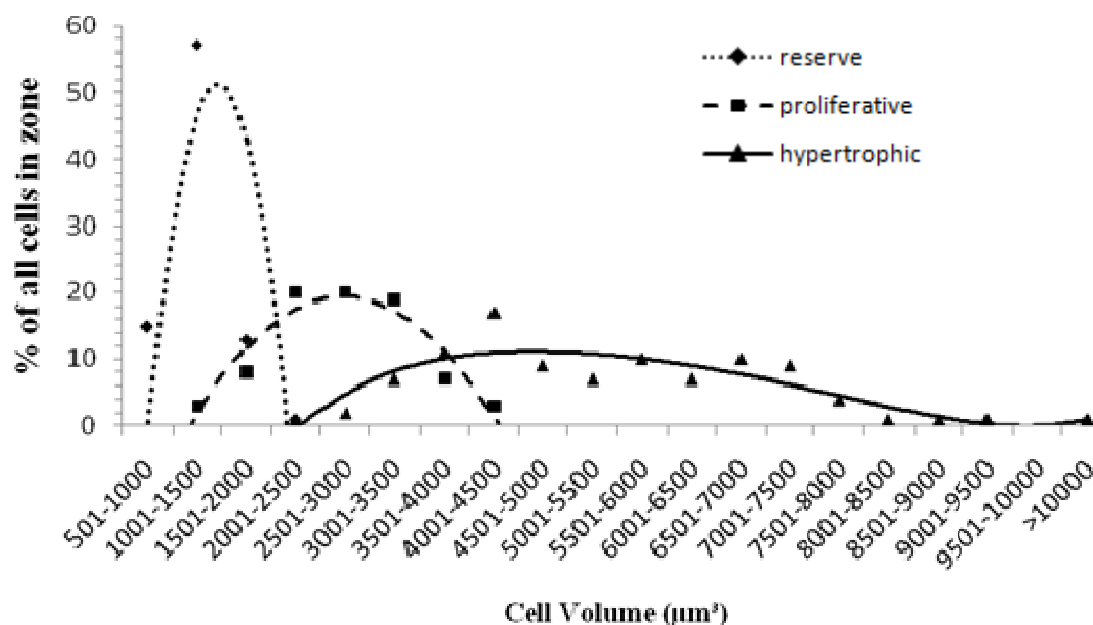


Figure 6-1 : Frequency distribution of chondrocytes volume within the three different zones of porcine growth plate. Polynomial curves were fitted to the data.

Hence, other morphometrical parameters such as sphericity (transition zone between proliferative and hypertrophic zones) and chondrocytes organization (transition zone between reserve and proliferative zone) are required to differentiate between chondrocytes coming from different histological zones. Based on the greater heterogeneity observed in chondrocytes volume within proliferative and hypertrophic zones, chondrocytes within these zones could indeed be considered

as two sub-histological zones (upper and lower) as indicated in the literature (C. E. Farnum & N. J. Wilsman, 1998; Kember, 1978).

This study characterized the morphometry of an intact, healthy growth plates from 4-week old porcine ulna. However, quantitative measurements of growth plate morphology and its variation with developmental stage, site and disease were not considered in this study. This may provide new insights into contribution of morphometry on growth plate physiology and pathology.

Another methodological limit in this study was cutting the explants in halves that may cause some changes in chondrocytes volume. However, using confocal microscopy we were able to go deep enough in the tissue (50-150 μm) to avoid the effects of the cutting step. This was confirmed by live/dead assays, which largely showed live chondrocytes from 50 μm and deeper into the growth plate tissue. Hence, the analyzed regions were free of cutting effects (Figure 6-2).

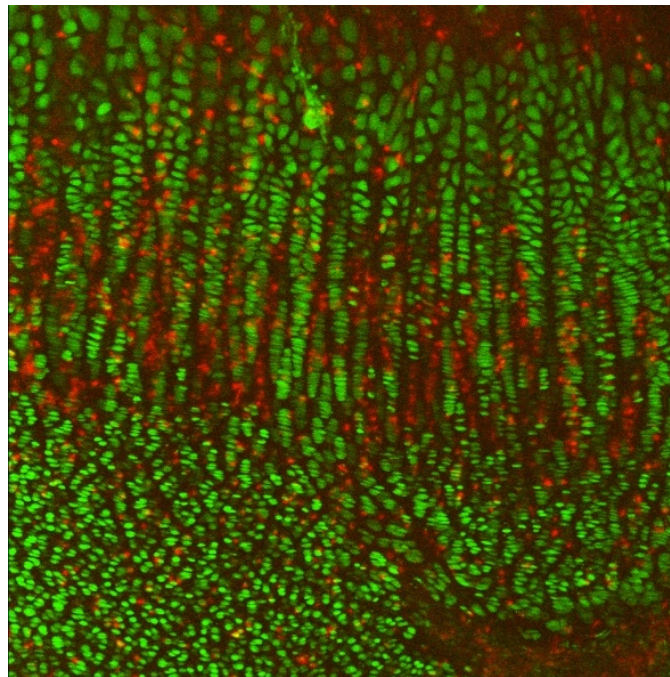


Figure 6-2 : Superposition of 2D confocal images of chondrocytes labeled with Calcein AM and Ethidium homodimer-1 through the growth plate thickness.

6.2 Growth plate mechanical behavior under compression

6.2.1 Three-dimensional *in situ* deformation under compressive loading

Cell morphology is implicated in the regulation of cell differentiation, phenotypic expression and proliferation (Watson, 1991). Changes in cell shape or size could initiate signals through stretch-activated ion channels on the cells plasma membrane, which may further regulate second messenger activity (Sachs, 1991; Watson, 1991). However, little is known about compression induced 3D morphological characteristics of intact growth plate chondrocytes maintained within their extracellular matrix. This information would further help us to understand the *in situ* effect of the mechanical environment on the biological response of growth plate chondrocytes. This is why the *in situ* three-dimensional growth plate morphology under compression was addressed at cell and tissue levels (Article No.2) using fluorescence labeling techniques combined with three-dimensional reconstruction of serial confocal sections.

Procedures, experimental tests and analyses conducted as part of this objective of the research project helped to highlight the following conclusions:

- ☑ Chondrocytes undergo significant zone-dependent shape and size changes with compression. In response to compression, larger changes in volume and surface area were found in the hypertrophic and proliferative zones compared to reserve zone, where lower bulk strains were found.
- ☑ Chondrocyte bulk strains were much greater than the applied platen-to-platen strain; they reached 1.7, 2.3 and 2.8 times the 15% applied strain, respectively, for the reserve, proliferative and hypertrophic zones.
- ☑ Decreases in cell/matrix volume ratio for the reserve and hypertrophic zones are reverse in the proliferative zone, where an increase in the cell/matrix volume ratio was observed, which implies that proliferative chondrocytes undergo less deformation compared to their extracellular matrix.

- ☑ Hypertrophic chondrocyte strains, with their greater chondrocyte bulk strains, could contribute to decreasing growth rate in response to growth plate compression as stated by Hueter-Volkmann law.

Additional items of discussion are discussed below.

Cell volume measurements done in this study were made using an intracellular stain, calcein AM. This stain rapidly bleaches and can cause apparent changes in volume. Thus, it was critical that the recovery of the volume be shown to confirm that photobleaching of the fluorescent dye did not introduce errors into the volume measurements over time. In a complementary analysis, no significant changes in chondrocyte volume were detected over the investigated period of time ($p > 0.75$). It was then confirmed that photobleaching of calcein AM did not introduce any significant error into the evaluated cell volumes in the present study (Figure 6-3).

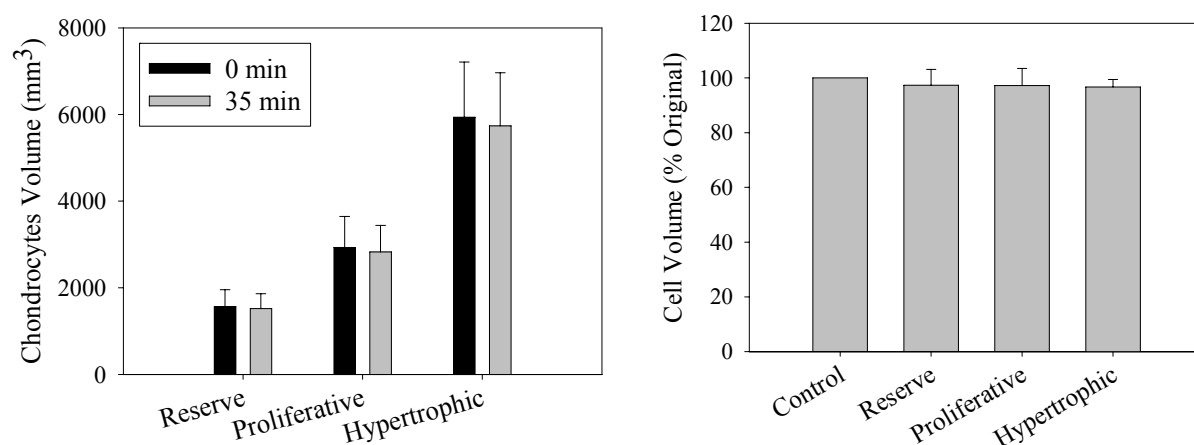


Figure 6-3 : Changes in chondrocytes volume within three histological zones of growth plate with two repeated confocal scans.

6.2.2 Two-dimensional *in situ* strain distribution through growth plate under compression

The mechanical environment is one of the regulating factors in the process of longitudinal bone growth through cartilaginous growth plates. It is clinically recognized that non-physiological compressive loading contributes to the progression of infantile and juvenile musculoskeletal

deformities, particularly during growth spurt. At the biomechanical level, mechanical properties of the growth plate and its zones have been studied. However, regional variations in growth plate mechanical behavior in animal models with lower growth rates, which most resemble humans, have never been determined under uniaxial compression. That is why we decided to characterize the strain distribution through growth plate thickness in swine model (mechanical part of Article No.3).

Procedures, experimental tests and analyses conducted as part of this objective of the research project led to the following conclusions:

- ☑ The compressive deformational behavior of the growth plate tissue was non uniform and zone dependent. Higher axial tissue strains were developed within the proliferative zone of the growth plate compared to two other histological zones. Higher transverse strains mainly arose in the proliferative and hypertrophic zones compared to the reserve zone.
- ☑ Conversely, lower and more homogenous axial as well as transverse strains were developed primarily within the reserve zone of 4-week old swine growth plates.
- ☑ The reserve and proliferative zones looked relatively homogenous between the samples compared to the hypertrophic zone, where both average strain magnitude and shape showed great variation among samples.

Additional items of discussion are discussed below

The relaxation criteria, used so that the explant reach equilibrium after application of compressive load, was chosen based on preliminary studies on the growth plate tissue. By visually monitoring the resulting applied forces, which were recorded by a single point load cell (Tedea-Huntleigh, Intertechnology Inc.) versus time, the chosen relaxation criterion (8×10^{-6} N/s) would let the samples to reach a relaxed state. Figure 6-4 shows a typical experimental stress relaxation curve of growth plate samples undergoing the two-step semi-confined compression. Both loading steps showed that the sample reached a relaxed state using the stress relaxation criterion of 8×10^{-6} N/s. Furthermore, this criterion has also been previously reported in different studies on growth plate biomechanics. In studies by Sergerie et al. (2009) and Wosu et al. (2011),

the same stress relaxation criteria was used for stress relaxation tests in unconfined compression to evaluate the mechanical properties of growth plates.

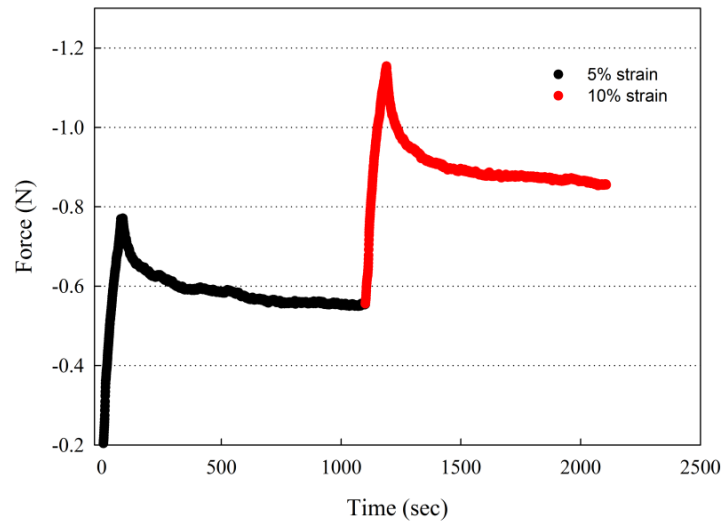


Figure 6-4 : Typical experimental stress relaxation curve of growth plate samples undergoing a two-step semi-confined compression

The results of this study will also guide the development of a more extensive *in vitro* study to compare mechanical behaviour of porcine growth plates loaded in equivalent static and dynamic loading conditions beforehand.

6.3 Growth plate structural characteristics

Growth plate extracellular matrix is mainly composed of water, proteoglycan within type II collagen fibers as well as type X collagen exclusively in the hypertrophic zones. All these elements are believed to be determinants of cartilaginous tissue biomechanical competence (Speer, 1982) and provide tissue with its mechanical stiffness (Mwale et al., 2002). However, up to date, no study had comprehensively analyzed the zonal growth plate compressive mechanical behavior with respect to its biochemical composition and collagen fiber organization. That is why Objective 3 (Section 2.2) and Objective 4 (Section 2.2) were defined in this research project to evaluate the biochemical content and collagen fiber orientation through growth plate thickness.

Procedures, experimental tests and analyses conducted as part of this objective of the research project led to the following conclusions:

- ☑ The growth plate has a non uniform collagen content but similar GAG and water contents through its thickness.
- ☑ A significant decrease in collagen content from the reserve zone to the chondro-osseous junction was observed.
- ☑ The growth plate collagen fiber orientation was non uniform through its thickness.
- ☑ The random dispersion of chondrocytes in the reserve zone and the columnar arrangement of chondrocytes in proliferative and hypertrophic zones correlate with the orientation of collagen fibers in these zones.
- ☑ An increase in the intensity of birefringence with decreasing the width of the longitudinal septa from the proliferative zone to the hypertrophic zone was observed.

This study includes some technical limits. First of all, the biochemical study, investigating the growth plate zonal biocomposition, and the mechanical study, used to determine the strain distribution, were not done on the same growth plate samples due to methodological limits at tissue preparation level. The explants had to be cut in halves for the mechanical experiments in order to image the samples using the inverted confocal microscope while the samples used in the biochemical assays had to be trimmed along the three growth plate zones. The challenging procedure of cutting a semi-cylindrical explants along the three zones was not attempted, as it would have increased the manipulation on the explants and most probably caused defects in the resulting samples. This consequently limited the statistical analyses to establish relationships between mechanical behavior and biochemical contents. However, all the experimental analyses were completed on one animal model (porcine ulna) at a fixed developmental stage (4 week old). Given that we have completed this objective on separate growth plate samples, multiple analyses that could have improved the statistics were consequently not done.

It is also noteworthy to mention that the study of collagen fiber organization using PLM, Objective 4 (Section 2.2), was added to this research project further in the time, since we thought it would further our understanding of growth plate collagen organization and its effect on mechanical response of the tissue.

6.4 Global discussion and overall limits of the research project

At the histomorphological level, major differences in tissue and cellular morphology as well as cellular arrangements may explain growth plate mechanical behavior during the growth process. In this light, the ability to measure *in situ* cell surface area and volume directly and monitor their changes in the direction of growth would allow better understanding of the possible mechanisms through which abnormal growth is triggered. More specifically, at the mechanobiological level, chondrocytes hypertrophy, which is believed to be mostly involved in the bone growth process compared to cellular proliferation and matrix synthesis (Wilsman, Farnum, Leiferman, et al., 1996), could be monitored with anatomical sites, developmental stage as well as disease to further our understanding of the mechanisms through which morphometric regulation of hypertrophic chondrocytes could trigger abnormal growth.

At the mechanical level, the less rigid hypertrophic and proliferative zones at both cellular and tissue levels could be more prone to trigger abnormal endochondral growth under compressive loading, whereas the reserve zone would act like a mechanical support to the growth plate. At the structural level, collagen content and collagen fiber orientation are two significant elements influencing the mechanical behavior of the growth plate at early developmental stages of growth. Proliferative and hypertrophic zones of the growth plate, where lower collagen content was found and in which the collagen fibers were oriented along the growth direction, could be more involved in abnormal endochondral growth process in response to compressive loading. First of all, therapies aiming to direct or influence pathologic growth plate maturation should take into consideration that the proliferative and hypertrophic zones are more susceptible to compressive strains, and hence are more likely to be involved in the process of mechanical growth modulation exploited in the minimally invasive treatment approaches of progressive skeletal deformities to correct abnormal growth. Second of all, more research could be conducted at the mechanobiological level to investigate the effect of mechanical loading on these zones. In this light, cellular proliferation and hypertrophy could be investigated with developmental stage and disease using special markers such as type X collagen for hypertrophy and Ki-67 or Bromodeoxyuridine (BrdU) for cellular proliferation.

These studies include some technical limits. First of all, the study is limited to a single animal model. Hence, it is important to be cautious when interpreting the results and the generalization of conclusions. However, this study was done in an animal model with a low growth rate that most resembles human. Secondly, the mechanical tests were performed with loading parameters limited to one single amplitude. With additional mechanical tests, it might be interesting to investigate the effect of amplitude of loading (physiological and pathophysiological) on the growth plate morphology. Furthermore, the loading apparatus used in this thesis has the potential to be modified to apply dynamic loading, which is believed to be as effective as static loading with less detrimental effects on the growth plate (Valteau et al., 2011). Comparative studies on static and dynamic loading might provide complementary knowledge to better understand the process of mechanical modulation of growth and provide an objective justification for non-invasive surgical treatments of progressive musculoskeletal deformities. Additionally, evaluating the variation between sites, developmental stages, and with species as well as diseases could also be very interesting. Finally, although general trends were observed, the difficulty of demonstrating statistical differences may be due to the limited sample size.

At the biochemical and structural level, having evaluated the biocomposition in separate growth plate samples than mechanical analyses as stated before, no multiple statistical analyses were performed. This would have allowed establishing more concrete relationships between the mechanical behavior and structural characteristics of the growth plate tissue.

CONCLUSIONS AND RECOMMENDATIONS

The main objective of the present research project was to characterize histomorphological (cell and tissue morphology) and structural (biochemical composition, fibrillar collagen organization) characteristics as well as mechanical behaviour (in terms of developed strains) of growth plate at cellular and tissue levels in its three distinct histological zones and to establish relationships between zonal mechanical behaviour and biochemical composition of the growth plate. The development of protocols, of an experimental set-up and of a research methodology allowed to answer the research hypotheses and to meet the five project objectives. Histomorphology, mechanical behavior, and structural characteristics (biochemical content and collagen fiber organization) of swine growth plates were addressed in this research project. As the first step, morphometric characteristics of growth plate were evaluated by combining fluorescent labeling, confocal microscopy and three-dimensional reconstruction techniques. Afterwards, mechanical tests were performed on explants of porcine growth plate to address its mechanical behavior at the cellular level, using fluorescent labeling, confocal microscopy and three-dimensional reconstruction techniques, and at the tissue level, using a combination of fluorescent labeling, confocal microscopy and two-dimensional digital image correlation (DIC) approaches. As the third step, the biocomposition of growth plate extracellular matrix was evaluated using proper biochemical assays and collagen fiber orientation was characterized in swine growth plate extracellular matrix using polarized light microscopy. Finally, a study was conducted to analyze the possible association between the mechanical behavior and structural characteristics of swine growth plates.

First of all, a marked heterogeneity in *in situ* cell and tissue morphology through the different histological zones of the growth plate was observed. Cell size as well as cell/matrix volume ratio were shown to increase from the pool of chondrocytes in the reserve zone approaching the chondro-osseous junction. Hence, the first research hypothesis, stating that *three-dimensional histomorphological characteristics of the growth plate at cellular (volume, surface area, major/minor radii and sphericity) and tissue (cell/matrix volume ratio) levels are non-uniform and change with its histological zone*, was confirmed. It is now clear that histomorphological characteristics across the growth plate is heterogeneous and zone-dependent.

Secondly, it was shown that uniform compressive loading results in a significant, zone-dependent changes in cellular and tissue morphology. In response to compression, greater changes in cellular morphology were found in the hypertrophic and proliferative zones compared to the reserve zone. Furthermore, proliferative chondrocytes were shown to undergo less deformation compared to their extracellular matrix, whereas higher deformations were shown to develop in chondrocytes of the reserve and hypertrophic zones compared to their surrounding extracellular matrix. At tissue level, mechanical behavior was also shown non uniform and zone-dependent. Higher strains along and perpendicular to loading direction arose in the proliferative zone and hypertrophic zone, respectively, where lower collagen content was found and collagen fibers were oriented parallel to growth direction. Conversely, lower strains were developed in the reserve zone, which contained the maximum collagen content and fibers principally aligned perpendicular to growth direction. Therefore, the second hypothesis, affirming that *in response to uniform compressive loading, non-uniform three-dimensional cellular strain as well as two-dimensional tissue strain will develop depending on the histological zone under study*, was also established. It was indeed confirmed that growth plate mechanical behavior at both cellular and tissue levels is non uniform and zone-dependent through its thickness. Indeed, it was further shown that among the structural properties of the growth plate extracellular matrix, collagen content and collagen fiber orientation is zone-dependent across the growth plate thickness. However, water and GAG content was shown to be indistinguishable and hence constant across the growth plate thickness. Therefore, the third hypothesis, stating that *biochemical composition (collagen, GAG and water content) and type II collagen fiber orientation change with the histological zone throughout the growth plate thickness* was partially confirmed. It was further shown that each histological zone plays a noticeable role in response to compressive loading. Furthermore, it was shown that the structural characteristics of each distinct zone of growth plate play an utmost role in the zonal mechanical behavior. Histological zones with lower collagen content and vertically oriented type II collagen fibers (proliferative, hypertrophic) developed higher cellular and tissue strains, whereas the histological zone with higher collagen content and horizontally oriented type II collagen fibers (reserve) developed lower cellular and tissue strain. Therefore, the final hypothesis of the present thesis, stating that *developed strain within the three zones of the growth plate is related to the corresponding biochemical composition (collagen,*

GAG and water content) as well as type II collagen fiber organization, was also partly established.

This study is the first that provides relevant information on the growth plate histomorphology, mechanical behavior, and structural characteristics and their relationships in an animal model with low growth rate, which most resembles humans. The knowledge gained from this study, combined with results of other mechanobiological studies of the growth plate, adds to our understanding of the fundamental relationship between compressive forces experienced by growth plate chondrocytes and their extracellular environment structural characteristics. This information will further help us to better understand the effect of the mechanical environment on the biological response of growth plate and provide a more scientific basis for medical treatment of progressive skeletal deformities. This could have a long-term impact on the development of new strategies for the orthopaedic treatment of musculoskeletal deformities, which aim at exploiting local bone growth to reverse and optimally correct these deformities.

Considering the multidisciplinary nature of the research project, some recommendations and avenues for future work could be investigated to provide some answers to the points raised in this research project:

- ☑ Increasing the sample size of each group of study;
- ☑ Confirming the results in other anatomical sites.
- ☑ Investigating the effect of developmental stages on the mechanical behaviour and biochemical content of the growth plate to see if trends remain unchanged with the growth development.
- ☑ Performing other mechanical tests to investigate the effects of loading amplitude on mechanical behaviour of growth plate.
- ☑ Investigating the effect of type of loading (dynamic versus static) on the mechanical behaviour of growth plate by modification of the loading apparatus.
- ☑ Performing other mechanical tests on pathological tissue to investigate the effect of pathology on the mechanical behavior of growth plate tissue.

- ☑ Developing a new methodology in order to perform both mechanical tests and biochemical assays on the same explant.
- ☑ Looking at collagen fibers using scanning electron microscopy (SEM) in order to quantify variations in collagen fiber characteristics such as fiber diameter and confirming the fiber orientation in the three histological zones of the growth plate.

From a clinical point of view, it is of great interest to determine whether the mechanical behavior of the growth plate contributes to the rapid progression of musculoskeletal deformities coinciding with periods of accelerated growth. The results of this study demonstrate that morphometry, mechanical behavior, and structural characteristics of growth plate are zone-dependent and interconnected. Disease progression could be due to the interplay between these factors in one or certain zones of the growth plate as well as other factors related to the disease. Knowledge on the interplay between these factors could contribute to understanding the abnormal growth as well as development of new approaches for treatment of progressive musculoskeletal deformities.

BIBLIOGRAPHY

- Abad, V., Meyers, J. L., Weise, M., Gafni, R. I., Barnes, K. M., Nilsson, O., . . . Baron, J. (2002). The role of the resting zone in growth plate chondrogenesis. *Endocrinology*, 143(5), 1851-1857.
- Abbaszade, I., Liu, R. Q., Yang, F., Rosenfeld, S. A., Ross, O. H., Link, J. R., . . . et al. (1999). Cloning and characterization of ADAMTS11, an aggrecanase from the ADAMTS family. *J Biol Chem*, 274(33), 23443-23450.
- Alberty, A., Peltonen, J., & Ritsila, V. (1993). Effects of distraction and compression on proliferation of growth plate chondrocytes. A study in rabbits. *Acta orthopaedica Scandinavica*, 64(4), 449-455.
- Alini, M., Matsui, Y., Dodge, G. R., & Poole, A. R. (1992). The extracellular matrix of cartilage in the growth plate before and during calcification: changes in composition and degradation of type II collagen. *Calcif Tissue Int*, 50(4), 327-335.
- Alvarez-Leefmans, F. J., Altamirano, J., & Crowe, W. E. (1995). Use of ion-selective microelectrodes and fluorescent probes to measure cell volume. In K. Jacob & S. J. Dixon (dir.), *Methods in neurosciences*. (Vol. 27, pp. 361-391). London: Academic Press.
- Alvarez, J., Balbin, M., Santos, F., Fernandez, M., Ferrando, S., & Lopez, J. M. (2000). Different bone growth rates are associated with changes in the expression pattern of types II and X collagens and collagenase 3 in proximal growth plates of the rat tibia. *J Bone Miner Res*, 15(1), 82-94. doi:10.1359/jbmr.2000.15.1.82 [doi]
- Amini, S., Veilleux, D., & Villemure, I. (2010). Tissue and cellular morphological changes in growth plate explants under compression. *J Biomech*, 43(13), 2582-2588. doi:S0021-9290(10)00280-0 [pii]10.1016/j.jbiomech.2010.05.010 [doi]
- Anderson, H. C. (1995). Molecular biology of matrix vesicles. *Clin Orthop Relat Res*(314), 266-280.
- Apte, S. S., & Kenwright, J. (1994). Physeal distraction and cell proliferation in the growth plate. *J Bone Joint Surg Br*, 76(5), 837-843.
- Arkin, A. M., & Katz, J. F. (1956). The effects of pressure on epiphyseal growth; the mechanism of plasticity of growing bone. *J Bone Joint Surg Am*, 38-A(5), 1056-1076.
- Arnoczky, S. P., Lavagnino, M., Whallon, J. H., & Hoonjan, A. (2002). In situ cell nucleus deformation in tendons under tensile load; a morphological analysis using confocal laser microscopy. *Journal of orthopaedic research : official publication of the Orthopaedic Research Society*, 20(1), 29-35. doi:10.1016/S0736-0266(01)00080-8 [doi]
- Arokoski, J. P., Hyttinen, M. M., Lapvetelainen, T., Takacs, P., Kosztaczky, B., Modis, L., . . . Helminen, H. (1996). Decreased birefringence of the superficial zone collagen network in the canine knee (stifle) articular cartilage after long distance running training, detected by quantitative polarised light microscopy. *Ann Rheum Dis*, 55(4), 253-264.

- Aronsson, D. D., Stokes, I. A., Rosovsky, J., & Spence, H. (1999). Mechanical modulation of calf tail vertebral growth: implications for scoliosis progression. *J Spinal Disord*, 12(2), 141-146.
- Arriola, F., Forriol, F., & Canadell, J. (2001). Histomorphometric study of growth plate subjected to different mechanical conditions (compression, tension and neutralization): an experimental study in lambs. Mechanical growth plate behavior. *J Pediatr Orthop B*, 10(4), 334-338.
- Aspden, R. M., Yarker, Y. E., & Hukins, D. W. (1985). Collagen orientations in the meniscus of the knee joint. *J Anat*, 140 (Pt 3), 371-380.
- Bachrach, N. M. (1995). *Growth plate chondrocyte deformation in situ and a biphasic inclusion model for cells within hydrated soft tissues*. (Ph.D.), Columbia University, New York. Tiré de <http://proquest.umi.com/pqdweb?did=742588631&Fmt=7&clientId=43390&RQT=309&VName=PQD>
- Bachrach, N. M., Valhmu, W. B., Stazzone, E., Ratcliffe, A., Lai, W. M., & Mow, V. C. (1995). Changes in proteoglycan synthesis of chondrocytes in articular cartilage are associated with the time-dependent changes in their mechanical environment. *J Biomech*, 28(12), 1561-1569. doi:0021-9290(95)00103-4 [pii]
- Baker, J., Liu, J. P., Robertson, E. J., & Efstratiadis, A. (1993). Role of insulin-like growth factors in embryonic and postnatal growth. *Cell*, 75(1), 73-82. doi:0092-8674(93)90680-O [pii]
- Ballock, R. T., Heydemann, A., Wakefield, L. M., Flanders, K. C., Roberts, A. B., & Sporn, M. B. (1993). TGF-beta 1 prevents hypertrophy of epiphyseal chondrocytes: regulation of gene expression for cartilage matrix proteins and metalloproteases. *Dev Biol*, 158(2), 414-429. doi:10.1006/dbio.1993.1200 [doi] S0012-1606(83)71200-5 [pii]
- Ballock, R. T., & O'Keefe, R. J. (2003a). The biology of the growth plate. *J Bone Joint Surg Am*, 85-A(4), 715-726.
- Ballock, R. T., & O'Keefe, R. J. (2003b). Physiology and pathophysiology of the growth plate. *Birth Defects Res C Embryo Today*, 69(2), 123-143. doi:<http://dx.doi.org10.1002/bdrc.10014>
- Balmain, N., Leguellec, D., Elkak, A., Nars, G., Toury, R., & Schoevaert, D. (1995). Zonal variations of types II, IX and XI collagen mRNAs in rat epiphyseal cartilage chondrocytes: quantitative evaluation of in situ hybridization by image analysis of radioautography. *Cell Mol Biol (Noisy-le-grand)*, 41(1), 197-212.
- Bassett, J. H., Swinhoe, R., Chassande, O., Samarut, J., & Williams, G. R. (2006). Thyroid hormone regulates heparan sulfate proteoglycan expression in the growth plate. *Endocrinology*, 147(1), 295-305. doi:en.2005-0485 [pii] 10.1210/en.2005-0485 [doi]
- Basso, N., & Heersche, J. N. (2006). Effects of hind limb unloading and reloading on nitric oxide synthase expression and apoptosis of osteocytes and chondrocytes. *Bone*, 39(4), 807-814. doi:S8756-3282(06)00409-1 [pii] 10.1016/j.bone.2006.04.014 [doi]

- Bay, B. K. (1995). Texture correlation: a method for the measurement of detailed strain distributions within trabecular bone. *Journal of orthopaedic research : official publication of the Orthopaedic Research Society*, 13(2), 258-267. doi:<http://dx.doi.org/10.1002/jor.1100130214>
- Bay, B. K., Yerby, S. A., McLain, R. F., & Toh, E. (1999). Measurement of strain distributions within vertebral body sections by texture correlation. *Spine*, 24(1), 10-17.
- Betz, R. R., D'Andrea, L. P., Mulcahey, M. J., & Chafetz, R. S. (2005). Vertebral body stapling procedure for the treatment of scoliosis in the growing child. *Clin Orthop Relat Res*(434), 55-60. doi:00003086-200505000-00009 [pii]
- Beutler, W. J., Fredrickson, B. E., Murtland, A., Sweeney, C. A., Grant, W. D., & Baker, D. (2003). The natural history of spondylolysis and spondylolisthesis: 45-year follow-up evaluation. *Spine (Phila Pa 1976)*, 28(10), 1027-1035; discussion 1035. doi:10.1097/01.BRS.00000061992.98108.A0 [doi]
- Bey, M. J., Song, H. K., Wehrli, F. W., & Soslowsky, L. J. (2002). A noncontact, nondestructive method for quantifying intratissue deformations and strains. *Journal of biomechanical engineering*, 124(2), 253-258.
- Blatter, L. A. (1999). Cell volume measurements by fluorescence confocal microscopy: theoretical and practical aspects. *Methods Enzymol*, 307, 274-295.
- Bonnel, F., Dimeglio, A., Baldet, P., & Rabischong, P. (1984). Biomechanical activity of the growth plate. Clinical incidences. *Anat Clin*, 6(1), 53-61.
- Bonnel, F., Peruchon, E., Baldet, P., Dimeglio, A., & Rabischong, P. (1983). Effects of compression on growth plates in the rabbit. *Acta Orthop Scand*, 54(5), 730-733.
- Brashear, H. R., Jr. (1963). Epiphyseal avascular necrosis and its relation to longitudinal bone growth. *J Bone Joint Surg Am*, 45, 1423-1438.
- Braun, J. T., Akyuz, E., Ogilvie, J. W., & Bachus, K. N. (2005). The efficacy and integrity of shape memory alloy staples and bone anchors with ligament tethers in the fusionless treatment of experimental scoliosis. *J Bone Joint Surg Am*, 87(9), 2038-2051. doi:87/9/2038 [pii] 10.2106/JBJS.D.02103 [doi]
- Breur, G. J., Lapierre, M. D., Kazmierczak, K., Stechuchak, K. M., & McCabe, G. P. (1997). The domain of hypertrophic chondrocytes in growth plates growing at different rates. *Calcif Tissue Int*, 61(5), 418-425.
- Breur, G. J., Turgai, J., Vanenkevort, B. A., Farnum, C. E., & Wilsman, N. J. (1994). Stereological and serial section analysis of chondrocytic enlargement in the proximal tibial growth plate of the rat. *Anat Rec*, 239(3), 255-268. doi:10.1002/ar.1092390304 [doi]
- Breur, G. J., VanEnkevort, B. A., Farnum, C. E., & Wilsman, N. J. (1991). Linear relationship between the volume of hypertrophic chondrocytes and the rate of longitudinal bone growth in growth plates. *Journal of orthopaedic research*, 9(3), 348-359. doi:10.1002/jor.1100090306 [doi]

- Bruckner, P., Vaughan, L., & Winterhalter, K. H. (1985). Type IX collagen from sternal cartilage of chicken embryo contains covalently bound glycosaminoglycans. *Proc Natl Acad Sci U S A*, 82(9), 2608-2612.
- Bruns, J., Kahrs, J., Kampen, J., Behrens, P., & Plitz, W. (1998). Autologous perichondral tissue for meniscal replacement. *J Bone Joint Surg Br*, 80(5), 918-923.
- Bruns, J., Kampen, J., Kahrs, J., & Plitz, W. (2000). [Autologous meniscus replacement with rib perichondrium. Experimental results]. *Orthopade*, 29(2), 145-150.
- Buckwalter, J. A., & Mower, D. (1987). Alterations of growth plate associated with slowing of bone growth. *Annual meeting of orthopaedic research society, San Francisco, CA, USA*. (Vol. 33, pp. 490).
- Buckwalter, J. A., Mower, D., Schafer, J., Ungar, R., Ginsberg, B., & Moore, K. (1985). Growth-plate-chondrocyte profiles and their orientation. *The Journal of bone and joint surgery. American volume*, 67(6), 942-955.
- Buckwalter, J. A., Mower, D., Ungar, R., Schaeffer, J., & Ginsberg, B. (1986). Morphometric analysis of chondrocyte hypertrophy. *The Journal of bone and joint surgery. American volume*, 68(2), 243-255.
- Buridan, F., Szumilo, J., Korobowicz, A., Farooquee, R., Patel, S., Patel, A., . . . Dudka, J. (2009). Morphology and physiology of the epiphyseal growth plate. *Folia Histochem Cytobiol*, 47(1), 5-16. doi:LM04K3M612476K04 [pii] 10.2478/v10042-009-0007-1 [doi]
- Burleigh, M. C., Barrett, A. J., & Lazarus, G. S. (1974). Cathepsin B1. A lysosomal enzyme that degrades native collagen. *Biochem J*, 137(2), 387-398.
- Buschmann, M. D., Gluzband, Y. A., Grodzinsky, A. J., Kimura, J. H., & Hunziker, E. B. (1992). Chondrocytes in agarose culture synthesize a mechanically functional extracellular matrix. *Journal of orthopaedic research : official publication of the Orthopaedic Research Society*, 10(6), 745-758. doi:10.1002/jor.1100100602 [doi]
- Bush, P. G., & Hall, A. C. (2001). The osmotic sensitivity of isolated and in situ bovine articular chondrocytes. *Journal of orthopaedic research : official publication of the Orthopaedic Research Society*, 19(5), 768-778. doi:S0736026601000134 [pii] 10.1016/S0736-0266(01)00013-4 [doi]
- Bush, P. G., & Hall, A. C. (2003). The volume and morphology of chondrocytes within non-degenerate and degenerate human articular cartilage. *Osteoarthritis Cartilage*, 11(4), 242-251. doi:S1063458402003692 [pii]
- Bush, P. G., Hall, A. C., & Macnicol, M. F. (2008). New insights into function of the growth plate: clinical observations, chondrocyte enlargement and a possible role for membrane transporters. *The Journal of bone and joint surgery. British volume*, 90(12), 1541-1547. doi:90-B/12/1541 [pii] 10.1302/0301-620X.90B12.20805 [doi]
- Bush, P. G., Parisinos, C. A., & Hall, A. C. (2008). The osmotic sensitivity of rat growth plate chondrocytes in situ; clarifying the mechanisms of hypertrophy. *J Cell Physiol*, 214(3), 621-629. doi:10.1002/jcp.21249

- Bush, P. G., Wokosin, D. L., & Hall, A. C. (2007). Two-versus one photon excitation laser scanning microscopy: critical importance of excitation wavelength. *Front Biosci*, 12, 2646-2657. doi:2261 [pii]
- Byers, S., van Rooden, J. C., & Foster, B. K. (1997). Structural changes in the large proteoglycan, aggrecan, in different zones of the ovine growth plate. *Calcif Tissue Int*, 60(1), 71-78.
- Callister, W. D. (2002). *Materials Science and Engineering: An introduction* (6^e éd.): Wiley.
- Canal, C. E., Hung, C. T., & Ateshian, G. A. (2008). Two-dimensional strain fields on the cross-section of the bovine humeral head under contact loading. *J Biomech*, 41(15), 3145-3151. doi:S0021-9290(08)00449-1 [pii] 10.1016/j.jbiomech.2008.08.031 [doi]
- Cancel, M., Grimard, G., Thuillard-Crisinel, D., Moldovan, F., & Villemure, I. (2009). Effects of in vivo static compressive loading on aggrecan and type II and X collagens in the rat growth plate extracellular matrix. *Bone*, 44(2), 306-315. doi:S8756-3282(08)00778-3 [pii] 10.1016/j.bone.2008.09.005 [doi]
- Cassorla, F. G., Skerda, M. C., Valk, I. M., Hung, W., Cutler, G. B., Jr., & Loriaux, D. L. (1984). The effects of sex steroids on ulnar growth during adolescence. *J Clin Endocrinol Metab*, 58(4), 717-720.
- Chandrasekhar, S., Esterman, M. A., & Hoffman, H. A. (1987). Microdetermination of proteoglycans and glycosaminoglycans in the presence of guanidine hydrochloride. *Anal Biochem*, 161(1), 103-108. doi:0003-2697(87)90658-0 [pii]
- Changoor, A., Tran-Khanh, N., Methot, S., Garon, M., Hurtig, M. B., Shive, M. S., & Buschmann, M. D. (2011). A polarized light microscopy method for accurate and reliable grading of collagen organization in cartilage repair. *Osteoarthritis Cartilage*, 19(1), 126-135. doi:S1063-4584(10)00351-1 [pii] 10.1016/j.joca.2010.10.010 [doi]
- Cheng, P., Sutton, M., Schreier, H., & McNeill, S. (2002). Full-field speckle pattern image correlation with B-Spline deformation function. *Experimental Mechanics*, 42(3), 344-352. doi:10.1177/001448502321548445
- Choi, J. B., Youn, I., Cao, L., Leddy, H. A., Gilchrist, C. L., Setton, L. A., & Guilak, F. (2007). Zonal changes in the three-dimensional morphology of the chondron under compression: the relationship among cellular, pericellular, and extracellular deformation in articular cartilage. *J biomech*, 40(12), 2596-2603. doi:<http://dx.doi.org/10.1016/j.jbiomech.2007.01.009>
- Cohen, B., Chorney, G. S., Phillips, D. P., Dick, H. M., Buckwalter, J. A., Ratcliffe, A., & Mow, V. C. (1992). The microstructural tensile properties and biochemical composition of the bovine distal femoral growth plate. *Journal of orthopaedic research : official publication of the Orthopaedic Research Society*, 10(2), 263-275. doi:10.1002/jor.1100100214 [doi]
- Cohen, B., Chorney, G. S., Phillips, D. P., Dick, H. M., & Mow, V. C. (1994). Compressive stress-relaxation behavior of bovine growth plate may be described by the nonlinear biphasic theory. *Journal of orthopaedic research : official publication of the Orthopaedic Research Society*, 12(6), 804-813. doi:10.1002/jor.1100120608 [doi]

- Cohen, B., Lai, W. M., & Mow, V. C. (1998). Transversely isotropic biphasic model for unconfined compression of growth plate and chondroepiphysis. *Journal of Biomechanical Engineering, Transactions of the ASME*, 120(4), 491-496.
- Courvoisier, A., Eid, A., & Merloz, P. (2009). Epiphyseal stapling of the proximal tibia for idiopathic genu valgum. *J Child Orthop*, 3(3), 217-221. doi:10.1007/s11832-009-0178-5 [doi]
- Cowell, H. R., Hunziker, E. B., & Rosenberg, L. (1987). The role of hypertrophic chondrocytes in endochondral ossification and in the development of secondary centers of ossification. *J Bone Joint Surg Am*, 69(2), 159-161.
- Coxam, V., Bowman, B. M., Mecham, M., Roth, C. M., Miller, M. A., & Miller, S. C. (1996). Effects of dihydrotestosterone alone and combined with estrogen on bone mineral density, bone growth, and formation rates in ovariectomized rats. *Bone*, 19(2), 107-114. doi:8756328296001354 [pii]
- Cutler, G. B., Jr. (1997). The role of estrogen in bone growth and maturation during childhood and adolescence. *J Steroid Biochem Mol Biol*, 61(3-6), 141-144.
- Darling, E. M., Zauscher, S., & Guilak, F. (2006). Viscoelastic properties of zonal articular chondrocytes measured by atomic force microscopy. *Osteoarthritis Cartilage*, 14(6), 571-579. doi:S1063-4584(05)00349-3 [pii] 10.1016/j.joca.2005.12.003 [doi]
- Demarquay, D., Dumontier, M. F., Tsagris, L., Bourguignon, J., Nataf, V., & Corvol, M. T. (1990). In vitro insulin-like growth factor I interaction with cartilage cells derived from postnatal animals. *Horm Res*, 33(2-4), 111-114; discussion 115.
- Desrochers, J., & Duncan, N. A. (2010). Strain transfer in the annulus fibrosus under applied flexion. *J Biomech*, 43(11), 2141-2148. doi:S0021-9290(10)00208-3 [pii] 10.1016/j.jbiomech.2010.03.045 [doi]
- Diab, M., Wu, J. J., & Eyre, D. R. (1996). Collagen type IX from human cartilage: a structural profile of intermolecular cross-linking sites. *Biochem J*, 314 (Pt 1), 327-332.
- DiSilvestro, M. R., & Suh, J. K. (2001). A cross-validation of the biphasic poroviscoelastic model of articular cartilage in unconfined compression, indentation, and confined compression. *J Biomech*, 34(4), 519-525. doi:S0021929000002244 [pii]
- Duncan, N. A. (2006). Cell deformation and micromechanical environment in the intervertebral disc. *J Bone Joint Surg Am*, 88 Suppl 2, 47-51. doi:88/1_suppl_2/47 [pii] 10.2106/JBJS.F.00035 [doi]
- Duncan, R. L., & Turner, C. H. (1995). Mechanotransduction and the functional response of bone to mechanical strain. *Calcif Tissue Int*, 57(5), 344-358.
- Eerola, I., Elima, K., Markkula, M., Kananen, K., & Vuorio, E. (1996). Tissue distribution and phenotypic consequences of different type X collagen gene constructs in transgenic mice. *Ann N Y Acad Sci*, 785, 248-250.
- Egerbacher, M., & Haeusler, G. (2003). Integrins in growth plate cartilage. *Pediatr Endocrinol Rev*, 1(1), 2-8.

- Eggli, P. S., Herrmann, W., Hunziker, E. B., & Schenk, R. K. (1985). Matrix compartments in the growth plate of the proximal tibia of rats. *The Anatomical record*, 211(3), 246-257. doi:10.1002/ar.1092110304 [doi]
- Ehrlich, M. G., Mankin, H. J., & Treadwell, B. V. (1972). Biochemical and physiological events during closure of the stapled distal femoral epiphyseal plate in rats. *J Bone Joint Surg Am*, 54(2), 309-322.
- Erne, O. K., Reid, J. B., Ehmke, L. W., Sommers, M. B., Madey, S. M., & Bottlang, M. (2005). Depth-dependent strain of patellofemoral articular cartilage in unconfined compression. *J Biomech*, 38(4), 667-672. doi:10.1016/j.jbiomech.2004.04.005
- Eyre, D. R., Apon, S., Wu, J. J., Ericsson, L. H., & Walsh, K. A. (1987). Collagen type IX: evidence for covalent linkages to type II collagen in cartilage. *FEBS Lett*, 220(2), 337-341. doi:0014-5793(87)80842-6 [pii]
- Farndale, R. W., Buttle, D. J., & Barrett, A. J. (1986). Improved quantitation and discrimination of sulphated glycosaminoglycans by use of dimethylmethylene blue. *Biochim Biophys Acta*, 883(2), 173-177. doi:0304-4165(86)90306-5 [pii]
- Farndale, R. W., Sayers, C. A., & Barrett, A. J. (1982). A direct spectrophotometric microassay for sulfated glycosaminoglycans in cartilage cultures. *Connect Tissue Res*, 9(4), 247-248.
- Farnum, C. E., Lee, R., O'Hara, K., & Urban, J. P. (2002). Volume increase in growth plate chondrocytes during hypertrophy: the contribution of organic osmolytes. *Bone*, 30(4), 574-581. doi:S8756328201007104 [pii]
- Farnum, C. E., Nixon, A., Lee, A. O., Kwan, D. T., Belanger, L., & Wilsman, N. J. (2000). Quantitative three-dimensional analysis of chondrocytic kinetic responses to short-term stapling of the rat proximal tibial growth plate. *Cells, tissues, organs*, 167(4), 247-258.
- Farnum, C. E., & Wilsman, N. J. (1993). Determination of proliferative characteristics of growth plate chondrocytes by labeling with bromodeoxyuridine. *Calcif Tissue Int*, 52(2), 110-119.
- Farnum, C. E., & Wilsman, N. J. (1998). Effects of distraction and compression on growth plate function. In J. A. Buckwalter, M. G. Ehrlich, L. J. Sandell & S. B. Trippel (dir.), *Skeletal Growth and Development*. (pp. 517-530). Rosemont: AAOS.
- Farnum, C. E., & Wilsman, N. J. (1998). Growth plate cellular function. In J. A. Buckwalter, M. G. Ehrlich, L. J. Sandell & S. B. Trippel (dir.), *Advances in the basis and clinical understanding of the growth plate*. (pp. 203-223). Chicago, IL: American Academy of Orthopaedic Surgeons.
- Farnum, C. E., & Wilsman, N. J. (2001). Converting a differentiation cascade into longitudinal growth: stereology and analysis of transgenic animals as tools for understanding growth plate function. *Curr Opin Orthop*, 12, 428-433.
- Francomano, C. A. (1995). Key role for a minor collagen. *Nat Genet*, 9(1), 6-8. doi:10.1038/ng0195-6 [doi]

- Fredrickson, B. E., Baker, D., McHolick, W. J., Yuan, H. A., & Lubicky, J. P. (1984). The natural history of spondylolysis and spondylolisthesis. *J Bone Joint Surg Am*, 66(5), 699-707.
- Freeman, P. M., Natarajan, R. N., Kimura, J. H., & Andriacchi, T. P. (1994). Chondrocyte cells respond mechanically to compressive loads. *Journal of orthopaedic research : official publication of the Orthopaedic Research Society*, 12(3), 311-320. doi:10.1002/jor.1100120303 [doi]
- Frost, H. M. (1990). Skeletal structural adaptations to mechanical usage (SATMU): 3. The hyaline cartilage modeling problem. *The Anatomical record*, 226(4), 423-432. doi:10.1002/ar.1092260404 [doi]
- Fujii, T., Takai, S., Arai, Y., Kim, W., Amiel, D., & Hirasawa, Y. (2000). Microstructural properties of the distal growth plate of the rabbit radius and ulna: biomechanical, biochemical, and morphological studies. *Journal of orthopaedic research : official publication of the Orthopaedic Research Society*, 18(1), 87-93. doi:10.1002/jor.1100180113 [doi]
- Gannon, J. M., Walker, G., Fischer, M., Carpenter, R., Thompson, R. C., Jr., & Oegema, T. R., Jr. (1991). Localization of type X collagen in canine growth plate and adult canine articular cartilage. *Journal of orthopaedic research : official publication of the Orthopaedic Research Society*, 9(4), 485-494. doi:10.1002/jor.1100090404 [doi]
- Glade, M. J., & Belling, T. H., Jr. (1984). Growth plate cartilage metabolism, morphology and biochemical composition in over- and underfed horses. *Growth*, 48(4), 473-482.
- Gray, M. L., Pizzanelli, A. M., Grodzinsky, A. J., & Lee, R. C. (1988). Mechanical and physiochemical determinants of the chondrocyte biosynthetic response. *Journal of orthopaedic research : official publication of the Orthopaedic Research Society*, 6(6), 777-792. doi:10.1002/jor.1100060602 [doi]
- Gray, M. L., Pizzanelli, A. M., Lee, R. C., Grodzinsky, A. J., & Swann, D. A. (1989). Kinetics of the chondrocyte biosynthetic response to compressive load and release. *Biochimica et biophysica acta*, 991(3), 415-425.
- Guilak, F. (1994). Volume and surface area measurement of viable chondrocytes in situ using geometric modelling of serial confocal sections. *J Microsc*, 173(Pt 3), 245-256.
- Guilak, F. (1995). Compression-induced changes in the shape and volume of the chondrocyte nucleus. *Journal of Biomechanics*, 28(12), 1529-1541. doi:[http://dx.doi.org/10.1016/0021-9290\(95\)00100-x](http://dx.doi.org/10.1016/0021-9290(95)00100-x)
- Guilak, F., & Hung, C. T. (2005). Physical regulation of cartilage metabolism. In V. C. Mow & R. Huiskes (dir.), *Basic Orthopaedic Biomechanics and Mechano-biology*. (3^e éd.). Philadelphia: Lippincott William and Wilkins.
- Guilak, F., Ratcliffe, A., & Mow, V. C. (1995). Chondrocyte deformation and local tissue strain in articular cartilage: a confocal microscopy study. *Journal of orthopaedic research : official publication of the Orthopaedic Research Society*, 13(3), 410-421. doi:10.1002/jor.1100130315 [doi]

- Guille, J. T., D'Andrea, L. P., & Betz, R. R. (2007). Fusionless treatment of scoliosis. *Orthop Clin North Am*, 38(4), 541-545, vii. doi:S0030-5898(07)00078-8 [pii] 10.1016/j.ocl.2007.07.003 [doi]
- Gupta, S., Lin, J., Ashby, P., & Pruitt, L. (2009). A fiber reinforced poroelastic model of nanoindentation of porcine costal cartilage: a combined experimental and finite element approach. *J Mech Behav Biomed Mater*, 2(4), 326-337; discussion 337-328. doi:S1751-6161(08)00079-9 [pii] 10.1016/j.jmbbm.2008.09.003 [doi]
- Haeusler, G., Walter, I., Helmreich, M., & Egerbacher, M. (2005). Localization of matrix metalloproteinases, (MMPs) their tissue inhibitors, and vascular endothelial growth factor (VEGF) in growth plates of children and adolescents indicates a role for MMPs in human postnatal growth and skeletal maturation. *Calcif Tissue Int*, 76(5), 326-335. doi:10.1007/s00223-004-0161-6
- Hall, A. C. (1995). Volume-sensitive taurine transport in bovine articular chondrocytes. *The Journal of physiology*, 484 (Pt 3), 755-766.
- Hausler, G., Helmreich, M., Marlovits, S., & Egerbacher, M. (2002). Integrins and extracellular matrix proteins in the human childhood and adolescent growth plate. *Calcif Tissue Int*, 71(3), 212-218. doi:10.1007/s00223-001-2083-x [doi]
- Hausser, H. J., Ruegg, M. A., Brenner, R. E., & Ksiazek, I. (2007). Agrin is highly expressed by chondrocytes and is required for normal growth. *Histochem Cell Biol*, 127(4), 363-374. doi:10.1007/s00418-006-0258-2 [doi]
- Heinegard, D., & Paulsson, M. (1984). Structure and metabolism of proteoglycans. In P. K. A. & R. A. H. (dir.), *Extracellular Matrix Biochemistry*. (pp. 277-328). Newyork, NY: Elsevier.
- Hoemann, C., Kandel, R., Roberts, S., Saris, D. B. F., Creemers, L., Mainil-Varlet, P., . . . Buschmann, M. D. (2011). International Cartilage Repair Society (ICRS) Recommended Guidelines for Histological Endpoints for Cartilage Repair Studies in Animal Models and Clinical Trials. *Cartilage*, 2(2), 153-172. doi:10.1177/1947603510397535
- Hoemann, C. D. (2004a). Cartilage and Osteoarthritis. In F. De Ceuninck, M. Sabatini & P. Pastoureau (dir.), *Methods in Molecular Medicine*. (2004/08/10^e éd., Vol. 101, pp. 127-156). doi:1-59259-821-8:127 [pii]10.1385/1-59259-821-8:127 [doi]
- Hoemann, C. D. (2004b). Molecular and biochemical assays of cartilage components. *Methods Mol Med*, 101, 127-156. doi:1-59259-821-8:127 [pii] 10.1385/1-59259-821-8:127 [doi]
- Hoemann, C. D., Sun, J., Chrzanowski, V., & Buschmann, M. D. (2002). A multivalent assay to detect glycosaminoglycan, protein, collagen, RNA, and DNA content in milligram samples of cartilage or hydrogel-based repair cartilage. *Anal Biochem*, 300(1), 1-10. doi:10.1006/abio.2001.5436 [doi] S0003269701954363 [pii]
- Hu, S. S., Tribus, C. B., Diab, M., & Ghanayem, A. J. (2008). Spondylolisthesis and spondylolysis. *Instr Course Lect*, 57, 431-445.
- Hughes, L. C., Archer, C. W., & ap Gwynn, I. (2005). The ultrastructure of mouse articular cartilage: collagen orientation and implications for tissue functionality. A polarised light

- and scanning electron microscope study and review. *Eur Cell Mater*, 9, 68-84. doi:vol009a09 [pii]
- Humbel, R., & Etringer, S. (1974). A colorimetric method for the determination of sulfated glycosaminoglycans. *Rev. Roum. Biochem.*, 11, 21-24.
- Huntley, J. S., Bush, P. G., Hall, A. C., & Macnicol, M. F. (2003). Looking at the living human growth plate. *CMAJ*, 168(4), 459-460.
- Hunziker, E. B. (1994). Mechanism of longitudinal bone growth and its regulation by growth plate chondrocytes. *Microsc Res Tech*, 28(6), 505-519. doi:10.1002/jemt.1070280606 [doi]
- Hunziker, E. B., & Schenk, R. K. (1989). Physiological mechanisms adopted by chondrocytes in regulating longitudinal bone growth in rats. *The Journal of physiology*, 414, 55-71.
- Hunziker, E. B., Schenk, R. K., & Cruz-Orive, L. M. (1987). Quantitation of chondrocyte performance in growth-plate cartilage during longitudinal bone growth. *The Journal of bone and joint surgery. American volume*, 69(2), 162-173.
- Hutchison, M. R., Bassett, M. H., & White, P. C. (2007). Insulin-like growth factor-I and fibroblast growth factor, but not growth hormone, affect growth plate chondrocyte proliferation. *Endocrinology*, 148(7), 3122-3130. doi:en.2006-1264 [pii] 10.1210/en.2006-1264 [doi]
- Isaksson, O. G., Jansson, J. O., & Gause, I. A. (1982). Growth hormone stimulates longitudinal bone growth directly. *Science*, 216(4551), 1237-1239.
- Iwamoto, M., Shapiro, I. M., Yagami, K., Boskey, A. L., Leboy, P. S., Adams, S. L., & Pacifici, M. (1993). Retinoic acid induces rapid mineralization and expression of mineralization-related genes in chondrocytes. *Exp Cell Res*, 207(2), 413-420. doi:S0014-4827(83)71209-7 [pii] 10.1006/excr.1993.1209 [doi]
- Jaramillo, D., Villegas-Medina, O. L., Doty, D. K., Rivas, R., Strife, K., Dwek, J. R., . . . Shapiro, F. (2004). Age-related vascular changes in the epiphysis, physis, and metaphysis: normal findings on gadolinium-enhanced MRI of piglets. *AJR Am J Roentgenol*, 182(2), 353-360.
- Jin, H., & Lewis, J. L. (2004). Determination of Poisson's ratio of articular cartilage by indentation using different-sized indenters. *Journal of biomechanical engineering*, 126(2), 138-145.
- Johnson, I. (1998). Fluorescent probes for living cells. *Histochem J*, 30(3), 123-140.
- Johnstone, E. W., Leane, P. B., Kolesik, P., Byers, S., & Foster, B. K. (2000). Spatial arrangement of physeal cartilage chondrocytes and the structure of the primary spongiosa. *J Orthop Sci*, 5(3), 294-301. doi:10.1007/s007760000050294.776 [doi]
- Julkunen, P., Korhonen, R. K., Herzog, W., & Jurvelin, J. S. (2008). Uncertainties in indentation testing of articular cartilage: a fibril-reinforced poroviscoelastic study. *Med Eng Phys*, 30(4), 506-515. doi:S1350-4533(07)00103-8 [pii] 10.1016/j.medengphy.2007.05.012 [doi]

- Kaab, M. J., Gwynn, I. A., & Notzli, H. P. (1998). Collagen fibre arrangement in the tibial plateau articular cartilage of man and other mammalian species. *J Anat*, 193 (Pt 1), 23-34.
- Keeling, J., & Herrera, G. A. (2008). Human matrix metalloproteinases: characteristics and pathologic role in altering mesangial homeostasis. *Microsc Res Tech*, 71(5), 371-379. doi:10.1002/jemt.20565 [doi]
- Kember, N. F. (1960). Cell division in endochondral ossification. A study of cell proliferation in rat bones by the method of tritiated thymidine autoradiography. *J Bone Joint Surg Br*, 42B, 824-839.
- Kember, N. F. (1978). Cell kinetics and the control of growth in long bones. *Cell Tissue Kinet*, 11(5), 477-485.
- Kerrigan, M. J., & Hall, A. C. (2008). Control of chondrocyte regulatory volume decrease (RVD) by $[Ca^{2+}]_i$ and cell shape. *Osteoarthritis Cartilage*, 16(3), 312-322. doi:S1063-4584(07)00256-7 [pii] 10.1016/j.joca.2007.07.006 [doi]
- Kim, Y. J., Sah, R. L., Doong, J. Y., & Grodzinsky, A. J. (1988). Fluorometric assay of DNA in cartilage explants using Hoechst 33258. *Anal Biochem*, 174(1), 168-176. doi:0003-2697(88)90532-5 [pii]
- Kiraly, K., Hyttinen, M. M., Lapvetelainen, T., Elo, M., Kiviranta, I., Dobai, J., . . . Arokoski, J. P. (1997). Specimen preparation and quantification of collagen birefringence in unstained sections of articular cartilage using image analysis and polarizing light microscopy. *Histochem J*, 29(4), 317-327.
- Knauper, V., Will, H., Lopez-Otin, C., Smith, B., Atkinson, S. J., Stanton, H., . . . Murphy, G. (1996). Cellular mechanisms for human procollagenase-3 (MMP-13) activation. Evidence that MT1-MMP (MMP-14) and gelatinase a (MMP-2) are able to generate active enzyme. *J Biol Chem*, 271(29), 17124-17131.
- Knight, M. M., Bomzon, Z., Kimmel, E., Sharma, A. M., Lee, D. A., & Bader, D. L. (2006). Chondrocyte deformation induces mitochondrial distortion and heterogeneous intracellular strain fields. *Biomechanics and Modeling in Mechanobiology*, 5(2-3), 180-191. doi:<http://dx.doi.org/10.1007/s10237-006-0020-7>
- Korhonen, R. K., Wong, M., Arokoski, J., Lindgren, R., Helminen, H. J., Hunziker, E. B., & Jurvelin, J. S. (2002). Importance of the superficial tissue layer for the indentation stiffness of articular cartilage. *Med Eng Phys*, 24(2), 99-108. doi:S1350453301001230 [pii]
- Kuhn, J. L., Hornovich, J. D., & Lee, E. E. (1993). The relationship between bone growth rate and hypertrophic chondrocyte volume in the New Zealand white rabbit of varying age. *Annual meeting of orthopaedic research society, San Francisco, CA, USA.*(Vol. 39, pp. 695).
- Kurien, B. T., & Scofield, R. H. (2006). Western blotting. *Methods*, 38(4), 283-293. doi:S1046-2023(06)00006-5 [pii] 10.1016/j.ymeth.2005.11.007 [doi]

- Langsjo, T. K., Vasara, A. I., Hyttinen, M. M., Lammi, M. J., Kaukinen, A., Helminen, H. J., & Kiviranta, I. (2010). Quantitative analysis of collagen network structure and fibril dimensions in cartilage repair with autologous chondrocyte transplantation. *Cells, tissues, organs*, 192(6), 351-360. doi:000319469 [pii] 10.1159/000319469 [doi]
- Leach, R. M., Jr., Richards, M. P., Praul, C. A., Ford, B. C., & McMurtry, J. P. (2007). Investigation of the insulin-like growth factor system in the avian epiphyseal growth plate. *Domest Anim Endocrinol*, 33(2), 143-153. doi:S0739-7240(06)00064-6 [pii] 10.1016/j.domaniend.2006.04.010 [doi]
- Lee, D. A., Knight, M. M., Bolton, J. F., Idowu, B. D., Kayser, M. V., & Bader, D. L. (2000). Chondrocyte deformation within compressed agarose constructs at the cellular and sub-cellular levels. *J Biomech*, 33(1), 81-95. doi:S0021929099001608 [pii]
- Leger, J., & Czernichow, P. (1989). Congenital hypothyroidism: decreased growth velocity in the first weeks of life. *Biol Neonate*, 55(4-5), 218-223.
- Lehmann, T. M., Gonner, C., & Spitzer, K. (1999). Survey: interpolation methods in medical image processing. *IEEE Trans Med Imaging*, 18(11), 1049-1075. doi:10.1109/42.816070 [doi]
- Leipzig, N. D., & Athanasiou, K. A. (2005). Unconfined creep compression of chondrocytes. *J Biomech*, 38(1), 77-85. doi:S0021929004001381 [pii] 10.1016/j.jbiomech.2004.03.013 [doi]
- Lerner, A. L., Kuhn, J. L., & Hollister, S. J. (1998). Are regional variations in bone growth related to mechanical stress and strain parameters? *J Biomech*, 31(4), 327-335. doi:S0021-9290(98)00015-3 [pii]
- LeVeau, B. F., & Bernhardt, D. B. (1984). Developmental biomechanics. Effect of forces on the growth, development, and maintenance of the human body. *Phys Ther*, 64(12), 1874-1882.
- Lu, X. L., Sun, D. D., Guo, X. E., Chen, F. H., Lai, W. M., & Mow, V. C. (2004). Indentation determined mechanoelectrochemical properties and fixed charge density of articular cartilage. *Annals of Biomedical Engineering*, 32(3), 370-379.
- Mainil-Varlet, P., Aigner, T., Brittberg, M., Bullough, P., Hollander, A., Hunziker, E., . . . Stauffer, E. (2003). Histological assessment of cartilage repair: a report by the Histology Endpoint Committee of the International Cartilage Repair Society (ICRS). *J Bone Joint Surg Am*, 85-A Suppl 2, 45-57.
- Mak, A. F. (1986). The apparent viscoelastic behavior of articular cartilage--the contributions from the intrinsic matrix viscoelasticity and interstitial fluid flows. *Journal of biomechanical engineering*, 108(2), 123-130.
- Makower, A. M., Wroblewski, J., & Pawlowski, A. (1988). Effects of IGF-I, EGF, and FGF on proteoglycans synthesized by fractionated chondrocytes of rat rib growth plate. *Exp Cell Res*, 179(2), 498-506.
- Mankin, K. P., & Zaleske, D. J. (1998). Response of physeal cartilage to low-level compression and tension in organ culture. *J Pediatr Orthop*, 18(2), 145-148.

- Mao, J. J., & Nah, H. D. (2004). Growth and development: hereditary and mechanical modulations. *American journal of orthodontics and dentofacial orthopedics* 125(6), 676-689. doi:10.1016/S0889540604001908 [doi] S0889540604001908 [pii]
- Marieb, E. N., & Hoehn, K. (2006). *Human anatomy and physiology* (7th^e éd.): Benjamin Cummings.
- Matsui, Y., Alini, M., Webber, C., & Poole, A. R. (1991). Characterization of aggregating proteoglycans from the proliferative, maturing, hypertrophic, and calcifying zones of the cartilaginous physis. *The Journal of bone and joint surgery. American volume*, 73(7), 1064-1074.
- Michalek, A. J., Buckley, M. R., Bonassar, L. J., Cohen, I., & Iatridis, J. C. (2009). Measurement of local strains in intervertebral disc anulus fibrosus tissue under dynamic shear: contributions of matrix fiber orientation and elastin content. *J Biomech*, 42(14), 2279-2285. doi:S0021-9290(09)00375-3 [pii] 10.1016/j.jbiomech.2009.06.047 [doi]
- Minsky, M. (1961). U.S. Patent No. 3013467.
- Mitani, H., Takahashi, I., Onodera, K., Bae, J. W., Sato, T., Takahashi, N., . . . Igarashi, K. (2006). Comparison of age-dependent expression of aggrecan and ADAMTSs in mandibular condylar cartilage, tibial growth plate, and articular cartilage in rats. *Histochem Cell Biol*, 126(3), 371-380. doi:10.1007/s00418-006-0171-8 [doi]
- Mitchell, P. G., Magna, H. A., Reeves, L. M., Lopresti-Morrow, L. L., Yocum, S. A., Rosner, P. J., . . . Hambor, J. E. (1996). Cloning, expression, and type II collagenolytic activity of matrix metalloproteinase-13 from human osteoarthritic cartilage. *J Clin Invest*, 97(3), 761-768. doi:10.1172/JCI118475 [doi]
- Modis, L. (1991). Physical backgrounds of polarization microscopy. In L. Modis (dir.), *Organization of the extracellular matrix: a polarization microscopic approach*. (pp. 9-30). Boca Raton: CRC Press.
- Monsonogo, E., Halevy, O., Gertler, A., Hurwitz, S., & Pines, M. (1995). Growth hormone inhibits differentiation of avian epiphyseal growth-plate chondrocytes. *Mol Cell Endocrinol*, 114(1-2), 35-42.
- Mort, J. S., & Roughley, P. J. (2007). Measurement of glycosaminoglycan release from cartilage explants. *Methods Mol Med*, 135, 201-209. doi:1-59745-401-X:201 [pii]
- Mow, V. C., Gu, W. Y., & Chen, F. H. (2005). Structure and function of articular cartilage and meniscus. In V. C. Mow & R. Huiskes (dir.), *Basic Orthopaedic Biomechanics and Mechano-biology*. (3^e éd., pp. 182-258). Philadelphia: Lippincott William and Wilkins.
- Mow, V. C., & Hung, C. T. (2001). Biomechanics of articular cartilage. In M. Nordin & V. H. Frankel (dir.), *Basic biomechanics of the musculoskeletal system*. (3^e éd.). Philadelphia: Lippincott William and Wilkins.
- Mow, V. C., & Ratcliffe, A. (1997). Structure and function of articular cartilage and meniscus. In V. C. Mow & W. C. Hayes (dir.), *Basic Orthopaedic Biomechanics*. (2^e éd.). Philadelphia: Lippincott-Raven.

- Mow, V. C., Wang, C. C., & Hung, C. T. (1999). The extracellular matrix, interstitial fluid and ions as a mechanical signal transducer in articular cartilage. *Osteoarthritis Cartilage*, 7(1), 41-58. doi:S1063-4584(98)90161-3 [pii] 10.1053/joca.1998.0161 [doi]
- Mow, V. C., Zhu, W., Lai, W. M., Hardingham, T. E., Hughes, C., & Muir, H. (1989). The influence of link protein stabilization on the viscometric properties of proteoglycan aggregate solutions. *Biochim Biophys Acta*, 992(2), 201-208.
- Murphy, G., Nagase, H., & Brinckerhoff, C. E. (1988). Relationship of procollagenase activator, stromelysin and matrix metalloproteinase 3. *Coll Relat Res*, 8(4), 389-391.
- Mwale, F., Tchetina, E., Wu, C. W., & Poole, A. R. (2002). The assembly and remodeling of the extracellular matrix in the growth plate in relationship to mineral deposition and cellular hypertrophy: an in situ study of collagens II and IX and proteoglycan. *J Bone Miner Res*, 17(2), 275-283.
- Nerlich, A. G. (2003). Histochemical and Immunohistochemical Staining of Cartilage Sections. In Y. H. An & K. L. Martin (dir.), *Handbook of Histology Methods for Bone and Cartilage*. (pp. 295-313). Totowa, NJ: Humana Press.
- Newman, P. H. (1955). Spondylolisthesis, its cause and effect. *Ann R Coll Surg Engl*, 16(5), 305-323.
- Newton, P. O., Faro, F. D., Farnsworth, C. L., Shapiro, G. S., Mohamad, F., Parent, S., & Fricka, K. (2005). Multilevel spinal growth modulation with an anterolateral flexible tether in an immature bovine model. *Spine (Phila Pa 1976)*, 30(23), 2608-2613. doi:00007632-200512010-00005 [pii]
- Niehoff, A., Kersting, U. G., Zaucke, F., Morlock, M. M., & Bruggemann, G. P. (2004). Adaptation of mechanical, morphological, and biochemical properties of the rat growth plate to dose-dependent voluntary exercise. *Bone*, 35(4), 899-908. doi:10.1016/j.bone.2004.06.006 [doi] S875632820400256X [pii]
- Nilsson, O., & Baron, J. (2004). Fundamental limits on longitudinal bone growth: growth plate senescence and epiphyseal fusion. *Trends Endocrinol Metab*, 15(8), 370-374. doi:10.1016/j.tem.2004.08.004 [doi] S1043-2760(04)00185-7 [pii]
- O'Keefe, R. J., Loveys, L. S., Hicks, D. G., Reynolds, P. R., Crabb, I. D., Puzas, J. E., & Rosier, R. N. (1997). Differential regulation of type-II and type-X collagen synthesis by parathyroid hormone-related protein in chick growth-plate chondrocytes. *Journal of orthopaedic research : official publication of the Orthopaedic Research Society*, 15(2), 162-174. doi:10.1002/jor.1100150203 [doi]
- Ohashi, N., Robling, A. G., Burr, D. B., & Turner, C. H. (2002). The effects of dynamic axial loading on the rat growth plate. *J Bone Miner Res*, 17(2), 284-292. doi:10.1359/jbmr.2002.17.2.284 [doi]
- Othman, H., Thonar, E. J., & Mao, J. J. (2007). Modulation of neonatal growth plate development by ex vivo intermittent mechanical stress. *J Biomech*, 40(12), 2686-2693. doi:S0021-9290(07)00003-6 [pii] 10.1016/j.jbiomech.2006.12.014 [doi]

- . Papain assay: Worthington enzymes and biochemicals. (2011). <http://www.worthington-biochem.com/pap/assay.html>.
- Patterson, M. L., Atkinson, S. J., Knauper, V., & Murphy, G. (2001). Specific collagenolysis by gelatinase A, MMP-2, is determined by the hemopexin domain and not the fibronectin-like domain. *FEBS Lett*, 503(2-3), 158-162.
- Pawley, J. B. (dir.). (1995). *Handbook of biological confocal microscopy* (2nd éd.). New York: Plenum Press.
- Pihlajamaa, T., Perala, M., Vuoristo, M. M., Nokelainen, M., Bodo, M., Schulthess, T., . . . Ala-Kokko, L. (1999). Characterization of recombinant human type IX collagen. Association of alpha chains into homotrimeric and heterotrimeric molecules. *J Biol Chem*, 274(32), 22464-22468.
- Poole, A. R., Matsui, Y., Hinek, A., & Lee, E. R. (1989). Cartilage macromolecules and the calcification of cartilage matrix. *Anat Rec*, 224(2), 167-179. doi:10.1002/ar.1092240207 [doi]
- Radhakrishnan, P., Lewis, N. T., & Mao, J. J. (2004). Zone-specific micromechanical properties of the extracellular matrices of growth plate cartilage. *Annals of Biomedical Engineering*, 32(2), 284-291. doi:<http://dx.doi.org/10.1023/B:ABME.0000012748.41851.b4>
- Ratcliffe, A., & Mow, V. C. (1996). The structure and function of articular cartilage. In W. D. Comper (dir.), *Structure and function of connective tissue*. (3^e éd.). Amsterdam: Harwood Academic Press.
- Rauch, F. (2005). Bone growth in length and width: the Yin and Yang of bone stability. *J Musculoskelet Neuronal Interact*, 5(3), 194-201.
- Revel, M., Andre-Deshays, C., Roudier, R., Roudier, B., Hamard, G., & Amor, B. (1992). Effects of repetitive strains on vertebral end plates in young rats. *Clin Orthop Relat Res*(279), 303-309.
- Rieppo, J., Toyra, J., Nieminen, M. T., Kovanen, V., Hyttinen, M. M., Korhonen, R. K., . . . Helminen, H. J. (2003). Structure-function relationships in enzymatically modified articular cartilage. *Cells, tissues, organs*, 175(3), 121-132. doi:10.1159/000074628 [doi] 74628 [pii]
- Roach, H. I., & Clarke, N. M. (2000). Physiological cell death of chondrocytes in vivo is not confined to apoptosis. New observations on the mammalian growth plate. *J Bone Joint Surg Br*, 82(4), 601-613.
- Roberts, S., McCall, I. W., Darby, A. J., Menage, J., Evans, H., Harrison, P. E., & Richardson, J. B. (2003). Autologous chondrocyte implantation for cartilage repair: monitoring its success by magnetic resonance imaging and histology. *Arthritis Res Ther*, 5(1), R60-73.
- Rodeo, S. A., Seneviratne, A., Suzuki, K., Felker, K., Wickiewicz, T. L., & Warren, R. F. (2000). Histological analysis of human meniscal allografts. A preliminary report. *J Bone Joint Surg Am*, 82-A(8), 1071-1082.

- Ruggiero, F., Petit, B., Ronziere, M. C., Farjanel, J., Hartmann, D. J., & Herbage, D. (1993). Composition and organization of the collagen network produced by fetal bovine chondrocytes cultured at high density. *J Histochem Cytochem*, 41(6), 867-875.
- Russell, S. M., & Spencer, E. M. (1985). Local injections of human or rat growth hormone or of purified human somatomedin-C stimulate unilateral tibial epiphyseal growth in hypophysectomized rats. *Endocrinology*, 116(6), 2563-2567.
- Sachs, F. (1991). Mechanical transduction by membrane ion channels: a mini review. *Molecular and cellular biochemistry* 104(1-2), 57-60.
- Sairyo, K., Katoh, S., Ikata, T., Fujii, K., Kajiura, K., & Goel, V. K. (2001). Development of spondylolytic olisthesis in adolescents. *Spine J*, 1(3), 171-175. doi:S1529-9430(01)00018-3 [pii]
- Sakai, T., Sairyo, K., Suzue, N., Kosaka, H., & Yasui, N. Incidence and etiology of lumbar spondylolysis: review of the literature. *J Orthop Sci*, 15(3), 281-288. doi:10.1007/s00776-010-1454-4 [doi]
- Sandell, L. J., Sugai, J. V., & Trippel, S. B. (1994). Expression of collagens I, II, X, and XI and aggrecan mRNAs by bovine growth plate chondrocytes in situ. *Journal of orthopaedic research : official publication of the Orthopaedic Research Society*, 12(1), 1-14. doi:10.1002/jor.1100120102 [doi]
- Schinagl, R. M., Gurskis, D., Chen, A. C., & Sah, R. L. (1997). Depth-dependent confined compression modulus of full-thickness bovine articular cartilage. *Journal of orthopaedic research : official publication of the Orthopaedic Research Society*, 15(4), 499-506. doi:10.1002/jor.1100150404
- Schinagl, R. M., Ting, M. K., Price, J. H., & Sah, R. L. (1996). Video microscopy to quantitate the inhomogeneous equilibrium strain within articular cartilage during confined compression. *Annals of Biomedical Engineering*, 24(4), 500-512.
- Schoenle, E., Zapf, J., Humbel, R. E., & Froesch, E. R. (1982). Insulin-like growth factor I stimulates growth in hypophysectomized rats. *Nature*, 296(5854), 252-253.
- Schrier, L., Ferns, S. P., Barnes, K. M., Emons, J. A., Newman, E. I., Nilsson, O., & Baron, J. (2006). Depletion of resting zone chondrocytes during growth plate senescence. *J Endocrinol*, 189(1), 27-36. doi:189/1/27 [pii] 10.1677/joe.1.06489 [doi]
- Scott, J. H. (1957). The mechanical basis of bone formation. *J Bone Joint Surg Br*, 39-B(1), 134-144.
- Seinsheimer, F., 3rd, & Sledge, C. B. (1981). Parameters of longitudinal growth rate in rabbit epiphyseal growth plates. *J Bone Joint Surg Am*, 63(4), 627-630.
- Sergerie, K., Lacoursiere, M. O., Levesque, M., & Villemure, I. (2009). Mechanical properties of the porcine growth plate and its three zones from unconfined compression tests. *Journal of biomechanics*, 42(4), 510-516. doi:S0021-9290(08)00587-3 [pii] 10.1016/j.jbiomech.2008.11.026 [doi]

- Sergerie, K., Parent, S., Beauchemin, P. F., Londono, I., Moldovan, F., & Villemure, I. (2011). Growth plate explants respond differently to in vitro static and dynamic loadings. *Journal of orthopaedic research : official publication of the Orthopaedic Research Society*, 29(4), 473-480. doi:10.1002/jor.21282 [doi]
- Setton, L. A., Gu, W. Y., Lai, W. M., & Mow, V. C. (1995). Predictions of the swelling induced pre-stress in articular cartilage. In A. P. S. Selvadurai (dir.), *Mechanics of Porous Media*. Dordrecht: Kluwer Academic Publishers.
- Shieh, A. C., & Athanasiou, K. A. (2006). Biomechanics of single zonal chondrocytes. *J Biomech*, 39(9), 1595-1602. doi:S0021-9290(05)00217-4 [pii] 10.1016/j.jbiomech.2005.05.002 [doi]
- Simon, M. R. (1978). The effect of dynamic loading on the growth of epiphyseal cartilage in the rat. *Acta Anat (Basel)*, 102(2), 176-183.
- Skaggs, D. L., Warden, W. H., & Mow, V. C. (1994). Radial tie fibers influence the tensile properties of the bovine medial meniscus. *Journal of orthopaedic research : official publication of the Orthopaedic Research Society*, 12(2), 176-185. doi:10.1002/jor.1100120205 [doi]
- Speer, D. P. (1982). Collagenous architecture of the growth plate and perichondrial ossification groove. *J Bone Joint Surg Am*, 64(3), 399-407.
- Speer, D. P., & Dahners, L. (1979). The collagenous architecture of articular cartilage. Correlation of scanning electron microscopy and polarized light microscopy observations. *Clin Orthop Relat Res*(139), 267-275.
- Stegemann, H., & Stalder, K. (1967). Determination of hydroxyproline. *Clin Chim Acta*, 18(2), 267-273. doi:0009-8981(67)90167-2 [pii]
- Stickens, D., Behonick, D. J., Ortega, N., Heyer, B., Hartenstein, B., Yu, Y., . . . Werb, Z. (2004). Altered endochondral bone development in matrix metalloproteinase 13-deficient mice. *Development*, 131(23), 5883-5895. doi:131/23/5883 [pii] 10.1242/dev.01461 [doi]
- Stokes, I. A. (2002). Mechanical effects on skeletal growth. *Journal of musculoskeletal & neuronal interactions*, 2(3), 277-280.
- Stokes, I. A., Aronsson, D. D., Dimock, A. N., Cortright, V., & Beck, S. (2006). Endochondral growth in growth plates of three species at two anatomical locations modulated by mechanical compression and tension. *Journal of orthopaedic research*, 24(6), 1327-1334. doi:10.1002/jor.20189 [doi]
- Stokes, I. A., Clark, K. C., Farnum, C. E., & Aronsson, D. D. (2007). Alterations in the growth plate associated with growth modulation by sustained compression or distraction. *Bone*, 41(2), 197-205. doi:S8756-3282(07)00372-9 [pii] 10.1016/j.bone.2007.04.180 [doi]
- Stokes, I. A., Gwadera, J., Dimock, A., Farnum, C. E., & Aronsson, D. D. (2005). Modulation of vertebral and tibial growth by compression loading: diurnal versus full-time loading. *Journal of orthopaedic research*, 23(1), 188-195. doi:S0736-0266(04)00154-8 [pii] 10.1016/j.orthres.2004.06.012 [doi]

- Stokes, I. A., Mente, P. L., Iatridis, J. C., Farnum, C. E., & Aronsson, D. D. (2002). Enlargement of growth plate chondrocytes modulated by sustained mechanical loading. *J Bone Joint Surg Am*, 84-A(10), 1842-1848.
- Stokes, I. A. F., Spence, H., Aronsson, D. D., & Kilmer, N. (1996). Mechanical modulation of vertebral body growth. Implications for scoliosis progression. *Spine*, 21(10), 1162-1167.
- Stoltz, J. F., & Wang, X. (2002). From biomechanics to mechanobiology. *Biorheology*, 39(1-2), 5-10.
- Suttmuller, M., Bruijn, J. A., & de Heer, E. (1997). Collagen types VIII and X, two non-fibrillar, short-chain collagens. Structure homologies, functions and involvement in pathology. *Histol Histopathol*, 12(2), 557-566.
- Takahashi, I., Onodera, K., Bae, J. W., Mitani, H., & Sasano, Y. (2005). Age-related changes in the expression of gelatinase and tissue inhibitor of metalloproteinase genes in mandibular condylar, growth plate, and articular cartilage in rats. *J Mol Histol*, 36(5), 355-366. doi:10.1007/s10735-005-9007-4 [doi]
- Takano, H., Aizawa, T., Irie, T., Kokubun, S., & Itoi, E. (2007). Estrogen deficiency leads to decrease in chondrocyte numbers in the rabbit growth plate. *J Orthop Sci*, 12(4), 366-374. doi:10.1007/s00776-007-1145-y [doi]
- Tanaka, N., Ohno, S., Honda, K., Tanimoto, K., Doi, T., Ohno-Nakahara, M., . . . Tanne, K. (2005). Cyclic mechanical strain regulates the PTHrP expression in cultured chondrocytes via activation of the Ca²⁺ channel. *Journal of dental research*, 84(1), 64-68. doi:84/1/64 [pii]
- Tang, M., & Mao, J. J. (2006). Matrix and gene expression in the rat cranial base growth plate. *Cell Tissue Res*, 324(3), 467-474. doi:10.1007/s00441-005-0143-7 [doi]
- Taylor, K. B., & Jeffree, G. M. (1969). A new basic metachromatic dye, I:9-dimethyl methylene blue. *Histochem J*, 1(3), 199-204.
- Thorngren, K. G., & Hansson, L. I. (1974). Bioassay of growth hormone, I, Determination of longitudinal bone growth with tetracycline in hypophysectomized rats. *Acta Endocrinol (Copenh)*, 75(4), 653-668.
- Thorp, B. H., Anderson, I., & Jakowlew, S. B. (1992). Transforming growth factor-beta 1, -beta 2 and -beta 3 in cartilage and bone cells during endochondral ossification in the chick. *Development*, 114(4), 907-911.
- Tong, W. (2005). An evaluation of digital image correlation criteria for strain mapping applications. *Strain*, 41(4), 167-175. doi:10.1111/j.1475-1305.2005.00227.x
- Tortorella, M., Pratta, M., Liu, R. Q., Abbaszade, I., Ross, H., Burn, T., & Arner, E. (2000). The thrombospondin motif of aggrecanase-1 (ADAMTS-4) is critical for aggrecan substrate recognition and cleavage. *J Biol Chem*, 275(33), 25791-25797. doi:10.1074/jbc.M001065200 [doi] M001065200 [pii]

- Tortorella, M. D., Burn, T. C., Pratta, M. A., Abbaszade, I., Hollis, J. M., Liu, R., . . . Arner, E. C. (1999). Purification and cloning of aggrecanase-1: a member of the ADAMTS family of proteins. *Science*, 284(5420), 1664-1666.
- Trickey, W. R., Lee, G. M., & Guilak, F. (2000). Viscoelastic properties of chondrocytes from normal and osteoarthritic human cartilage. *Journal of orthopaedic research : official publication of the Orthopaedic Research Society*, 18(6), 891-898. doi:10.1002/jor.1100180607 [doi]
- Trueta, J., & Little, K. (1960). The vascular contribution to osteogenesis. II. Studies with the electron microscope. *J Bone Joint Surg Br*, 42-B, 367-376.
- Trueta, J., & Trias, A. (1961). The vascular contribution to osteogenesis. IV. The effect of pressure upon the epiphyseal cartilage of the rabbit. *J Bone Joint Surg Br*, 43-B, 800-813.
- Urban, J. P., Hall, A. C., & Gehl, K. A. (1993). Regulation of matrix synthesis rates by the ionic and osmotic environment of articular chondrocytes. *J Cell Physiol*, 154(2), 262-270. doi:10.1002/jcp.1041540208 [doi]
- Valteau, B., Grimard, G., Londono, I., Moldovan, F., & Villemure, I. (2011). In vivo dynamic bone growth modulation is less detrimental but as effective as static growth modulation. *Bone*. doi:S8756-3282(11)01086-6 [pii] 10.1016/j.bone.2011.07.008 [doi]
- van der Eerden, B. C., Karperien, M., & Wit, J. M. (2003). Systemic and local regulation of the growth plate. *Endocr Rev*, 24(6), 782-801.
- van der Meulen, M. C., & Huiskes, R. (2002). Why mechanobiology? A survey article. *J Biomech*, 35(4), 401-414. doi:S0021929001001841 [pii]
- van der Rest, M., & Mayne, R. (1988). Type IX collagen proteoglycan from cartilage is covalently cross-linked to type II collagen. *J Biol Chem*, 263(4), 1615-1618.
- Vasara, A. I., Hyttinen, M. M., Pulliainen, O., Lammi, M. J., Jurvelin, J. S., Peterson, L., . . . Kiviranta, I. (2006). Immature porcine knee cartilage lesions show good healing with or without autologous chondrocyte transplantation. *Osteoarthritis Cartilage*, 14(10), 1066-1074. doi:S1063-4584(06)00105-1 [pii] 10.1016/j.joca.2006.04.003 [doi]
- Villemure, I., Chung, M. A., Seck, C. S., Kimm, M. H., Matyas, J. R., & Duncan, N. A. (2005). Static compressive loading reduces the mRNA expression of type II and X collagen in rat growth-plate chondrocytes during postnatal growth. *Connective tissue research* 46(4-5), 211-219. doi:M258PM3635J18233 [pii] 10.1080/03008200500344058 [doi]
- Villemure, I., Cloutier, L., Matyas, J. R., & Duncan, N. A. (2007). Non-uniform strain distribution within rat cartilaginous growth plate under uniaxial compression. *Journal of Biomechanics*, 40(1), 149-156. doi:<http://dx.doi.org/10.1016/j.jbiomech.2005.11.008>
- Villemure, I., & Stokes, I. A. (2009). Growth plate mechanics and mechanobiology. A survey of present understanding. *Journal of Biomechanics*, 42(12), 1793-1803. doi:S0021-9290(09)00270-X [pii] 10.1016/j.jbiomech.2009.05.021 [doi]

- Vu, T. H., Shipley, J. M., Bergers, G., Berger, J. E., Helms, J. A., Hanahan, D., . . . Werb, Z. (1998). MMP-9/gelatinase B is a key regulator of growth plate angiogenesis and apoptosis of hypertrophic chondrocytes. *Cell*, 93(3), 411-422.
- Wall, E. J., Bylski-Austrow, D. I., Kolata, R. J., & Crawford, A. H. (2005). Endoscopic mechanical spinal hemiepiphysiodesis modifies spine growth. *Spine (Phila Pa 1976)*, 30(10), 1148-1153. doi:00007632-200505150-00008 [pii]
- Wang, C. C., Chahine, N. O., Hung, C. T., & Ateshian, G. A. (2003). Optical determination of anisotropic material properties of bovine articular cartilage in compression. *J Biomech*, 36(3), 339-353.
- Wang, C. C. B., Jian-Ming, D., Ateshian, G. A., & Hung, C. T. (2002). An automated approach for direct measurement of two-dimensional strain distributions within articular cartilage under unconfined compression. *Transactions of the ASME. Journal of Biomechanical Engineering*, 124(5), 557-567. doi:<http://dx.doi.org/10.1115/1.1503795>
- Wang, W., & Kirsch, T. (2002). Retinoic acid stimulates annexin-mediated growth plate chondrocyte mineralization. *J Cell Biol*, 157(6), 1061-1069. doi:10.1083/jcb.200203014 [doi] jcb.200203014 [pii]
- Wang, X., & Mao, J. J. (2002). Chondrocyte proliferation of the cranial base cartilage upon in vivo mechanical stresses. *Journal of dental research*, 81(10), 701-705.
- Watson, P. A. (1991). Function follows form: generation of intracellular signals by cell deformation. *The FASEB journal* 5(7), 2013-2019.
- Webb, R. H. (1996). Confocal optical microscopy *Reports on Progress in Physics*, 59(3), 427-471.
- Webb, R. H., & Dorey, C. K. (1995). The pixelated image. In J. B. Pawley (dir.), *Handbook of biological confocal microscopy*. (2nd^e éd.). New York: Plenum Press.
- Wiemann, J. M. t., Tryon, C., & Szalay, E. A. (2009). Physeal stapling versus 8-plate hemiepiphysiodesis for guided correction of angular deformity about the knee. *J Pediatr Orthop*, 29(5), 481-485. doi:10.1097/BPO.0b013e3181aa24a8 [doi] 01241398-200907000-00013 [pii]
- Williams, R. M., Zipfel, W. R., Tinsley, M. L., & Farnum, C. E. (2007). Solute transport in growth plate cartilage: in vitro and in vivo. *Biophys J*, 93(3), 1039-1050. doi:S0006-3495(07)71360-7 [pii] 10.1529/biophysj.106.097675 [doi]
- Wilsman, N. J., Farnum, C. E., Green, E. M., Lieferman, E. M., & Clayton, M. K. (1996). Cell cycle analysis of proliferative zone chondrocytes in growth plates elongating at different rates. *Journal of Orthopaedic Research*, 14(4), 562-572. doi:10.1002/jor.1100140410 [doi]
- Wilsman, N. J., Farnum, C. E., Lieferman, E. M., Fry, M., & Barreto, C. (1996). Differential growth by growth plates as a function of multiple parameters of chondrocytic kinetics. *Journal of orthopaedic research*, 14(6), 927-936. doi:10.1002/jor.1100140613

- Wirth, T., Syed Ali, M. M., Rauer, C., Suss, D., Griss, P., & Syed Ali, S. (2002). The blood supply of the growth plate and the epiphysis: a comparative scanning electron microscopy and histological experimental study in growing sheep. *Calcif Tissue Int*, 70(4), 312-319. doi:10.1007/s00223-001-2006-x [doi]
- Wit, J. M., Kamp, G. A., & Rikken, B. (1996). Spontaneous growth and response to growth hormone treatment in children with growth hormone deficiency and idiopathic short stature. *Pediatr Res*, 39(2), 295-302.
- Woessner, J. F., Jr. (1961). The determination of hydroxyproline in tissue and protein samples containing small proportions of this imino acid. *Arch Biochem Biophys*, 93, 440-447.
- Wosu, R., Sergerie, K., Levesque, M., & Villemure, I. (2011). Mechanical properties of the porcine growth plate vary with developmental stage. *Biomech Model Mechanobiol*. doi:10.1007/s10237-011-0310-6 [doi]
- Wroblewski, J., & Edwall-Arvidsson, C. (1995). Inhibitory effects of basic fibroblast growth factor on chondrocyte differentiation. *J Bone Miner Res*, 10(5), 735-742. doi:10.1002/jbmr.5650100510 [doi]
- Wuthier, R. E. (1969). A zonal analysis of inorganic and organic constituents of the epiphysis during endochondral calcification. *Calcif Tissue Res*, 4(1), 20-38.
- Yoshida, E., Noshiro, M., Kawamoto, T., Tsutsumi, S., Kuruta, Y., & Kato, Y. (2001). Direct inhibition of Indian hedgehog expression by parathyroid hormone (PTH)/PTH-related peptide and up-regulation by retinoic acid in growth plate chondrocyte cultures. *Exp Cell Res*, 265(1), 64-72. doi:10.1006/excr.2001.5161 [doi] S0014-4827(01)95161-4 [pii]
- Youn, I., Choi, J. B., Cao, L., Setton, L. A., & Guilak, F. (2006). Zonal variations in the three-dimensional morphology of the chondron measured in situ using confocal microscopy. *Osteoarthritis Cartilage*, 14(9), 889-897. doi:S1063-4584(06)00047-1 [pii] 10.1016/j.joca.2006.02.017 [doi]
- Zerath, E., Holy, X., Mouillon, J. M., Farbos, B., Machwate, M., Andre, C., . . . Marie, P. J. (1997). TGF-beta2 prevents the impaired chondrocyte proliferation induced by unloading in growth plates of young rats. *Life Sci*, 61(24), 2397-2406. doi:S0024320597009570 [pii]
- Zioudrou, C., Fujii, S., & Fruton, J. S. (1958). LABELING OF PROTEINS BY ISOTOPIC AMINO ACID DERIVATIVES. *Proc Natl Acad Sci U S A*, 44(5), 439-446.
- Zung, A., Phillip, M., Chalew, S. A., Palese, T., Kowarski, A. A., & Zadik, Z. (1999). Testosterone effect on growth and growth mediators of the GH-IGF-I axis in the liver and epiphyseal growth plate of juvenile rats. *J Mol Endocrinol*, 23(2), 209-221. doi:JME00814 [pii]